FER-LIKE IRON DEFICIENCY-INDUCED TRANSCRIPTION FACTOR (FIT) activity is controlled by protein phosphorylation.

Inaugural-Dissertation

zur Erlangung des Doktorgrades
der Mathematisch-Naturwissenschaftlichen Fakultät
der Heinrich-Heine-Universität Düsseldorf

vorgelegt von

Regina M. Gratz
aus Saarlouis

Düsseldorf, Februar 2018

aus dem Institut für Botanik
der Heinrich-Heine-Universität Düsseldorf

Gedruckt mit der Genehmigung der Mathematisch-Naturwissenschaftlichen Fakultät der Heinrich-Heine-Universität Düsseldorf

Berichterstatter:

1. Prof. Dr. P. Bauer

2. Prof. Dr. A. Weber

Tag der mündlichen Prüfung:
29.03.2018

EIDESSTATTLICHE ERKLÄRUNG

Ich versichere an Eides Statt, dass diese Dissertation von mir selbständig und ohne unzulässige fremde Hilfe unter Beachtung der „Grundsätze zur Sicherung guter wissenschaftlicher Praxis an der Heinrich-Heine-Universität Düsseldorf“ erstellt worden ist.

Die Dissertation habe ich in der vorgelegten oder in ähnlicher Form noch bei keiner anderen Institution eingereicht.

Ich habe bisher keine erfolglosen Promotionsversuche unternommen.

Regina Gratz

Düsseldorf, 05.02.2018

“Everything is going to be fine in the end.

-If it's not fine, it's not the end.”

-Oscar Wilde

Acknowledgment

First and foremost I would like to thank Prof. Petra Bauer. Thank you Petra for all your support over the last years! I appreciate many helpful discussions, your trust and also the freedom of implementing my own ideas. I happily returned to the lab for this PhD thesis.

I would like to thank my mentor Prof. Andreas Weber for his time and valuable input during the last years. Also I am thankful for my committee members Prof. Laura Rose as well as Dr. Nicole Linka for the fruitful discussions.

A big “Thank You” goes out to all of our collaborators and co-authors such as Prof. Matias Zurbriggen, Prof. Jörg Kudla and Prof. Uwe Karst and their teams. Thank you Prabha, Rocio, Tim and Alexander for help in the lab.

A special thanks goes to all old and new members of the Bauer Lab. I had a very pleasant time with you, especially during many coffee and cake breaks, movie nights and our BBQs. Maria Augusta- desde el fondo de mi corazón, gracias por tu gran apoyo, desde el momento en que heredaste mi escritorio en Saarbrücken. Sin ti los últimos 4 años hubieran sido diferentes. Quédate como eres porque eres una persona maravillosa! Birte- thank you very much for the great time in the office, during the day but also in the evenings, for good advice in all aspects of life and moral support! Thank you Hansi, Andreas, Cham, Anna, Dani, Inga, Claudia, Ksenia and everyone else for the good spirit! Thanks to Elke, Ginte, Angelika, Kai and Ulrike for help in the lab. Thanks to my students Chris, Laura, Dana, Bianca and Hristina for your help!

Dank je well Pieter (+Nemo) voor uw steun! Lazar- thanks for the one or the other bottle of wine, your hospitality in Toronto and the proofs! Ulrika och Siglinde- stort tack för ert stöd! Johnson Family- alt er love! Anika, Anja, Mara, Judith, Bernard, Michi and Hoffi, thank you very much for your friendship throughout all the years. Thank you Martin for the overall support during the critical phase! Thank you Yannic and the Spengli Family.

Изключително съм благодарна за подкрепата на Цветина и Румен. Научих толкова много от вас и в лабораторията, и извън нея. Бъдете винаги такива, каквито сте! Ще се видим това лято!

Letztlich möchte ich mich ganz herzlich bei meiner Familie, insbesondere bei Andreas und Tatjana sowie meinen Eltern für die Unterstützung in allen Lebenslagen bedanken.

Table of Contents

1 Preface

In the beginning of this PhD thesis, the work will be summarized in both languages, English and German. The following introduction will provide insight into iron deficiency and the importance of post-translational modifications as an integration tool for environmental stimuli on plant protein regulation. Subsequently, the aims of this work are summarized. The main body of this thesis comprises two manuscripts:

1. **CIPK11-dependent phosphorylation modulates dynamic cellular activity of the key transcription factor FIT, promoting iron acquisition**

   Regina Gratz*, Prabha Manishankar*, Rumen Ivanov, Philipp Köster, Inga Mohr, Ksenia Trofimov, Leonie Steinhorst, Johannes Meiser, Maria Drerup, Sibylle Arendt, Michael Holtkamp, Uwe Karst, Jörg Kudla, Petra Bauer, and Tzvetina Brumbarova -***submitted***

In this manuscript, we showed for the first time that the bHLH transcription factor FER-LIKE IRON DEFICIENCY-INDUCED TRANSCRIPTION FACTOR (FIT) undergoes protein phosphorylation. Phosphorylation of a C-terminal serine was demonstrated to have a positive impact on protein activity. Further, we identified the involved kinase, CBL-INTERACTING PROTEIN KINASE 11 (CIPK11), as an integrator of an iron deficiency-triggered calcium signature.

2. **Evidence for two-step regulation of FIT, using phospho-mutant activity screening**

   Regina Gratz, Tzvetina Brumbarova, Rumen Ivanov, Ksenia Trofimov, Rocio Ochoa-Fernandez, Tim Blomeier, Johannes Meiser, Matias Zurbriggen, Petra Bauer -***in preparation***

The second manuscript extends the knowledge of FIT protein regulation by the identification of potential, additional phosphorylation target sites. We suggest a dual regulation of the iron deficiency response through FIT phosphorylation. Possible serine phosphorylation might enhance FIT activity in contrast to potential tyrosine phosphorylation, which might abolish the functionality of the protein. This regulation might affect the fine-tuning of FIT protein activity.

In a final concluding remark paragraph, findings of both manuscripts are put into context.

2 Summary

An insufficient iron- (Fe) based nutrition accounts for severe health problems in humans. Likewise, plants may suffer from iron malnutrition. Plant Fe-deficiency can originate from inaccessible Fe pools, which are widely spread in agronomically used soils. This often leads to leaf chlorosis and poor growth, which can result in complete crop failure. Under certain conditions, however, plants tend to take up too much Fe, which then has detrimental effects on the plant's fitness. To ensure a balanced Fe uptake and tight regulation of its transport and storage, plants have developed complex Fe uptake and homeostasis strategies. *Arabidopsis thaliana*, a representative of non-graminaceous plants, follows a reduction-based Fe uptake strategy (Strategy I). First, the rhizosphere is acidified in order to solubilize ferric iron (Fe^{3+}). Subsequently, Fe^{3+} is chelated and reduced to ferrous iron (Fe^{2+}), before it is imported into root epidermal cells. The master regulator for this uptake mechanism is the bHLH transcription factor FER-LIKE IRON DEFICIENCY-INDUCED TRANSCRIPTION FACTOR (FIT). FIT itself is regulated on transcriptional and post-transcriptional levels and is divided into two pools of active and inactive FIT forms. It remained an open question, which molecular mark defines and controls the activity status of FIT.

This work has contributed to the elucidation of phosphorylation-mediated regulation of FIT activity. First, based on a protein interaction screen, CBL-INTERACTING PROTEIN KINASE 11 (CIPK11) was identified as a novel FIT interactor. Fe-deficiency generated a cytosolic Ca^{2+} signature, potentially perceived by the Ca^{2+} sensors CBL1/CBL9. We propose that CBL-mediated activation of CIPK11 serves to transduce the Fe-deficiency signal to downstream transcriptional processes. This is mediated via CIPK11-dependant FIT phosphorylation. We found that Ser272 phosphorylation is a prerequisite for FIT activation.

Further, we analyzed the activity of several FIT phospho-mimicking and non-phosphorylatable FIT mutants in different cellular assays. In this phospho-mutant activity screening, we identified several novel, possible phosphorylation target sites in FIT. We suggest a model, in which FIT activity might be differentially regulated upon phosphorylation. Possible serine phosphorylation might contribute to FIT activity, while tyrosine phosphorylation might have an inhibiting effect.

These novel findings contribute to the elucidation of FIT regulation and improved understanding of Fe stress signaling.

3 Zusammenfassung

Eine unzureichend eisenhaltige Ernährung kann zu schwerwiegenden gesundheitlichen Problemen bei Menschen führen. Gleichermaßen können Pflanzen unter Eisenmangelernährung leiden. Die Eisenunterversorgung bei Pflanzen kann von unzugänglichen Eisenvorkommen herrühren, die in landwirtschaftlich genutzten Böden weit verbreitet sind. Dies führt oft zu Blattchlorosen und schlechtem Wachstum, was zu Missernten führen kann. Unter bestimmten Bedingungen neigen Pflanzen dazu, zu viel Eisen aufzunehmen, was sich nachteilig auf deren Fitness auswirkt. Um eine ausgewogene Eisenaufnahme und eine strikte Regulation von Transport und Speicherung zu gewährleisten, haben Pflanzen komplexe Eisenaufnahme- und Eisenhomöostase-Strategien entwickelt. *Arabidopsis thaliana*, ein Vertreter der nicht-grasartigen Pflanzen, verfolgt eine reduktionsbasierte Eisenaufnahmestrategie (Strategie I). Zunächst wird die Rhizosphäre angesäuert, um dreiwertiges Eisen (Fe^{3+}) zu lösen. Anschließend wird Fe^{3+} komplexiert und zu zweiwertigem Eisen (Fe^{2+}) reduziert, bevor es in epidermale Wurzelzellen importiert wird. Der Hauptregulator für diesen Aufnahmemechanismus ist der bHLH-Transkriptionsfaktor FER-LIKE IRON DEFICIENCY-INDUCED TRANSCRIPTION FACTOR (FIT). FIT selbst ist auf transkriptionaler und post-transkriptionaler Ebene reguliert und liegt in zwei verschiedenen Formen vor, einer aktiven und einer inaktiven. Es war lange unbekannt, welches molekulare Signal den Aktivitätsstatus von FIT festlegt und kontrolliert.

Diese Arbeit hat zur Aufklärung der phosphorylierungsbasierten Regulation der FIT-Aktivität beigetragen. Zuerst wurde, basierend auf einer Protein-Interaktionsstudie, CBL-INTERACTING PROTEIN KINASE 11 (CIPK11) als neuer Interaktionspartner von FIT identifiziert. Eisenmangel erzeugte eine zytosolische Ca^{2+}-Signatur, die wahrscheinlich von den Ca^{2+}-Sensoren CBL1/CBL9 wahrgenommen wird. Wir vermuten, dass die CBL-basierte CIPK11-Aktivierung der Übermittlung des Eisenmangel-Signals auf nachfolgende Transkriptionsprozesse dient. Dies wird über eine CIPK11-abhängige FIT-Phosphorylierung vermittelt. Wir konnten zeigen, dass eine Phosphorylierung von Ser272 eine Voraussetzung für die Aktivierung von FIT ist.

Zudem haben wir in verschiedenen Untersuchungen die Aktivität von mehreren phosphorylierungsimitierenden und nicht phosphorylierbaren FIT-Mutanten analysiert. Innerhalb dieser Phospho-Mutanten-Aktivitätsuntersuchung konnten wir mehrere neue, potentielle Phosphorylierungsstellen von FIT identifizieren. Daher schlagen wir ein neues

Modell vor, in welchem die Aktivität von FIT durch potentielle Phosphorylierung differenziell reguliert ist. Die mögliche Phosphorylierung von Serinen könnte somit zur Aktivität von FIT beitragen, während die Phosphorylierung von Tyrosinen möglicherweise einen inhibierenden Effekt hat.

Diese neuen Ergebnisse tragen zur Aufklärung der FIT-Regulation und somit zur Verbesserung des Verständnisses der Eisenstress-Signalübermittlung bei.

4 Introduction

4.1 Iron Displays a Vital Nutrient for Humans and Plants

4.1.1 Iron Deficiency Anemia Affects Human Health

A recent study from the World Health Organization revealed that iron (Fe) deficiency anemia not only accounts for the most widespread nutrition disorder by influencing 2 billion people, but also for the only one significantly present in industrialized countries. Approximately every other pregnant woman as well as 40% of children under the age of six are affected when living in developing countries (www.who.int/nutrition/topics/ida/en). Often people that live in rural places have reduced access to a well-balanced diet, dietary supplements or fortified staple foods. Regions with prevailing malnutrition due to the lack of accessibility to high quality nutritious food show the highest numbers of affected people [1, 2].

In humans, approximately 70% of the Fe is needed for the production of hemoglobin and is therefore involved in erythrocyte-mediated oxygen transport in the blood. Whereas, roughly 4% is needed for the myoglobin-mediated transport within the muscle cells. The remaining Fe is utilized for energy production [3]. Hence, Fe-deficiency anemia can have a severe impact on the physical well-being and overall health. For instance, Fe-deficiency diminishes infection resistance by impairing the immune system, alters cognitive performance, impairs growth and physical performance [3].

One long-term and cost-efficient way to counteract this problem is to increase the amount of Fe in staple foods. This can be done by selective breeding or genetic modification of plants in order to enrich their edible parts with the needed Fe. This strategy, however, can only succeed if certain basic principles are preserved, such as the combination of nutrient enrichment with high yield (ensuring profitability), a decrease in Fe-deficiency anemia in humans (ensuring efficiency) as well as acceptance by farmers (ensuring applicability) [1, 4]. This biofortification approach has been applied, for example, in rice plants by overexpressing Fe storage, homeostasis, uptake, translocation or transportation genes [5]. Recently, a new variety of beans, which are rich in Fe, has been reported successfully to increase Fe levels in Rwandan women, highlighting the potential of biofortification [6].

For a successful application of this promising tool to enhance bio-available nutrients in staple foods, an understanding of the importance of nutrients for plants in general as well as an in-depth understanding of plant nutrient uptake and homeostasis systems are critical.

4.1.2 A Well-Balanced Fe Nutrition is Pivotal for Plants

As sessile organisms, plants are dependent on a balanced nutrient soil composition. This includes the presence of macronutrients, such as nitrogen, phosphorous, magnesium and potassium, as well as micronutrients, which are considerably less abundant. Most essential micronutrients are metal elements, such as Fe, manganese, nickel, copper, zinc and molybdenum. These metal ions are much needed cofactors for enzymes, which are crucial for enzyme activity. In addition, metal ions have the ability to change redox-states, which renders them indispensable for metabolic pathways. Fe, for instance, is involved in the mitochondrial electron transport chain. In chloroplasts, a major sink for Fe, it is involved in photosynthesis and present in all electron transfer complexes [7]. Fe limitation causes a re-organization of the photosynthetic pathway as well as interveinal leaf chlorosis, since chlorophyll production is dependent on an Fe-cofactor containing enzyme [8]. Fe as a co-factor is also present in DNA polymerases and helicases and is therefore involved in DNA replication and repair [9].

Two forms of Fe can be utilized by the plant, ferric iron (Fe^{3+}) and ferrous iron (Fe^{2+}). The concentration of both forms in the soil as well as soil composition, pH, and other factors affect the accessibility of Fe and thus plant nutrition. Although Fe at 4.32% abundance is the fourth most abundant element found in the continental crust [10], it is mostly present as Fe^{3+} oxides, such as ferric hydroxide $Fe(OH)_3$, which is a limiting factor for plants due to its low solubility. Neutral or alkaline soil pH, as is the case for one-third of the soils [11], as well as the presence of oxygen leads to an increased proportion of insoluble Fe forms [12]. Under such conditions, the plant's demand for approximately 10^{-9} to 10^{-4} M of Fe for optimal development is far from met. In addition to developing leaf chlorosis, this often accounts for reduced crop yield or complete crop failure [12, 13]. As a response to low amounts of Fe, plants employ different strategies to buffer and minimize these effects. The synthesis of Fe-containing proteins or metabolic pathways can be reduced in favor of Fe sparing and nutrient recycling. This is executed in a hierarchical manner, where the transcript abundance of individual genes is preferentially reduced over others or the degradation of certain Fe-containing proteins is favored upon Fe limitations [7, 14, 15]. In order to elevate Fe uptake capacity, the root architecture is altered, for example, by increasing the amount of root hairs, varying the length of the primary root as well as the lateral roots [16]. Ultimately, Fe-deficiency results in the expression of Fe uptake and homeostasis genes, which include respective transcription factors, Fe transporters as well as chelators [17, 18]. External foliage application of Fe or fertilization with chelates or bio-available Fe is possible but inefficient for agricultural application, partly due to its tremendous costs [11].

Fe overaccumulation frequently occurs in acidic soils or when plants are grown submerged in water. This can lead to severe problems because Fe is highly reactive when freely present in the cell. In aerobic conditions, Fe can participate in the Fenton reaction, which leads to the formation of highly reactive oxygen species and oxidative damage of cells [2, 19]. A first indication of Fe overload is the appearance of necrotic spots and bronzing of leaves, which can ultimately lead to yield loss [20]. Hence, plants quickly have to react to high amounts of Fe, especially if unbound, by applying different chelation, transportation and storage mechanisms. Given the crucial function of Fe in plastids and mitochondria, both organelles display major Fe sinks. There, Fe^{3+} is sequestered by the Fe storage protein ferritin [21, 22]. In both organelles, the synthesis of prosthetic groups, such as heme and Fe-S clusters, provides a second way of sequestering free Fe. Heme and Fe-S clusters are either directly involved in the respective metabolic pathways or used for the assembly of holoproteins [22]. Fraxatin displays another Fe storage protein, which is suggested to be involved in the assembly of Fe-S clusters in mitochondria [23, 24]. The vacuole is associated Fe storage, which is of special importance in seeds [25]. Besides, Fe can also be stored in the apoplast [26]. Long-distance transport is mediated through Fe^{2+}-NA chelates, which are transported via the phloem as well as Fe^{3+}-citrate complexes in the xylem [22, 27, 28]. This demonstrates that a well-balanced Fe uptake and homeostasis system is critical, serving the need for Fe in plant metabolism and to avoid excessive Fe accumulation, which in contrast exceeds the cell sequestering capacities.

It is of high importance to note that decreased nutrient availability in soils not only affects the well-being of plants and thus agricultural economy. Affected plants do not provide high quality nutrition, which consequently leads to a malnourished human population.

4.2 Plants Employ Different Fe Uptake Strategies

It is evident that nutrient uptake in plants needs to be fine-tuned to counteract nutrient deficiency but also overaccumulation and thus toxicity. To date, two Fe uptake strategies have been investigated concerning Fe uptake from the soil into epidermal cells. All plants, except the *Poaceae*, execute an Fe^{3+} reduction-based uptake strategy (Strategy I). *Poaceae*, however, excrete non-proteinogenic amino acids, phytosiderophores, to complex Fe^{3+} (Strategy II) [29, 30].

4.2.1 Reduction-based Fe Uptake (Strategy I)

The Fe uptake strategy employed by non-graminaceous plants consists of three steps that are executed by Fe-responsive, plasma-membrane-localized proteins located in epidermal root cells. *Arabidopsis thaliana* belongs to the non-graminaceous plants (Figure 1).

Soil acidification allows solubilizing Fe^{3+}, which is bound to negatively charged soil particles (Step 1) [29]. Several Arabidopsis ATPases were shown to be responsive to Fe limitations, but one promising candidate was Arabidopsis H(+)-ATPASE 2 (*AHA2)*. *aha2* knock-out mutants displayed a significant reduction in net proton flux compared to WT when grown under sufficient and deficient Fe conditions, confirming a major role of AHA2 in rhizosphere acidification [31].

Secretion of secondary metabolites can positively affect the Fe uptake response. As seen in red clover, secreted phenolic compounds enhance the utilization of apoplastic Fe^{3+} [32]. Similarly, the expression of the respective efflux transporter and the presence of phenolic compounds promote Fe uptake under limiting conditions in Arabidopsis. *FERULOYL-COA 6'-HYDROXYLASE 1* (F6'H1), a player in the phenylpropanoid biosynthesis pathway, as well as the phenolic transporter *PLEIOTROPIC DRUG RESISTANCE 9 (PDR9)* (also called *ABCG37*) are key players in Arabidopsis. Generally, the secretion of phenolic compounds and expression of *ABCG37* are upregulated under Fe-deficiency. Thus, it is believed that the secretion of different phenolic compounds, such as coumarins, increase Fe^{3+} assimilation and mobilization. The coumarin scopoletin in particular seems to play an important role in Arabidopsis [33-37].

Once Fe^{3+} is readily available, it is subsequently reduced to Fe^{2+} by FERRIC REDUCTASE-OXIDASE 2 (FRO2) [38]. FRO2 was identified based on its sequence similarity to yeast ferric-chelate reductases and the human phagocytic NADPH oxidase [38]. The respective loss-of-function mutant *frd1* shows decreased Fe chelate reductase activity [39]. When grown under Fe-deficient conditions, the *frd1* mutant phenotype, characterized by severe leaf chlorosis, could be complemented by *FRO2* expression. Overexpression of *FRO2* even enhanced tolerance to Fe-deficiency [38, 40] (Step 2).

In the last step, Fe^{2+} is transported across the membrane from the rhizosphere into epidermal cells. In a yeast -complementation assay, IRON REGULATED TRANSPORTER 1 (IRT1) was able to rescue the growth defect of the Fe uptake mutant strain *fet3/fet4* under limiting Fe supply [41]. *irt1-1* knock-out mutants display severe Fe-deficiency chlorosis, growth defects, disturbed photosynthetic capacity under Fe-deficient conditions as well as reduced leaf Fe content when grown in soil. Hence, IRT1 is responsible for Fe uptake in plants. Interestingly, IRT1 is not highly selective, since it also transports other divalent metals in the plant [42-44].

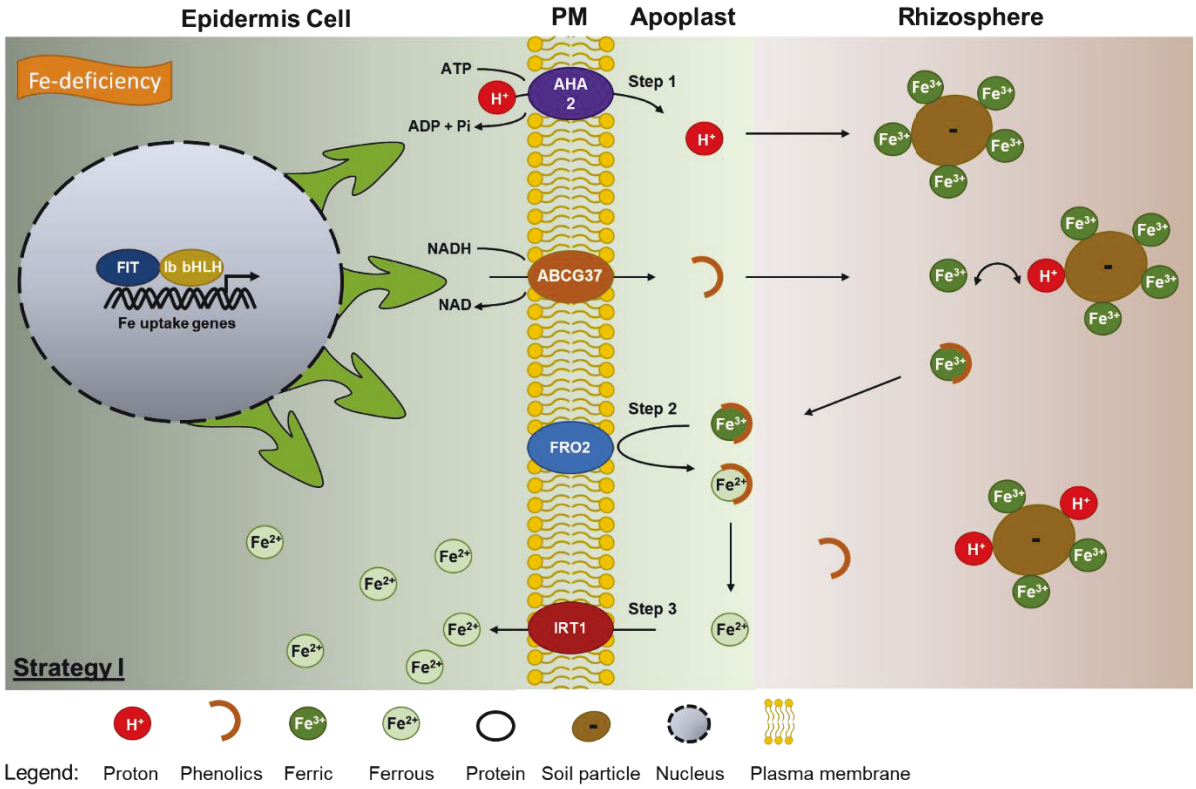

Figure 1: Fe-deficiency response of *Arabidopsis thaliana*. AHA2 mediates reduction of the soil pH. The competitive binding of protons (red) to negatively charged soil particles (brown) solubilizes Fe^{3+} ions (dark green), which are subsequently chelated by phenolic compounds (brown hook). Phenolics are secreted by ABCG37. Reduction of Fe^{3+} is conferred by FRO2 and Fe^{2+} uptake (light green) in epidermal cells is performed by IRT1. At the genetic level, involved proteins are controlled by the nuclear-localized hetero-dimer of FIT and members of the Ib bHLH subgroup (green arrows). The system is upregulated by Fe-deficiency.

The question remains: which upstream located regulator coordinates those processes and thus fine tunes the action of the respective proteins involved in Strategy I? The basic helix-loop-helix (bHLH) transcription factor FER-LIKE IRON DEFICIENCY-INDUCED TRANSCRIPTION FACTOR (FIT, bHLH029), belonging to subgroup IIIa within the *A. thaliana* bHLH family [45], was shown to execute this task. Upon dimerization with bHLH subgroup Ib proteins, bHLH038, bHLH039, bHLH100 and bHLH101, which are upregulated by Fe-deficiency independently of FIT, FIT induces the expression of *AHA2*, *FRO2* and *IRT1* upon Fe limitation [45-56].

4.2.2 Chelation-based Fe Uptake (Strategy II)

Graminaceous plants, however, do not rely on the uptake of reduced Fe. The plasma membrane-located TRANSPORTER OF MUGINEIC ACID 1 (TOM1) [57] releases phytosiderophores (PS) that efficiently chelate ferrous Fe over a wide pH range, from pH 4 to pH 9 under Fe-deficiency [29, 58, 59]. These non-proteinogenic amino acids, such as mugineic acid (MA) or

avenic acid (AA) are produced from the initial precursor methionine [29, 60]. In a first step, the enzyme S-ADENOSYLMETHIONINE (SAM) SYNTHETHASE uses methionine to catalyze the synthesis of SAM. Three SAM molecules are subsequently condensed by the enzyme NICOTIANAMINE SYNTHASE (NAS) to produce the PS precursor nicotianamine (NA). The metal chelator NA facilitates intracellular as well as short- and long-distance metal transport [61-63]. Secreted PS solubilize and form Fe^{3+} complexes in the rhizosphere, giving rise to a stable complex that is subsequently taken up into epidermis cells , for example, by the maize proton-coupled transporter YELLOW STRIPE 1 (ZmYS1) [29, 30, 64, 65]. For barley and rice, homologous transporters, YS-likes (YSL), were reported [66-68].

Several bHLH transcription factors were reported to be Fe regulated and involved in the Fe uptake control in graminaceous plants. In rice, OsIRO2 is a positive regulator of *e.g. OsNAS1*, *OsNAS2* or *YSL15* and exhibits a similar amino acid sequence as subgroup Ib bHLH transcription factors in Arabidopsis. OsIRO2 has homologues in other graminaceous plants, such as in barley and is not only involved in Fe uptake, but also in Fe transport and translocation [69-71]. OsIRO3, however, has a negative effect on Fe uptake and is suggested to be an orthologue of Arabidopsis POPEYE (PYE) [72]. No orthologue of AtFIT has yet been presented. Recent findings indicate that *Zea mays*, with *ZmIRT1* [73, 74]*, Oryza sativa,* with *OsIRT1* and *OsIRT2* [41, 75-77], and *Hordeum vulgare*, with *HvIRT1* [78], express functional homologues of genes employed by Strategy I plants. This raises the question, however, whether this strict separation into Strategy I and Strategy II can be applied.

4.3 Different Co-Expression Clusters Control Fe-Deficiency Responses

In *Arabidopsis thaliana*, genes associated with the Fe-deficiency response can be grouped into sub-clusters. Genes involved in Fe uptake and transport that are directly or indirectly dependent on the major regulator of Strategy I, FIT, are grouped into the so-called “FIT target network” and contains root-expressed genes like *IRT1* [46, 49, 54]. An additional cluster contains FIT-independent genes, such as *PYE* and its direct targets as well as *BHLH039* and *BHLH101*. As associated genes function mainly in Fe homeostasis, this sub-cluster can be referred to as the “Fe homeostasis network”, [49].

4.3.1 Regulation of Fe-Deficiency Response by the FIT Target Network

The Fe-regulated, root-specific bHLH transcription factor, FER, is responsible for the transcriptional regulation of Fe uptake genes and was first identified in *Solanum lycopersicum* [79, 80]. The *FIT* gene encodes the respective FER homolog in Arabidopsis [46, 48, 81, 82].

FIT promotor activity was detected in epidermal cells within the differentiation- and elongation zone of the main root, in lateral roots and in the central cylinder. *fit-3* loss-of-function causes lethality if not supplemented with Fe [82]. FIT robustly regulates the expression of 34 Fe-responsive genes in roots and seedlings. Regulated genes are involved in Fe uptake, *e.g.* *IRT1* or *ABCG37*, and Fe homeostasis, *e.g.*, *ZRT/IRT-LIKE PROTEIN 8* (*ZIP8*) [54].
This highlights that FIT holds a central role in the Fe-Deficiency response. Hence, it is of vital importance to analyze the molecular regulation of FIT as central regulator of the Fe uptake pathway.

4.3.1.1 Transcriptional and Post-Transcriptional Modifications of FIT Ensure Fine-Tuning of the Plants' Fe Uptake Capacity

FIT gene expression is 2-4-fold upregulated during Fe limiting conditions [46, 47]. When Fe is present, however, *FIT* is only transcriptionally induced upon the application of cycloheximide (CHX), an inhibitor of protein biosynthesis. As speculated by Meiser et al., 2011, a repressor might inhibit *FIT* expression, which responds to the Fe status and also underlies a turnover control mechanism. With application of CHX, this repressor is absent. Therefore, the repression of *FIT* does not take place. This raises the question: which positive regulator accounts for the removal of the repressor to initiate gene transcription under Fe-deprived conditions [83, 84]? Interestingly, *FIT* gene expression is reduced in the EMS mutant *fru-C497T*, which contains a premature stop codon, thus impeding correct protein translation of FIT [82]. Together with the finding of decreased promotor activity under Fe-limited conditions in the *fit-3* mutant expressing a promoter *pFIT-GUS* construct, it becomes obvious that the FIT protein has a positive influence on its own promoter activity [50]. Recently, it was shown that the Fe-deficiency-responsive bHLH039 also promotes *FIT* expression [56]. Hence, both bHLH proteins could account for the unknown regulator.
More factors are known to enhance *FIT* expression, such as nitric oxide (NO), which accumulates in response to Fe-deficiency [83, 85-87]. NO facilitates the expression of the 14-3-3 protein GENERAL REGULATORY FACTOR 11 (GRF11), which in turn promotes *FIT* expression [88]. Hormones can also directly or indirectly influence the post-transcriptional regulation of *FIT*. This control mechanism is very complex due to the fact that different hormones share signaling pathways that engage with each other, leading to hormonal crosstalk [89]. Also, hormones as well as small molecules can influence their synthesis in a reciprocal way, thereby controlling their mutual accumulation, such as NO, ethylene and auxin [90]. Fe limitation promotes gene expression of several enzymes needed for ethylene synthesis and thus

leads to an accumulation of the hormone [91-93]. Ethylene promotes *FIT* gene expression, most likely through the feed-forward cycle of the FIT protein on its promoter activity [82, 91, 94-96]. Accumulated auxin in roots in response to Fe-deficiency acts upstream of NO, which became evident after analyzing a large set of respective auxin and NO mutants. Presumably, an Fe-deficiency-induced increase in root sucrose level mediates auxin-signaling, which causes the regulation of Fe uptake via NO [83, 87, 97]. Repression of *FIT* translational activity by the application of jasmonate and cytokinins was demonstrated. However, it does not account for the repression of FIT target gene expression [98, 99].
RNA polymerase II (RNA POL II) CARBOXYL-TERMINAL DOMAIN PHOSPHATASE-LIKE 1 (CPL1) is inhibiting *FIT* and subgroup Ib *BHLH* gene expression (Aksoy 2013). CPL1 interacts with REGULATOR OF CBF GENE EXPRESSION 3 (RCF3), which also affects the transcript abundance of *FIT* and additional Fe homeostasis genes [100].

FIT protein accumulates under the presence and absence of Fe, when being overexpressed. However, transcriptional regulation of downstream target genes is only mediated by a lack of Fe. This leads to the conclusion that the accumulated FIT under sufficient Fe conditions is inactive until an unknown but Fe-dependent signal renders it active. This suggests post-transcriptional regulation of FIT [46, 82, 83]. Several authors have speculated that FIT is present in active and inactive forms. However, the question arouse: what the molecular difference is, that divides active and inactive forms of FIT [83, 94, 101]. Hence, FIT protein-protein interactions were investigated (Figure 2). Mediator subunit 16 (MED16, also called SFR6), part of the multi-subunit Mediator complex, facilitates the interconnection of RNA POLYMERASE II (RNA Pol II) and respective transcription factors in eukaryotes. The knock-down insertion-mutant *yellow and sensitive to iron-deficiency 1* (*yid1*), encoding MED16, accumulated reduced amounts of *FIT*, *IRT1* and *FRO2* transcripts and displayed increased sensitivity in response to low Fe. Protein-protein interaction studies revealed that MED16 dimerizes with MED25, which in turn interacts with EIN3/EIL1. The authors concluded that MED16 and MED25 are needed to activate the Fe-deficiency-response by stabilizing FIT through the action of EIN3/EIL1 [94, 102]. Interestingly, ethylene-dependent EIN3/EIL1 interacts with the FIT protein, which in turn prevents its degradation. This contributes to the positive feedback regulation of FIT on its own promoter [47, 50, 94]. Additional research revealed the direct interaction between MED16 and FIT. Chromatin immunoprecipitation (ChIP) confirmed that MED16 promotes the binding of the FIT-bHLH038/039/100/101-complex to downstream *FRO2* and *IRT1* promoters under Fe limiting conditions [103].

This detailed control of FIT enables a precise and quick regulation of the Fe uptake machinery. In addition to the transcriptional control of *FIT* by NO, it also contributes to FIT protein stabilization, similar to ethylene. With application of NO scavengers, an enhanced proteasomal FIT degradation was previously demonstrated [83].

In addition to protein stabilization conferred by either different interaction partners or external stimuli, two interactors have been identified to repress FIT activity. FIT is negatively regulated by the DELLA proteins. Interaction of DELLA proteins with FIT, bHLH038 and bHLH039 inhibit the binding of the transcription factors to downstream promoters and thus prevent transcription. To overcome this inhibiting effect, Fe-deficiency causes a GA-mediated de-stabilization of DELLA proteins in epidermal cells of the root differentiation zone. This shows that special distribution of regulators enlarge the complexity of the Fe uptake network [104].

Upon prolonged Fe-deficiency, hydrogen peroxide (H_2O_2) levels increase in a FIT-dependent manner. Subsequently, *FIT* expression is repressed and the transcription of *ZINC FINGER OF ARABIDOPSIS THALIANA 12* (*ZAT12*) is enhanced. ZAT12 dimerizes with FIT, thus withdrawing FIT from other possible protein-protein interactions that might activate FIT. Hence, the subsequent downregulation of *FIT* expression might be caused by accumulation of inactive FIT which is not capable of enhancing its own transcription [47, 50, 105].

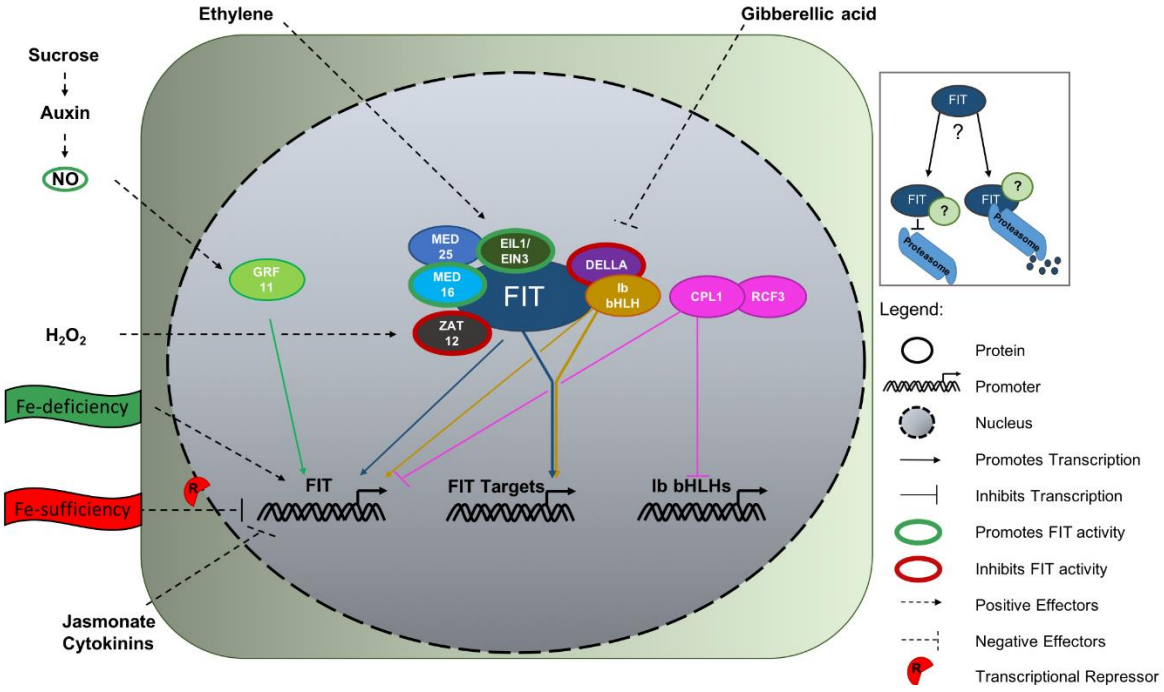

Figure 2: Transcriptional- and post-transcriptional regulation of the Fe uptake machinery. Different external stimuli, such as the presence of Fe or hormones, display either positive or negative effectors on gene expression or protein activity (dashed lines). The presence of individual proteins regulate transcription of downstream genes (solid lines). FIT protein-protein interactions affect FIT stability or activity. A positive regulator is indicated by a green frame. A negative effect conferred by the respective interaction partner is shown by a red frame. The box highlights that FIT undergoes proteasomal degradation. However it is not yet known, which signal determines the fate of FIT stability.

To date, several authors reported the proteasomal degradation of FIT. A combination of CHX and MG132 treatment initially demonstrated that FIT is degraded, which is pronounced under Fe-deficiency [83, 101]. It is controversially discussed why this turn-over control is needed and how this is regulated. It cannot be ruled out that the proteasome targets FIT independently of its activity status. Besides, a large pool of inactive FIT could exist, from which FIT is recruited and subsequently activated by a yet unknown mechanism [94]. This study was supported by the finding that smallest traces of active FIT are sufficient for downstream transcriptional control [83]. Another hypothesis suggests that the degradation of active, but "exhausted" FIT forms increases the need for constant re-synthesis, which ensures accumulation of "fresh" forms that mediate downstream gene expression [101]. Therefore, it might be that the Fe uptake response is regulated by the stability of FIT protein, since the protein can affect its own gene transcription [82, 95].

In addition to that, differential protein-protein interactions that might contribute to a selection between different activity levels of FIT, post-translational modifications (PTMs) might also be involved. This might be needed in order to mediate the hetero-dimerization with other proteins, such as subgroup Ib bHLH transcription factors, which are exclusively up-regulated under Fe limiting conditions and are needed for FIT target gene expression [50, 51, 54-56]. In agreement with this hypothesis, the observed molecular weight of FIT is higher as previously predicted [101]. This points to the possibility that FIT undergoes additional, yet undetected PTMs, which might have a regulatory impact on its activity.

4.3.2 Regulation of Fe-Deficiency Responses by the Fe Homeostasis Network

A second, FIT-independent gene network (Figure 3) controls various aspects within the Fe-deficiency response, putting a focus on the subgroup IVb bHLH protein PYE and its homologs [45]. PYE was found in a T-DNA screen for transcription factors, showing impaired Fe stress tolerance. *PYE* is mainly upregulated in the pericycle upon Fe-deficiency, but PYE protein accumulates in all root cell types. *pye-1* knock-out mutants display altered formation of root hairs, deformation of lateral roots cells, severe leaf chlorosis and reduced root growth, chlorophyll- and Fe content under Fe limiting conditions. Hence, PYE is suggested to positively regulate Fe-deficiency responses in plants [106]. However, it negatively regulates transcription of Fe homeostasis genes, such as *FERRIC REDUCTASE OXIDASE 3* (*FRO3*), *NAS4* and *ZINC-INDUCED FACILITATOR 1* (*ZIF1*), by binding to their promotors under Fe-deficiency [106]. The protein interacts with all four homologues from subgroup IVc bHLH034, bHLH104,

bHLH105 (ILR3) and bHLH115, collective called PYE-likes (PYELs) [45, 106-108]. All PYELs can form homo- and hetero-dimers [45, 107-110]. Overexpression of *BHLH101* partially rescues the *bhlh034 bhlh104* double mutant phenotype, suggesting that PYELs are upstream regulators of subgroup Ib *BHLH*s [109]. Indeed, they bind to the promoters of *PYE* and *BHLH038/039/100/101*. However, the binding of bHLH034 to PYE_{pro} is only anticipated [108-110]. The generation of PYELs knock-out mutants demonstrate reduced tolerance to Fe-deficiency, whereas PYELs overexpression lines show increased accumulation of Fe and improved fitness. Hence, PYELs positively mediate Fe-deficiency responses [108-110]. The decreased Fe stress tolerance phenotype of *bhlh115-1* knock-out mutant could be rescued by the overexpression of any PYEL, suggesting functional redundancy. Although, it cannot be ruled out that PYELs might have additive, tissue specific functions, since they only in part display the same expression pattern [110].

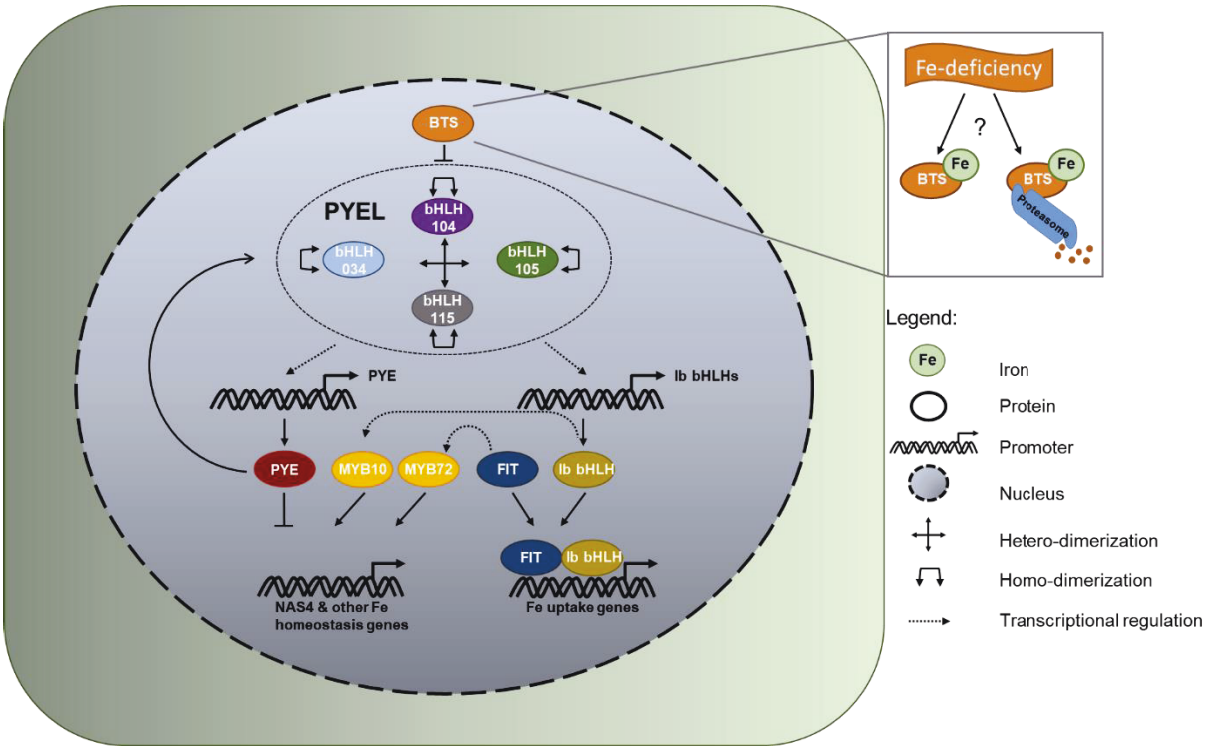

Figure 3: Regulatory network of the Fe homeostasis sub-cluster during Fe-deficiency. BTS negatively affects the four PYEL proteins bHLH034, bHLH104, bHLH105 and bHLH115 (grouped within the dotted circle), upon direct interaction. It is not yet known whether an Fe signal stabilizes BTS protein or displays a turn-over control (box). PYEL actively controls transcription of PYE and Ib bHLHs. PYE negatively affects *e.g.*, NAS4 transcription. In contrast, MYB10 and MYB72 positively regulate NAS4. Ib bHLH transcription factors interact with FIT to initiate Fe uptake. Ib bHLHs, FIT and both MYB proteins act as a link between Fe uptake and Fe homeostasis.

Under Fe deprivation, PYE is co-expressed with BRUTUS (BTS), a protein with a RING E3 ligase function that contains a haemerythrin / HHE cation-binding motif for metal binding such as Fe and Zn [106, 107, 111]. *bts-1* knock-down mutants have longer roots, increased acidification capacity and contain more Fe. Hence, they are more robust to Fe-deficiency, which suggests an opposite function of BTS compared to the positive regulator PYE [106, 108].

Likewise, the two redundant Arabidopsis BTS paralogs, BTS LIKE 1 (BTSL1) and BTS LIKE 2 (BTSL2), as well as the rice homologs, OzHRZ1 and OzHRZ2, negatively affect the Fe-deficiency response [111, 112]. Besides its expression in the vasculature, BTS is broadly expressed in other tissues, which matches its additional function in developing processes [107]. Interestingly, PYELs, but not PYE, interact with BTS [106, 107, 110]. The interaction inhibits the activity of PYELs and it is suggested that this is conferred by their ubiquitination and subsequent degradation [107]. The interaction and degradation is likely mediated via the BTS RING E3 domain, since $BTS_{\Delta E3}$ deletion mutants cannot form heterodimers [107]. The RING E3 domain is additionally important for BTS activity [113]. The HHE domain renders BTS less stable, as seen by the accumulation of BTS-GFP in $BTS_{\Delta HHE}$ mutants [107, 113]. *In vitro* expressed BTS was shown to be degraded in a dose-dependent manner following an increasing concentration of Fe. Similar results were obtained upon transient expression of BTS-EGFP in tobacco leaves, in which excess Fe promoted the degradation of the fusion protein. Chelation of Fe^{3+}, arrested the degradation [107]. This suggests that BTS is less stable upon Fe binding, which is controversially discussed in the literature [107, 112]. It is not very beneficial for the plant to degrade a negative regulator of Fe-deficiency responses in the presence of Fe, leading to enhanced expression of subgroup Ib transcription factors and thus further Fe accumulation. The degradation of BTS was, however, solely shown in an *in vitro* situation, where problems during wheat germ-based protein translation cannot be ruled out, particularly since MG132 treatment could not prevent BTS degradation. In contrast, BTS might display a modulator to prevent Fe over-accumulation in a nutrient-deprived situation. This could be conferred by constantly degrading PYELs in order to finely adjust initiation of subgroup Ib bHLH translation. This in turn also depicts an effective mechanism to quickly respond to changing Fe conditions [107, 112]. A similar model was suggested for FIT regulation [83, 94, 101]. Hence, Hindt and colleagues suggested a model, where BTS is stabilized upon metal binding, as seen for the human Fe sensor, FBXL5 [114], and rice, OsHRZ [111], and therefore blocking subgroup Ib-mediated upregulation of Fe-deficiency genes [112].

In addition, two Fe-regulated transcription factors are associated with the PYE regulation network, which are the functionally redundant MYELOBLASTOSIS 10 (MYB10) and MYB72 [115]. Both proteins are positive regulators of *NAS2* and *NAS4* and therefore connected to Fe homeostasis regulation. MYB72 positively mediates the transcription of the ß-glucosidase *BGLU42* and thus promotes the deglycosylation of coumarinyl glycosides, which contribute to induced systemic resistance against pathogens in Arabidopsis [116-118]. Interestingly, *MYB10*

is regulated by bHLH039 [56] and *MYB72* by FIT [46, 119]. Hence, MYB10 and MYB72 seem to represent not only a link interconnecting the Fe uptake FIT network and the Fe homeostasis PYE network, but also connecting Fe regulation in general with pathogen defense.

4.4 bHLH Transcription Factors are Involved in Numerous Signaling Pathways

Transcription factors are proteins that regulate the transcription of genes by binding to *cis* regulatory DNA sequences at the respective promoter region. This mechanism is conserved in all forms of life and enables the organism to quickly adapt to changing conditions. Hence, transcription factors are vital components in all life-sustaining processes. About 6% of all Arabidopsis proteins are transcription factors [120], which can be classified in different families. The fact that central regulators in both co-expression clusters of genes regulating Fe uptake are bHLH proteins makes this family very interesting. First discovered in animals [121], the second largest family in Arabidopsis is the group of bHLH proteins with 162 members [45, 122-124]. bHLHs possess a characteristic stretch of 60 amino acids, comprising a N-terminal region with 13-17 mostly basic residues (basic region) and a helix-loop-helix (HLH) region. Specific DNA binding to a 5' CANNTG 3' E-box motif, such as the G-box motif 5'CACGTG 3', is conferred by the basic region. The HLH region contains two amphipatic α-helices that are connected with a loop and mostly possess hydrophobic amino acids [121, 123, 125]. It is suggested that bHLH proteins mostly form homo- or heterodimers with other bHLHs, since dimers are needed to bind to the DNA [125-127]. A bimolecular fluorescence complementation (BiFC) assay showed that FIT interacts with itself as well as bHLH038/039/100/101 in protoplasts [51, 52].

4.4.1 Regulation of bHLH Transcription Factors in Plants

PTMs enable an increase in proteomic complexity and facilitate a quick response to various internal and external stimuli, for example, by a covalent addition of a functional group to the target protein. bHLH proteins can be modified by the addition of various functional groups, such as N-glycosylation, phosphorylation and N-myristoylation events (as suggested for mulberry MabHLH144-like [128] or acetylation (as suggested for OsbHLH089 [129], to name a few. This suggests a complex protein regulation, allowing the integration of different signaling pathways.

A well-studied example for the transduction of different stimuli via diverse PTMs is the bHLH protein INDUCER OF CBF EXPRESSION 1 (ICE1), which regulates the transcription of C-REPEAT/DRE BINDING FACTORS (CBFs). CBFs in turn activate cold-regulated genes

(CORs), providing freezing tolerance [130-132]. ICE1 belongs to bHLH subgroup IIIb within the *A. thaliana* bHLH family and is therefore closely related to FIT (subgroup IIIa) [45]. Interestingly, the ICE1-CBF-COR cascade presents a central integration platform for many signaling pathways that are also associated with the Fe-deficiency response [17, 105, 133, 134], such as ABA, RO-, ethylene or SA signaling [130, 135-141].

PTMs of ICE1 were shown to have different effects on protein stability and activity (Figure 4). Upon perceiving a cold signal, ICE1 is antagonistically regulated by a series of phosphorylation events [142-144]. Phosphorylation of ICE1 at position Ser278 is mediated by cold-activated Ser/Thr protein kinase SnRK2.6 / OPEN STOMATA 1 (OST1), increases its stability and thus promotes downstream gene expression of cold-tolerance genes [142]. This increase in stability results from a competitive binding between OST1 and RING-type E3 ligase HIGH EXPRESSION OF OSMOTICALLY RESPONSIVE GENE 1 (HOS1) to ICE1 and a disabled interaction between phosphorylated ICE1 and HOS1, which, upon interaction with ICE1, facilitates proteasomal degradation of the protein [142, 145, 146]. Small ubiquitin-like modifier E3-ligase SIZ1-mediated SUMOylation of ICE1 also interferes with ICE1 degradation and stabilizes the protein [147-149].

It was further shown that an alanine substitution of Ser403 leads to enhanced protein activity, decreased ubiquitination and degradation of ICE1, suggesting additional, negatively acting PTMs [150]. Indeed, phosphorylation of Ser94, Ser403 and Thr366 by the cold-activated MITOGEN-ACTIVATED PROTEIN KINASES (MPKs) MPK3/MPK6 cascade was shown to decrease ICE1 stability and therefore to negatively influence freezing tolerance [143]. These findings were confirmed and extended by showing an enhanced transcriptional activity in a transient transactivation assay and reduced proteasomal degradation in a 6x alanine mutant ($ICE1^{6A}$), highlighting the importance of Ser94, Ser203, Ser403, Thr366, Thr382 and Thr384. This suggests a negative effect of MPK3/MPK6-mediated phosphorylation on ICE1 activity and stability [144]. This inhibition of a positive regulator in freezing tolerance is proposed to occur under prolonged cold-stress [142, 145].

It is of interest to understand how the cold signal is perceived by the cell. Low temperatures affect plasma membrane fluidity, which leads to the activation of calcium (Ca^{2+}) channels and therefore Ca^{2+} influx into the cell. The Ca^{2+}-mediated signal transduction cascade involves several calcium-responsive kinases, affecting downstream located expression of cold-responsive genes [151].

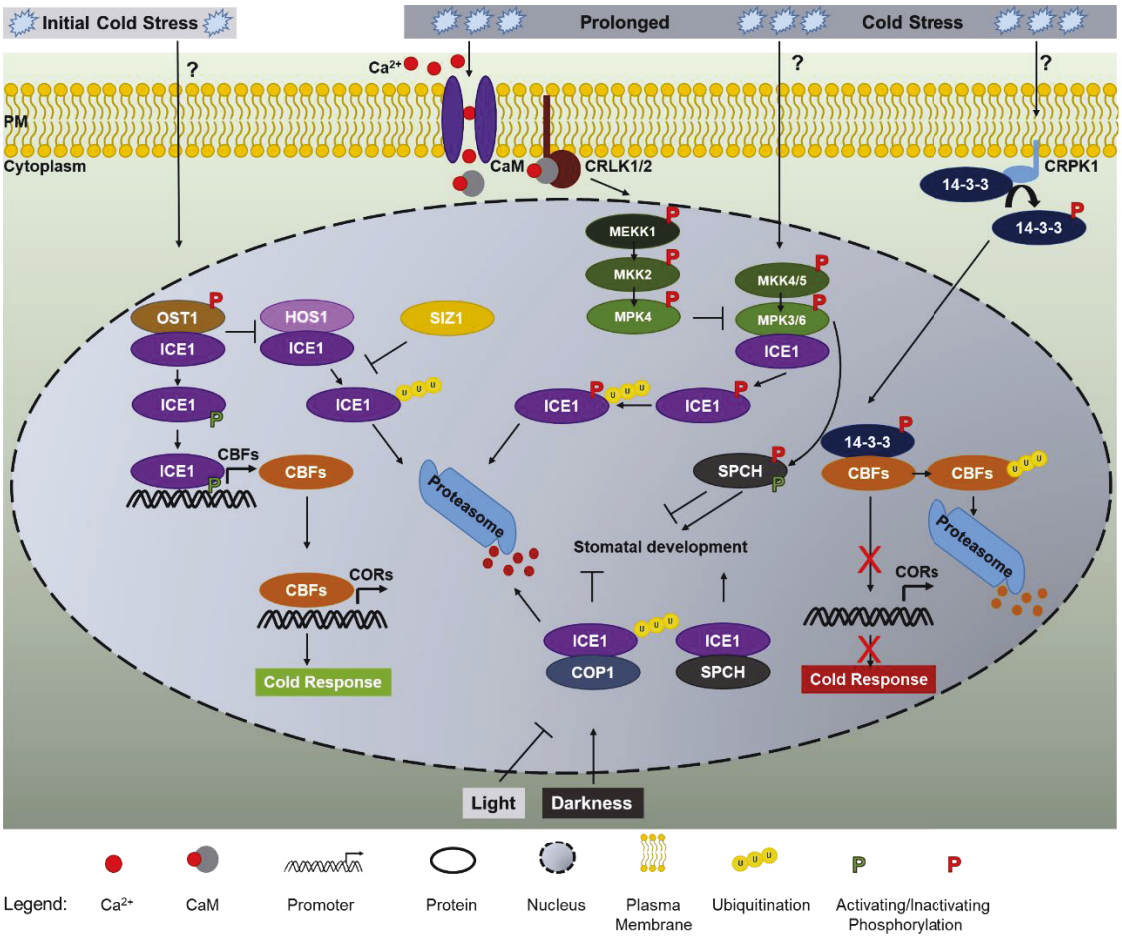

Figure 4: Post-translational regulation of bHLH transcription factor ICE1 as an example for multi-site protein phosphorylation. Upon initial / prolonged cold stress, different signaling cascades are active that involve protein phosphorylation events. Different kinases, such as OST1, MPKs, CRLKs and CRPKs, are involved. Phosphorylation can lead to stabilization or destabilization of the target protein and thus affect their activity. In addition, the crosstalk between signaling pathways is displayed by linking cold responses to stomatal development, mediated by the bHLH protein SPCH.

In order to quickly respond to changing environmental stimuli and counteract the negative regulation via MPK3/6, the CALCIUM/CALMODULIN-REGULATED RECEPTOR-LIKE KINASE 1 (CRLK1) and CRLK2 are activated, promoting freezing tolerance in plants [143, 152]. CRLKs interact with MITOGEN-ACTIVATED PROTEIN KINASE KINASE KINASE1 (MEKK1), which activates the MITOGEN-ACTIVATED PROTEIN KINASE KINASE2 (MKK2) - MPK4 cascade [143, 153, 154]. Cold-responsive MKK2 was already described as a positive regulator of cold responses [155]. The subsequent phosphorylation and activation of MPK4 inhibits the MPK3/6-mediated phosphorylation and degradation of ICE1 [143]. Ca^{2+}-signals are also perceived via other transduction mechanisms, such as a CALCINEURIN B-LIKE PROTEIN (CBL) / CBL-INTERACTING PROTEIN KINASE (CIPK) module. In the context of freezing tolerance, Ca^{2+} is sensed by CBL1, which was described to have a negative effect on freezing tolerance [156]. It was further speculated that CBL1 affects CBF gene expression in a dose-responsive manner [157]. Recently, Huang et al., 2011 identified the respective CBL1 interaction partner, CIPK7, both of which are induced by

cold and affect cold responses [158]. CBL1 potentially interferes with another CBL/CIPK module, comprising of CBL9 and CIPK3, involved in cold signaling as a response to ABA - signaling [156, 159, 160]. Further CALCIUM-DEPENDENT PROTEIN KINASES (CDPK) were shown to be involved [161, 162].

ICE1 stability is additionally regulated in a light-dependent manner. Darkness facilitates CONSTITUTIVELY PHOTOMORPHOGENIC 1 (COP1)-mediated ubiquitination and proteasomal degradation of ICE1, which also leads to reduced production of stomata [163, 164]. Light-signaling and COP1-involvement indicates that the freezing tolerance module is an integration point for different environmental stimuli, linking adaptation to abiotic stresses and stomatal development.

This further becomes evident by the interaction between ICE1 and SPEECHLESS (SPCH) [165], a group Ia bHLH transcription factor responsible for the asymmetric cell divisions and production of paired guard cells in Arabidopsis [45, 166]. SPCH itself undergoes MPK3/MPK6-mediated phosphorylation, which mostly has a repressive effect on SPCH activity. The failure of the non-phosphorylatable mutant S193A to rescue *spch-3* knock-out phenotype demonstrated that phosphorylation of one Ser193, however, is required for full activity [167]. MPK-regulated phosphorylation of SPCH is controlled by different stimuli, such as brassinosteroids (BRs). The presence of BR lead to degradation of the BRASSINOSTEROID-INSENSITIVE 2 (BIN2) [168-170], which can no longer phosphorylate and therefore inactivate MAPKKK YODA (YDA) [171-173]. YDA is upstream of MKK4/MKK5 - MPK3/MPK6 [174], initiating MPK signaling and thus inhibiting SPCH activation by phosphorylation [167]. The degradation of BIN2 also interferes with the BIN2-mediated phosphorylation, and therefore inactivation, of MKK4 and MKK5, consequently leading to reduced stomatal development [175]. Therefore, BR impede stomatal development.

An opposing effect mediated by the same stimuli can be demonstrated by the finding that BIN2 phosphorylates SPCH directly [176]. BR-mediated degradation of BIN2 therefore leads to impaired phosphorylation of SPCH and stomatal development can be initiated [176]. Besides the mostly negative regulation of SPCH activity by the BR- or MPK signaling pathways, it was recently shown that CYCLIN-DEPENDENT KINASE A;1 (CDKA;1) phosphorylation of SPCH Ser186 is needed for mutant complementation [177]. This ambivalent regulation of SPCH is a well-studied example of how complex the activity of a bHLH transcription factor can be regulated and fine-tuned.

Hence, similar to the effects of different stimuli, such as hormones, protein phosphorylation by one kinase at different residues can have opposing effects on the activity. It can become more

complex by the integration of different kinases, simultaneously modifying the same protein. Subsequently, the need arises to understand the molecular mechanism that alters protein activity in response to a phosphorylation event.

The activity of bHLH transcription factor ABA-RESPONSIVE KINASE SUBSTRATE 1 (AKS1), connected to guard cell regulation under drought stress, was shown to be diminished upon ABA-mediated phosphorylation, leading to an interrupted binding to the promoter of the target gene, *POTASSIUM CHANNEL IN ARABIDOPSIS THALIANA 1* (*KAT1*) and decreased stomatal opening [178, 179]. *KAT1* promoter binding is only possible when AKS1 forms homo-multimers. Hence, phosphorylation of AKS1 interrupts the multi-merization and renders the monomer inactive [180].

In addition to an interrupted DNA binding capacity, phosphorylation can also lead to the degradation or stabilization of a protein, which is another well-studied mechanism to fine-tuned protein activity. The light-inducible, atypical bHLH protein, LONG HYPOCOTYL IN FAR-RED 1 (HFR1), is involved in photomorphogenesis, combining phytochrome A (phyA)-mediated far-red light- and CRYPTOCHROME1 (cry-1) mediated blue light signaling [181-184]. HFR1 interacts with COP1 during darkness, which leads to its proteasomal degradation [185-187]. Reciprocal results propose that phosphorylation of HFR1 promotes its degradation in a COP1 dependent manner [185]. In contrast, light-dependent phosphorylation of preferentially Ser122 by CASEIN KINASE II (CKII) renders the protein more stable [188].
HFR1 also interacts with the negative regulator of light signaling PHYTOCHROME-INTERACTING FACTOR 3 (PIF3), whose protein stability is also regulated via proteasomal degradation, similar to other PIF proteins [182, 189-195]. Active forms of phytochromes (Pfr), which are localized in the nucleus after light-induced translocation from the cytosol, interact with PIFs. Pfr-mediated PIF phosphorylation leads to subsequent proteasomal degradation and initiation of photomorphogenesis [196]. It was reported that BR have an impact on the PIF regulation by BIN2-mediated phosphorylation of PIF4 [197]. In addition to CK2 modifying PIF1 [198], PHOTOREGULATORY PROTEIN KINASE 1 (PPK1) was also shown to phosphorylate PIF3 [199]. Interestingly, phytochromes can also act as kinases, as shown for *Avena sativa* phyA, phosphorylating PIF3 [200].

Protein phosphorylation alone might not always be sufficient to directly alter downstream actions, which is why dimerization in response to a post-translational modification depicts

another molecular mechanism for protein regulation. Phospho-peptide binding proteins, such as phospho-serine / -threonine binding 14-3-3 proteins, are well characterized [201-203]. This interaction can retain target proteins in a specific subcellular compartment to either prevent or facilitate their action, as shown for the transcription factor BRASSINAZOLE-RESISTANT 1 (BZR1). Stabilization of BIN2 under exhausted BR availability leads to the phosphorylation of BZR1, which in turn is bound by 14-3-3 protein. This leads to a maintained cytosolic localization. Hence, BZR1 cannot be imported into the nucleus and initiate gene expression [204].

The direct phosphorylation of 14-3-3 proteins, however, is another means of phosphorylation-based signal transduction, as seen for COLD-RESPONSIVE PROTEIN KINASE 1 (CRPK1)-mediated phosphorylation of 14-3-3 proteins during cold stress (Figure 4*Figure 4)*. In this scenario, the modified 14-3-3 protein subsequently translocates to the nucleus, interacts with CBFs and thus promotes their degradation, which causes negative regulation of freezing tolerance [205, 206]. Oppositely, hetero-dimerization with 14-3-3 proteins can also prevent degradation of the target protein [207]. This highlights that the dimerization with this class of proteins can mediate protein regulation in response to phosphorylation. The regulation mechanism, however, can be expanded to homo-/ or hetero-dimerization processes in general, since protein phosphorylation can confer changed binding preferences [208].

The involvement of different bHLH transcription factors in multiple signaling pathways was shown to be regulated by post-translational modifications, notably by protein phosphorylation. Hence, protein functionality was affected by either activating or inactivating the protein in part by its stabilization or destabilization, or by affecting the dimerization capacity of the protein. Also in the context of Fe deprivation, protein regulation via phosphorylation plays a vital role.

4.5 Post-translational Modifications are Involved in Fe-Deficiency Signaling

As sessile organisms, it is of importance for plants to sense nutrient availability in the soil. PTMs enable a quick response to changing nutrient occurrences, such as Fe-deficiency, and allow a fine-tuned signal transduction to adjust respective gene expression accordingly. Exemplary, histone PTMs are described to be involved in Fe homeostasis. Under sufficient Fe conditions, the gene expression of BHLH038/039/100/101 is reduced due to SHK1-BINDING PROTEIN 1 (SKB1)-mediated dimethylation of histone 4 arginine 3 (H4R3), suggesting a negative effect on Fe uptake [209]. Further, it was reported, that GENERAL CONTROL NONREPRESSED PROTEIN 5 (GCN5)-mediated acetylation and HISTONE

DEACETYLASE 7 (HDA7)-mediated deacetylation of *FRD3* has a direct impact on Fe root-to-shoot transportation [210].

It was also shown that ubiquitination-dependent regulation of several proteins are involved in Fe-uptake or homeostasis. As described previously, PYELs are targeted for ubiquitination and subsequent proteasomal degradation by BTS [107]. Also, one PYEL homologue in *Malus domestica*, MdbHLH104, was shown to be ubiquitinated and subsequently degraded via the proteasome to avoid Fe over-accumulation under Fe sufficient conditions [211].

A constant ubiquitin-mediated turnover was also reported for FIT, securing the accessibility of a pool of active FIT within the cell. Hence, the cell can remain responsive to incoming signals [83, 94, 101]. Ubiquitination also affects protein localization and stability of IRON REGULATED TRANSPORTER 1 (IRT1). IRT1 DEGRADATION FACTOR 1 (IDF1)-facilitated mono-ubiquitination of lysines K154 and K179 is needed for clathrin-mediated endocytosis of IRT1 from the plasma membrane to the *trans*-Golgi network. There, IRT1 undergoes both exocytosis and is either re-located to the PM or is marked for vacuolar degradation [200, 212, 213]. However, it is speculated that two more lysine residues are targets for ubiquitination [214] which might depend on prior phosphorylation events [215].

The MAP kinase cascade is involved in the regulation of the Fe-deficiency response via ethylene signaling. Under Fe limiting conditions, *MPK3* and *MPK6* gene expression and their corresponding enzymatic activity was increased. *mpk3* and *mpk6* knock-out mutant plants were chlorotic and displayed reduced Fe content. Molecular analysis highlighted a diminished expression of ACC SYNTHASE (ACS) genes, *ACS2* and *ACS6*, responsible for the production of the ethylene precursor ACC, and reduced Fe-deficiency responses [216]. Further, it was shown that MPK3 and MPK6-mediated phosphorylation of ACS2 and ACS6 prevents their proteasomal degradation [217-219]. Another MPK3 and MPK6 substrate is the transcription factor WRKY33 [220]. Upon phosphorylation, WRKY33 can bind to *ACS2* and *ACS6* promotors and induce gene expression [221]. Additionally, other kinases promote *ACS2* and *ACS6* gene expression such as CALCIUM-DEPENDENT PROTEIN KINASE (CPK) CPK5 and CPK6 [222]. Transcription of *ACS* genes were shown to be upregulated under Fe-limited conditions [91, 216, 223]. This supports the observed increase of ethylene biosynthesis in plant roots upon Fe-deficiency [224, 225]. Further, it is known, that *FIT* gene expression is reduced in ethylene omitted conditions [91, 226]. Hence, ethylene is not only a positive regulator of *FIT* gene expression, but also FIT protein stability, mediated by EIN3/EIL1 protein-protein interaction [91, 94, 226].

Recently, it was shown that Fe-deficiency causes the accumulation of cytosolic Ca^{2+} within cells of the elongation and root-hair zone in primary Arabidopsis roots. In addition, *lsk* knock-out mutant plants, which contain a lesion in *CIPK23* gene, displayed stronger chlorosis, reduced chlorophyll- and Fe content, altered root structure as well as reduced FRO2 activity than WT under Fe-deficient conditions. This led to the conclusion, that kinases from the CIPK-family are involved in Fe accumulation and uptake by positively mediating FRO2 activity [227]. CBL1 and CBL9 were identified to act as respective Ca^{2+} sensors upstream of CIPK23 in this process [227, 228].

Under low Fe, the plasma membrane ATPase AHA2 reduces the soil pH and facilitates the solubilization of Fe^{3+} from soil particles [31]. Hence, differential regulation of AHA2 via protein phosphorylation indirectly affects Fe accumulation and uptake. AHA2 interaction with 14-3-3 proteins has an activating effect on the proton pump [229-232]. Phosphorylation of C-terminal threonine, Thr947, located within a Tyr-Thr-Val recognition site for 14-3-3 proteins, facilitates the interaction of both proteins and activates AHA2 [233-236]. In addition, the binding of the peptide hormone PLANT PEPTIDE CONTAINING SULFATED TYROSINE 1 (PSY1) to the respective LEUCINE-RICH REPEAT RECEPTOR KINASE (LRR-RK) PSY1R has a positive effect on AHA2 activity. The activated PSY1R interacts with and phosphorylates AHA2 at Thr881, assisting protein extrusion [237]. Pump activation by Thr881 phosphorylation appears to be independent of subsequent 14-3-3 binding [238]. The phosphorylation of C-terminal Ser931 by the CBL2 - CIPK11 module however causes inhibition of AHA2 activity by prohibiting the interaction with 14-3-3 proteins. *cikp11* loss-of-function mutants display an increase in tolerance towards high external pH [239]. Flagellin-mediated phosphorylation of Ser899 also inhibits AHA2 action [240]. In addition, peptide RAPID ALKALINIZATION FACTOR (RALF)-triggered activation of the cell surface receptor FERONIA also prompts Ser899 phosphorylation [241].

The described phosphorylation of AHA2 is conveyed by different overlapping environmental and biochemical stimuli, which mediate the signal integration into downstream actions, either activating or inactivating the enzyme [242].

These examples show, which potential post-translational modifications are involved in the regulation of signaling pathways. Hence, it is of interest for further study, focusing on phosphorylation-based protein regulation, since it is probable that more proteins involved in Fe-deficiency signaling might undergo post-translational control.

5 Aims of the Thesis

FIT was proposed to be present in active and inactive forms [83, 94, 101]. Previous work in the group has identified the protein kinase CIPK11 as a novel potential interaction partner of FIT, suggesting possible involvement of phosphorylation in FIT activity regulation. Phosphorylation of other bHLH proteins was shown to mediate opposing effects on the respective protein activity, either rendering the protein active or inactive. To add even further complexity, the involvement of different kinases can trigger a set of different phosphorylation events with opposing effects, thus, as part of a fine-tuned activity. This raises two important questions: (i) which signal renders the FIT protein active and (ii) how is the Fe-deficiency signal incorporated into downstream transcriptional programs? In order to answer these questions, the following aims were formulated as a framework for this thesis:

1. *The first aim was to verify the interaction between FIT and CIPK11 and to characterize the effects of potential phosphorylation of FIT by the kinase.*
   In order to confirm the interaction of both proteins, different targeted protein-protein interaction assays were to be executed in yeast and *in planta*. An *in vitro* kinase assay was to be performed to address whether FIT is phosphorylated by CIPK11. Additionally, a phospho-mimicking approach was to be applied and respective FIT phospho-mutants were to be created. This was to be performed to identify kinase target sites and to demonstrate the effects of FIT phosphorylation on its activity. If possible evidence was to be provided for *in vivo* phosphorylation and, if possible, phospho-peptides were to be obtained.

2. *A second aim was to map and characterize additional, potential phosphorylation sites in FIT-C to test the hypothesis that FIT-C acts as a regulatory platform for its activity.*
   By creating selected, novel phospho-mutations in FIT-C, a broad phospho-mutant activity screening was to be applied to elucidate the function of potential additional phosphorylation sites. As part of this assay, FIT protein properties such as subcellular localization, nuclear mobility and dimerization capacity were be compared between WT and phospho-mutants. In order to build a more general, final model of FIT protein activity regulation through phosphorylation, a FIT activity assay was to be established.

References

1. Saltzman, A., et al., *Biofortification: Progress toward a more nourishing future.* Global Food Security, 2013. 2(1): p. 9-17.
2. Naranjo- Arcos, M.A. and P. Bauer, *Nutritional Deficiency. Chapter 4: Iron Nutrition, Oxidative Stress, and Pathogen Defense*. 2016, INTECH Open Access Publisher.
3. Scrimshaw, N.S., *Functional consequences of iron deficiency in human populations.* Journal of nutritional science and vitaminology, 1984. 30(1): p. 47-63.
4. Bouis, H.E., et al., *Biofortification: a new tool to reduce micronutrient malnutrition.* Food Nutr Bull, 2011. 32(1 Suppl): p. S31-40.
5. Masuda, H., M.S. Aung, and N.K. Nishizawa, *Iron biofortification of rice using different transgenic approaches.* Rice, 2013. 6(1): p. 40-40.
6. Haas, J.D., et al., *Consuming Iron Biofortified Beans Increases Iron Status in Rwandan Women after 128 Days in a Randomized Controlled Feeding Trial.* Journal of Nutrition, 2016. 146(8): p. 1586-1592.
7. Blaby-Haas, C.E. and S.S. Merchant, *Iron sparing and recycling in a compartmentalized cell.* Current opinion in microbiology, 2013. 16(6): p. 10.1016/j.mib.2013.07.019.
8. López-Millán, A.F., D. Duy, and K. Philippar, *Chloroplast Iron Transport Proteins – Function and Impact on Plant Physiology.* Frontiers in Plant Science, 2016. 7: p. 178.
9. Zhang, C., *Essential functions of iron-requiring proteins in DNA replication, repair and cell cycle control.* Protein & Cell, 2014. 5(10): p. 750-760.
10. Wedepohl, K.H., *The Composition of the Continental-Crust.* Geochimica Et Cosmochimica Acta, 1995. 59(7): p. 1217-1232.
11. Chen, Y. and P. Barak, *Iron nutrition of plants in calcareous soils.* Advances in agronomy, 1982. 35: p. 217-240.
12. Guerinot, M.L. and Y. Yi, *Iron: Nutritious, Noxious, and Not Readily Available.* Plant Physiol, 1994. 104(3): p. 815-820.
13. Briat, J.-F., et al., *Cellular and molecular aspects of iron metabolism in plants.* Biology of the Cell, 1995. 84(1): p. 69-81.
14. Page, M.D., et al., *Fe Sparing and Fe Recycling Contribute to Increased Superoxide Dismutase Capacity in Iron-Starved Chlamydomonas reinhardtii.* The Plant Cell, 2012. 24(6): p. 2649-2665.
15. Hantzis, L.J., et al., *A program for iron economy during deficiency targets specific Fe proteins.* Plant Physiol, 2018. 176(1): p. 596-610.
16. Li, G., H.J. Kronzucker, and W. Shi, *The Response of the Root Apex in Plant Adaptation to Iron Heterogeneity in Soil.* Frontiers in Plant Science, 2016. 7: p. 344.
17. Brumbarova, T., P. Bauer, and R. Ivanov, *Molecular mechanisms governing Arabidopsis iron uptake.* Trends Plant Sci, 2015. 20(2): p. 124-33.
18. Kim, S.A. and M.L. Guerinot, *Mining iron: iron uptake and transport in plants.* FEBS Lett, 2007. 581(12): p. 2273-80.
19. Ravet, K., et al., *Ferritins control interaction between iron homeostasis and oxidative stress in Arabidopsis.* Plant J, 2009. 57(3): p. 400-12.
20. Sperotto, R.A., et al., *Iron stress in plants: dealing with deprivation and overload.* Plant Stress, 2010. 4: p. 57-69.
21. Zancani, M., et al., *Evidence for the presence of ferritin in plant mitochondria.* European Journal of Biochemistry, 2004. 271(18): p. 3657-3664.
22. Morrissey, J. and M.L. Guerinot, *Iron uptake and transport in plants: the good, the bad, and the ionome.* Chemical reviews, 2009. 109(10): p. 4553-4567.
23. Busi, M.V., et al., *Functional and molecular characterization of the frataxin homolog from Arabidopsis thaliana.* FEBS Lett, 2004. 576(1-2): p. 141-4.

24. Bencze, K.Z., et al., *The Structure and Function of Frataxin.* Critical reviews in biochemistry and molecular biology, 2006. 41(5): p. 269-291.
25. Kim, S.A., et al., *Localization of iron in Arabidopsis seed requires the vacuolar membrane transporter VIT1.* Science, 2006. 314(5803): p. 1295-1298.
26. Krämer, U. and S. Clemens, *Functions and homeostasis of zinc, copper, and nickel in plants*, in *Molecular Biology of Metal Homeostasis and Detoxification: From Microbes to Man*, M.J. Tamas and E. Martinoia, Editors. 2006, Springer Berlin Heidelberg: Berlin, Heidelberg. p. 215-271.
27. Briat, J.-F., C. Curie, and F. Gaymard, *Iron utilization and metabolism in plants.* Current opinion in plant biology, 2007. 10(3): p. 276-282.
28. Curie, C. and J.-F. Briat, *Iron Transport and Signaling in Plants.* Annual Review of Plant Biology, 2003. 54(1): p. 183-206.
29. Marschner, H., V. Romheld, and M. Kissel, *Different Strategies in Higher-Plants in Mobilization and Uptake of Iron.* Journal of Plant Nutrition, 1986. 9(3-7): p. 695-713.
30. Romheld, V. and H. Marschner, *Evidence for a specific uptake system for iron phytosiderophores in roots of grasses.* Plant Physiol, 1986. 80(1): p. 175-80.
31. Santi, S. and W. Schmidt, *Dissecting iron deficiency-induced proton extrusion in Arabidopsis roots.* New Phytol, 2009. 183(4): p. 1072-84.
32. Jin, C.W., et al., *Iron Deficiency-Induced Secretion of Phenolics Facilitates the Reutilization of Root Apoplastic Iron in Red Clover.* Plant Physiology, 2007. 144(1): p. 278-285.
33. Rodriguez-Celma, J., et al., *Mutually exclusive alterations in secondary metabolism are critical for the uptake of insoluble iron compounds by Arabidopsis and Medicago truncatula.* Plant Physiol, 2013. 162(3): p. 1473-85.
34. Fourcroy, P., et al., *Involvement of the ABCG37 transporter in secretion of scopoletin and derivatives by Arabidopsis roots in response to iron deficiency.* New Phytol, 2014. 201(1): p. 155-67.
35. Fourcroy, P., et al., *Facilitated Fe Nutrition by Phenolic Compounds Excreted by the Arabidopsis ABCG37/PDR9 Transporter Requires the IRT1/FRO2 High-Affinity Root Fe(2+) Transport System.* Mol Plant, 2016. 9(3): p. 485-8.
36. Schmid, N.B., et al., *Feruloyl-CoA 6'-Hydroxylase1-dependent coumarins mediate iron acquisition from alkaline substrates in Arabidopsis.* Plant Physiol, 2014. 164(1): p. 160-72.
37. Schmidt, H., et al., *Metabolome analysis of Arabidopsis thaliana roots identifies a key metabolic pathway for iron acquisition.* PLoS One, 2014. 9(7): p. e102444.
38. Robinson, N.J., et al., *A ferric-chelate reductase for iron uptake from soils.* Nature, 1999. 397(6721): p. 694-7.
39. Yi, Y. and M.L. Guerinot, *Genetic evidence that induction of root Fe(III) chelate reductase activity is necessary for iron uptake under iron deficiency.* Plant J, 1996. 10(5): p. 835-44.
40. Connolly, E.L., et al., *Overexpression of the FRO2 ferric chelate reductase confers tolerance to growth on low iron and uncovers posttranscriptional control.* Plant Physiology, 2003. 133(3): p. 1102-1110.
41. Eide, D., et al., *A novel iron-regulated metal transporter from plants identified by functional expression in yeast.* Proc Natl Acad Sci U S A, 1996. 93(11): p. 5624-8.
42. Vert, G., et al., *IRT1, an Arabidopsis transporter essential for iron uptake from the soil and for plant growth.* Plant Cell, 2002. 14(6): p. 1223-33.
43. Varotto, C., et al., *The metal ion transporter IRT1 is necessary for iron homeostasis and efficient photosynthesis in Arabidopsis thaliana.* The Plant Journal, 2002. 31(5): p. 589-599.

44. Henriques, R., et al., *Knock-out of Arabidopsis metal transporter gene IRT1 results in iron deficiency accompanied by cell differentiation defects.* Plant molecular biology, 2002. 50(4-5): p. 587-597.
45. Heim, M.A., et al., *The basic helix-loop-helix transcription factor family in plants: A genome-wide study of protein structure and functional diversity.* Molecular Biology and Evolution, 2003. 20(5): p. 735-747.
46. Colangelo, E.P. and M.L. Guerinot, *The essential basic helix-loop-helix protein FIT1 is required for the iron deficiency response.* Plant Cell, 2004. 16(12): p. 3400-12.
47. Jakoby, M., et al., *FRU (BHLH029) is required for induction of iron mobilization genes in Arabidopsis thaliana.* FEBS Lett, 2004. 577(3): p. 528-34.
48. Yuan, Y.X., et al., *AtbHLH29 of Arabidopsis thaliana is a functional ortholog of tomato FER involved in controlling iron acquisition in strategy I plants.* Cell Research, 2005. 15(8): p. 613-621.
49. Ivanov, R., T. Brumbarova, and P. Bauer, *Fitting into the harsh reality: regulation of iron-deficiency responses in dicotyledonous plants.* Mol Plant, 2012. 5(1): p. 27-42.
50. Wang, H.Y., et al., *Iron deficiency-mediated stress regulation of four subgroup Ib BHLH genes in Arabidopsis thaliana.* Planta, 2007. 226(4): p. 897-908.
51. Yuan, Y., et al., *FIT interacts with AtbHLH38 and AtbHLH39 in regulating iron uptake gene expression for iron homeostasis in Arabidopsis.* Cell Res, 2008. 18(3): p. 385-97.
52. Wang, N., et al., *Requirement and functional redundancy of Ib subgroup bHLH proteins for iron deficiency responses and uptake in Arabidopsis thaliana.* Mol Plant, 2013. 6(2): p. 503-13.
53. Vorwieger, A., et al., *Iron assimilation and transcription factor controlled synthesis of riboflavin in plants.* Planta, 2007. 226(1): p. 147-158.
54. Mai, H.-J., S. Pateyron, and P. Bauer, *Iron homeostasis in Arabidopsis thaliana: transcriptomic analyses reveal novel FIT-regulated genes, iron deficiency marker genes and functional gene networks.* BMC plant biology, 2016. 16(1): p. 211.
55. Mai, H.-J., et al., *Iron and FER-LIKE IRON DEFICIENCY-INDUCED TRANSCRIPTION FACTOR-dependent regulation of proteins and genes in Arabidopsis thaliana roots.* PROTEOMICS, 2015. 15(17): p. 3030-3047.
56. Naranjo-Arcos, M.A., et al., *Dissection of iron signaling and iron accumulation by overexpression of subgroup Ib bHLH039 protein.* Scientific Reports, 2017. 7.
57. Nozoye, T., et al., *Phytosiderophore efflux transporters are crucial for iron acquisition in graminaceous plants.* J Biol Chem, 2011. 286(7): p. 5446-54.
58. Takagi, S.-i., *Naturally occurring iron-chelating compounds in oat-and rice-root washings: I. Activity measurement and preliminary characterization.* Soil science and plant nutrition, 1976. 22(4): p. 423-433.
59. Takagi, S.i., K. Nomoto, and T. Takemoto, *Physiological aspect of mugineic acid, a possible phytosiderophore of graminaceous plants.* Journal of Plant Nutrition, 1984. 7(1-5): p. 469-477.
60. Mori, S. and N. Nishizawa, *Methionine as a dominant precursor of phytosiderophores in Graminaceae plants.* Plant and Cell Physiology, 1987. 28(6): p. 1081-1092.
61. Schuler, M. and P. Bauer, *Heavy metals need assistance: the contribution of nicotianamine to metal circulation throughout the plant and the Arabidopsis NAS gene family.* Frontiers in Plant Science, 2011. 2.
62. Ling, H.-Q., et al., *Map-based cloning of chloronerva, a gene involved in iron uptake of higher plants encoding nicotianamine synthase.* Proceedings of the National Academy of Sciences of the United States of America, 1999. 96(12): p. 7098-7103.
63. Higuchi, K., et al., *Cloning of Nicotianamine Synthase Genes, Novel Genes Involved in the Biosynthesis of Phytosiderophores.* Plant Physiology, 1999. 119(2): p. 471-480.

64. Curie, C., et al., *Maize yellow stripe1 encodes a membrane protein directly involved in Fe(III) uptake.* Nature, 2001. 409(6818): p. 346-9.
65. Schaaf, G., et al., *ZmYS1 functions as a proton-coupled symporter for phytosiderophore- and nicotianamine-chelated metals.* Journal of Biological Chemistry, 2004. 279(10): p. 9091-9096.
66. Murata, Y., et al., *A specific transporter for iron (III)–phytosiderophore in barley roots.* The Plant Journal, 2006. 46(4): p. 563-572.
67. Inoue, H., et al., *Rice OsYSL15 is an iron-regulated iron(III)-deoxymugineic acid transporter expressed in the roots and is essential for iron uptake in early growth of the seedlings.* J Biol Chem, 2009. 284(6): p. 3470-9.
68. Araki, R., J. Murata, and Y. Murata, *A novel barley yellow stripe 1-like transporter (HvYSL2) localized to the root endodermis transports metal-phytosiderophore complexes.* Plant Cell Physiol, 2011. 52(11): p. 1931-40.
69. Ogo, Y., et al., *The rice bHLH protein OsIRO2 is an essential regulator of the genes involved in Fe uptake under Fe-deficient conditions.* The Plant Journal, 2007. 51(3): p. 366-377.
70. Ogo, Y., et al., *Isolation and characterization of IRO2, a novel iron-regulated bHLH transcription factor in graminaceous plants.* J Exp Bot, 2006. 57(11): p. 2867-78.
71. Ogo, Y., et al., *OsIRO2 is responsible for iron utilization in rice and improves growth and yield in calcareous soil.* Plant Mol Biol, 2011. 75(6): p. 593-605.
72. Zheng, L., et al., *Identification of a novel iron regulated basic helix-loop-helix protein involved in Fe homeostasis in Oryza sativa.* BMC Plant Biol, 2010. 10: p. 166.
73. Li, S., et al., *Identification and characterization of the zinc-regulated transporters, iron-regulated transporter-like protein (ZIP) gene family in maize.* BMC plant biology, 2013. 13(1): p. 114.
74. Li, S., et al., *Overexpression of ZmIRT1 and ZmZIP3 enhances iron and zinc accumulation in transgenic Arabidopsis.* PloS one, 2015. 10(8): p. e0136647.
75. Bughio, N., et al., *Cloning an iron-regulated metal transporter from rice.* J Exp Bot, 2002. 53(374): p. 1677-82.
76. Ishimaru, Y., et al., *Rice plants take up iron as an Fe3+-phytosiderophore and as Fe2+.* Plant J, 2006. 45(3): p. 335-46.
77. Lee, S. and G. An, *Over-expression of OsIRT1 leads to increased iron and zinc accumulations in rice.* Plant, Cell & Environment, 2009. 32(4): p. 408-416.
78. Pedas, P., et al., *Manganese efficiency in barley: identification and characterization of the metal ion transporter HvIRT1.* Plant physiology, 2008. 148(1): p. 455-466.
79. Ling, H.Q., et al., *The tomato fer gene encoding a bHLH protein controls iron-uptake responses in roots.* Proc Natl Acad Sci U S A, 2002. 99(21): p. 13938-43.
80. Brumbarova, T. and P. Bauer, *Iron-mediated control of the basic helix-loop-helix protein FER, a regulator of iron uptake in tomato.* Plant Physiol, 2005. 137(3): p. 1018-26.
81. Bauer, P., et al., *Analysis of sequence, map position, and gene expression reveals conserved essential genes for iron uptake in Arabidopsis and tomato.* Plant Physiol, 2004. 136(4): p. 4169-83.
82. Jakoby, M., et al., *FRU (BHLH029) is required for induction of iron mobilization genes in Arabidopsis thaliana.* FEBS letters, 2004. 577(3): p. 528-534.
83. Meiser, J., S. Lingam, and P. Bauer, *Posttranslational regulation of the iron deficiency basic helix-loop-helix transcription factor FIT is affected by iron and nitric oxide.* Plant Physiol, 2011. 157(4): p. 2154-66.
84. Meiser, J. and P. Bauer, *Looking for the hub in Fe signaling.* Plant signaling & behavior, 2012. 7(6): p. 688-690.

85. Garcia, M.J., et al., *A new model involving ethylene, nitric oxide and Fe to explain the regulation of Fe-acquisition genes in Strategy I plants.* Plant Physiol Biochem, 2011. 49(5): p. 537-44.
86. Graziano, M. and L. Lamattina, *Nitric oxide accumulation is required for molecular and physiological responses to iron deficiency in tomato roots.* Plant J, 2007. 52(5): p. 949-60.
87. Chen, W.W., et al., *Nitric Oxide Acts Downstream of Auxin to Trigger Root Ferric-Chelate Reductase Activity in Response to Iron Deficiency in Arabidopsis.* Plant Physiology, 2010. 154(2): p. 810-819.
88. Yang, J.L., et al., *The 14-3-3 protein GENERAL REGULATORY FACTOR11 (GRF11) acts downstream of nitric oxide to regulate iron acquisition in Arabidopsis thaliana.* New Phytol, 2013. 197(3): p. 815-24.
89. Kohli, A., et al., *The phytohormone crosstalk paradigm takes center stage in understanding how plants respond to abiotic stresses.* Plant Cell Reports, 2013. 32(7): p. 945-957.
90. Romera, F.J., et al., *Latest findings about the interplay of auxin, ethylene and nitric oxide in the regulation of Fe-deficiency responses by Strategy I plants.* Plant Signaling & Behavior, 2011. 6(1): p. 167-170.
91. Garcia, M.J., et al., *Ethylene and nitric oxide involvement in the up-regulation of key genes related to iron acquisition and homeostasis in Arabidopsis.* J Exp Bot, 2010. 61(14): p. 3885-99.
92. Romera, F.J., C. Lucena, and E. Alcàntara, *Plant hormones influencing iron uptake in plants*, in *Iron nutrition in plants and rhizospheric microorganisms*. 2006, Springer. p. 251-278.
93. Romera, F.J. and E. Alcántara, *Ethylene involvement in the regulation of Fe-deficiency stress responses by Strategy I plants.* Functional Plant Biology, 2004. 31(4): p. 315-328.
94. Lingam, S., et al., *Interaction between the bHLH transcription factor FIT and ETHYLENE INSENSITIVE3/ETHYLENE INSENSITIVE3-LIKE1 reveals molecular linkage between the regulation of iron acquisition and ethylene signaling in Arabidopsis.* Plant Cell, 2011. 23(5): p. 1815-29.
95. Wang, H.-Y., et al., *Iron deficiency-mediated stress regulation of four subgroup Ib BHLH genes in Arabidopsis thaliana.* Planta, 2007. 226(4): p. 897-908.
96. Lucena, C., et al., *Ethylene could influence ferric reductase, iron transporter, and H+-ATPase gene expression by affecting FER (or FER-like) gene activity.* Journal of Experimental Botany, 2006. 57(15): p. 4145-4154.
97. Lin, X.Y., et al., *Increased Sucrose Accumulation Regulates Iron-Deficiency Responses by Promoting Auxin Signaling in Arabidopsis Plants.* Plant Physiology, 2016. 170(2): p. 907-920.
98. Séguéla, M., et al., *Cytokinins negatively regulate the root iron uptake machinery in Arabidopsis through a growth-dependent pathway.* The Plant Journal, 2008. 55(2): p. 289-300.
99. Maurer, F., S. Müller, and P. Bauer, *Suppression of Fe-deficiency gene expression by jasmonate.* Plant Physiology and Biochemistry, 2011. 49(5): p. 530-536.
100. Jeong, I.S., et al., *Regulation of Abiotic Stress Signalling by Arabidopsis C-Terminal Domain Phosphatase-Like 1 Requires Interaction with a K-Homology Domain-Containing Protein.* PLOS ONE, 2013. 8(11): p. e80509.
101. Sivitz, A., et al., *Proteasome-mediated turnover of the transcriptional activator FIT is required for plant iron-deficiency responses.* Plant J, 2011. 66(6): p. 1044-52.

102. Yang, Y., et al., *The Arabidopsis Mediator subunit MED16 regulates iron homeostasis by associating with EIN3/EIL1 through subunit MED25.* Plant J, 2014. 77(6): p. 838-51.
103. Zhang, Y., et al., *Mediator subunit 16 functions in the regulation of iron uptake gene expression in Arabidopsis.* New Phytol, 2014. 203(3): p. 770-83.
104. Wild, M., et al., *Tissue-Specific Regulation of Gibberellin Signaling Fine-Tunes Arabidopsis Iron-Deficiency Responses.* Developmental Cell, 2016. 37(2): p. 190-200.
105. Le, C.T.T., et al., *ZINC FINGER OF ARABIDOPSIS THALIANA12 (ZAT12) Interacts with FER-LIKE IRON DEFICIENCY- INDUCED TRANSCRIPTION FACTOR (FIT) Linking Iron Deficiency and Oxidative Stress Responses.* Plant Physiology, 2016. 170(1): p. 540-557.
106. Long, T.A., et al., *The bHLH Transcription Factor POPEYE Regulates Response to Iron Deficiency in Arabidopsis Roots.* The Plant Cell, 2010. 22(7): p. 2219-2236.
107. Selote, D., et al., *Iron-binding E3 ligase mediates iron response in plants by targeting basic helix-loop-helix transcription factors.* Plant Physiol, 2015. 167(1): p. 273-86.
108. Zhang, J., et al., *The bHLH Transcription Factor bHLH104 Interacts with IAA-LEUCINE RESISTANT3 and Modulates Iron Homeostasis in Arabidopsis.* The Plant Cell, 2015. 27(3): p. 787-805.
109. Li, X., et al., *Two bHLH Transcription Factors, bHLH34 and bHLH104, Regulate Iron Homeostasis in Arabidopsis thaliana.* Plant Physiology, 2016. 170(4): p. 2478-2493.
110. Liang, G., et al., *bHLH transcription factor bHLH115 regulates iron homeostasis in Arabidopsis thaliana.* Journal of Experimental Botany, 2017. 68(7): p. 1743-1755.
111. Kobayashi, T., et al., *Iron-binding haemerythrin RING ubiquitin ligases regulate plant iron responses and accumulation.* Nature communications, 2013. 4.
112. Hindt, M.N., et al., *BRUTUS and its paralogs, BTS LIKE1 and BTS LIKE2, encode important negative regulators of the iron deficiency response in Arabidopsis thaliana.* Metallomics, 2017. 9(7): p. 876-890.
113. Matthiadis, A. and T.A. Long, *Further insight into BRUTUS domain composition and functionality.* Plant signaling & behavior, 2016. 11(8): p. e1204508.
114. Salahudeen, A.A., et al., *An E3 Ligase Possessing an Iron-Responsive Hemerythrin Domain Is a Regulator of Iron Homeostasis.* Science (New York, N.Y.), 2009. 326(5953): p. 722-726.
115. Palmer, C.M., et al., *MYB10 and MYB72 Are Required for Growth under Iron-Limiting Conditions.* PLOS Genetics, 2013. 9(11): p. e1003953.
116. Van der Ent, S., et al., *MYB72 is required in early signaling steps of rhizobacteria-induced systemic resistance in Arabidopsis.* Plant Physiol, 2008. 146(3): p. 1293-304.
117. Zamioudis, C., J. Hanson, and C.M. Pieterse, *beta-Glucosidase BGLU42 is a MYB72-dependent key regulator of rhizobacteria-induced systemic resistance and modulates iron deficiency responses in Arabidopsis roots.* New Phytol, 2014. 204(2): p. 368-79.
118. Zamioudis, C., et al., *Rhizobacterial volatiles and photosynthesis-related signals coordinate MYB72 in Arabidopsis roots during onset of induced systemic resistance and iron deficiency responses.* Plant J, 2015.
119. Sivitz, A.B., et al., *Arabidopsis bHLH100 and bHLH101 Control Iron Homeostasis via a FIT-Independent Pathway.* PLOS ONE, 2012. 7(9): p. e44843.
120. Riechmann, J.L., et al., *Arabidopsis Transcription Factors: Genome-Wide Comparative Analysis Among Eukaryotes.* Science, 2000. 290(5499): p. 2105-2110.
121. Murre, C., P.S. McCaw, and D. Baltimore, *A new DNA binding and dimerization motif in immunoglobulin enhancer binding, daughterless, MyoD, and myc proteins.* Cell, 1989. 56(5): p. 777-83.
122. Bailey, P.C., et al., *Update on the basic helix-loop-helix transcription factor gene family in Arabidopsis thaliana.* Plant Cell, 2003. 15(11): p. 2497-2501.

123. Toledo-Ortiz, G., E. Huq, and P.H. Quail, *The Arabidopsis basic/helix-loop-helix transcription factor family.* Plant Cell, 2003. 15(8): p. 1749-70.
124. Feller, A., et al., *Evolutionary and comparative analysis of MYB and bHLH plant transcription factors.* Plant J, 2011. 66(1): p. 94-116.
125. Ferré-D'Amaré, A.R., et al., *Recognition by Max of its cognate DNA through a dimeric b/HLH/Z domain.* Nature, 1993. 363: p. 38.
126. Ma, P.C.M., et al., *Crystal structure of MyoD bHLH domain-DNA complex: Perspectives on DNA recognition and implications for transcriptional activation.* Cell, 1994. 77(3): p. 451-459.
127. Shimizu, T., et al., *Crystal structure of PHO4 bHLH domain-DNA complex: flanking base recognition.* Embo j, 1997. 16(15): p. 4689-97.
128. Sajeevan, R.S. and K.N. Nataraja, *Molecular cloning and characterization of a novel basic helix–loop–helix-144 (bHLH144)-like transcription factor from Morus alba (L.).* Plant Gene, 2016. 5(Supplement C): p. 109-117.
129. Nallamilli, B.R.R., et al., *Global Analysis of Lysine Acetylation Suggests the Involvement of Protein Acetylation in Diverse Biological Processes in Rice (Oryza sativa).* PLoS ONE, 2014. 9(2): p. e89283.
130. Chinnusamy, V., et al., *ICE1: a regulator of cold-induced transcriptome and freezing tolerance in Arabidopsis.* Genes Dev, 2003. 17(8): p. 1043-54.
131. Shi, Y., et al., *The precise regulation of different COR genes by individual CBF transcription factors in Arabidopsis thaliana.* Journal of Integrative Plant Biology, 2017. 59(2): p. 118-133.
132. Stockinger, E.J., S.J. Gilmour, and M.F. Thomashow, *Arabidopsis thaliana CBF1 encodes an AP2 domain-containing transcriptional activator that binds to the C-repeat/DRE, a cis-acting DNA regulatory element that stimulates transcription in response to low temperature and water deficit.* Proceedings of the National Academy of Sciences of the United States of America, 1997. 94(3): p. 1035-1040.
133. Shen, C., et al., *Involvement of endogenous salicylic acid in iron-deficiency responses in Arabidopsis.* Journal of Experimental Botany, 2016. 67(14): p. 4179-4193.
134. Maurer, F., M.A. Naranjo Arcos, and P. Bauer, *Responses of a Triple Mutant Defective in Three Iron Deficiency-Induced BASIC HELIX-LOOP-HELIX Genes of the Subgroup Ib(2) to Iron Deficiency and Salicylic Acid.* PLOS ONE, 2014. 9(6): p. e99234.
135. Kurepin, L.V., et al., *Role of CBFs as Integrators of Chloroplast Redox, Phytochrome and Plant Hormone Signaling during Cold Acclimation.* International Journal of Molecular Sciences, 2013. 14(6): p. 12729-12763.
136. Lee, B.-h., et al., *A Mitochondrial Complex I Defect Impairs Cold-Regulated Nuclear Gene Expression.* The Plant Cell, 2002. 14(6): p. 1235.
137. Dong, C.-H., et al., *Disruption of Arabidopsis CHY1 Reveals an Important Role of Metabolic Status in Plant Cold Stress Signaling.* Molecular Plant, 2009. 2(1): p. 59-72.
138. Maruta, T., et al., *H2O2-triggered retrograde signaling from chloroplasts to nucleus plays specific role in response to stress.* J Biol Chem, 2012. 287(15): p. 11717-29.
139. Xiong, L.M., M. Ishitani, and J.K. Zhu, *Interaction of osmotic stress, temperature, and abscisic acid in the regulation of gene expression in arabidopsis.* Plant Physiology, 1999. 119(1): p. 205-211.
140. Knight, H., et al., *Abscisic Acid Induces CBF Gene Transcription and Subsequent Induction of Cold-Regulated Genes via the CRT Promoter Element.* Plant Physiology, 2004. 135(3): p. 1710-1717.
141. Christmann, A., et al., *Integration of abscisic acid signalling into plant responses.* Plant Biol (Stuttg), 2006. 8(3): p. 314-25.
142. Ding, Y., et al., *OST1 Kinase Modulates Freezing Tolerance by Enhancing ICE1 Stability in Arabidopsis.* Developmental Cell, 2015. 32(3): p. 278-289.

143. Zhao, C., et al., *MAP Kinase Cascades Regulate the Cold Response by Modulating ICE1 Protein Stability.* Developmental Cell, 2017.
144. Li, H., et al., *MPK3- and MPK6-Mediated ICE1 Phosphorylation Negatively Regulates ICE1 Stability and Freezing Tolerance in Arabidopsis.* Developmental Cell, 2017.
145. Dong, C.H., et al., *The negative regulator of plant cold responses, HOS1, is a RING E3 ligase that mediates the ubiquitination and degradation of ICE1.* Proc Natl Acad Sci U S A, 2006. 103(21): p. 8281-6.
146. Lee, H., et al., *The Arabidopsis HOS1 gene negatively regulates cold signal transduction and encodes a RING finger protein that displays cold-regulated nucleo–cytoplasmic partitioning.* Genes & Development, 2001. 15(7): p. 912-924.
147. Miura, K., et al., *SIZ1-Mediated Sumoylation of ICE1 Controls CBF3/DREB1A Expression and Freezing Tolerance in Arabidopsis.* The Plant Cell, 2007. 19(4): p. 1403.
148. Miura, K. and P.M. Hasegawa, *Regulation of cold signaling by sumoylation of ICE1.* Plant Signaling & Behavior, 2008. 3(1): p. 52-53.
149. Miura, K., et al., *The Arabidopsis SUMO E3 ligase SIZ1 controls phosphate deficiency responses.* Proc Natl Acad Sci U S A, 2005. 102(21): p. 7760-5.
150. Miura, K., et al., *ICE1 Ser403 is necessary for protein stabilization and regulation of cold signaling and tolerance.* The Plant Journal, 2011. 67(2): p. 269-279.
151. Zhu, J.K., *Abiotic Stress Signaling and Responses in Plants.* Cell, 2016. 167(2): p. 313-324.
152. Yang, T., et al., *A calcium/calmodulin-regulated member of the receptor-like kinase family confers cold tolerance in plants.* J Biol Chem, 2010. 285(10): p. 7119-26.
153. Furuya, T., D. Matsuoka, and T. Nanmori, *Phosphorylation of Arabidopsis thaliana MEKK1 via Ca2+ signaling as a part of the cold stress response.* Journal of Plant Research, 2013. 126(6): p. 833-840.
154. Yang, T., et al., *Calcium/calmodulin-regulated receptor-like kinase CRLK1 interacts with MEKK1 in plants.* Plant Signaling & Behavior, 2010. 5(8): p. 991-994.
155. Teige, M., et al., *The MKK2 pathway mediates cold and salt stress signaling in Arabidopsis.* Molecular Cell, 2004. 15(1): p. 141-152.
156. Cheong, Y.H., et al., *CBL1, a Calcium Sensor That Differentially Regulates Salt, Drought, and Cold Responses in Arabidopsis.* The Plant Cell, 2003. 15(8): p. 1833.
157. Albrecht, V., et al., *The calcium sensor CBL1 integrates plant responses to abiotic stresses.* Plant J, 2003. 36(4): p. 457-70.
158. Huang, C., et al., *CIPK7 is involved in cold response by interacting with CBL1 in Arabidopsis thaliana.* Plant Science, 2011. 181(1): p. 57-64.
159. Kim, K.-N., et al., *CIPK3, a Calcium Sensor–Associated Protein Kinase That Regulates Abscisic Acid and Cold Signal Transduction in Arabidopsis.* The Plant Cell, 2003. 15(2): p. 411.
160. Pandey, G.K., et al., *Calcineurin-B-Like Protein CBL9 Interacts with Target Kinase CIPK3 in the Regulation of ABA Response in Seed Germination.* Molecular Plant, 2008. 1(2): p. 238-248.
161. Komatsu, S., et al., *Over-expression of calcium-dependent protein kinase 13 and calreticulin interacting protein 1 confers cold tolerance on rice plants.* Mol Genet Genomics, 2007. 277(6): p. 713-23.
162. Bohmer, M. and T. Romeis, *A chemical-genetic approach to elucidate protein kinase function in planta.* Plant Mol Biol, 2007. 65(6): p. 817-27.
163. Lee, J.-H., J.-H. Jung, and C.-M. Park, *Light Inhibits COP1-Mediated Degradation of ICE Transcription Factors to Induce Stomatal Development in Arabidopsis.* The Plant Cell, 2017. 29(11): p. 2817.

164. Salomé, P.A., *This ICE/SCRM Melts in the Dark: Light-Dependent COP1-Mediated Protein Degradation in Stomatal Formation.* The Plant Cell, 2017. 29(11): p. 2680.
165. Kanaoka, M.M., et al., *SCREAM/ICE1 and SCREAM2 Specify Three Cell-State Transitional Steps Leading to Arabidopsis Stomatal Differentiation.* The Plant Cell, 2008. 20(7): p. 1775-1785.
166. MacAlister, C.A., K. Ohashi-Ito, and D.C. Bergmann, *Transcription factor control of asymmetric cell divisions that establish the stomatal lineage.* Nature, 2007. 445(7127): p. 537-540.
167. Lampard, G.R., C.A. Macalister, and D.C. Bergmann, *Arabidopsis stomatal initiation is controlled by MAPK-mediated regulation of the bHLH SPEECHLESS.* Science, 2008. 322(5904): p. 1113-6.
168. Peng, P., et al., *Regulation of the Arabidopsis GSK3-like Kinase BRASSINOSTEROID-INSENSITIVE 2 through Proteasome-Mediated Protein Degradation.* Molecular Plant, 2008. 1(2): p. 338-346.
169. Kim, T.-W., et al., *Brassinosteroid signal transduction from cell surface receptor kinases to nuclear transcription factors.* Nature cell biology, 2009. 11(10): p. 1254-1260.
170. Jonak, C. and H. Hirt, *Glycogen synthase kinase 3/SHAGGY-like kinases in plants: an emerging family with novel functions.* Trends in Plant Science, 2002. 7(10): p. 457-461.
171. Kim, T.W., et al., *Brassinosteroid regulates stomatal development by GSK3-mediated inhibition of a MAPK pathway.* Nature, 2012. 482(7385): p. 419-U1526.
172. Lukowitz, W., et al., *A MAPKK kinase gene regulates extra-embryonic cell fate in Arabidopsis.* Cell, 2004. 116(1): p. 109-19.
173. Bergmann, D.C., W. Lukowitz, and C.R. Somerville, *Stomatal Development and Pattern Controlled by a MAPKK Kinase.* Science, 2004. 304(5676): p. 1494-1497.
174. Wang, H., et al., *Stomatal Development and Patterning Are Regulated by Environmentally Responsive Mitogen-Activated Protein Kinases in Arabidopsis.* The Plant Cell, 2007. 19(1): p. 63-73.
175. Khan, M., et al., *Brassinosteroid-regulated GSK3/Shaggy-like Kinases Phosphorylate Mitogen-activated Protein (MAP) Kinase Kinases, Which Control Stomata Development in Arabidopsis thaliana.* Journal of Biological Chemistry, 2013. 288(11): p. 7519-7527.
176. Gudesblat, G.E., et al., *SPEECHLESS integrates brassinosteroid and stomata signalling pathways.* Nature Cell Biology, 2012. 14(5): p. 548-U214.
177. Yang, K.Z., et al., *Phosphorylation of Serine 186 of bHLH Transcription Factor SPEECHLESS Promotes Stomatal Development in Arabidopsis.* Molecular Plant, 2015. 8(5): p. 783-795.
178. Takahashi, Y., et al., *bHLH Transcription Factors That Facilitate K+ Uptake During Stomatal Opening Are Repressed by Abscisic Acid Through Phosphorylation.* Science Signaling, 2013. 6(280): p. ra48.
179. Leonhardt, N., et al., *Microarray Expression Analyses of Arabidopsis Guard Cells and Isolation of a Recessive Abscisic Acid Hypersensitive Protein Phosphatase 2C Mutant.* The Plant Cell, 2004. 16(3): p. 596.
180. Takahashi, Y., et al., *Inhibition of the Arabidopsis bHLH transcription factor by monomerization through abscisic acid-induced phosphorylation.* The Plant Journal, 2016. 87(6): p. 559-567.
181. Fankhauser, C. and J. Chory, *RSF1, an Arabidopsis locus implicated in phytochrome A signaling.* Plant Physiology, 2000. 124(1): p. 39-45.
182. Fairchild, C.D., M.A. Schumaker, and P.H. Quail, *HFR1 encodes an atypical bHLH protein that acts in phytochrome A signal transduction.* Genes & Development, 2000. 14(18): p. 2377-2391.

183. Soh, M.S., et al., *REP1, a basic helix-loop-helix protein, is required for a branch pathway of phytochrome A signaling in arabidopsis.* Plant Cell, 2000. 12(11): p. 2061-74.
184. Duek, P.D. and C. Fankhauser, *HFR1, a putative bHLH transcription factor, mediates both phytochrome A and cryptochrome signalling.* Plant J, 2003. 34(6): p. 827-36.
185. Duek, P.D., et al., *The degradation of HFR1, a putative bHLH class transcription factor involved in light signaling, is regulated by phosphorylation and requires COP1.* Current Biology, 2004. 14(24): p. 2296-2301.
186. Yang, J.P., et al., *Light regulates COP1-mediated degradation of HFR1, a transcription factor essential for light signaling in arabidopsis.* Plant Cell, 2005. 17(3): p. 804-821.
187. Jang, I.C., et al., *HFR1 is targeted by COP1 E3 ligase for post-translational proteolysis during phytochrome A signaling.* Genes Dev, 2005. 19(5): p. 593-602.
188. Park, H.J., et al., *Multisite phosphorylation of Arabidopsis HFR1 by casein kinase II and a plausible role in regulating its degradation rate.* J Biol Chem, 2008. 283(34): p. 23264-73.
189. Al-Sady, B., et al., *Photoactivated phytochrome induces rapid PIF3 phosphorylation prior to proteasorne-mediated degradation.* Molecular Cell, 2006. 23(3): p. 439-446.
190. Nozue, K., et al., *Rhythmic growth explained by coincidence between internal and external cues.* Nature, 2007. 448(7151): p. 358-U11.
191. Shen, H., J. Moon, and E. Huq, *PIF1 is regulated by light-mediated degradation through the ubiquitin-26S proteasome pathway to optimize photomorphogenesis of seedlings in Arabidopsis.* Plant J, 2005. 44(6): p. 1023-35.
192. Shen, Y., et al., *Phytochrome induces rapid PIF5 phosphorylation and degradation in response to red-light activation.* Plant Physiology, 2007. 145(3): p. 1043-1051.
193. Lorrain, S., et al., *Phytochrome-mediated inhibition of shade avoidance involves degradation of growth-promoting bHLH transcription factors.* Plant Journal, 2008. 53(2): p. 312-323.
194. Park, E., et al., *Degradation of phytochrome interacting factor 3 in phytochrome-mediated light signaling.* Plant Cell Physiol, 2004. 45(8): p. 968-75.
195. Monte, E., et al., *The phytochrome-interacting transcription factor, PIF3, acts early, selectively, and positively in light-induced chloroplast development.* Proc Natl Acad Sci U S A, 2004. 101(46): p. 16091-8.
196. Bhattacharya, J., U.K. Singh, and A. Ranjan, *Interaction of Light and Temperature Signaling at the Plant Interphase: From Cue to Stress*, in *Plant Tolerance to Individual and Concurrent Stresses*, M. Senthil-Kumar, Editor. 2017, Springer India: New Delhi. p. 111-132.
197. Bernardo-García, S., et al., *BR-dependent phosphorylation modulates PIF4 transcriptional activity and shapes diurnal hypocotyl growth.* Genes & Development, 2014. 28(15): p. 1681-1694.
198. Bu, Q., et al., *Phosphorylation by CK2 Enhances the Rapid Light-induced Degradation of Phytochrome Interacting Factor 1 in Arabidopsis.* The Journal of Biological Chemistry, 2011. 286(14): p. 12066-12074.
199. Ni, W., et al., *PPKs mediate direct signal transfer from phytochrome photoreceptors to transcription factor PIF3.* Nat Commun, 2017. 8: p. 15236.
200. Shin, A.Y., et al., *Evidence that phytochrome functions as a protein kinase in plant light signalling.* Nature Communications, 2016. 7.
201. Yaffe, M.B. and A.E.H. Elia, *Phosphoserine/threonine-binding domains.* Current Opinion in Cell Biology, 2001. 13(2): p. 131-138.
202. Yaffe, M.B., et al., *The structural basis for 14-3-3 : phosphopeptide binding specificity.* Cell, 1997. 91(7): p. 961-971.

203. Muslin, A.J., et al., *Interaction of 14-3-3 with Signaling Proteins Is Mediated by the Recognition of Phosphoserine.* Cell, 1996. 84(6): p. 889-897.
204. Gampala, S.S., et al., *An essential role for 14-3-3 proteins in brassinosteroid signal transduction in Arabidopsis.* Developmental Cell, 2007. 13(2): p. 177-189.
205. Guo, X., S. Xu, and K. Chong, *Cold Signal Shuttles from Membrane to Nucleus.* Molecular Cell, 2017. 66(1): p. 7-8.
206. Liu, Z.Y., et al., *Plasma Membrane CRPK1-Mediated Phosphorylation of 14-3-3 Proteins Induces Their Nuclear Import to Fine-Tune CBF Signaling during Cold Response.* Molecular Cell, 2017. 66(1): p. 117.
207. Cotelle, V., et al., *14-3-3s regulate global cleavage of their diverse binding partners in sugar-starved Arabidopsis cells.* The EMBO Journal, 2000. 19(12): p. 2869-2876.
208. Betts, M.J., et al., *Systematic identification of phosphorylation-mediated protein interaction switches.* PLOS Computational Biology, 2017. 13(3): p. e1005462.
209. Fan, H., et al., *SKB1/PRMT5-mediated histone H4R3 dimethylation of Ib subgroup bHLH genes negatively regulates iron homeostasis in Arabidopsis thaliana.* The Plant Journal, 2014. 77(2): p. 209-221.
210. Xing, J., et al., *GENERAL CONTROL NONREPRESSED PROTEIN5-Mediated Histone Acetylation of FERRIC REDUCTASE DEFECTIVE3 Contributes to Iron Homeostasis in Arabidopsis.* Plant Physiol, 2015. 168(4): p. 1309-20.
211. Zhao, Q., et al., *Ubiquitination-Related MdBT Scaffold Proteins Target a bHLH Transcription Factor for Iron Homeostasis.* Plant Physiology, 2016. 172(3): p. 1973-1988.
212. Barberon, M., et al., *Monoubiquitin-dependent endocytosis of the iron-regulated transporter 1 (IRT1) transporter controls iron uptake in plants.* Proc Natl Acad Sci U S A, 2011. 108(32): p. E450-8.
213. Kerkeb, L., et al., *Iron-induced turnover of the Arabidopsis IRON-REGULATED TRANSPORTER1 metal transporter requires lysine residues.* Plant Physiol, 2008. 146(4): p. 1964-73.
214. Shin, L.J., et al., *IRT1 DEGRADATION FACTOR1, a RING E3 Ubiquitin Ligase, Regulates the Degradation of IRON-REGULATED TRANSPORTER1 in Arabidopsis.* Plant Cell, 2013. 25(8): p. 3039-3051.
215. Ivanov, R. and P. Bauer, *Sequence and coexpression analysis of iron-regulated ZIP transporter genes reveals crossing points between iron acquisition strategies in green algae and land plants.* Plant and Soil, 2017. 418(1-2): p. 61-73.
216. Ye, L.X., et al., *MPK3/MPK6 are involved in iron deficiency-induced ethylene production in Arabidopsis.* Frontiers in Plant Science, 2015. 6.
217. Liu, Y.D. and S.Q. Zhang, *Phosphorylation of 1-aminocyclopropane-1-carboxylic acid synthase by MPK6, a stress-responsive mitogen-activated protein kinase, induces ethylene biosynthesis in Arabidopsis.* Plant Cell, 2004. 16(12): p. 3386-3399.
218. Joo, S., et al., *MAPK phosphorylation-induced stabilization of ACS6 protein is mediated by the non-catalytic C-terminal domain, which also contains the cis-determinant for rapid degradation by the 26S proteasome pathway.* Plant J, 2008. 54(1): p. 129-40.
219. Han, L., et al., *Mitogen-activated protein kinase 3 and 6 regulate Botrytis cinerea-induced ethylene production in Arabidopsis.* Plant Journal, 2010. 64(1): p. 114-127.
220. Mao, G., et al., *Phosphorylation of a WRKY transcription factor by two pathogen-responsive MAPKs drives phytoalexin biosynthesis in Arabidopsis.* Plant Cell, 2011. 23(4): p. 1639-53.
221. Li, G.J., et al., *Dual-Level Regulation of ACC Synthase Activity by MPK3/MPK6 Cascade and Its Downstream WRKY Transcription Factor during Ethylene Induction in Arabidopsis.* Plos Genetics, 2012. 8(6).

222. Li, S., et al., *Mitogen-activated protein kinases and calcium-dependent protein kinases are involved in wounding-induced ethylene biosynthesis in Arabidopsis thaliana.* Plant Cell Environ, 2017.
223. Chae, H.S. and J.J. Kieber, *Eto Brute? Role of ACS turnover in regulating ethylene biosynthesis.* Trends in Plant Science, 2005. 10(6): p. 291-296.
224. Romera, F.J., E. Alcantara, and M.D. De la Guardia, *Ethylene production by Fe-deficient roots and its involvement in the regulation of Fe-deficiency stress responses by strategy I plants.* Annals of Botany, 1999. 83(1): p. 51-55.
225. Romera, F.J. and E. Alcantara, *Ethylene involvement in the regulation of Fe-deficiency stress responses by Strategy I plants.* Functional Plant Biology, 2004. 31(4): p. 315-328.
226. Lucena, C., et al., *Ethylene could influence ferric reductase, iron transporter, and H+-ATPase gene expression by affecting FER (or FER-like) gene activity.* J Exp Bot, 2006. 57(15): p. 4145-54.
227. Tian, Q.Y., et al., *CIPK23 is involved in iron acquisition of Arabidopsis by affecting ferric chelate reductase activity.* Plant Science, 2016. 246: p. 70-79.
228. Xu, J., et al., *A protein kinase, interacting with two calcineurin B-like proteins, regulates K+ transporter AKT1 in Arabidopsis.* Cell, 2006. 125(7): p. 1347-60.
229. Baunsgaard, L., et al., *The 14-3-3 proteins associate with the plant plasma membrane H(+)-ATPase to generate a fusicoccin binding complex and a fusicoccin responsive system.* Plant J, 1998. 13(5): p. 661-71.
230. Jahn, T., et al., *The 14-3-3 protein interacts directly with the C-terminal region of the plant plasma membrane H (+)-ATPase.* The Plant Cell, 1997. 9(10): p. 1805-1814.
231. Oecking, C., et al., *Topology and target interaction of the fusicoccin- binding 14- 3-3 homologs of Commelina communis.* The Plant Journal, 1997. 12(2): p. 441-453.
232. Fullone, M.R., et al., *Fusicoccin effect on the in vitro interaction between plant 14-3-3 proteins and plasma membrane H+-ATPase.* Journal of Biological Chemistry, 1998. 273(13): p. 7698-7702.
233. Fuglsang, A.T., et al., *Binding of 14-3-3 protein to the plasma membrane H(+)-ATPase AHA2 involves the three C-terminal residues Tyr(946)-Thr-Val and requires phosphorylation of Thr(947).* J Biol Chem, 1999. 274(51): p. 36774-80.
234. Kinoshita, T. and K.i. Shimazaki, *Blue light activates the plasma membrane H(+)-ATPase by phosphorylation of the C-terminus in stomatal guard cells.* The EMBO Journal, 1999. 18(20): p. 5548-5558.
235. Svennelid, F., et al., *Phosphorylation of Thr-948 at the C terminus of the plasma membrane H(+)-ATPase creates a binding site for the regulatory 14-3-3 protein.* The Plant Cell, 1999. 11(12): p. 2379-2391.
236. Maudoux, O., et al., *A plant plasma membrane H+-ATPase expressed in yeast is activated by phosphorylation at its penultimate residue and binding of 14-3-3 regulatory proteins in the absence of fusicoccin.* Journal of Biological Chemistry, 2000. 275(23): p. 17762-17770.
237. Fuglsang, A.T., et al., *Receptor kinase-mediated control of primary active proton pumping at the plasma membrane.* The Plant Journal, 2014. 80(6): p. 951-964.
238. Niittyla, T., et al., *Temporal analysis of sucrose-induced phosphorylation changes in plasma membrane proteins of Arabidopsis.* Mol Cell Proteomics, 2007. 6(10): p. 1711-26.
239. Fuglsang, A.T., et al., *Arabidopsis protein kinase PKS5 inhibits the plasma membrane H+ -ATPase by preventing interaction with 14-3-3 protein.* Plant Cell, 2007. 19(5): p. 1617-34.

240. Nuhse, T.S., et al., *Quantitative phosphoproteomic analysis of plasma membrane proteins reveals regulatory mechanisms of plant innate immune responses.* Plant J, 2007. 51(5): p. 931-40.
241. Haruta, M., et al., *A peptide hormone and its receptor protein kinase regulate plant cell expansion.* Science, 2014. 343(6169): p. 408-11.
242. Haruta, M., W.M. Gray, and M.R. Sussman, *Regulation of the plasma membrane proton pump (H+-ATPase) by phosphorylation.* Current opinion in plant biology, 2015. 28: p. 68-75.

6 Manuscript 1

CIPK11-dependent phosphorylation modulates dynamic cellular activity of the key transcription factor FIT, promoting iron acquisition.

CIPK11-dependent phosphorylation modulates dynamic cellular activity of the key transcription factor FIT, promoting iron acquisition

Regina Gratz,[1,5] Prabha Manishankar,[2,5] Rumen Ivanov,[1] Philipp Köster,[2] Inga Mohr,[1] Ksenia Trofimov,[1] Leonie Steinhorst,[2] Johannes Meiser,[1] Maria Drerup,[2] Sibylle Arendt,[2] Michael Holtkamp,[3] Uwe Karst,[3] Jörg Kudla,[2] Petra Bauer[1,4,6,7], and Tzvetina Brumbarova[1,6]

[1] Institute of Botany, Heinrich-Heine University, 40225 Düsseldorf, Germany
[2] Institute of Plant Biology and Biotechnology, University of Münster, 48149 Münster, Germany
[3] Institute of Inorganic and Analytical Chemistry, University of Münster, 48149 Münster, Germany
[4] Cluster of Excellence on Plant Sciences, Heinrich-Heine University, 40225 Düsseldorf, Germany
[5] Co-first Author
[6] Shared Corresponding Authors
[7] Lead Contact

* Correspondence: Tzvetina.Brumbarova@uni-duesseldorf.de (T. B.),
Petra.Bauer@uni-duesseldorf.de (P. B.)

SUMMARY

Nutrient acquisition is entangled with growth and stress in sessile organisms. The bHLH transcription factor FIT is a key regulator of Arabidopsis iron (Fe) acquisition and post-translationally activated upon low Fe. Based on protein interaction screens we identified CBL-INTERACTING PROTEIN KINASE CIPK11 to phosphorylate FIT at Ser272. Cytosolic Ca^{2+} concentration and *CIPK11* expression are induced by Fe-deficiency. *cipk11* mutant plants display compromised root Fe mobilization and seed Fe content. Fe uptake is dependent on CBL1/CBL9. Mutation of the CIPK11 phosphorylation target site, Ser272, modulates cellular and *in planta* FIT nuclear accumulation, homo-dimerization, interaction with bHLH039 and transcriptional activity, and affects the plant's Fe uptake ability. We propose that Ca^{2+}-triggered CBL1/9-mediated activation of CIPK11 and subsequent phosphorylation of FIT shifts inactive into active FIT, allowing regulatory protein interactions in the nucleus. This biochemical link between Fe-deficiency and the cellular Ca^{2+} decoding machinery represents an environment-sensing mechanism to adjust nutrient uptake.

HIGHLIGHTS

- Iron-regulated and calcium-dependent protein kinase CIPK11 was identified in a screen to interact with FIT.
- CIPK11 phosphorylates FIT at Ser272 and activates iron deficiency responses, and iron acquisition.
- Mutation at FIT Ser272 modulates cellular and *in planta* FIT nuclear mobility, protein interactions and activity, affecting plant iron utilization capacity and seed iron content.

INTRODUCTION

Plant growth follows a progressive developmental path, being dynamically influenced by a changing environment that challenges sessile land organisms. This life style requires deep entanglement of parallel signaling pathways that process information cues to allow precise and coordinated decisions on plant development, physiology and stress response outputs.

In nutritional plant cell biology, iron uptake regulation is a model system for investigating integration of parallel signaling events. Nutrient, particularly iron (Fe), availability is of crucial importance for plant growth and development, and hence for the amount and quality of food available for humans. Fe is highly abundant in the soil but poorly accessible for plants (Guerinot and Yi, 1994). However, plants can actively mobilize Fe in the soil according to their needs. Many species, including the model plant Arabidopsis, use a reduction-based strategy, where Fe is solubilized through active proton (H^+) extrusion, then reduced at the root surface and imported in the form of bivalent Fe (Brumbarova et al., 2015). The lack of Fe triggers the induction of several clusters of genes responsible for the maintenance of Fe homeostasis (Ivanov et al., 2012; Mai et al., 2016). The basic helix-loop-helix (bHLH) FER-LIKE IRON DEFICIENCY-INDUCED TRANSCRIPTION FACTOR (FIT) plays a key role in regulating the Fe acquisition process in the roots of Arabidopsis to balance beneficial but also potentially harmful effects of Fe in the cells. Following the induced *FIT* gene expression in response to a regulatory Fe-deficiency cascade (Wang et al., 2007; Zhang et al., 2015; Li et al., 2016; Naranjo-Arcos et al., 2017), FIT upregulates the genes encoding the H^+ pump ARABIDOPSIS H^+-ATPase2 (AHA2), the FERRIC REDUCTASE-OXIDASE2 (FRO2) and the divalent metal ion transporter IRON-REGULATED TRANSPORTER1 (IRT1) (Colangelo and Guerinot, 2004; Jakoby et al., 2004; Yuan et al., 2005; Ivanov et al., 2012).

The response of the plant to Fe-deficiency is affected by different signaling pathways. FIT activity responds not only to the Fe status of the plant but also to different plant hormones like ethylene and gibberellic acid, and oxidative stress (Yuan et al., 2008; Lingam et al., 2011; Wang et al., 2013; Le et al., 2016; Wild et al., 2016). The integration of this information flow occurs through the post-translational regulation of FIT activity and results in adjusting the Fe-deficiency response to the environmental conditions (Brumbarova et al., 2015).

It was shown that FIT overexpression alone is not sufficient to induce downstream activation of FIT target genes, suggesting that FIT protein exists in active and inactive forms (Lingam et al., 2011; Meiser et al., 2011; Sivitz et al., 2011). FIT protein turnover, regulated by the 26S proteasome, was very pronounced under Fe-deficiency conditions, where FIT activity is crucial.

The current models suggest that the active FIT form is rapidly degraded and replaced through the activation of new molecules from the pool of inactive FIT (Lingam et al., 2011; Meiser et al., 2011; Sivitz et al., 2011).

Another important mechanism of FIT activity regulation is through protein-protein interactions. The four subgroup Ib (2) bHLH proteins, bHLH038, bHLH039, bHLH100, and bHLH101, are upregulated by Fe-deficiency (Wang et al., 2007). Their physical interaction with FIT activates it and induces FIT target genes (Yuan et al., 2008; Wang et al., 2013). The ethylene-responsive transcription factors ETHYLENE-INSENSITIVE3 (EIN3) and EIN3-LIKE1 (EIL1) also directly interact with and activate FIT, linking Fe uptake regulation and ethylene signaling at the molecular level (Lingam et al., 2011). On the other side, the abiotic stress-induced transcription factor ZINC FINGER OF ARABIDOPSIS THALIANA12 (ZAT12) negatively regulates FIT (Le et al., 2016). It was proposed that FIT can be kept in an inactive state by engaging in a complex with ZAT12, thus balancing FIT activity under conditions of prolonged Fe-deficiency or excess Fe to prevent the detrimental effects of reactive oxygen species (ROS) accumulation (Le et al., 2016). The gibberellin (GA)-responsive DELLA proteins inhibit the transcriptional activity of FIT in a root zone-specific manner by preventing FIT binding to its target promoters (Wild et al., 2016). It is tempting to speculate that active FIT molecules engage in protein interactions that promote FIT function and that interactions with negative FIT regulators serve to keep FIT inactive. However, it is still unclear how the pools of active and inactive FIT can be molecularly distinguished from each other, and which are the mechanisms that affect the formation of different regulatory protein-protein interactions of FIT.

Besides their nutrient autotrophy, sessile plants profit from their high competency to respond fast to environmental changes. Increase in cytosolic calcium concentration $[Ca^{2+}]_{cyt}$ serves as second messenger signaling. It is an ancient and versatile mechanism to transmit information among cells and cellular compartments. The large expansion of Ca^{2+}-decoding networks during plant evolution and their link with abiotic stress signaling argue in favor of a remarkable role that Ca^{2+} signaling plays during plant growth (Edel and Kudla, 2015). CBL-INTERACTING PROTEIN KINASEs (CIPKs), working together with calcineurin B-like proteins (CBLs), represent one class of Ca^{2+} signal decoders catalyzing serine/threonine protein phosphorylation elicited by different environmental stimuli (Batistic and Kudla, 2012; Shabala et al., 2016; Edel et al., 2017). CIPKs target enzymes, transporters and channels linked with abiotic stress, ion transport, reactive oxygen species (ROS) production but also nutrient transport (Quintero et al., 2002; Xu et al., 2006; Fuglsang et al., 2007; Lee et al., 2007; Ho et al., 2009; Drerup et al., 2013). Few reports indicate that CIPKs may also target transcription factor proteins and thereby

play an upstream regulatory role (Song et al., 2005; Lyzenga et al., 2013; Lumba et al., 2014; Zhou et al., 2015).

Here, we show that a member of this family, CIPK11, interacts with FIT and modulates FIT activity by phosphorylation at the target site Ser272. Using a phospho-mutant approach we can show that Ser272 impacts diverse cellular activities of FIT, namely transcription factor mobility, protein interaction and transcriptional regulation activity in plant cells and at whole plant level. Thus, CIPK11 is a positive factor that promotes Fe acquisition responses downstream of FIT. We propose that CIPK11 activation is triggered by an increased $[Ca^{2+}]_{cyt}$ sensed through plasma-membrane-localized CBL1/CBL9.

RESULTS

FIT interaction with CIPK family members is highly selective

Observations that FIT protein exists in active and inactive forms (Lingam et al., 2011; Meiser et al., 2011; Sivitz et al., 2011) prompted us to search for potential proteins and mechanisms involved in FIT protein modification. A previously reported yeast two-hybrid (Y2H) screen for FIT protein interaction partners enabled us to identify relevant FIT-interacting transcription factors (Lingam et al., 2011; Le et al., 2016). In this same screen, we also retrieved a member of the CIPK protein kinase family as a potential interactor. Since FIT protein interaction partners known to date are related to the composition of transcription factor complexes, a possible interaction of FIT with a protein kinase would represent a new mechanism of FIT regulation. Moreover, since CIPKs convey substrate phosphorylation upon interaction with and activation by Calcineurin B-like (CBL) Ca^{2+} sensor proteins, the association of FIT with a CIPK opened up the possibility that Ca^{2+} signaling may be involved in Fe-deficiency response regulation. In order to address the interaction specificity of the C-terminal part of FIT (FIT-C) (Lingam et al., 2011; Le et al., 2016) with different members of the CIPK family (Weinl and Kudla, 2009), we performed an extensive targeted yeast two-hybrid (Y2H) interaction assay with all annotated full-length CIPKs. From the 26 CIPKs, only two caused significant reporter gene activation, indicative of interaction with FIT, namely CIPK11 and CIPK21 (Figure 1). Interestingly, both *CIPK11* and *CIPK21* genes are Fe-regulated in seedlings. *CIPK11* is upregulated, while *CIPK21* is downregulated under Fe-deficiency (Mai et al., 2016). *CIPK11* is also upregulated in the early root differentiation zone (Dinneny et al., 2008), which is primarily responsible for Fe uptake (Ivanov et al., 2012; Blum et al., 2014). The result of the

Y2H screen against the full CIPK family points out that the interaction of FIT with CIPK proteins is highly selective and involves only Fe-regulated members of the family.

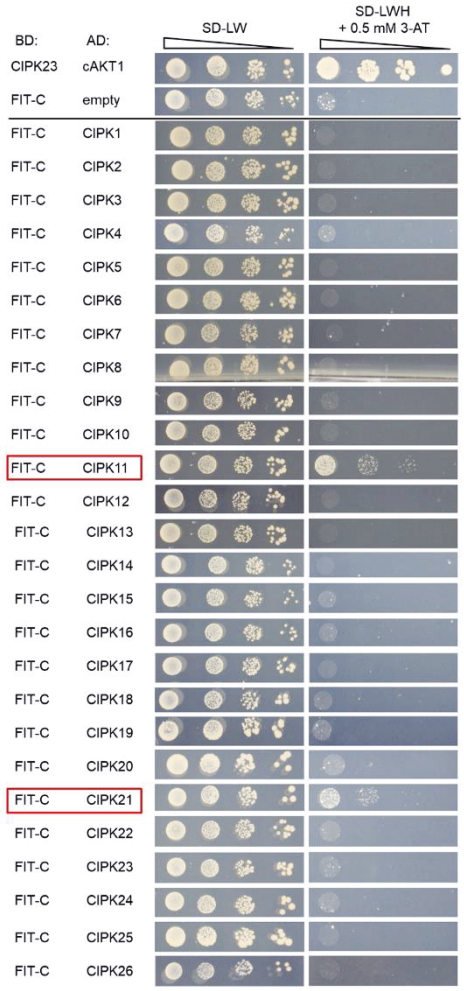

Figure 1. Selective interaction between FIT and CIPK family members.

Targeted Y2H screen for protein interactions between the C-terminal part of FIT (FIT-C), fused to the DNA-binding domain (BD) of GAL4, and the full 26-member CIPK family. CIPK1 to CIPK26 were fused to the GAL4 activation domain (AD). Yeast co-transformed with different BD and AD plasmid combinations were spotted in parallel in ten-fold dilution series on SD-LW plates (co-transformation control) and on SD-LWH + 0.5 mM 3-AT plates (selection for protein interaction). CIPK23/cAKT1 served as a positive control (Xu et al., 2006), FIT-C/empty plasmid as a negative control. Plates were photographed after one-week incubation at 30 °C. The two strongest interactions are labeled with red boxes.

FIT and CIPK11 interact in plant cells

CIPK11, unlike *CIPK21*, is upregulated by Fe-deficiency (Mai et al., 2016). Therefore, CIPK11 represented a promising candidate for a kinase involved in Fe-deficiency-triggered signaling potentially leading to FIT activation and was selected for further investigations.

After reconfirming the interaction between FIT-C and CIPK11 in yeast (Figure 2A), we investigated whether *FIT* and *CIPK11* are expressed in similar parts of the plant. We analyzed Arabidopsis plants stably transformed with *FIT* or *CIPK11* promoters driving the β-glucuronidase (GUS) reporter gene. Indeed, the spatial expression pattern revealed that *FIT* and *CIPK11* are expressed in similar root zones (Figure 2B and Supplemental Figure 1). *FIT* promoter activity was detected throughout the root differentiation zone, as previously reported (Jakoby et al., 2004). *CIPK11* promoter activity was absent at the root tip, while it was mainly present in the epidermis, including root hair cells, of the early root differentiation zone in the two examined lines. The similar expression pattern of *FIT* and *CIPK11* promoters, especially

in the early root differentiation zone, where the majority of Fe uptake takes place (Ivanov et al., 2012; Blum et al., 2014), suggested that FIT and CIPK11 could exert their function in the same cells. FIT and CIPK11 also share a similar subcellular localization. Nuclear and cytoplasmic GFP signals were detected for both FIT-GFP and GFP-CIPK11 (Figure 2C). The localization of both proteins did not change when FIT-mCherry and GFP-CIPK11 were co-transformed into the same plant cells (Figure 2D). Thus, FIT and CIPK11 proteins co-localize inside plant cells. *In planta* interaction between FIT and CIPK11 was confirmed by bimolecular fluorescence complementation (BiFC) (Figure 2E). YFP fluorescent signals, indicative of an interaction between FIT and CIPK11, were detected predominantly in the nucleus and weakly in the cytoplasm of plant cells. No interaction was observed between CIPK11 and another Fe-regulated bHLH transcription factor that interacts with FIT, bHLH039 (Yuan et al., 2008), or between FIT and another CIPK, CIPK15, which did not show interaction with FIT-C in the Y2H assay against the CIPK family (Figure 1). These negative BiFC controls underline the specificity of the CIPK11-FIT interaction.

Taken together, *FIT* and *CIPK11* are induced by Fe-deficiency, the proteins interact with each other and function in the same subcellular compartments, and root zones.

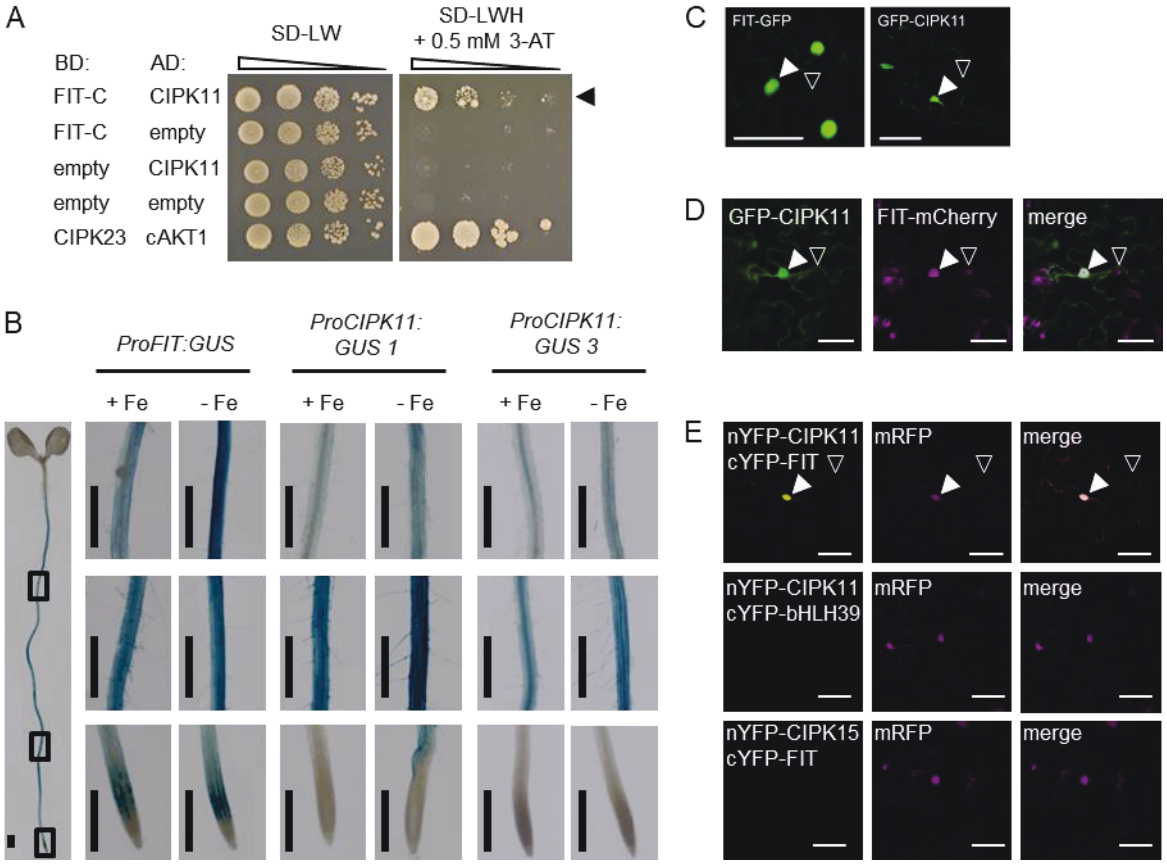

Figure 2. FIT and CIPK11 co-localize and interact with each other.

(A) Targeted Y2H interaction assay for investigating the interaction of the C-terminal part of FIT (FIT-C), fused to the DNA-binding domain (BD) of GAL4, with CIPK11, fused to the GAL4 activation domain (AD). Yeast co-

transformed with different BD and AD plasmid combinations were spotted in parallel in ten-fold dilution series on a SD-LW plate (co-transformation control) and on a SD-LWH + 0.5 mM 3-AT plate (selection for protein interaction). CIPK23/cAKT1 served as a positive control (Xu et al., 2006), combinations with empty plasmids as negative controls. An arrow indicates the physical interaction between FIT-C and CIPK11. **(B)** Promoter-driven GUS reporter activity in roots. Transgenic plants with *ProFIT:GUS* and *ProCIPK11:GUS* (lines 1 and 3) were grown in the 6-day system under sufficient (+ Fe) or deficient (- Fe) supply and stained for GUS activity. Rectangles in the left side seedling picture indicate the positions of the enlarged images corresponding to, from top to bottom, the differentiated cell zone, the early differentiation zone, and the root tip. Bars: 1 mm. Full-size plants are shown in Supplemental Figure 1. **(C)** Laser-scanning confocal images showing GFP fluorescence of FIT-GFP and GFP-CIPK11 in tobacco leaf epidermis cells. Nuclear and cytoplasmic GFP fluorescence signals are indicated by arrowheads (filled and empty, respectively). Bars: 50 µm. **(D)** Laser-scanning confocal images showing co-localization of GFP-CIPK11 and FIT-mCherry in tobacco leaf epidermis cells. Arrowheads show examples of co-localized GFP and mCherry fluorescent signals in the nucleus (filled arrowheads) and in the cytoplasm (empty arrowheads). Bars: 50 µm. **(E)** Laser-scanning confocal images showing Bimolecular Fluorescence Complementation (BiFC) of nYFP-CIPK11 and cYFP-FIT in tobacco leaf epidermis cells. nYFP-CIPK11 and cYFP-bHLH039, as well as nYFP-CIPK15 and cYFP-FIT, serve as negative control pairs with a non-interacting related bHLH TF and a non-interacting CIPK, respectively. Reconstituted YFP signals are indicated by arrowheads (filled for nuclear YFP, empty for cytoplasmic YFP). The interaction between FIT and CIPK11 was detected predominantly in the nucleus. Presence of mRFP signal served as a transformation control. Bars: 50 µm.

CIPK11 is a positive regulator of FIT-dependent Fe-deficiency responses

To genetically address the function of CIPK11 in FIT-dependent Fe acquisition, we examined the Fe-deficiency responses of *cipk11* loss-of-function mutant plants (Fuglsang et al., 2007) and three independent *cipk11*-complemented plant lines. Under Fe-deficiency, wild-type (WT) plants had increased root length compared to Fe-sufficient conditions, potentially representing a foraging strategy of exploiting the medium for Fe. At the same time, the severely Fe-deficient *fit* loss-of-function mutant was unable to sustain this growth response. In contrast, *cipk11* mutants displayed an even further increased root length compared to WT under both Fe supply conditions, a phenotype which was reverted in *cipk11*-complemented lines (Supplemental Figure 2A, B). The compromised Fe-deficiency response phenotype of *cipk11* roots indicated that CIPK11 might fine-tune Fe acquisition responses.

Because of the protein interaction with FIT we tested the hypothesis that CIPK11 might possibly affect Fe-deficiency responses through regulating FIT. *FRO2* and *IRT1* are generally used as marker genes for the responsiveness of a plant to limited Fe supply (Colangelo and Guerinot, 2004; Jakoby et al., 2004; Yuan et al., 2005; Lingam et al., 2011; Ivanov et al., 2012). Gene expression analysis confirmed the genotypes of the plant lines analyzed with respect to *cipk11* loss-of-function and complementation (Figure 3A). The three *cipk11*-complemented

lines showed *CIPK11* expression levels that exceeded WT levels (Figure 3A). *CIPK11* was induced in WT roots upon Fe-deficiency and expressed at similar level in WT and *fit* (Figure 3A). Since *CIPK11* was not expressed at higher level in the Fe-deficient *fit* mutant plants than in WT, we conclude that *CIPK11* is not a direct target gene of the core Fe-deficiency regulon controlled by FIT and bHLH039. *FIT* transcript levels were not significantly deregulated in *cipk11*, and only one out of the three complemented lines showed enhanced *FIT* expression at – Fe versus + Fe conditions (Figure 3B). *BHLH039* is one of the four *BHLH* genes from subgroup Ib (2) that is upregulated by Fe-deficiency and functions upstream of FIT in the Fe-deficiency response signaling cascade (Wang et al., 2007; Zhang et al., 2015; Li et al., 2016; Naranjo-Arcos et al., 2017). *BHLH039* transcript abundance was not dependent on CIPK11, indicating that the upstream Fe-deficiency response signaling cascade was not perturbed in *cipk11* (Figure 3C). However, lack of functional CIPK11 led to downregulation of the transcript abundance of the FIT target genes *FRO2* (Figure 3D) and *IRT1* (Figure 3E) under deficient Fe supply, although not to the same extent as in *fit* mutants. In the *cipk11*-complemented lines, *FRO2* and *IRT1* transcript levels were again restored at least to WT levels (Figure 3D, E). Interestingly, the expression of Fe homeostasis genes co-regulated with *BHLH039*, *NICOTIANAMINE SYNTHASE4* (*NAS4*) and *FERRIC REDUCTASE OXIDASE3* (*FRO3*) was not affected by the lack of functional CIPK11 (Figure 3F, G), and was very similar to that described above for *BHLH039* (Figure 3F, G). These findings argue against a function of CIPK11 further upstream of FIT, suggesting that CIPK11 directly affects Fe signaling at the level of FIT. Moreover, CIPK11 plays a positive role in regulating FIT target genes, but not in regulating Fe-deficiency genes, that are not targets of FIT, such as *BHLH039*, *NAS4* or *FRO3*. Physiological analyses confirmed the Fe-deficiency response phenotype of *cipk11* mutant plants observed at the gene expression level. Root ferric reductase activity represents a physiological read-out for the plant's response when exposed to Fe limitation (Robinson et al., 1999). Indeed, *cipk11* mutant plants showed reduced Fe reductase activity in comparison to the WT under Fe-deficient conditions, whereas the *cipk11*-complemented lines had Fe reductase activity levels similar to the WT, consistent with the observed *FRO2* transcript abundance in these plants (Figure 3H). Reduced Fe content of *cipk11* mutant seeds reflected the decreased capacity of the mutant to acquire Fe. Importantly, *cipk11*-complemented lines with elevated *CIPK11* gene expression showed a tendency to accumulate more Fe in their seeds (Figure 3I).

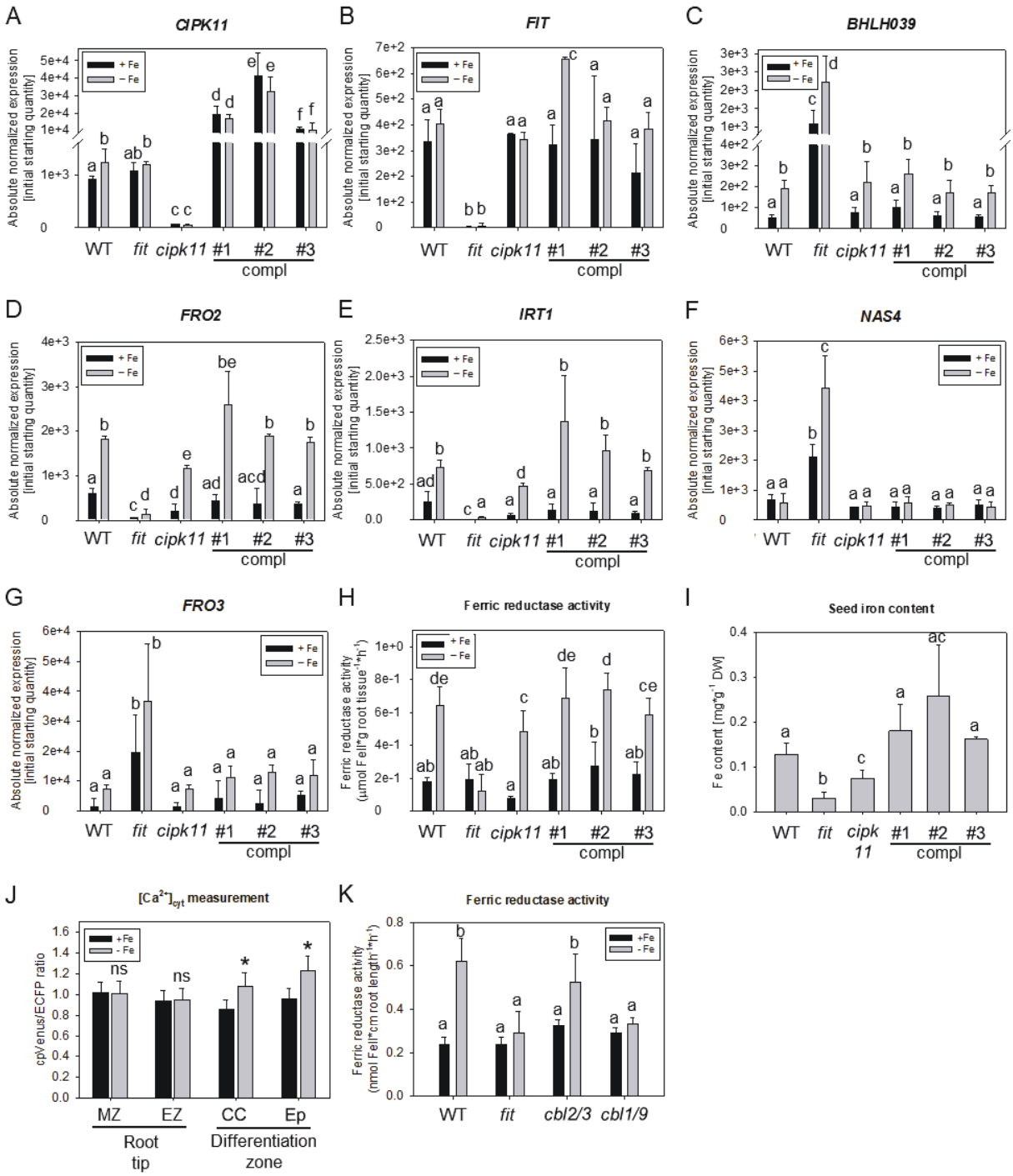

Figure 3. CIPK11 is a positive regulator of FIT-dependent Fe-deficiency responses.

cipk11 mutant and three *cipk11*-complemented lines (compl #1, #2, and #3) (A-H) or *cbl2/3* and *cbl1/9* double loss-of-function mutant plants (K) were analyzed in comparison with wild type (WT) and *fit* mutant. (A-H, K) Plants were grown in the 2-week system with sufficient (+Fe, black bars) and deficient (-Fe, gray bars) Fe supply. Error bars represent standard deviations. Different letters indicate statistically significant differences ($P < 0.05$). **(A-G)** Gene expression analysis in roots of *CIPK11* (A), *FIT* (B), *BHLH039* (C), *FRO2* (D), *IRT1* (E), *NAS4* (F), and *FRO3* (G). (n = 3) **(H)** Root Fe reductase activity. (n = 4) **(I)** Fe content of seeds collected from soil-grown plants. DW, dry weight. (n = 3) **(J)** Changes in free $[Ca^{2+}]_{cyt}$ in response to Fe-deficiency measured by ratiometric imaging of the genetically encoded Fluorescence Resonance Energy Transfer (FRET)-based Ca^{2+} sensor YC3.6. The emission ratios between cpVenus and ECFP fluorescence intensities indicate changes in free cytosolic $[Ca^{2+}]$

in roots of plants grown under sufficient (+Fe, black bars) and deficient (-Fe, gray bars) Fe supply. $[Ca^{2+}]_{cyt}$ changes were measured in different roots zones: meristematic (MZ) and elongation (EZ) of the root tip, central cylinder (CC) and epidermis (Epi) of the early root differentiation zone. Error bars represent standard deviations. Asterisks indicate statistically significant differences ($P < 0.05$) to the respective Fe sufficient condition of the same genotype. **(K)** Root Fe reductase activity. (n = 4)

Since the CBL-CIPK network serves to decode Ca^{2+} signals, we asked whether Fe-deficiency leads to a change in $[Ca^{2+}]_{cyt}$ in our growth conditions. Using the genetically encoded Ca^{2+} sensor Yellow Cameleon 3.6 (YC3.6) (Krebs et al., 2012), we could confirm an Fe-deficiency-dependent $[Ca^{2+}]_{cyt}$ increase in the early root differentiation zone. In this zone, crucial for Fe uptake (Ivanov et al., 2012; Blum et al., 2014), the $[Ca^{2+}]_{cyt}$ increase was observed both in the central cylinder and in the epidermis (Figure 3J, Supplemental Figure 2C). The existence of a Ca^{2+} signal in the context of Fe uptake regulation through CIPK11 raises the question of the identity of the potential Ca^{2+} sensor and the subcellular compartment where the sensing takes place. To answer this question we examined the Fe mobilization capacity of the double loss-of-function mutants *cbl2/3* (Eckert et al., 2014) and *cbl1/9* (Xu et al., 2006) representing plants deficient in Ca^{2+} perception at the tonoplast (Batistic et al., 2008; Tang et al., 2012) and the plasma membrane (D'Angelo et al., 2006; Cheong et al., 2007; Batistic et al., 2010), respectively (Figure 3K). The Fe reductase activity of *cbl2/3* mutant plants was not significantly different from that of WT plants under both sufficient and deficient Fe supply. However, *cbl1*/9 mutant plants were unable to induce Fe reductase activity under Fe-deficiency (Figure 3K), suggesting that the plasma membrane-localized CBL1 and CBL9, similarly to CIPK11, act as positive regulators of Fe uptake. In summary, CIPK11 function affected Fe-deficiency responses downstream of FIT in a positive manner. Hence, we conclude that CIPK11, potentially activated by CBL1/9-mediated Ca^{2+} sensing, positively modulates the activity of FIT through their protein interaction and the observed alterations in gene expression manifest physiologically in modulated Fe acquisition.

CIPK11 phosphorylates FIT at Ser272

Next, we asked whether differences in FIT activity could be attributed to differences in the FIT phosphorylation status, considering that FIT interacts with a protein kinase affecting Fe acquisition.

First, we looked for *in vivo* evidence of FIT phosphorylation. We employed phosphate affinity Zn^{2+}-Phos-tag SDS-PAGE which leads to retarded electrophoretic mobility of phosphorylated proteins in comparison to their corresponding non-phosphorylated forms (Kinoshita and

Kinoshita-Kikuta, 2011; Bekesova et al., 2015) in combination with HA-FIT immunodetection using transgenic HA_7-FIT plants (Meiser et al., 2011). Standard SDS-PAGE resulted in a single HA-FIT protein band (Supplemental Figure 3A), whereas the Phos-tag SDS-PAGE revealed three distinct HA-FIT protein bands (Supplemental Figure 3B), indicating the presence of phosphorylated HA-FIT in roots of Fe-sufficient and Fe-deficient plants. Calf Intestinal phosphatase (CIP) treatment of the protein extracts prior to electrophoresis led to a clear decrease in the relative protein abundance of the low mobility (LM) FIT form versus the total FIT pool (Supplemental Figure 3C), supporting the identity of the LM form as a phosphorylated form of HA-FIT. The two HA-FIT bands with high mobility were potentially non-phosphorylated or had a lower phosphorylation grade. Both extracts from plants grown under sufficient and deficient Fe supply showed the presence of a phosphorylated LM HA-FIT form. It is likely that FIT is phosphorylated under both Fe supply conditions at different FIT target sites, potentially also by different protein kinases.

We next proved that CIPK11 phosphorylates FIT. Since the interaction between CIPK11 and FIT in yeast involved the C-terminal part of FIT, we performed an *in silico* prediction of potential phosphorylation sites in this region (Figure 4A) and especially considered potential target sites that were conserved between FIT-C and the C-terminal part of SlFER, the tomato homolog of FIT (Ling et al., 2002; Yuan et al., 2005). This led to the identification of Ser272 as predicted potential FIT/SlFER phosphorylation site (Figure 4A). Site-directed mutagenesis was used to create non-phosphorylatable, FITm(AA), and phospho-mimicking, FITm(E), FIT forms to investigate the potential impact of Ser272 phosphorylation (Figure 4A).

We observed efficient phosphorylation of FIT and FIT-C by CIPK11 *in vitro* (Figure 4B). CIPK11 also underwent auto-phosphorylation which served as CIPK11 activity control. FIT or FIT-C without exposure to CIPK11 and StrepII-GST protein incubated with CIPK11 were not phosphorylated, confirming the specificity of the detected FIT phosphorylation. Both non-phosphorylatable FITm-C(AA) and phospho-mimicking FITm-C(E) forms displayed decreased radioactive signals when incubated with CIPK11 in comparison to the non-mutagenized FIT-C (Figure 4B), suggesting that Ser272 is a prominent CIPK11 target site in FIT-C.

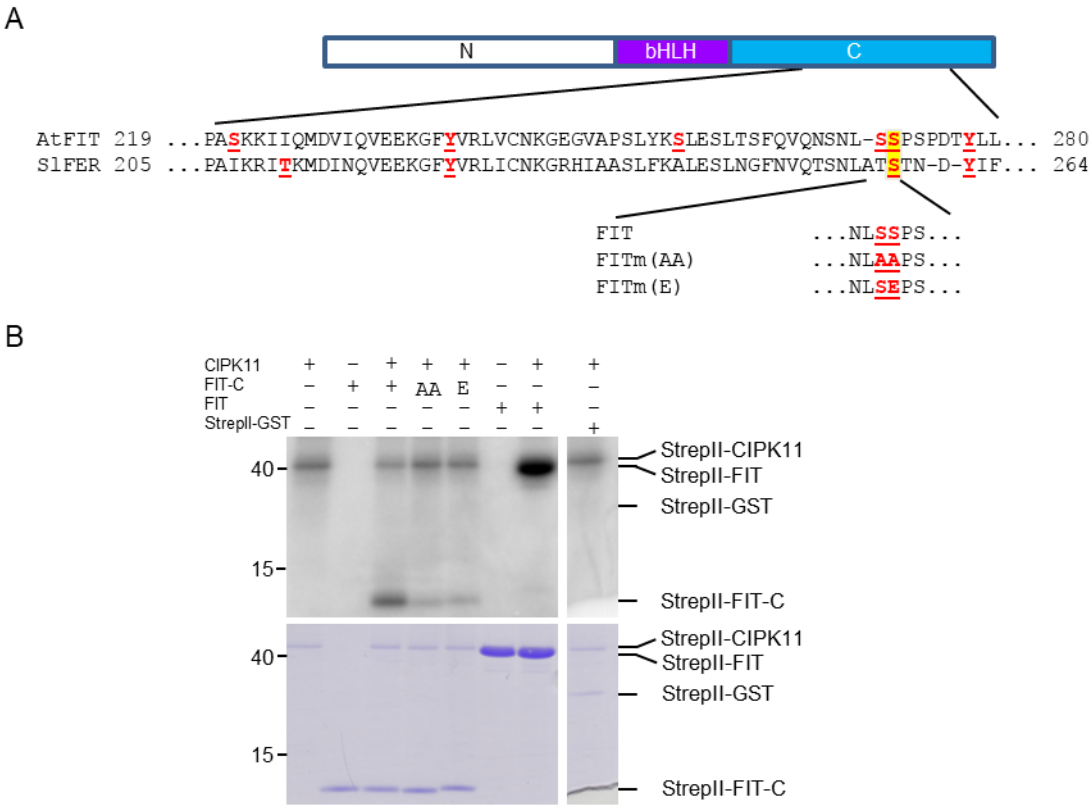

Figure 4. CIPK11 phosphorylates FIT at Ser272.

(A) NetPhos2.0 (http://www.cbs.dtu.dk/services/NetPhos-2.0/) predicts several Ser and Tyr residues in FIT-C as putative phosphorylation sites (highlighted in red and underlined). S272 (in yellow) is conserved between SlFER and AtFIT and was therefore selected as target site for further investigations. Non-phosphorylatable, FITm(AA), and phospho-mimicking, FITm(E), FITm forms were generated by site-directed mutagenesis for this site. **(B)** *In vitro* kinase assay. Affinity-purified recombinant StrepII-tagged CIPK11 (produced in a wheat germ-based cell-free system) and StrepII-tagged substrates (produced in *E. coli*) were incubated together in the assay, as specified by + and -. StrepII-FIT-C was assayed either as non-mutagenized protein or as phospho-mutant forms StrepII-FITm-C(AA) (AA) and StrepII-FITm(E) (E). StrepII-GST was used as a negative and specificity control. Lower panel, protein staining as loading control. Upper panel, auto-radiography image showing phosphorylation signals. Protein molecular weights (in kDa) are indicated on the left side of both panels. Respective protein bands are indicated on the right side. CIPK11 auto-phosphorylation served as a positive control for CIPK11 activity.

Ser272 phosphorylation target site mutation modulates the cellular localization, mobility, homo- and hetero-dimerization of FIT

Next, we investigated whether and how Ser272 phosphorylation status impacts on FIT functional properties. To this end, we first verified the functionality of the C-terminal GFP fusion of wild-type FIT and found that the Fe-deficient phenotype of *fit* mutant plants was rescued by constitutive expression of FIT-GFP. These FIT/*fit* plants expressed *FIT*, *BHLH039*, *FRO2*, and *IRT1* at levels comparable to the WT, and displayed WT-like Fe reductase activity and seed Fe content levels (Supplemental Figure 4).

The observation that this functional FIT-GFP was present both in the nucleus and in the cytoplasm (Figure 2C, D) implied that the amount of transcriptionally active nuclear FIT may be regulated through a partitioning between the nucleus and the cytoplasm, as shown for other transcription factors (Meier and Somers, 2011). We found that the non-phosphorylatable FITm(AA)-GFP form displayed enhanced accumulation in the cytoplasm compared to FIT-GFP, while the phospho-mimicking FITm(E)-GFP form did not show statistically significant difference from FIT-GFP in subcellular distribution (Figure 5A). In addition, protein mobility of nuclear FIT was affected by its phosphorylation status. Fluorescent Recovery after Photobleaching (FRAP) experiments revealed an increased mobility of the FITm(AA)-GFP form in comparison to FIT-GFP and FITm(E)-GFP (Figure 5B, Supplemental Figure 5). This suggests that FIT abundance and mobility in the nucleus are modulated by its phosphorylation status at Ser272.

Next, we addressed whether Ser272 mutations affect the transcription factor self-activation capacity of full-length BD-FIT in yeast (Figure 5C, Lingam et al., 2011). Indeed, we found that BD-FITm(AA) caused a decreased transcriptional self-activation in comparison to BD-FITm(E) and WT BD-FIT (Figure 5C), pointing out the importance of Ser272 phosphorylation for FIT transcription factor activity. Hence, Ser272 affects the cellular localization, nuclear mobility and self-activation capacities of FIT.

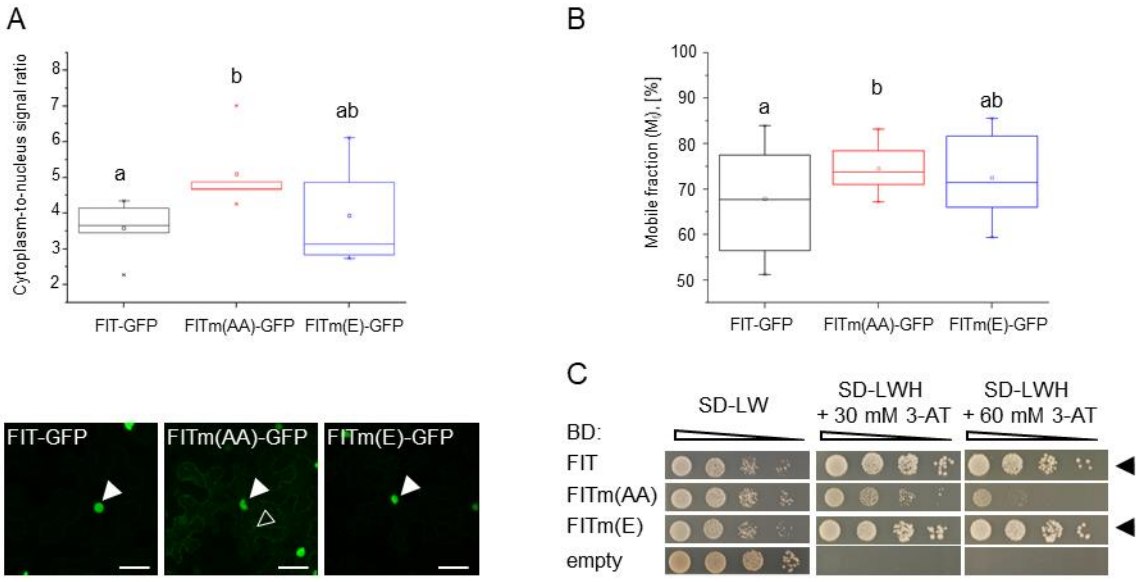

Figure 5. Mutation at the Ser272 phosphorylation target site alters FIT cellular localization, protein mobility and self-activation.

(A) Laser-scanning confocal imaging of the subcellular localization of FIT-GFP and FITm-GFP in plant cells. Upper part, quantification of the cytoplasm-to-nucleus GFP signal ratios for FIT-GFP (black), FITm(AA)-GFP (red) and FITm(E)-GFP (blue). (n=3). Lower part, representative images of GFP fluorescent signals in tobacco leaf epidermis cells transiently transformed with FIT-GFP, FITm(AA)-GFP and FITm(E)-GFP. Full and empty

arrowheads indicate nuclear and cytoplasmic GFP signals, respectively. Bars: 50 µm. **(B)** Protein mobility analysis of FIT-GFP and FITm-GFP by Fluorescence Recovery after Photobleaching (FRAP) in plant cells. The percentage of the mobile protein fraction for each FIT form was calculated from the recovery rate of its GFP fluorescence and shown for FIT-GFP (black), FITm(AA)-GFP (red) and FITm(E)-GFP (blue). (n = 12-21) **(C)** FIT and FITm transcriptional self-activation capacity assay. Yeast co-transformed with non-mutagenized or mutagenized BD-FIT and empty AD vector were spotted in parallel in ten-fold dilution series on a SD-LW plate (co-transformation control) and on SD-LWH + 30 and 60 mM 3-AT plates (selection for self-activation). Empty BD plasmids served as negative controls. Arrowheads indicate self-activation.

Proteins from the bHLH transcription factor family are known to form dimers (Heim et al., 2003). In order to understand the mechanism by which Ser272 phosphorylation of FIT affects its activity, we asked whether it can potentially alter the ability of FIT to form homo- or hetero-dimers. First, we used an Y2H assay to test the homo-dimerization of WT FIT-C and phospho-mutated FITm-C in yeast. As a result, FITm(AA)-C showed a decreased, and FITm(E)-C an increased tendency for homo-dimerization, compared to FIT-C (Figure 6A). FIT homo-dimer formation and its dependence on Ser272 phosphorylation status was further confirmed for full-length FIT forms *in planta* by Förster Resonance Energy Transfer - Acceptor Photo Bleaching (FRET-APB) (Figure 6B) and BiFC (Supplemental Figure 6) analyses. In both cases, non-phosphorylatable FIT displayed a reduced, and phospho-mimicking FIT an increased homo-dimerization capacity.

Since the physical interaction between bHLH039 and FIT was shown to be the key event leading to the activation of the downstream target genes in response to Fe-deficiency (Yuan et al., 2008; Wang et al., 2013), we investigated the effect of a potential FIT phosphorylation at Ser272 on the interaction between FIT and bHLH039. The hetero-dimerization assay between FIT-C and bHLH039 in yeast did not show significant differences in the interaction strength between FIT-C/bHLH039 and FITm-C/bHLH039 (Figure 6C). However, FRET-APB analysis of the interaction between full-length FIT or FITm and bHLH039 *in planta* revealed a decrease in FRET efficiency for the bHLH039-GFP/FITm(AA)-mCherry pair (Figure 6D). This suggests that the phosphorylation of the FIT C-terminus at Ser272 has a direct effect on FIT homo-dimerization but only indirectly affects the hetero-dimerization with bHLH039 in the nucleus, which may be dependent on a different interaction surface, probably the bHLH domain.

Taken together, the non-phosphorylatable FITm(AA) form showed an increased abundance in the cytoplasm and higher mobility, combined with a decreased homo-dimerization and bHLH039 interaction capacity in the nucleus. This is consistent with a decreased ability of FITm(AA) to participate in protein-protein interactions in the nucleus and, therefore, to remain active therein. This hypothesis is supported by the observation that FITm(AA) has a decreased

self-activation capacity, underlining the importance of the phosphorylation status of Ser272 for the proper localization and activity of FIT.

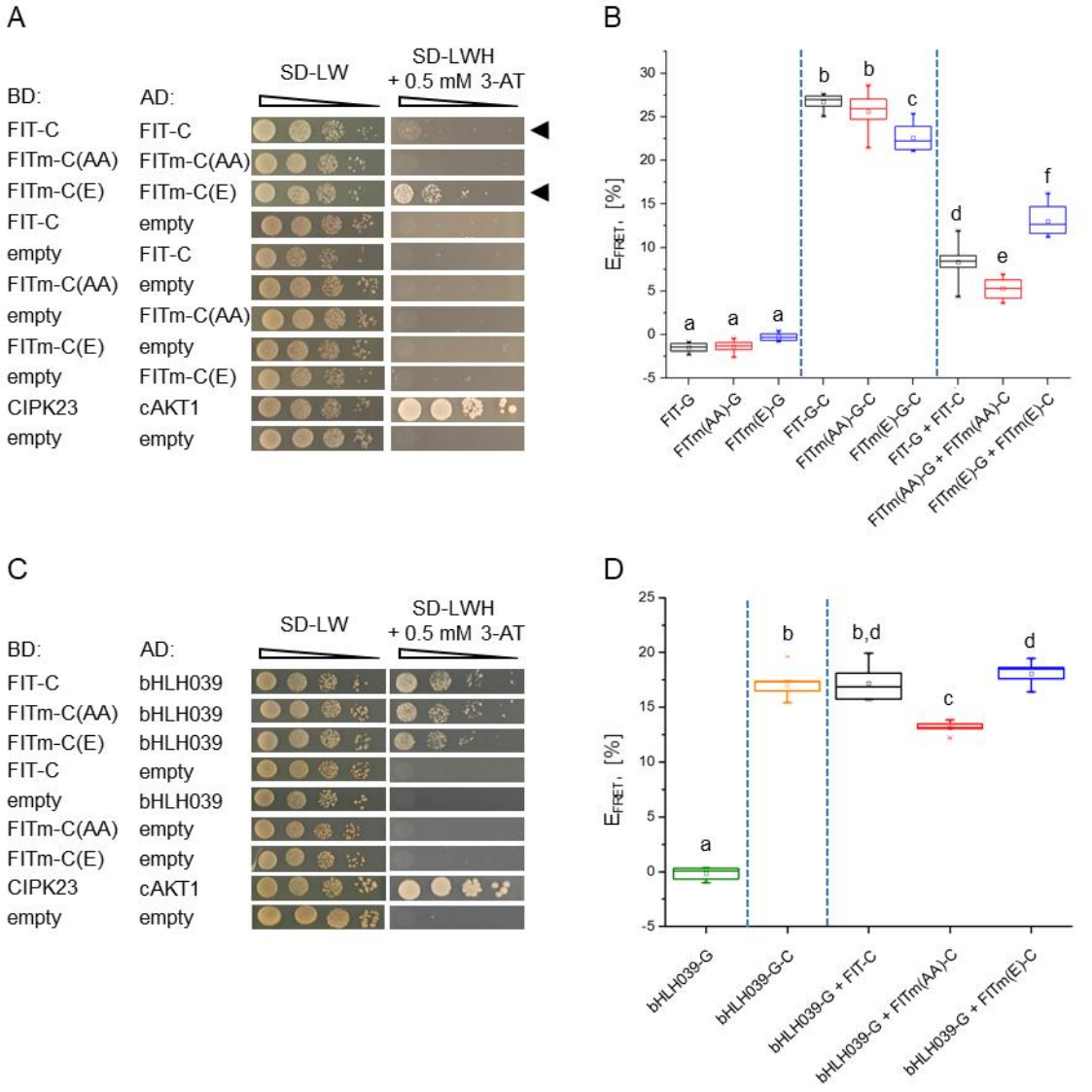

Figure 6. Mutation at the Ser272 phosphorylation target site alters FIT homo-dimerization and FIT-bHLH039 interaction.

(A) FIT protein homo-dimerization assay in yeast. Yeast co-transformed with different combinations of non-mutagenized and mutagenized BD- and AD-FIT-C/FITm-C vectors were spotted in parallel in ten-fold dilution series on a SD-LW plate (co-transformation control) and on SD-LWH + 0.5 mM 3-AT plates (selection for protein interaction). CIPK23/cAKT1 served as a positive control (Xu et al., 2006), empty plasmids as negative controls. Arrowheads indicate homo-dimerization. **(B)** FIT and FITm homo-dimerization *in planta*. Förster Resonance Energy Transfer - Acceptor Photo Bleaching (FRET-APB) for GFP and mCherry-tagged FIT and FITm couples was measured to assess the strength of homo-dimer formation in plant cell nuclei. GFP-tagged fusions were used as donor-only (negative) controls. Fusions of the respective proteins with both GFP and mCherry for intra-molecular FRET were used as positive controls. FRET efficiency (E_{FRET}) in percent was calculated as the relative increase of GFP intensity following photobleaching of the mCherry acceptor. G, GFP; C, mCherry; G-C, GFP-mCherry. Different letters indicate statistically significant differences ($P < 0.05$). (n = 10) **(C)** FIT-bHLH039

protein hetero-dimerization assay in yeast. Yeast co-transformed with different combinations of non-mutagenized and mutagenized BD-FIT-C/FITm-C and AD-bHLH039 vectors were spotted in parallel in ten-fold dilution series on a SD-LW plate (co-transformation control) and on SD-LWH + 0.5 mM 3-AT plates (selection for protein interaction). CIPK23/cAKT1 served as a positive control (Xu et al., 2006), empty plasmids as negative controls. Arrowheads indicate hetero-dimerization. **(D)** bHLH039 and FIT/FITm homo-dimerization *in planta*. FRET-APB for GFP-tagged bHLH039 and mCherry-tagged FIT/FITm couples was measured to assess the strength of hetero-dimer formation in plant cell nuclei. bHLH039-GFP was used as a donor-only (negative) control. bHLH039 fusion with both GFP and mCherry for intra-molecular FRET was used as a positive control. FRET efficiency (E_{FRET}) in percent was calculated as the relative increase of GFP intensity following photobleaching of the mCherry acceptor. G, GFP; C, mCherry; G-C, GFP-mCherry. Different letters indicate statistically significant differences ($P < 0.05$). ($n = 10$)

Mutation of the CIPK11 target site affects FIT activity *in vivo*

Loss of functional CIPK11 led to a decreased capacity of the plant to cope with Fe-deficiency (Figure 3) and mutation at the Ser272 phosphorylation target site of CIPK11 negatively affected FIT nuclear accumulation, activity and interaction capacity (Figures 4, 5 and 6). Therefore, we investigated whether plants stably expressing only a non-phosphorylatable FITm(AA) form in a *fit* mutant background would indeed exhibit Fe-deficiency phenotypes compared to the WT. Two independent FITm(AA)/*fit* lines were assayed for their ability to complement the *fit* mutant phenotype (Figure 7). Line AA#1 had *FIT* levels comparable to Fe-deficient WT and line AA#2 to Fe-sufficient WT (Figure 7A). Both lines were unable to fully rescue the *fit* mutant phenotype. This became evident by the increased *BHLH039* (Figure 7B) and decreased *FRO2* (Figure 7C), and *IRT1* (Figure 7D) transcript abundances in comparison to WT, which were in all cases similar to the corresponding levels in *fit*. Thus, even though phospho-mutated *FIT* transcript levels were comparable to the WT, this was not sufficient to reach the WT expression levels of the FIT target genes *FRO2* and *IRT1*. In contrast, complementation was clearly achieved in *fit* plants expressing non-mutated WT FIT-GFP (Supplemental Figure 4). Like *fit* mutants, AA#1 and AA#2 plants did not show increased Fe reductase activity upon Fe-deficiency (Figure 7E) and their seeds accumulated less Fe (Figure 7F) compared to WT. These results support the conclusion that the non-phosphorylatable mutation at Ser272 renders FIT less active and impedes its role as a transcriptional activator of *FRO2* and *IRT1*.

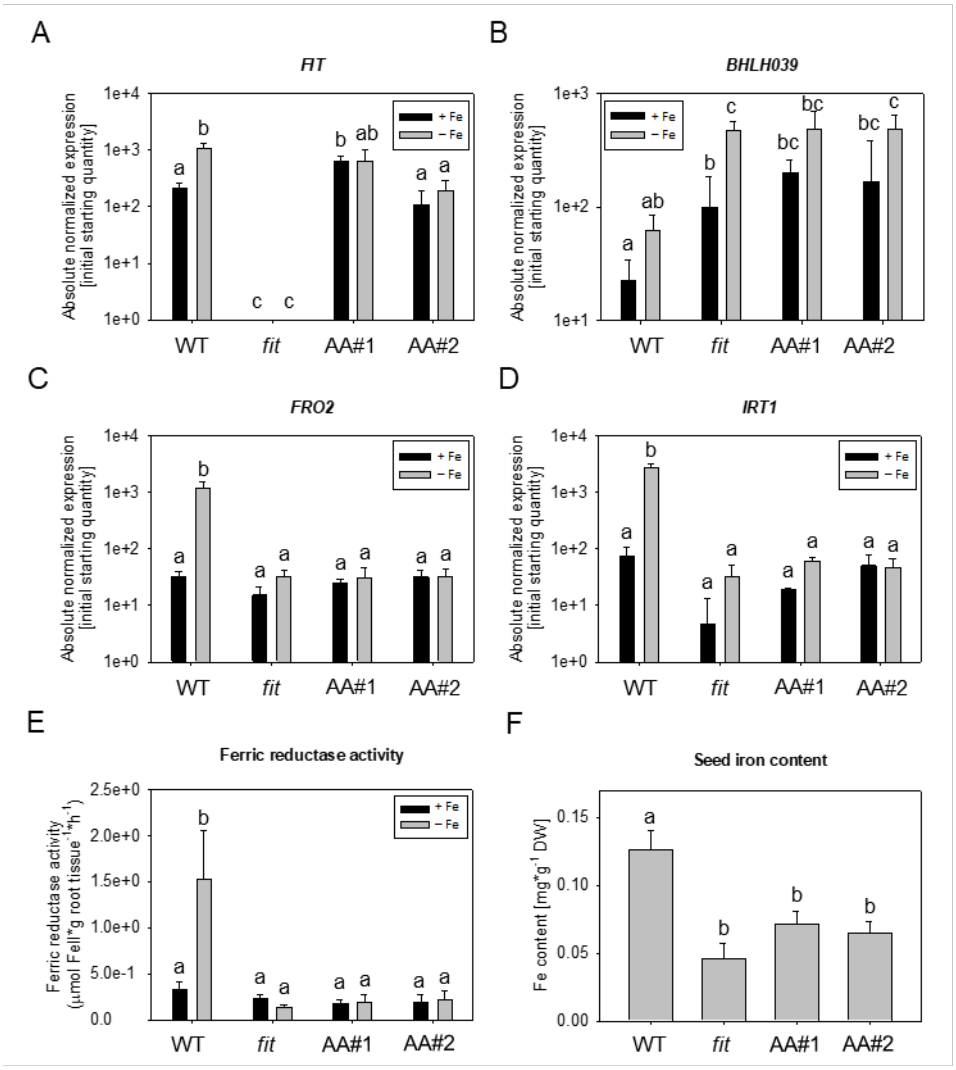

Figure 7. Non-phosphorylatable FIT at Ser272 has reduced activity in Arabidopsis.

Two independent FITm(AA)-GFP/*fit* lines (AA#1 and AA#2) were analyzed in comparison with wild-type (WT) and *fit* mutant plants in a *fit* mutant complementation assay. Plants were grown in response to sufficient (+Fe, black bars, A-E) and deficient (-Fe, gray bars, A-E) Fe supply. Error bars represent standard deviations. Different letters indicate statistically significant differences ($P < 0.05$). **(A-D)** Gene expression analysis in roots, represented in base-10 logarithmic scale. The expression of *FIT* (A), *BHLH039* (B), *FRO2* (C), and *IRT1* (D) was investigated. (n = 3) **(E)** Root Fe reductase activity. (n = 4) **(F)** Fe content of seeds collected from soil-grown plants. DW, dry weight. (n = 3)

DISCUSSION

Here, we identified the protein kinase CIPK11 as a positive regulator of Fe acquisition. *CIPK11* is induced by Fe-deficiency in roots irrespective of FIT, potentially through CBL1/9-dependent Ca^{2+} sensing. CIPK11 interacts with FIT and phosphorylates it at Ser272. Ser272 phosphorylation is needed to enhance FIT mobility and nuclear localization, and facilitates homo-dimerization, and interaction of FIT with bHLH039. Ser272 is important for full FIT activity and Fe acquisition in Arabidopsis plants. Thus, we propose that CIPK11 mediates the transformation of inactive FIT into active Ser272-phosphorylated FIT.

CIPK11 acts as a positive regulator of Fe acquisition by forming a pool of active FIT

The notion that two pools of active and inactive FIT exist is based on the observation that in an overexpression situation FIT is very abundant upon Fe sufficiency but inactive in terms of target gene activation, thus representing a large pool of inactive FIT. On the other side, in a WT situation FIT protein is hardly detectable upon Fe-deficiency, but it is active in terms of downstream gene activation, thus representing a small pool of active FIT (Lingam et al., 2011; Meiser et al., 2011). The same holds true for tomato FER (Brumbarova and Bauer, 2005). Here, we provide evidence for another two pools of FIT, namely a large pool of non-phosphorylated FIT and a small pool of phosphorylated FIT, detectable by Phos-tag analysis. The *in planta* and *in vitro* FIT phosphorylation data, combined with the detailed investigation of diverse cellular characteristics of WT and Ser272 phospho-mutant FIT forms, convincingly show that FIT is phosphorylated, and that phosphorylation at Ser272 by CIPK11 renders FIT more active than the non-phosphorylatable FITm(AA). Hence, our data strongly infer that FIT phosphorylated at position Ser272 has the characteristics that would allow discriminating it as active FIT from the non-phosphorylated inactive FIT. Thus, the phosphorylation status discriminates active from inactive FIT and Ser272 is required to render the FIT status from inactive into active. Our subcellular localization studies found both FIT and CIPK11 in the nucleus and in the cytoplasm. The interaction between the two proteins was detected predominantly in the nucleus but also in the cytoplasm. Therefore, it is possible that the phosphorylation of FIT by CIPK11 occurs at both cellular locations.

FIT protein alone may not be active upon sufficient Fe because CIPK11 may not fully activate FIT under this condition. Gene expression of this kinase may need to be induced upon Fe-deficiency, independently from that of *BHLH039* and *FIT*. *CIPK11* is expressed similarly to *FIT* in the early differentiation zone of the root, where Fe uptake predominantly takes place.

CIPK11 exerts its function in Fe-deficiency response regulation by acting predominantly on FIT. This is supported by the findings that CIPK11 interacts with FIT but not with bHLH039, and that expression of FIT downstream targets is affected in *cipk11* mutants, but not that of other tested Fe-deficiency-regulated genes. The positive role of CIPK11 in regulating FIT activity and Fe acquisition has been convincingly underlined by numerous Fe-deficiency phenotypes of the *cipk11* loss-of-function plants that are phenocopied in *fit* knockout mutants expressing non-phosphorylatable FIT at the CIPK11 target site Ser272. The common phenotypes include down-regulation of the Fe-deficiency marker genes *FRO2* and *IRT1*, decreased Fe reductase activity and compromised seed Fe content. Interestingly, the yeast self-activation capacity assay which showed decreased transcriptional activity of FITm(AA) was in line with our *in planta* data showing decreased activity of FIT in FITm(AA)-GFP/*fit* plants, demonstrating the utility of such assays.

The two extensive Y2H screens for FIT interaction partners, first against a library of Fe-deficiency-induced genes and second, against the full 26-member family of CIPKs, strongly underline the selectivity of FIT for just a few, Fe-deficiency regulated CIPKs, and points towards a dependence of the FIT-CIPK11 interaction on the Fe status of the plant.

The identification of CIPK11 as the first enzyme shown to interact with FIT and post-translationally modify it, allows to better understand the mechanisms leading to the attachment of regulatory marks on FIT. This knowledge should help to manipulate and better fine-tune Fe uptake regulation in response to different signals.

Taken together, we suggest that CIPK11 is a positive regulator of FIT action because it mediates phosphorylation at Ser272, the prime event rendering FIT active in the cell (Figure 8).

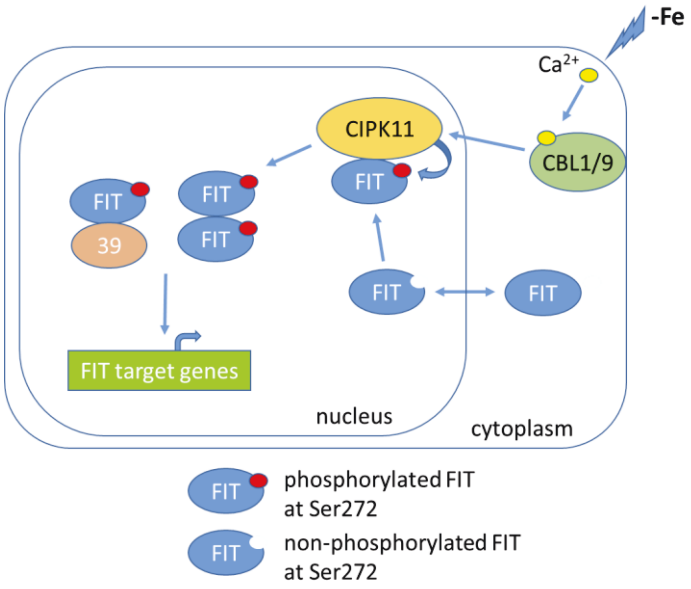

Figure 8. Involvement of CIPK11-mediated FIT phosphorylation in modulating FIT activity and Fe acquisition.

A model illustrating the role of protein kinase CIPK11 as a positive regulator of Fe acquisition. Fe-deficiency leads to the activation of CIPK11, potentially through perception of an elevated $[Ca^{2+}]_{cyt}$ by CBL1/9. Lack of Fe also upregulates *CIPK11* and independently from that *BHLH039*, and *FIT* transcript abundances. CIPK11 exerts its function by interacting with and phosphorylating FIT at Ser272, thereby defining two pools of FIT protein – active FIT (Ser272-phosphorylated) and inactive FIT (non-Ser272-phosphorylated). Phosphorylation at Ser272 triggers a distinct nucleocytoplasmic distribution and mobility of FIT towards higher nuclear accumulation, increasing the amount of available active FIT in the nucleus. Combined with the enhanced capacity to form homo-dimers and to interact with bHLH039, the phosphorylation of FIT at Ser272 leads to enhanced FIT transcriptional activity and, thus, FIT target gene expression. Consequently, the regulation of the FIT phosphorylation status presents a fundamental mechanism to fine-tune and dynamically adjust the pool of functionally active FIT protein in the cell, thus altering the plant's Fe utilization capacity.

FIT activation via the CIPK11 pathway involves nucleocytoplasmic redistribution and mobility, and differential capacities for protein interaction

The next question we answered was how active FIT performs its function in the cell, different from inactive FIT. Indeed, in a number of cellular assays we could narrow down the mechanism by which active FIT exerts its function. Active FIT, phosphorylated at Ser272, has a distinct nucleocytoplasmic distribution compared to inactive FIT, not phosphorylated at this Ser site. Active FIT accumulates to a greater extent than inactive FIT in the nucleus versus the cytoplasm and has decreased nuclear mobility, both favoring an enrichment of active FIT in the nucleus. Furthermore, active FIT has an increased capacity to form homo-dimers and to interact with bHLH039. The consequence of the interaction among active FIT molecules is currently unclear. Perhaps FIT dimerization or FIT multimerization is facilitated upon the CIPK11-mediated

phosphorylation at Ser272 and the FIT-FIT complex formation could be at the origin of nuclear accumulation and decreased mobility of FIT. Protein phosphorylation is one of the potential mechanisms involved in regulated nucleocytoplasmic partitioning of transcription factors (Meier and Somers, 2011). Phosphorylation may lead to a conformational change that either masks or exposes a nuclear localization signal (NLS) or a nuclear exclusion signal (NES). Indeed, FIT has been shown to possess an NLS at the C-terminal part of the basic region in the bHLH domain (Zhang et al., 2006). Additionally, phosphorylation may affect FIT interaction with a nuclear shuttle protein or with a protein that retains FIT in the cytoplasm. One of these or a combination of these mechanisms may be responsible for the observed increased mobility and decreased nuclear accumulation of the non-phosphorylatable FITm(AA) form. In addition, FIT-FIT interaction could be a prerequisite for further attraction of bHLH subgroup Ib proteins such as bHLH039 into this complex. Interestingly, we could show that FIT homo-dimerization and interaction with bHLH039 can occur through the C-terminus, which opens up the possibility that alterations in the conformation of the C-terminus through, for example, phosphorylation, can contribute, together with the bHLH domain, to the overall strength of FIT homo- and hetero-dimer formation. Subsequently, bHLH039-FIT complexes will stimulate further *FIT* gene induction and Fe acquisition (Wang et al., 2007; Yuan et al., 2008; Wang et al., 2013; Naranjo-Arcos et al., 2017).

Consequently, the regulation of the FIT phosphorylation status presents a fundamental mechanism to fine-tune and dynamically adjust the pool of functionally active FIT protein in the cell nucleus where it is available for protein-protein interactions, thus altering the plant's iron utilization capacity (Figure 8).

The CIPK11-mediated FIT activation pathway is integrated in plant stress response networks

The mechanism of CIPK11 activation by Fe-deficiency is an interesting aspect of the role of this protein kinase in Fe acquisition. Both *CIPK11* promotor activity and transcript abundance were upregulated by Fe-deficiency. Since we found *CIPK11* expression to be regulated in a FIT-independent manner, it is possible that this is achieved by the subgroup IVc bHLH transcription factors bHLH034, bHLH104 and bHLH105 (IAA-LEUCINE RESISTANT3) that have already been shown to positively regulate Fe homeostasis upstream of FIT and bHLH038/039/100/101 (Zhang et al., 2015; Li et al., 2016). On post-translational level, CIPK11 is likely activated by one of the 10 Arabidopsis CBLs (Weinl and Kudla, 2009) in response to Fe-deficiency-induced elevation of cytosolic Ca^{2+} concentration. A wide variety of

extracellular stimuli lead to the generation of the so-called Ca^{2+} transients which serve as a signal perceived by the cell and transmitted downstream to specifically regulate the cellular responses (Batistic and Kudla, 2012; Steinhorst and Kudla, 2013, 2014). Indeed, we could observe an increase in $[Ca^{2+}]_{cyt}$ in the early root differentiation zone of Fe-deficient plants, consistent with the recent report by Tian et al. (2016). Interestingly, we found the increase in $[Ca^{2+}]_{cyt}$ upon Fe-deficiency to be significant in both epidermis and central cylinder, where both *FIT* (Jakoby et al., 2004) and *IRT1* (Marques-Bueno et al., 2016) are expressed. Furthermore, it has been shown that lack of IRT1 not only from the epidermis but also from the central cylinder compromises the capacity of the plant to mobilize Fe (Marques-Bueno et al., 2016). Therefore, it is likely that FIT-dependent Fe uptake regulation responds to Ca^{2+} signals in both epidermis and central cylinder.

In order to clarify which CBLs are involved in decoding Fe-deficiency dependent changes in $[Ca^{2+}]_{cyt}$, we tested loss-of-function *cbl* mutant plants deficient in either tonoplast (*cbl2/3*) or plasma membrane (*cbl1/9*) CBL function. Indeed, *cbl2/3* plants did not show altered Fe reductase activity under Fe-deficient conditions which speaks against a significant role of these tonoplast CBLs in Fe-deficiency-dependent Ca^{2+} sensing. The contrary was true, however, for *cbl1/9* plants pointing towards an involvement of the plasma membrane localized CBL1 and CBL9 in perceiving Fe-deficiency. CBL9 is the closest homolog of CBL1 in Arabidopsis (Kolukisaoglu et al., 2004), and both CBL1 and CBL9 have been shown to interact with CIPK11 (Albrecht et al., 2001; Kolukisaoglu et al., 2004). Additionally, *cbl1/9* mutant plants were shown to have reduced shoot Fe content (Tian et al., 2016). Apart from their subcellular localization, CBL1/9 and CBL2/3 differ also in their number of canonical EF hands that serve to bind Ca^{2+} ions. While CBL1 and CBL9 contain two canonical and two noncanonical EF hands, CBL2 and CBL3 have only a single canonical EF hand (Kolukisaoglu et al., 2004). This implies different affinities of the proteins for Ca^{2+} and, therefore, their participation in decoding Ca^{2+} signals with different strengths at different subcellular compartments, providing spatiotemporal specificity (Batistic et al., 2011). Under alkaline stress, CIPK11 was shown to act as a negative regulator of AHA2 activity, evident from the increased tolerance of *cipk11* loss-of-function plants to growth on alkaline medium. Surprisingly, CIPK11 action on the plasma membrane-localized AHA2 was mediated by the tonoplast-localized CBL2 (Fuglsang et al., 2007). The role of CBL2 under Fe-deficiency is still unclear. First, because lack of Fe is a stress principally different form a high external pH stress and, second, because the activity of AHA2 is strongly increased under Fe-deficiency (Santi and Schmidt, 2009), inconsistent with CIPK11-mediated negative regulation on AHA2 under this condition.

Collectively, our data allow proposing a novel model on the integration of Fe signaling with plant development and other stress response networks. CIPK proteins, including CIPK11, target membrane proteins, which are involved in signaling and nutrient uptake. Several CIPK transcription factor targets participate in the abscisic acid (ABA) response (Sanyal et al., 2015; Sanyal et al., 2017). In these cases, CIPKs play a dual role in the phosphorylation of plasma membrane and transcription factor proteins, causing an activation or repression of ABA signaling responses. In this regard, Fe signaling in root cells, similarly to ABA signaling, also involves communication between the plasma membrane and the nucleus via a CIPK. Since CIPK11 has been proposed to be a regulatory hub in the ABA signaling network (Lumba et al., 2014; Zhou et al., 2015), this opens up the possibility that CIPK11 may serve as a connecting point, perhaps to coordinate Fe acquisition with adverse abiotic stress conditions via ABA signaling.

AUTHOR CONTRIBUTIONS

Conceptualization, T.B., R.G., P.M., R.I., J.K. and P.B. Investigation, T.B., R.G., P.M., R.I., P.K., I.M., K.T. and M.H. Resources, L.S., J.M., M.D., S. A. and U.K. Writing – Original Draft, T.B. and R.G. Writing – Review & Editing, T.B., R.G., P.M., R.I., J.K. and P.B. Supervision, T.B., J.K. and P.B. Project Administration, T.B. and L.S. Funding Acquisition, J.K. and P.B.

ACKNOWLEDGEMENTS

We thank Angelika Anna, Ulrike Ellersiek, Gintaute Matthäi and Elke Wieneke (Heinrich-Heine University) for excellent technical assistance. We acknowledge the contribution of the diploma and bachelor students Julia Mohrbacher, Florence Hermal and Dana Wiebel. We are thankful for the excellent assistance from Stefanie Weidtkamp-Peters and the members of the CAi imaging platform at the Heinrich-Heine University. P.M. is a member of CiM-IMPRS graduate school, Münster, Germany. Funding from the German Research Foundation is greatly acknowledged (grants Ba1610/5-2 and Ba1610/7-1 to P. B., and Ku931/X-1 to J. K.).

REFERENCES

Abdallah, H.B., and Bauer, P. (2016). Quantitative Reverse Transcription-qPCR-Based Gene Expression Analysis in Plants. Methods Mol Biol 1363, 9-24.

Albrecht, V., Ritz, O., Linder, S., Harter, K., and Kudla, J. (2001). The NAF domain defines a novel protein-protein interaction module conserved in Ca2+-regulated kinases. EMBO J 20, 1051-1063.

Bancaud, A., Huet, S., Rabut, G., and Ellenberg, J. (2010). Fluorescence perturbation techniques to study mobility and molecular dynamics of proteins in live cells: FRAP, photoactivation, photoconversion, and FLIP. Cold Spring Harb Protoc 2010, pdb top90.

Batistic, O., and Kudla, J. (2012). Analysis of calcium signaling pathways in plants. Biochim Biophys Acta 1820, 1283-1293.

Batistic, O., Sorek, N., Schultke, S., Yalovsky, S., and Kudla, J. (2008). Dual fatty acyl modification determines the localization and plasma membrane targeting of CBL/CIPK Ca2+ signaling complexes in Arabidopsis. Plant Cell 20, 1346-1362.

Batistic, O., Waadt, R., Steinhorst, L., Held, K., and Kudla, J. (2010). CBL-mediated targeting of CIPKs facilitates the decoding of calcium signals emanating from distinct cellular stores. Plant J 61, 211-222.

Batistic, O., Kim, K.N., Kleist, T., Kudla, J., and Luan, S. (2011). The CBL–CIPK Network for Decoding Calcium Signals in Plants. In Coding and Decoding of Calcium Signals in Plants S. Luan, ed (Berlin, Heidelberg: Springer), pp. 235-258.

Behera, S., Krebs, M., Loro, G., Schumacher, K., Costa, A., and Kudla, J. (2013). Ca2+ imaging in plants using genetically encoded Yellow Cameleon Ca2+ indicators. Cold Spring Harb Protoc 2013, 700-703.

Bekesova, S., Komis, G., Krenek, P., Vyplelova, P., Ovecka, M., Luptovciak, I., Illes, P., Kucharova, A., and Samaj, J. (2015). Monitoring protein phosphorylation by acrylamide pendant Phos-Tag in various plants. Front Plant Sci 6, 336.

Bleckmann, A., Weidtkamp-Peters, S., Seidel, C.A., and Simon, R. (2010). Stem cell signaling in Arabidopsis requires CRN to localize CLV2 to the plasma membrane. Plant Physiol 152, 166-176.

Blum, A., Brumbarova, T., Bauer, P., and Ivanov, R. (2014). Hormone influence on the spatial regulation of expression in iron-deficient roots. Plant Signal Behav 9.

Brumbarova, T., and Bauer, P. (2005). Iron-mediated control of the basic helix-loop-helix protein FER, a regulator of iron uptake in tomato. Plant Physiol 137, 1018-1026.

Brumbarova, T., and Ivanov, R. (2016). Differential Gene Expression and Protein Phosphorylation as Factors Regulating the State of the Arabidopsis SNX1 Protein Complexes in Response to Environmental Stimuli. Front Plant Sci 7, 1456.

Brumbarova, T., Bauer, P., and Ivanov, R. (2015). Molecular mechanisms governing Arabidopsis iron uptake. Trends Plant Sci 20, 124-133.

Cheong, Y.H., Pandey, G.K., Grant, J.J., Batistic, O., Li, L., Kim, B.G., Lee, S.C., Kudla, J., and Luan, S. (2007). Two calcineurin B-like calcium sensors, interacting with protein kinase CIPK23, regulate leaf transpiration and root potassium uptake in Arabidopsis. Plant J 52, 223-239.

Clough, S.J., and Bent, A.F. (1998). Floral dip: a simplified method for Agrobacterium-mediated transformation of Arabidopsis thaliana. Plant J 16, 735-743.

Colangelo, E.P., and Guerinot, M.L. (2004). The essential basic helix-loop-helix protein FIT1 is required for the iron deficiency response. Plant Cell 16, 3400-3412.

Curtis, M.D., and Grossniklaus, U. (2003). A gateway cloning vector set for high-throughput functional analysis of genes in planta. Plant Physiol 133, 462-469.

D'Angelo, C., Weinl, S., Batistic, O., Pandey, G.K., Cheong, Y.H., Schultke, S., Albrecht, V., Ehlert, B., Schulz, B., Harter, K., Luan, S., Bock, R., and Kudla, J. (2006). Alternative

complex formation of the Ca-regulated protein kinase CIPK1 controls abscisic acid-dependent and independent stress responses in Arabidopsis. Plant J 48, 857-872.

Dinneny, J.R., Long, T.A., Wang, J.Y., Jung, J.W., Mace, D., Pointer, S., Barron, C., Brady, S.M., Schiefelbein, J., and Benfey, P.N. (2008). Cell identity mediates the response of Arabidopsis roots to abiotic stress. Science 320, 942-945.

Drerup, M.M., Schlucking, K., Hashimoto, K., Manishankar, P., Steinhorst, L., Kuchitsu, K., and Kudla, J. (2013). The Calcineurin B-like calcium sensors CBL1 and CBL9 together with their interacting protein kinase CIPK26 regulate the Arabidopsis NADPH oxidase RBOHF. Mol Plant 6, 559-569.

Eckert, C., Offenborn, J.N., Heinz, T., Armarego-Marriott, T., Schultke, S., Zhang, C., Hillmer, S., Heilmann, M., Schumacher, K., Bock, R., Heilmann, I., and Kudla, J. (2014). The vacuolar calcium sensors CBL2 and CBL3 affect seed size and embryonic development in Arabidopsis thaliana. Plant J 78, 146-156.

Edel, K.H., and Kudla, J. (2015). Increasing complexity and versatility: how the calcium signaling toolkit was shaped during plant land colonization. Cell Calcium 57, 231-246.

Edel, K.H., Marchadier, E., Brownlee, C., Kudla, J., and Hetherington, A.M. (2017). The Evolution of Calcium-Based Signalling in Plants. Curr Biol 27, R667-R679.

Fuglsang, A.T., Guo, Y., Cuin, T.A., Qiu, Q., Song, C., Kristiansen, K.A., Bych, K., Schulz, A., Shabala, S., Schumaker, K.S., Palmgren, M.G., and Zhu, J.K. (2007). Arabidopsis protein kinase PKS5 inhibits the plasma membrane H+ -ATPase by preventing interaction with 14-3-3 protein. Plant Cell 19, 1617-1634.

Grefen, C., and Blatt, M.R. (2012). A 2in1 cloning system enables ratiometric bimolecular fluorescence complementation (rBiFC). BioTechniques 53, 311-314.

Guerinot, M.L., and Yi, Y. (1994). Iron: Nutritious, Noxious, and Not Readily Available. Plant Physiol 104, 815-820.

Hashimoto, K., Eckert, C., Anschutz, U., Scholz, M., Held, K., Waadt, R., Reyer, A., Hippler, M., Becker, D., and Kudla, J. (2012). Phosphorylation of calcineurin B-like (CBL) calcium sensor proteins by their CBL-interacting protein kinases (CIPKs) is required for full activity of CBL-CIPK complexes toward their target proteins. J Biol Chem 287, 7956-7968.

Heim, M.A., Jakoby, M., Werber, M., Martin, C., Weisshaar, B., and Bailey, P.C. (2003). The basic helix-loop-helix transcription factor family in plants: a genome-wide study of protein structure and functional diversity. Mol Biol Evol 20, 735-747.

Ho, C.H., Lin, S.H., Hu, H.C., and Tsay, Y.F. (2009). CHL1 functions as a nitrate sensor in plants. Cell 138, 1184-1194.

Holtkamp, M., Elseberg, T., Wehe, C.A., Sperling, M., and Karst, U. (2013). Complexation and oxidation strategies for improved TXRF determination of mercury in vaccines. Journal of Analytical Atomic Spectrometry 28, 719-723.

Holtkamp, M., Wehe, C.A., Blaske, F., Holtschulte, C., Sperling, M., and Karst, U. (2012). Nitrogen purged TXRF for the quantification of silver and palladium. Journal of Analytical Atomic Spectrometry 27, 1799-1802.

Hotzer, B., Ivanov, R., Brumbarova, T., Bauer, P., and Jung, G. (2012). Visualization of Cu(2)(+) uptake and release in plant cells by fluorescence lifetime imaging microscopy. FEBS J 279, 410-419.

Ivanov, R., Brumbarova, T., and Bauer, P. (2012). Fitting into the Harsh Reality: Regulation of Iron Deficiency Responses in Dicotyledonous Plants Mol Plant 5, 27-42.

Ivanov, R., Brumbarova, T., Blum, A., Jantke, A.M., Fink-Straube, C., and Bauer, P. (2014). SORTING NEXIN1 Is Required for Modulating the Trafficking and Stability of the Arabidopsis IRON-REGULATED TRANSPORTER1. Plant Cell.

Jakoby, M., Wang, H.Y., Reidt, W., Weisshaar, B., and Bauer, P. (2004). FRU (BHLH029) is required for induction of iron mobilization genes in *Arabidopsis thaliana*. FEBS Lett 577, 528-534.

Jefferson, R.A., Kavanagh, T.A., and Bevan, M.W. (1987). GUS fusions: beta-glucuronidase as a sensitive and versatile gene fusion marker in higher plants. EMBO J 6, 3901-3907.

Kinoshita, E., and Kinoshita-Kikuta, E. (2011). Improved Phos-tag SDS-PAGE under neutral pH conditions for advanced protein phosphorylation profiling. Proteomics 11, 319-323.

Kolukisaoglu, U., Weinl, S., Blazevic, D., Batistic, O., and Kudla, J. (2004). Calcium sensors and their interacting protein kinases: genomics of the Arabidopsis and rice CBL-CIPK signaling networks. Plant Physiol 134, 43-58.

Krebs, M., Held, K., Binder, A., Hashimoto, K., Den Herder, G., Parniske, M., Kudla, J., and Schumacher, K. (2012). FRET-based genetically encoded sensors allow high-resolution live cell imaging of Ca(2)(+) dynamics. Plant J 69, 181-192.

Kudla, J., and Bock, R. (2016). Lighting the Way to Protein-Protein Interactions: Recommendations on Best Practices for Bimolecular Fluorescence Complementation Analyses. Plant Cell 28, 1002-1008.

Le, C.T., Brumbarova, T., Ivanov, R., Stoof, C., Weber, E., Mohrbacher, J., Fink-Straube, C., and Bauer, P. (2016). ZINC FINGER OF ARABIDOPSIS THALIANA12 (ZAT12) Interacts with FER-LIKE IRON DEFICIENCY-INDUCED TRANSCRIPTION FACTOR (FIT) Linking Iron Deficiency and Oxidative Stress Responses. Plant Physiol 170, 540-557.

Lee, S.C., Lan, W.Z., Kim, B.G., Li, L., Cheong, Y.H., Pandey, G.K., Lu, G., Buchanan, B.B., and Luan, S. (2007). A protein phosphorylation/dephosphorylation network regulates a plant potassium channel. Proc Natl Acad Sci U S A 104, 15959-15964.

Li, X., Zhang, H., Ai, Q., Liang, G., and Yu, D. (2016). Two bHLH Transcription Factors, bHLH34 and bHLH104, Regulate Iron Homeostasis in Arabidopsis thaliana. Plant Physiol 170, 2478-2493.

Ling, H.Q., Bauer, P., Bereczky, Z., Keller, B., and Ganal, M. (2002). The tomato fer gene encoding a bHLH protein controls iron-uptake responses in roots. Proc Natl Acad Sci U S A 99, 13938-13943.

Lingam, S., Mohrbacher, J., Brumbarova, T., Potuschak, T., Fink-Straube, C., Blondet, E., Genschik, P., and Bauer, P. (2011). Interaction between the bHLH Transcription Factor FIT and ETHYLENE INSENSITIVE3/ETHYLENE INSENSITIVE3-LIKE1 Reveals Molecular Linkage between the Regulation of Iron Acquisition and Ethylene Signaling in Arabidopsis The Plant Cell 23 1815-1829.

Lumba, S., Toh, S., Handfield, L.F., Swan, M., Liu, R., Youn, J.Y., Cutler, S.R., Subramaniam, R., Provart, N., Moses, A., Desveaux, D., and McCourt, P. (2014). A mesoscale abscisic acid hormone interactome reveals a dynamic signaling landscape in Arabidopsis. Dev Cell 29, 360-372.

Lyzenga, W.J., Liu, H., Schofield, A., Muise-Hennessey, A., and Stone, S.L. (2013). Arabidopsis CIPK26 interacts with KEG, components of the ABA signalling network and is degraded by the ubiquitin-proteasome system. J Exp Bot 64, 2779-2791.

Mai, H.J., Pateyron, S., and Bauer, P. (2016). Iron homeostasis in Arabidopsis thaliana: transcriptomic analyses reveal novel FIT-regulated genes, iron deficiency marker genes and functional gene networks. BMC Plant Biol 16, 211.

Marques-Bueno, M.D.M., Morao, A.K., Cayrel, A., Platre, M.P., Barberon, M., Caillieux, E., Colot, V., Jaillais, Y., Roudier, F., and Vert, G. (2016). A versatile Multisite Gateway-compatible promoter and transgenic line collection for cell type-specific functional genomics in Arabidopsis. Plant J 85, 320-333.

Meier, I., and Somers, D.E. (2011). Regulation of nucleocytoplasmic trafficking in plants. Curr Opin Plant Biol 14, 538-546.

Meiser, J., Lingam, S., and Bauer, P. (2011). Posttranslational regulation of the iron deficiency basic helix-loop-helix transcription factor FIT is affected by iron and nitric oxide. Plant Physiol 157, 2154-2166.

Naranjo-Arcos, M.A., Maurer, F., Meiser, J., Pateyron, S., Fink-Straube, C., and Bauer, P. (2017). Dissection of iron signaling and iron accumulation by overexpression of subgroup Ib bHLH039 protein. Sci Rep 7.

Quintero, F.J., Ohta, M., Shi, H., Zhu, J.K., and Pardo, J.M. (2002). Reconstitution in yeast of the *Arabidopsis* SOS signaling pathway for Na^+ homeostasis. Proc Natl Acad Sci U S A 99, 9061–9066.

Robinson, N.J., Procter, C.M., Connolly, E.L., and Guerinot, M.L. (1999). A ferric-chelate reductase for iron uptake from soils. Nature 397, 694-697.

Santi, S., and Schmidt, W. (2009). Dissecting iron deficiency-induced proton extrusion in Arabidopsis roots. New Phytol 183, 1072-1084.

Sanyal, S.K., Pandey, A., and Pandey, G.K. (2015). The CBL-CIPK signaling module in plants: a mechanistic perspective. Physiol Plant.

Sanyal, S.K., Kanwar, P., Yadav, A.K., Sharma, C., Kumar, A., and Pandey, G.K. (2017). Arabidopsis CBL interacting protein kinase 3 interacts with ABR1, an APETALA2 domain transcription factor, to regulate ABA responses. Plant science : an international journal of experimental plant biology 254, 48-59.

Shabala, S., Bose, J., Fuglsang, A.T., and Pottosin, I. (2016). On a quest for stress tolerance genes: membrane transporters in sensing and adapting to hostile soils. J Exp Bot 67, 1015-1031.

Sivitz, A., Grinvalds, C., Barberon, M., Curie, C., and Vert, G. (2011). Proteasome-mediated turnover of the transcriptional activator FIT is required for plant iron-deficiency responses. Plant J.

Song, C.P., Agarwal, M., Ohta, M., Guo, Y., Halfter, U., Wang, P., and Zhu, J.K. (2005). Role of an Arabidopsis AP2/EREBP-Type Transcriptional Repressor in Abscisic Acid and Drought Stress Responses. The Plant Cell 17, 2384-2396.

Steinhorst, L., and Kudla, J. (2013). Calcium and reactive oxygen species rule the waves of signaling. Plant Physiol 163, 471-485.

Steinhorst, L., and Kudla, J. (2014). Signaling in cells and organisms - calcium holds the line. Curr Opin Plant Biol 22, 14-21.

Tang, R.J., Liu, H., Yang, Y., Yang, L., Gao, X.S., Garcia, V.J., Luan, S., and Zhang, H.X. (2012). Tonoplast calcium sensors CBL2 and CBL3 control plant growth and ion homeostasis through regulating V-ATPase activity in Arabidopsis. Cell Res 22, 1650-1665.

Tian, Q., Zhang, X., Yang, A., Wang, T., and Zhang, W.H. (2016). CIPK23 is involved in iron acquisition of Arabidopsis by affecting ferric chelate reductase activity. Plant science : an international journal of experimental plant biology 246, 70-79.

Walter, M., Chaban, C., Schutze, K., Batistic, O., Weckermann, K., Nake, C., Blazevic, D., Grefen, C., Schumacher, K., Oecking, C., Harter, K., and Kudla, J. (2004). Visualization of protein interactions in living plant cells using bimolecular fluorescence complementation. Plant J 40, 428-438.

Wang, H.Y., Klatte, M., Jakoby, M., Baumlein, H., Weisshaar, B., and Bauer, P. (2007). Iron deficiency-mediated stress regulation of four subgroup Ib BHLH genes in *Arabidopsis thaliana*. Planta 226, 897-908.

Wang, N., Cui, Y., Liu, Y., Fan, H., Du, J., Huang, Z., Yuan, Y., Wu, H., and Ling, H.Q. (2013). Requirement and functional redundancy of Ib subgroup bHLH proteins for iron deficiency responses and uptake in *Arabidopsis thaliana*. Mol Plant 6, 503-513.

Weinl, S., and Kudla, J. (2009). The CBL-CIPK Ca(2+)-decoding signaling network: function and perspectives. New Phytol 184, 517-528.

Wild, M., Daviere, J.M., Regnault, T., Sakvarelidze-Achard, L., Carrera, E., Lopez Diaz, I., Cayrel, A., Dubeaux, G., Vert, G., and Achard, P. (2016). Tissue-Specific Regulation of Gibberellin Signaling Fine-Tunes Arabidopsis Iron-Deficiency Responses. Dev Cell 37, 190-200.

Xu, J., Li, H.D., Chen, L.Q., Wang, Y., Liu, L.L., He, L., and Wu, W.H. (2006). A protein kinase, interacting with two calcineurin B-like proteins, regulates K+ transporter AKT1 in Arabidopsis. Cell 125, 1347-1360.

Yuan, Y., Wu, H., Wang, N., Li, J., Zhao, W., Du, J., Wang, D., and Ling, H.Q. (2008). FIT interacts with AtbHLH38 and AtbHLH39 in regulating iron uptake gene expression for iron homeostasis in Arabidopsis. Cell Res 18, 385-397.

Yuan, Y.X., Zhang, J., Wang, D.W., and Ling, H.Q. (2005). AtbHLH29 of *Arabidopsis thaliana* is a functional ortholog of tomato FER involved in controlling iron acquisition in strategy I plants. Cell Res 15, 613-621.

Zhang, J., Zhu, H.F., Liang, H., Liu, K.F., Zhang, A.M., Ling, H.Q., and Wang, D.W. (2006). Further analysis of the function of AtBHLH29 in regulating the iron uptake process in *Arabidopsis thaliana*. J Integr Plant Biol 48, 75-84.

Zhang, J., Liu, B., Li, M., Feng, D., Jin, H., Wang, P., Liu, J., Xiong, F., Wang, J., and Wang, H.B. (2015). The bHLH transcription factor bHLH104 interacts with IAA-LEUCINE RESISTANT3 and modulates iron homeostasis in Arabidopsis. Plant Cell 27, 787-805.

Zhou, X., Hao, H., Zhang, Y., Bai, Y., Zhu, W., Qin, Y., Yuan, F., Zhao, F., Wang, M., Hu, J., Xu, H., Guo, A., Zhao, H., Zhao, Y., Cao, C., Yang, Y., Schumaker, K.S., Guo, Y., and Xie, C.G. (2015). SOS2-LIKE PROTEIN KINASE5, an SNF1-RELATED PROTEIN KINASE3-Type Protein Kinase, Is Important for Abscisic Acid Responses in Arabidopsis through Phosphorylation of ABSCISIC ACID-INSENSITIVE5. Plant Physiol 168, 659-676.

CONTACT FOR REAGENT AND RESOURCE SHARING

Further information and requests for resources and reagents should be directed to and will be fulfilled by Petra Bauer (Petra.Bauer@uni-duesseldorf.de).

METHODS

Yeast Two-Hybrid Screens

For targeted Y2H interaction assays between FIT and the 26 members of the CIPK family, the GAL4 DNA binding domain (BD)-containing construct pGBKT7:FIT-C (BD-FIT-C; Lingam et al., 2011) was used as a bait and co-transformed in the yeast strain AH109 together with prey pGAD.GH, providing the GAL4 activation domain (AD)-containing full-length CIPK fusion constructs. pGAD.GH:CIPK1 to pGAD.GH:CIPK26 were described previously (Kolukisaoglu et al., 2004; Drerup et al., 2013). The combination of pGBT9.BS:CIPK23 and pGAD.GH:cAKT1 was used as a positive control (Xu et al., 2006; Lee et al., 2007). BD-FIT-C co-transformed with empty AD plasmid was used as a negative control. In the targeted yeast two-hybrid interaction assay combining FIT and CIPK11, empty BD and AD-CIPK11 plasmids, and empty BD with empty AD plasmids, were used as additional negative controls. Yeast transformation and subsequent cultivation were performed as previously described (Le et al., 2016). In short, aliquots of ten-fold serial dilutions (A_{600} = 10^{-1}–10^{-4}) of the transformed AH109 cells were spotted on synthetic defined (SD) agar plates lacking Leu (pGBKT7 auxotrophy selection) and Trp (pACT2-GW auxotrophy selection) (SD-LW, co-transformation control). In parallel, aliquots of the same serial dilutions were spotted on SD agar plates lacking Leu, Trp, and His, and supplemented with 0.5 mM 3-amino-1,2,4-triazole (SD-LWH + 0.5 mM 3-AT, selection for interaction). Plates were photographed after one-week incubation at 30 °C.

Plant Growth Conditions

Arabidopsis seeds were sterilized and seedlings grown on upright sterile plates containing modified half-strength Hoagland medium [1.5 mM $Ca(NO_3)_2$, 1.25 mM KNO_3, 0.75 mM $MgSO_4$, 0.5 mM KH_2PO_4, 50 µM KCl, 50 µM H_3BO_3, 10 µM $MnSO_4$, 2 µM $ZnSO_4$, 1.5 µM $CuSO_4$, 0.075 µM $(NH_4)_6Mo_7O_{24}$, 1% sucrose, pH 5.8, supplemented with 1.4 % Plant agar (Duchefa)] with sufficient (50 µM FeNaEDTA, + Fe) or deficient (0 µM FeNaEDTA, - Fe) Fe supply under long-day conditions, as described previously (Lingam et al., 2011). Plants were grown in plant growth chambers (CLF Plant Climatics) either for six days directly on sufficient or Fe-deficient medium (6-day system) or for 14 days at sufficient Fe supply and then transferred for three days to either sufficient or deficient Fe supply (2-week system). For $[Ca^{2+}]_{cyt}$ measurements, plants were grown for five days at sufficient Fe supply and then transferred for three days to either sufficient or deficient Fe supply.

Histochemical β-glucuronidase (GUS) Assay

ProFIT:GUS transgenic plants have been described previously (Jakoby et al., 2004). *ProCIPK11:GUS* plants were generated as follows: a 1882 bp *CIPK11* promoter fragment was amplified using the primers pCIPK11_forSpe and pCIPK11_reXho (Supplemental Table 1), cloned into pKS II Bluescript (Stratagene), and then subcloned into pGPTV-II-KOZ-BAR (Walter et al., 2004). The resulting *ProCIPK11:GUS* construct was transformed into Col-0 plants using the floral dip procedure (Clough and Bent, 1998). Positive transformants were identified by BASTA selection, selfed, and propagated until homozygous lines were obtained. Two independent *ProCIPK11:GUS* lines (1 and 3) were selected for detailed analysis. GUS plants were grown in the 6-day system and assayed for histochemical GUS activity using the substrate 5-bromo-4-chloro-3-indolyl-β-D-glucuronic acid (X-Gluc) (Jefferson et al., 1987; Jakoby et al., 2004). Chlorophyll was removed by a 16-hour incubation in 100 % ethanol. Seedlings were stored in 70 % ethanol before imaging. GUS staining was documented on an Axio Imager.M2 microscope (Zeiss). Single images obtained with 10x objective magnification were assembled using the Stitching function of the ZEN 2 Blue Edition software (Zeiss).

FIT Mutagenesis

pDONR207:gFIT was used as a template for FIT mutagenesis. To mutate FIT at position Ser272 to Glu and create a phospho-mimicking FIT form, termed gFITm(E), the primers FITmS272E-1 and FITmS272E-2 (Supplemental Table 1) were used. To create a non-phosphorylatable FIT form for position S272, gFITm(AA), Ser272 was mutated to Ala together with the adjacent Ser271 in order to exclude redundancy, using the primers FITmSS271AA-1 and FITmSS271AA-2 (Supplemental Table 1). The PCR conditions were as follows: 95 °C, 30 seconds; 18 cycles of: 95 °C, 30 seconds/ 55 °C, 1 minute/ 72 °C for 2 minutes per 1kb of plasmid length; 72 °C, 7 minutes. After the PCR, the reaction was treated with 10 units Dpn I for 1 h at 37 °C before *E. coli* transformation. The mutagenized *gFITm* forms in pDONR207 were subsequently used for creating plant expression constructs for C-terminal GFP fusions in the pMDC83 vector.

Generation of Fluorescent Protein Fusions

Generation of plant transformation vectors for fluorescent protein-fusion expression was performed as follows: *CIPK11* cDNA was amplified using primers CIPK11 SpeI forward and CIPK11 XhoI reverse (Supplemental Table 1) and inserted into pGPTV-II-BAR-pUBQ10-GFP for translational N-terminal GFP fusion. For cloning genomic *FIT* fragment (g*FIT*) into the

Gateway-compatible plasmids pJNC1 (Ivanov et al., 2014) and pMDC83 (Curtis and Grossniklaus, 2003) for translational C-terminal fusion of mCherry, and GFP, respectively, the entry clone pDONR207:gFIT was generated after amplification of g*FIT* from Col-0 gDNA using the primers FIT B1 and FITns B2 (Supplemental Table 1) (BP reaction; Life Technologies). gFIT-mCherry and gFIT-GFP fusions were created by subcloning g*FIT* (LR reaction; Life Technologies) into pJNC1 and pMDC83, respectively. The Agrobacterium (*Rhizobium radiobacter*) strain C58 (pGV2260) carrying pGPTV-II-BAR-pUBQ10-GFP:CIPK11, pJNC1:gFIT or pMDC83:gFIT, was used to transiently transform tobacco (*Nicotiana benthamiana*) leaves as previously described (Hotzer et al., 2012).

Bimolecular Fluorescence Complementation (BiFC)

The verification of FIT-CIPK11 interaction *in planta* was performed using rBiFC (Grefen and Blatt, 2012). *CIPK11* and *FIT* coding sequences were amplified using the primers CIPK11 B3 and CIPK11 B2, and FIT B1 and FITstop B4 (Supplemental Table 1). The resulting *CIPK11* and *FIT* PCR fragments were cloned by BP reaction (Life Technologies) into pDONR221 P3-P2 (Invitrogen) and pDONR221 P1-P4 (Invitrogen), respectively. Following LR reaction (Life Technologies) with the obtained vectors and pBiFC-2in1-NN (Grefen and Blatt, 2012), *CIPK11* and *FIT* were cloned together into pBiFC-2in1-NN:CIPK11-FIT. Following the recommendations for appropriate negative BiFC controls (Kudla and Bock, 2016), two pBiFC-2in1-NN constructs were created – *CIPK11* together with *BHLH039* and *FIT* together with *CIPK15*. *BHLH039* was amplified using the primers 39 B1 and 39st B4 (Supplemental Table 1). *CIPK15* was amplified using CIPK15 B3 and CIPK15st B2 (Supplemental Table 1). The obtained constructs were transformed into agrobacteria and used for tobacco leaf infiltration as described above. After 48 h, YFP fluorescent signals were detected by confocal microscopy. The BiFC experiments were performed in three independent repetitions on a total of six infiltrated leaves. Transformed cells were verified by mRFP fluorescence. The vector pBiFC-2in1-NN was kindly provided by Dr. Christopher Grefen, Tübingen, Germany.

For FIT and FITm homo-dimer formation analysis, full-length *FIT*, *FITm(AA)* and *FITm(E)* coding sequences were amplified using the primers FIT B3 and FITstop B2 (Supplemental Table 1) for cloning into pDONR221 P3-P2, and the primers FIT B1 and FITstop B4 (Supplemental Table 1) for cloning into pDONR221 P1-P4. pDONR207:cFIT, pDONR207:cFITm(AA) and pDONR207:cFITm(E) were used as templates, respectively. *FIT* and *FITm* were subcloned into pBiFC-2in1-NN:FIT-FIT, pBiFC-2in1-NN:FITm(AA)-FITm(AA) and pBiFC-2in1-NN:FITm(E)-FITm(E).

Confocal Microscopy

Laser-scanning confocal microscopy (LSM 780, Zeiss) controlled by ZEN 2 Black Edition software (Zeiss) was used for fluorescence imaging of YFP and GFP at an excitation wavelength of 488 nm and emission wavelength of 500 to 530 nm as previously described (Brumbarova and Ivanov, 2016; Le et al., 2016). mRFP and mCherry were detected 48 h after Agrobacterium leaf infiltration of tobacco plants with an excitation wavelength at 563 nm and emission wavelength of 560 to 615 nm. Pinholes for each channel were set at 1 Airy Unit with optical slices equivalent to 0.8 μm. Images were recorded in a 1024 pixel format.

Plant Material

The Arabidopsis (*Arabidopsis thaliana*) ecotype Col-0 was used as WT. The *fit* loss-of-function mutant allele *fit-3* (GABI_108C10, abbreviated as *fit* in the text) was described previously (Jakoby et al., 2004). The *cipk11* loss-of-function mutant allele *pks5-1* (named here *cipk11-1,* SALK_108074, briefly termed *cipk11* in the text) was previously reported (Fuglsang et al., 2007). Three independent *cipk11*-complemented lines were obtained by transforming *cipk11* mutant plants with *ProCIPK11:CIPK11* cloned into pGPTV-II-MCS-BAR and selecting them until homozygous. In order to obtain the *ProCIPK11:CIPK11* construct, 1882 bp *CIPK11* promoter fragment was amplified using CIPK11_forSpe and pCIPK11_reBam_2 (Supplemental Table 1), and cloned into pKS II Bluescript. The full-length *CIPK11* intron-containing coding sequence followed by the 3' UTR was amplified using the primers CIPK11_for_Bam and CIPK11UTRreXho (Supplemental Table 1), and cloned also into pKS II Bluescript. The *CIPK11* promotor and the *CIPK11*+3'UTR sequence were then subcloned into pGPTV-II-MCS-BAR. HA_7-FIT plants were previously described (HA-FIT 8; Meiser et al., 2011). The line stably expressing the genetically encoded Ca^{2+} sensor Yellow Cameleon 3.6 (YC3.6) under the control of the *UBQ10* promoter has been described previously by Krebs et al. (2012). The *cbl2/3* and *cbl1/9* double loss-of-function mutants were previously described (Xu et al., 2006; Eckert et al., 2014).

Root Length Measurement

Images of plants grown on agar plates were taken and primary root lengths of individual seedlings were measured using the JMicroVision software, version 1.2.7 (http://www.jmicrovision.com), as described previously (Ivanov et al., 2014). The line lengths were used for calculating average root length and standard deviations. Root lengths of 16 to 46 plants per condition were measured. (n = min 16).

Gene Expression Analysis by RT-qPCR

Gene expression analysis was performed as described previously (Abdallah and Bauer, 2016) from plants grown in the 2-week system. RT-qPCR was performed on SFX96 Touch™ Real-Time PCR Detection System (Bio-Rad). The results were processed on Bio-Rad SFX Manager™ (version 3.1) software. Primer pairs used in this study are listed in Supplemental Table 1. Absolute gene expression was determined by mass standard curve analysis and normalized to elongation factor *EF1Bα* expression as a reference. The assay was performed in three biological replicates (n = 3), each with two technical replicates.

Fe Reductase Activity Assay

Fe reductase activity was determined as described in (Le et al., 2016) with some modifications. Plants grown in the 2-week system, were washed in 100 mM $Ca(NO_3)_2$ solution followed by incubation at room temperature in 1 mL of Fe reductase solution (300 µM ferrozine and 100 µM FeNaEDTA) in the dark. After 1 h, the absorbance of the Fe reductase solution was measured at 562 nm using the Safire2 plate reader (Tecan). The Fe reductase activity normalized to root weight was calculated using the extinction coefficient $\varepsilon = 28.6\ mM^{-1}*cm^{-1}$. The assay was performed in four replicates (n = 4), each representing a pool of two plants.

Seed Fe Content Determination

For Fe content determination in seeds, plants were grown in parallel on soil under long-day conditions (16 hours day, 8 hours night, 21 °C). Harvested seeds were dried overnight at 120 °C, followed by two days exposure to 60 °C. Their Fe content was determined using Total Reflection X-Ray Fluorescence (TXRF) (Holtkamp et al., 2012; Holtkamp et al., 2013). TXRF was carried out on a S2-PICOFOX instrument (Bruker Nano) with an air-cooled molybdenum anode for X-ray generation. The excitation settings were 50 kV and 750 µA and quartz glass disks were used as sample carriers. As internal standard, arsenic (As, Fluka Chemie) with a concentration of 10 mg/L was applied. The samples of plant material were weighed into a vial and digested with nitric acid (70 %; Primar Plus®, Trace Analysis Grade, Fisher Scientific) over night at 95 °C. The dried samples were re-dissolved in 1 mL purified water (Aquatron A4000D system, Barloworld Scientific) and aliquots of 100 µL were mixed with the same volume of the 10 mg/L As standard solution. Aliquots of 5 µL of the samples were placed on the sample carriers and evaporated to dryness. The analysis was performed by signal integration over 500 seconds. For the determination, the signals of Fe (Kα1 = 6.405 keV) and As (Kα1 = 10.543 keV), as internal standard, were used. Quantification was performed by the Bruker

Spectra software (version 6.1.5.0) and based on the known concentration of the internal As standard. The assay was performed in three biological replicates (n = 3). Each biological replicate was measured two times.

$[Ca^{2+}]_{cyt}$ measurement

For monitoring Fe supply-dependent changes in free cytosolic $[Ca^{2+}]$, Arabidopsis seedlings stably expressing the genetically encoded Ca^{2+} sensor *ProUBQ10:YC3.6* were transferred to microscopic slides in liquid Hoagland medium containing the same amount of Fe as on the Hoagland agar plates where the plants grew for three days prior to imaging (50 µM FeNaEDTA for + Fe or 0 µM FeNaEDTA for – Fe supply). Imaging was performed using LSM780 confocal laser-scanning microscope (Zeiss) essentially as described in (Behera et al., 2013). In brief, fluorescence was excited at 458 nm and detected at 465-499 nm for ECFP, and 520-570 nm for cpVenus. 1024 x 1024 pixel images were acquired with 10x objective (pinhole 7 airy units) every 10 sec for 12 min.

ImageJ (http://rsbweb.nih.gov/ij/) was used to quantify changes in $[Ca^{2+}]$ in different root zones and tissues. Regions of interest (ROIs) were defined in the meristematic (MZ) and elongation (EZ) zones of the root tip, and in the central cylinder (CC) and epidermis with cortex (Ep) region of the early root differentiation zone. For each zone, a ROI with the same size was used to calculate background fluorescence in the ECFP and cpVenus channels. Background-corrected cpVenus and ECFP fluorescent intensities in the defined ROIs were used to calculate cpVenus/ECFP ratios. In order to exclude unspecific responses of the root to the mounting on the microscopic slide, the ratio values of the first 3 min were excluded from the subsequent analysis. The rest of the values were averaged for each zone and compared. The measurement was performed on 12 seedlings in two independent experiments.

***In vivo* FIT Phosphorylation Detection (Phos-tag SDS-PAGE)**

HA_7-FIT plants were grown in the 2-week system. Total protein was extracted from roots as previously described (Bekesova et al., 2015) by using RIPA buffer. Protein concentration was determined by Bradford Assay. 200 µg total root protein was precipitated with 80% v/v acetone for 4 hours at -20°C and pelleted at 15.000 x g at 4°C for ten minutes. The protein pellet was solubilized in 100 µl 1x CIP reaction buffer (Sigma-Aldrich) to a final concentration of 2 mg/ml. The samples were treated with 60 units of CIP or reaction buffer (mock treated) and incubated over night at 37 °C. The reaction was stopped by adding 5x Laemmli buffer (250 mM

Tris-Cl pH6.8, 10% SDS, 30% glycerol, 5% β-mercaptoethanol, 0,02% bromophenol blue), denatured at 95 °C for 10 min and kept on ice until loading. Approximately 20 µg root total protein was separated in a standard Mini-PROTEAN® TGX™ Precast Gel (BioRad). In parallel, the same samples were loaded on precast SuperSep Phos-tag™ gels (Wako Laboratory Chemicals), containing 50 µmol/L Phos-tag and 7.5% polyacrylamide. Electrophoresis was performed as described in Bekesova et al. 2015 (following instructions for Zn^{2+}- Phos-tag™ gels). HA_7-FIT protein detection was performed as previously described (Le et al., 2016).

Expression and Affinity Purification of Recombinant Proteins

CIPK11 and kinase target proteins were generated as follows: *CIPK11* coding sequence was amplified using the primers CIPK11 SpeI forward and CIPK11 XhoI reverse (Supplemental Table 1), and cloned into the pIVEX-WG-StrepII vector (Hashimoto et al., 2012). StrepII-tagged CIPK11 protein was generated using wheat germ-based cell-free protein synthesis with the RTS 500 Wheat Germ CECF Kit (5 PRIME) following the manufacturer's instructions. The purification of the StrepII-CIPK11 protein was performed as previously described (Hashimoto et al., 2012).

Constructs for recombinant protein expression of full-length and C-terminal part of non-mutated and mutagenized FIT forms were produced as follows: Full-length *FIT* coding sequence was amplified from Col-0 –Fe root cDNA using primers SpeI-noATG-FIT and FITstop-SacI (Supplemental Table 1). The C-terminal part of *FIT* or mutagenized *FIT* forms were amplified from cDNA prepared from tobacco leaves infiltrated with pMDC83:gFIT, pMDC83:gFITm(AA) or pMDC83:gFITm(E), respectively, using primers SpeI-FIT-C and FITstop-SacI (Supplemental Table 1). The obtained *FIT*, *FIT-C*, *FITm-C(AA)* and *FITm-C(E)* products were subsequently cloned into the pET-24a(+) plasmid (Novagen). The resulting constructs were transformed into the *E. coli* bacterial strain BL21(DE3)pLysS (Promega).

In order to obtain StrepII-tagged glutathione S-transferase (GST) protein, the *GST* coding sequence was amplified using primers GST_XbaI.for and GST_SpeI_BamHI_SalI.rev (Supplemental Table 1) and subcloned into the pIVEX-WG-StrepII vector (Hashimoto et al., 2012). The resulting StrepII-GST fusion was subsequently cloned into pET-24b(+) plasmid. The resulting construct was transformed into BL21(DE3)pLysS cells.

Recombinantly expressed StrepII-FIT, StrepII-FIT-C, StrepII-FITm-C(AA) and StrepII-FITm-C(E) proteins were produced from BL21(DE3)pLysS cell cultures carrying the pET-24a(+) plasmid containing the respective StrepII-tagged FIT form as described in (Hashimoto et al., 2012). The affinity purification of the StrepII-tagged FIT forms was performed using Strep-

Tactin® Macro Prep (IBA) following the manufacturer's instructions. The protein amount in the fractions was estimated using BSA standards on Coomassie-stained SDS gels.
The StrepII-GST protein was produced in a similar manner, with the following exception: after cell lysis and centrifugation, StrepII-GST protein remained in the supernatant, which was then directly used for affinity purification using Strep-Tactin® Macro Prep (IBA) following the manufacturer's instructions.

In Vitro Kinase Assay

In vitro kinase assays were performed according to (Hashimoto et al., 2012). StrepII-tagged purified CIPK11 (150 ng per reaction) and different substrate proteins (500 ng per reaction) were mixed according to the experimental setup. Following the kinase assay, the samples were subjected to SDS-PAGE and Coomassie staining. The SDS gels were exposed to phosphorimager screens and the radioactively labelled protein bands were visualized by auto-radiography using a Molecular Dynamics Typhoon 9200 Variable Mode Imager (Amersham Biosciences). The *in vitro* kinase assays were repeated two to three times, showing similar results.

Cytoplasm-to-Nucleus Ratio Determination

The localization of FIT-GFP and FITm-GFP fusion proteins was detected in tobacco 48 hours post infiltration by laser-scanning confocal microscopy (LSM 780, Zeiss). Cells were imaged using a 40x C-Apochromat water immersion objective at an excitation wavelength of 488 nm and an emission wavelength of 500 to 530 nm, pinhole diameter 90 µm, pixel resolution of 0.208 µm in X and Y, and 1 µm in Z. Z-stacks typically consisted of 20 - 40 slices ensuring the recording full cell dimensions. For nucleus-to-cytoplasm ratio analysis, a maximum intensity projection of the Z-stack was made in the ZEN 2 Blue Edition software. Images were exported to tiff files and each image was analyzed in ImageJ software after conversion to 12-bit grayscale format. Signal intensity values were obtained for the whole cell without the nucleus and for the nucleus separately. The nucleus-to-cytoplasm ratio was calculated for each cell separately. Six tobacco cells were imaged per construct per experiment. Three independent experiments were performed.

Fluorescence Recovery after Photobleaching (FRAP) Analysis

The mobility of FIT-GFP and FITm-GFP fusion proteins, transiently expressed in tobacco was quantified using laser-scanning confocal microscopy (LSM 780, Zeiss) as described above.

Data was recorded with a pinhole diameter of 41 µm and pixel resolution of 0.208 µm. Successive control scans were made to ensure that no acquisition bleaching occurred during imaging. After 20 scans, a bleach with 50 iterations of maximum laser intensity was performed of a rectangular region of interest (ROI) of 46 x 14 pixels in the nucleus. This was followed by 280 post-bleaching scans within 100 seconds. For each single acquisition, the background fluorescence was subtracted from the FRAP values, which were then normalized to the mean of the pre-bleach values. The kinetic parameter final fluorescence intensity (F_{end}) was determined after applying Exponential curve fitting in the Origin Lab software, taking into account the initial fluorescence intensity (F_{pre}) and the fluorescence intensity after photobleaching (F_{post}). The percentage of mobile (M_f) and immobile (I_f) fractions of FIT-GFP, FITm(AA)-GFP and FITm(E)-GFP was determined according to the following equations: $M_f = [(F_{end}-F_{post})/(F_{pre}-F_{post})] * 100$ and $I_f = 100 - M_f$ (Bancaud et al., 2010). Twelve to 21 nuclei were quantified per construct.

Transcriptional Self-activation Capacity Assay

In order to investigate the self-activation capacity of FIT and mutagenized FIT forms, full-length *FIT*, *FITm(AA)* and *FITm(E)* were amplified using primers FIT B1 and FITns B2 (Supplemental Table 1) from cDNA prepared from tobacco leaves transiently transformed with pMDC83:gFIT, pMDC83:gFITm(AA) and pMDC83:gFITm(E). The PCR products were cloned into pDONR207 (BP reaction; Life Technologies) and subcloned into the BD-containing yeast two-hybrid destination vector pGBKT7-GW (LR reaction; Life Technologies). The resulting constructs were co-transformed into AH109 yeast cells together with an empty AD-containing pACT2-GW plasmid. Growth of yeast colonies was assayed on SD-LWH media with two different high 3-AT concentrations (30 and 60 mM) after spotting in ten-fold serial dilutions. Growth on selective SD-LW media was used as a co-transformation control. pGBKT7-GW and pACT2-GW plasmids were kindly provided by Dr. Yves Jacob.

Protein Homo- and Hetero-dimerization Assay in Yeast

For assaying the homo-dimerization ability of FIT-C and FIT-C phospho-mutant forms, *FITm-C(AA)* and *FITm-C(E)* coding sequences were amplified from tobacco cDNA (primers FIT-C B1 and FITst B2, Supplemental Table 1) and the amplicons were transferred into the BD- and AD-containing vectors pGBKT7-GW and pACT2-GW, respectively, to obtain the final destination constructs. These constructs were used to co-transform yeast AH109 cells with the combinations BD-FIT-C with AD-FIT-C, BD-FITm-C(AA) with AD-FITm-C(AA), and BD-

FITm-C(E) with AD-FITm-C(E). Growth of yeast colonies was assayed on SD-LWH media with 0.5 mM 3-AT (selection for interaction) after spotting in ten-fold serial dilutions. Growth on selective SD-LW media was used as a co-transformation control.

For assaying the ability of FIT-C and FIT-C phospho-mutant forms to form hetero-dimers with bHLH039, the coding sequence of *BHLH039* was amplified using the primers 39 B1 and 39st B2 (Supplemental Table 1) and subcloned into pACT2-GW to obtain AD-bHLH039. AD-bHLH039 was co-transformed with AD-FIT-C, BD-FITm-C(AA) and AD-FITm-C(AA) in AH109 cells and the strength of their interaction was assayed as described above.

Protein Homo- and Hetero-dimerization Assays *in planta* (FRET-APB)

Full-length coding sequences of FIT and FITm were cloned into the pABind vector set [pABindGFP, pABindmCherry, and pABindFRET (named here pABindGFPmCherry)] (Bleckmann et al., 2010) by LR reaction (Life Technologies) using the constructs pDONR207:cFIT, pDONR207:cFITm(AA) and pDONR2017:cFITm(E). The Agrobacterium (*Rhizobium radiobacter*) strain C58 (pGV2260) carrying one of the obtained constructs was used to transiently transform tobacco (*Nicotiana benthamiana*) leaf epidermis cells as previously described (Hotzer et al., 2012). Direct application of β-estradiol allowed the inducible expression of GFP-, mCherry- and GFP-mCherry-tagged FIT, FITm(AA) and FITm(E) fusion proteins 24 hours post infiltration. Förster Resonance Energy Transfer - Acceptor Photo Bleaching (FRET-APB) for GFP and mCherry-tagged pairs was measured to assess the strength of homo-dimer formation in epidermis cell nuclei. GFP-tagged fusions were used as donor-only (negative) controls. Fusions of the respective proteins with both GFP and mCherry for intra-molecular FRET were used as positive controls. Similarly, bHLH039 coding sequence was also cloned into the pABind vector set to produce bHLH039-GFP and bHLH039-GFP-mCherry fusions. bHLH039-GFP FRET pairs with FIT/FITm(AA)/FITm(E)-mCherry were assayed for their FRET efficiency. bHLH039-GFP was used as a donor-only control. bHLH039-GFP-mCherry was used as a positive control. Laser-scanning confocal microscopy (LSM 780, Zeiss) controlled by ZEN 2 Black Edition software (Zeiss) was used for GFP and mCherry detection as described above. Series of images were acquired in a 256 x 256 pixel format. After the fifth image, mCherry was photobleached in a region within the nucleus using 80 iterations of 100 % laser power. FRET efficiency (E_{FRET}) in percent was calculated as the relative increase of GFP intensity following photobleaching of the mCherry acceptor. Ten nuclei were measured per construct. Two independent experiments were performed.

fit Mutant Complementation Assay

Arabidopsis *fit-3* mutant plants (Jakoby et al., 2004) complemented with FIT-GFP using pMDC83:gFIT (named FIT/*fit*) were generated by floral dip (Clough and Bent, 1998). Positive transformants were selected based on hygromycin resistance, GFP fluorescence and PCR genotyping, selfed, and propagated until homozygous lines were obtained. T3 plants were used for analysis.

Arabidopsis *fit* mutant plants were transformed with the phospho-null FIT form C-terminally fused to GFP, FITm(AA)-GFP, by floral dip (Clough and Bent, 1998). Positive transformants, selected based on hygromycin resistance, GFP fluorescence and PCR genotyping, were selfed and multiplied until homozygous lines were obtained. Two independent FITm(AA)-GFP/*fit* plant lines in T3 generation were used for further analysis, AA#1 and AA#2.

Quantification and Statistical Analysis

Statistical details of experiments, such as number of technical and biological repetitions, can be found in the respective Methods section and in the Figure legends. For statistical analysis, P values were obtained via one-way ANOVA followed by Fisher's LSD using the SPSS Statistics software (IBM). Different lower-case letters on the graphs were used to indicate statistically significant differences ($P < 0.05$).

Accession Numbers

Sequence data from this article can be found in the EMBL/GenBank data libraries under accession numbers:

AKT1 (At2g26650), *BHLH039* (At3g56980), *CIPK1* (At3g17510), *CIPK2* (At5g07070), *CIPK3* (At2g26980), *CIPK4* (At4g14580), *CIPK5* (At5g10930), *CIPK6* (At4g30960), *CIPK7* (At3g23000), CIPK8 (At4g24400), *CIPK9* (At1g01140), *CIPK10* (At5g58380), *CIPK11* (At2g30360), *CIPK12* (At4g18700), *CIPK13* (At2g34180), *CIPK14* (At5g01820), *CIPK15* (At5g01810), *CIPK16* (At2g25090), *CIPK17* (At1g48260), *CIPK18* (At1g29230), *CIPK19* (At5g45810), *CIPK20* (At5g45820), CIPK21 (At5g57630), CIPK22 (At2g38490), *CIPK23* (At1g30270), *CIPK24* (At5g35410), *CIPK25* (At5g25110), CIPK26 (At5g21326), *FIT* (At2g28160), *FRO2* (At1g01580), *FRO3* (At1g23020), *IRT1* (At4g19690), *NAS4* (At1g56430), *SlFER* (AF437878).

SUPPLEMENTAL INFORMATION

Supplemental Information includes six figures and one table.

SUPPLEMENTAL FIGURES AND LEGENDS

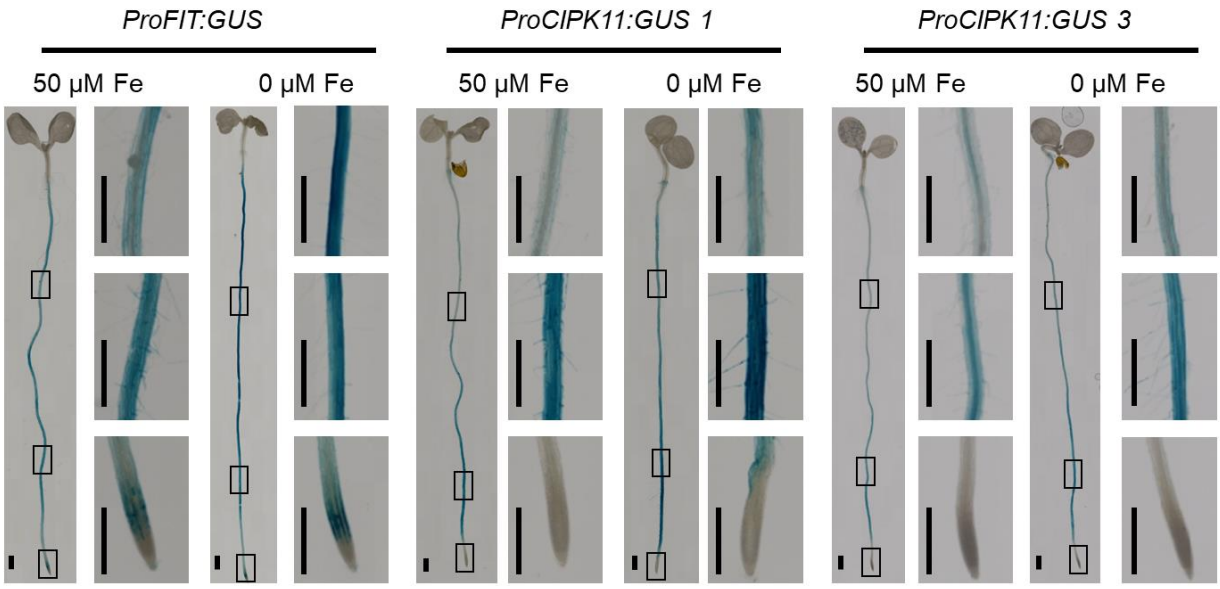

Supplemental Figure 1. Overlapping Fe-deficiency-induced *FIT* and *CIPK11* promoter activity.
Promoter-driven GUS reporter activity in whole seedlings and roots. Transgenic plants with *ProFIT:GUS* and *ProCIPK11:GUS* (lines 1 and 3) were grown in the 6-day system under sufficient (+ Fe) or deficient (- Fe) supply and stained for GUS activity. Rectangles in the respective seedling image indicate the positions of the enlarged images along the root for each genotype and condition, and correspond to, from top to bottom, the differentiated cell zone, the early differentiation zone, and the root tip. Bars: 1 mm.

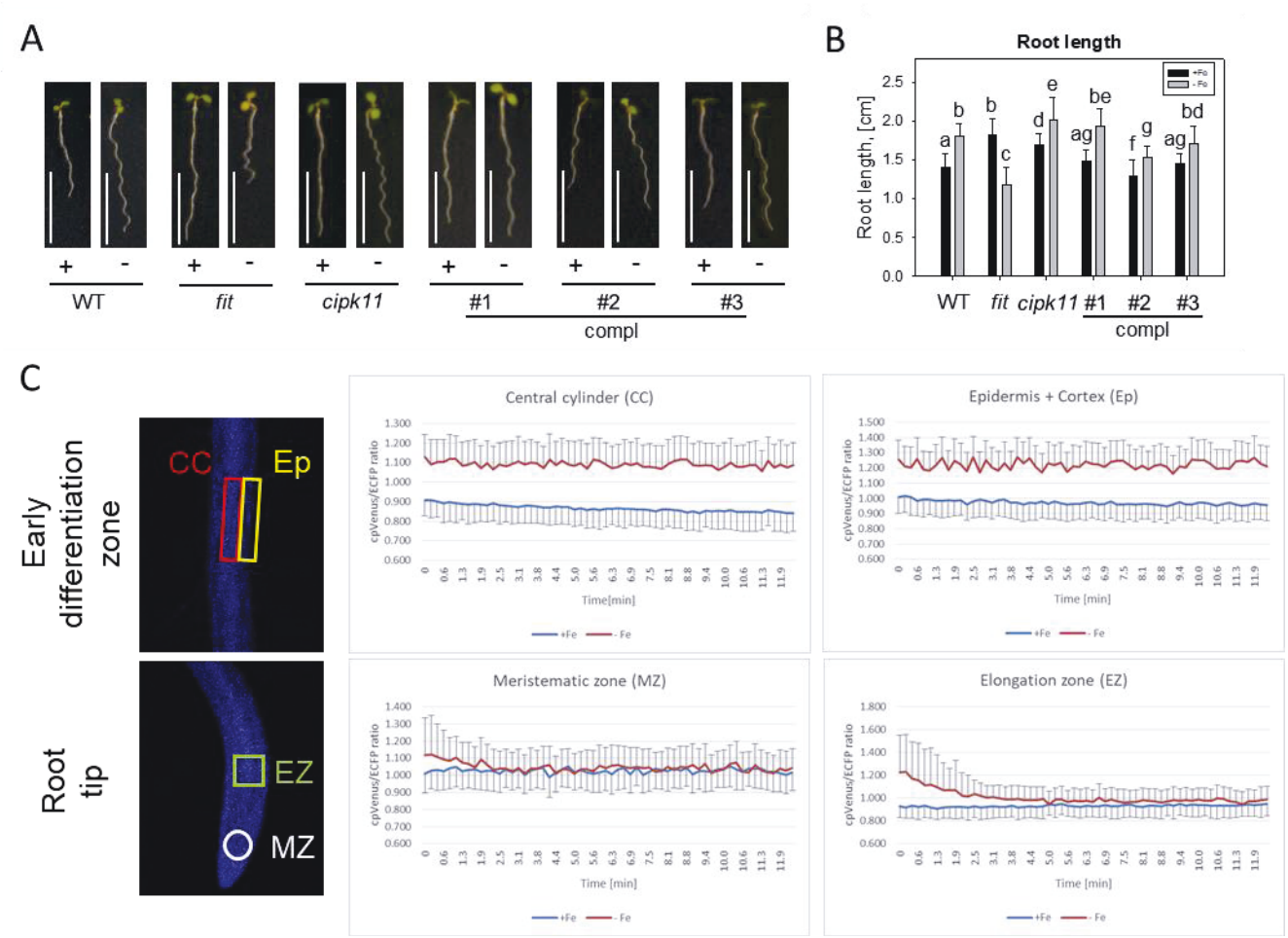

Supplemental Figure 2. *cipk11* root length phenotype and $[Ca^{2+}]_{cyt}$ measurements in Fe-deficient WT roots. **(A)** Phenotypes of plants grown in the 6-day system under sufficient (+ Fe) or deficient (- Fe) Fe supply. *cipk11* mutant and three *cipk11*-complemented lines (compl #1, #2, and #3) were analyzed in comparison with wild type (WT) and *fit* mutant. Bars: 1 mm. **(B)** Primary root lengths of plants grown as in (A). Bars represent mean values. Error bars represent standard deviations. (n = min 16). Different letters indicate statistically significant differences ($P < 0.05$). **(C)** Changes in free $[Ca^{2+}]_{cyt}$ in response to Fe-deficiency. The emission ratios between cpVenus and ECFP fluorescence intensities indicate changes in free cytosolic $[Ca^{2+}]$ in roots of plants grown under sufficient (+Fe, blue line) and deficient (-Fe, red line) Fe supply. $[Ca^{2+}]_{cyt}$ changes were measured for 12 min in different roots zones: meristematic (MZ) and elongation (EZ) of the root tip, central cylinder (CC) and epidermis with cortex (Ep) of the early root differentiation zone, as indicated. In order to exclude unspecific responses of the root to the mounting on the microscopic slide, the ratio values after the 3.3 min were averaged for each zone and represented in Figure 3J. Error bars represent standard deviations. (n = 12)

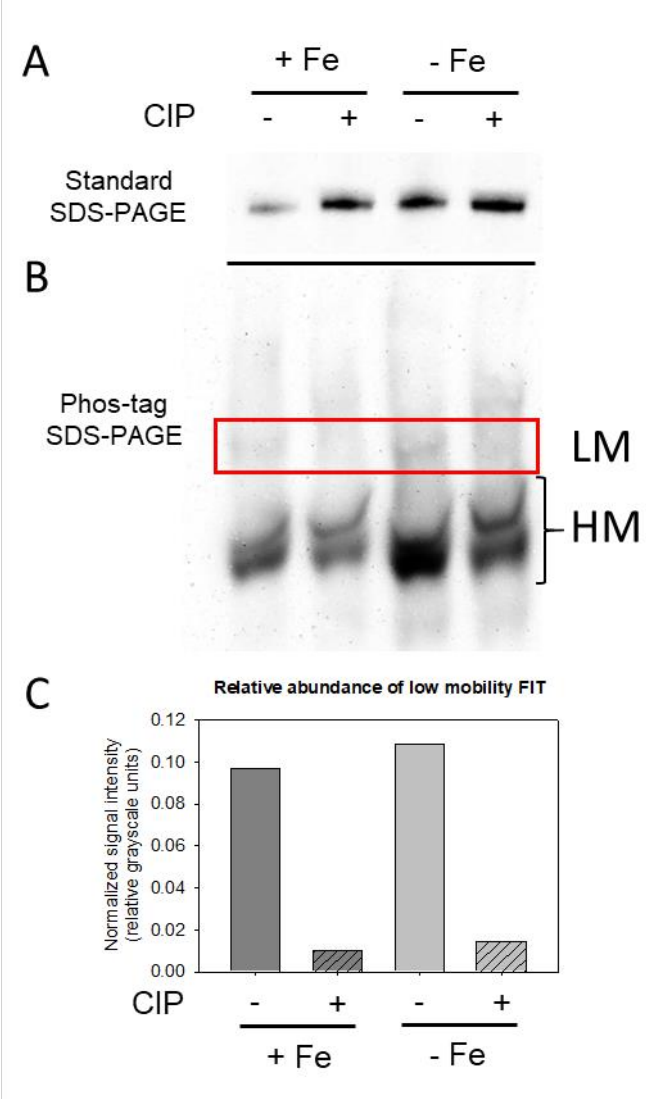

Supplemental Figure 3. *In vivo* phosphorylation of FIT.

(A) Immunoblot using anti-HA-HRP antibody after standard SDS-PAGE of protein extracts from roots of HA_7-FIT plants grown under sufficient (+ Fe) or deficient (- Fe) Fe supply and treated with Calf Intestinal Phosphatase (+ CIP) or mock treated (- CIP). **(B)** Immunoblot using anti-HA-HRP antibody after Phos-tag SDS-PAGE of the same protein extracts as in (A). Red rectangle surrounds the image area used for quantifying low mobility FIT forms (LM) in each sample. A bracket denotes the image area used for quantifying high mobility FIT forms (HM). **(C)** Quantification of the relative abundance of low mobility FIT vs the total FIT pool. The image shown in (B) was used to calculate normalized FIT signal intensity (in relative grayscale units) in the protein extracts from roots of plants grown under sufficient (dark gray bars) or deficient (light gray bars) Fe supply, mock treated (no pattern) or CIP treated (diagonal pattern).

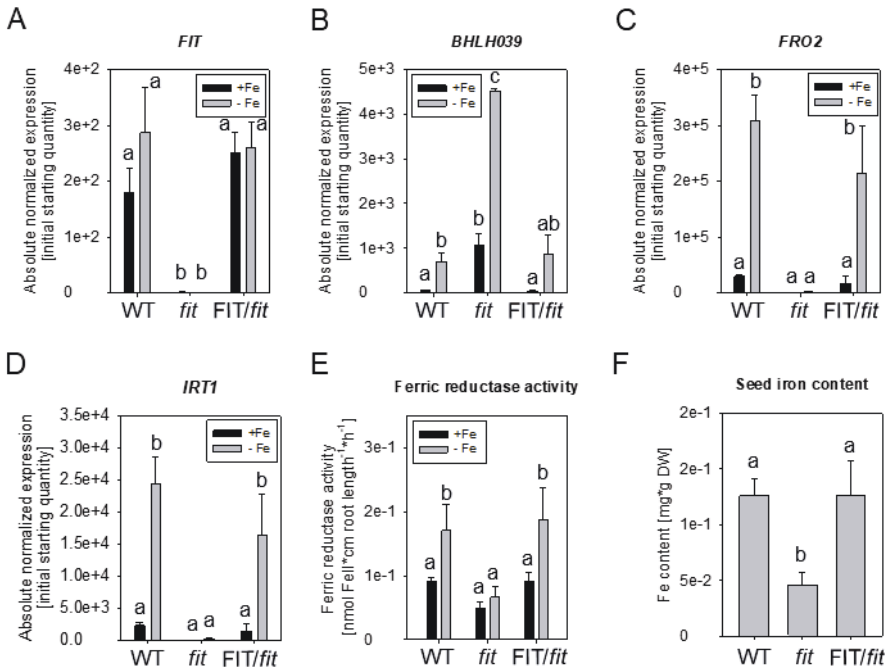

Supplemental Figure 4. FIT-GFP is a functional FIT fusion that can rescue the Fe-deficient *fit* mutant phenotype.

(A-D) Gene expression analysis in roots of plants grown in the 2-week system in response to sufficient (+Fe, black bars) and deficient (-Fe, gray bars) Fe supply. The expression of *FIT* (A), *BHLH039* (B), *FRO2* (C) and *IRT1* (D) was investigated in wild type (WT), *fit* mutant and *Pro35S:gFIT-GFP*-complemented *fit* mutant plants (FIT/*fit*). (n = 3) **(E)** Root Fe reductase activity of plants grown as in (A). (n = 4) **(F)** Fe content of seeds collected from soil-grown plants. DW, dry weight. (n = 3) Error bars represent standard deviations. Different letters indicate statistically significant differences ($P < 0.05$).

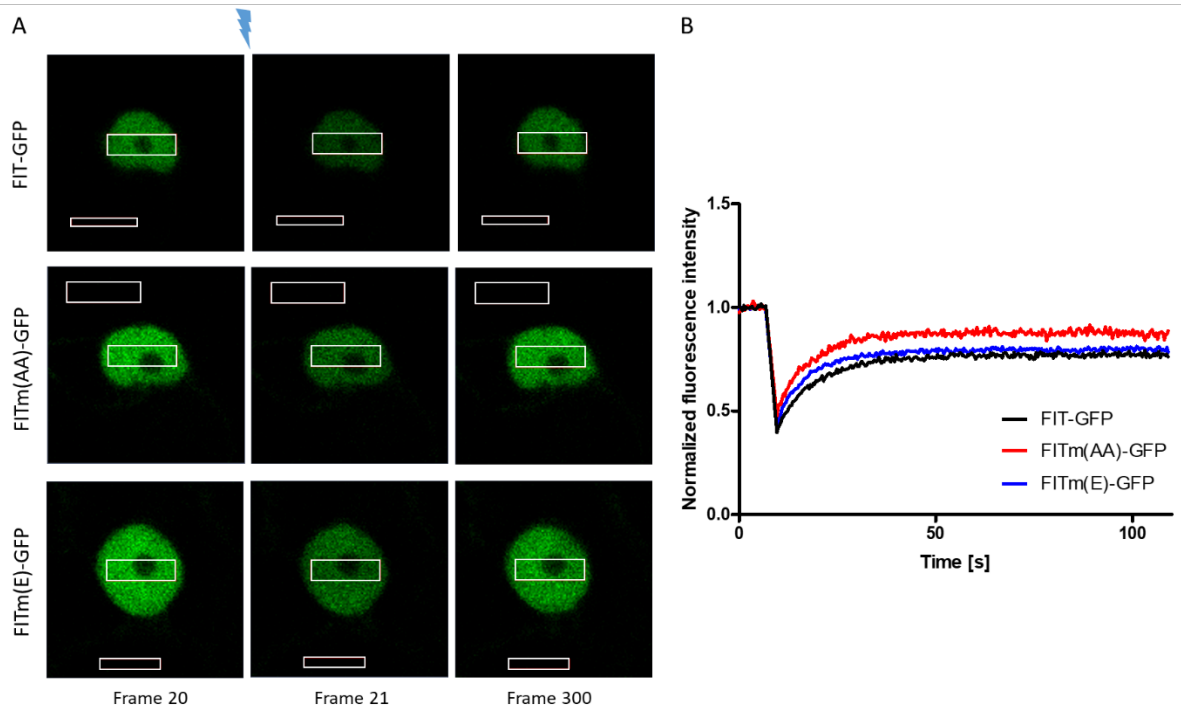

Supplemental Figure 5. Protein mobility of FIT-GFP and FITm-GFP analysis by Fluorescence Recovery after Photobleaching (FRAP).

(A) Nuclear-localized non-mutagenized FIT-GFP (upper horizontal panels), the phospho-null FITm(AA)-GFP (middle horizontal panels) and the phospho-mimicking FITm(E)-GFP forms (lower horizontal panels) were subjected to FRAP in transiently transformed tobacco leaf epidermis cells in order to compare the rate of their GFP-fluorescence recovery after photobleaching. Representative GFP fluorescence images for each FIT form show the GFP signal intensity just before bleaching (marked by a lightning sign) (left vertical panels, frame 20), immediately after bleaching (middle vertical panels, frame 21) and at the end of the GFP acquisition time (right vertical panels, frame 300). White rectangular shapes indicate the measured regions of interest (ROIs). The GFP fluorescence was bleached in the ROIs inside the nucleus. The ROIs outside the nucleus served the background fluorescence subtraction. **(B)** Background-corrected, normalized fluorescence intensities are plotted as a function of time. One representative curve is shown for each FIT form. The pre-bleach fluorescence intensities are set to 100 %. During the bleaching of the nuclei, a strong decline of the fluorescence signals by more than 50 % can be seen, indicative of successful bleaching. The GFP fluorescence signal recovery of the non-phosphorylatable FITm(AA)-GFP form (red) is accelerated in comparison to the recovery of the non-mutagenized FIT-GFP (black) and phospho-mimicking FITm(E)-GFP (blue). forms.

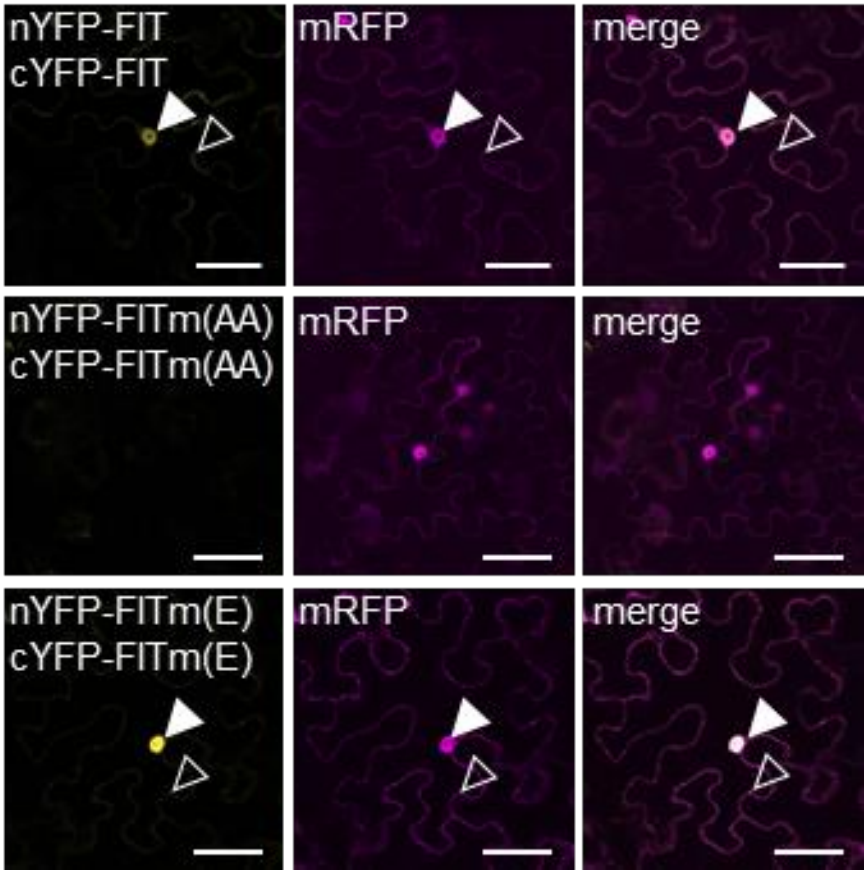

Supplemental Figure 6. FIT and FITm homo-dimerization analysis *in planta*.

Laser-scanning confocal images showing Bimolecular Fluorescence Complementation (BiFC) of nYFP- and cYFP-tagged FIT and FITm homo-dimer couples in tobacco leaf epidermis cells. Successful homo-dimer formation (YFP signal) was detected for FIT (nYFP-FIT and cYFP-FIT, upper horizontal panels) and FITm(E) (nYFP-FITm(E) and cYFP-FITm(E), lower horizontal panels), whereas FITm(AA) (nYFP-FITm(AA) and cYFP-FITm(AA), middle horizontal panels) homo-dimerization was barely detectable. Reconstituted YFP signals are indicated by arrowheads (filled for nuclear YFP, empty for cytoplasmic YFP). Positive mRFP signal served as a transformation control. Bars: 50 µm.

Supplemental Table 1. Primers used in this study.

Primer name	Primer sequence	Purpose	Origin
pCIPK11_forSpe	TTTACTAGTCAACGTGAAACTTTTGCTGATAAA	Cloning of ProCIPK11:GUS and pKS II Bluescript:ProCIPK11	This study
pCIPK11_reXho	TTTCTCGAGGATTGATGAATCCAGAGATTGATT	Cloning of ProCIPK11:GUS	This study
CIPK11 SpeI forward	TTTACTAGTATGCCAGAGATCGAGATTGC	Cloning of pGPTV-II-BAR-pUBQ10-GFP:CIPK11 and pIVEX-WG-StrepII:CIPK11	This study
CIPK11 XhoI reverse	TTTCTCGAGAATAGCCGCGTTTGTTGACG	Cloning of pGPTV-II-BAR-pUBQ10-GFP:CIPK11 and pIVEX-WG-StrepII:CIPK11	This study
FIT B1	GGGGACAAGTTTGTACAAAAAAGCAGGCTTAATGGAAGGAAGAGTCAACGC	Cloning of pDONR207:gFIT and pDONR221 P1-P4:cFIT	Le et al., 2016
FITns B2	GGGGACCACTTTGTACAAGAAAGCTGGGTTAGTAAATGACTTGATGAATTC	Cloning of pDONR207:gFIT	This study
CIPK11 B3	GGGGACAACTTTGTATAATAAAGTTGTAATGCCAGAGATCGAGATTGC	Cloning of pDONR221 P3-P2:CIPK11	This study
CIPK11 B2	GGGGACCACTTTGTACAAGAAAGCTGGGTTTTAAATAGCCGCGTTTGTTG	Cloning of pDONR221 P3-P2:CIPK11	This study
FITstop B4	GGGGACAACTTTGTATAGAAAAGTTGGGTGTCAAGTAAATGACTTGATGA	Cloning of pDONR221 P1-P4:cFIT	Le et al., 2016

39 B1	GGGGACAAGTTTGTACAAAAAAGCAGGCTTAATGTGTGCATTAGTACCTCC	Cloning of pDONR221 P1-P4:BHLH039	Le et al., 2016
39st B4	GGGGACAACTTTGTATAGAAAAGTTGGGTGTCATATATATGAGTTTCCAC	Cloning of pDONR221 P1-P4:BHLH039	Le et al., 2016
CIPK15 B3	GGGGACAACTTTGTATAATAAAGTTGTAATGGAGAAGAAAGGATCTGT	Cloning of pDONR221 P3-P2:CIPK15	This study
CIPK15st B2	GGGGACCACTTTGTACAAGAAAGCTGGGTTTCAGTGCCAAGCTAATACAA	Cloning of pDONR221 P3-P2:CIPK15	This study
pCIPK11_reBam_2	TTTGGATCCGATTGATGAATCCAGAGATTGATT	Cloning of pKS II Bluescript:ProCIPK11	This study
CIPK11_for_Bam	TTTGGATCCATGCCAGAGATCGAGATTGC	Cloning of pKS II Bluescript:gCIPK11+3'UTR	This study
CIPK11UTRreXho	TTTCTCGAGGGAAAATCCAAACTATAAATAGAAGA	Cloning of pKS II Bluescript:gCIPK11+3'UTR	This study
EFg1	TCCGAACAATACCAGAACTACG	*EF1Balpha* (genomic) RT-PCR	Wang et al., 2007
EFg2	CCGGGACATATGGAGGTAAG	*EF1Balpha* (genomic) RT-PCR	Wang et al., 2007
EFc1	ACTTGTACCAGTTGGTTATGGG	*EF1Balpha* RTPCR	Wang et al., 2007
EFc2	CTGGATGTACTCGTTGTTAGGC	*EF1Balpha* RTPCR	Wang et al., 2007

FITrt1	GGAGAAGGTGTTGCTCCATC	*FIT* RT-PCR	Wang et al., 2007
FITrt2	TCCGGAGAAGGAGAGCTTAG	*FIT* RT-PCR	Wang et al., 2007
BHLH39rt1	GACGGTTTCTCGAAGCTTG	*BHLH039* RT-PCR	Wang et al., 2007
BHLH39rt2	GGTGGCTGCTTAACGTAACAT	*BHLH039* RT-PCR	Wang et al., 2007
IRT1rt1	AAGCTTTGATCACGGTTGG	*IRT1* RT-PCR	Wang et al., 2007
IRT1rt2	TTAGGTCCCATGAACTCCG	*IRT1* RT-PCR	Wang et al., 2007
FRO2rt1	CTTGGTCATCTCCGTGAGC	*FRO2* RT-PCR	Wang et al., 2007
FRO2rt2	AAGATGTTGGAGATGGACGG	*FRO2* RT-PCR	Wang et al., 2007
C11 RT-F	GGATTTGTATTTCGCGGTTG	*CIPK11* RT-PCR	This study
C11 RT-R	GTCAACAAACGCGGCTATTT	*CIPK11* RT-PCR	This study
FITmS272E-1	AACTCTAACCTAAGCGAACCTTCTCCGGACACA	Cloning of pDONR2017:gFITm(E)	This study
FITmS272E-2	TGTGTCCGGAGAAGGTTCGCTTAGGTTAGAGTT	Cloning of pDONR2017:gFITm(E)	This study
FITmSS271AA-1	CAGAACTCTAACCTAGCCGCTCCTTCTCCGGACA	Cloning of pDONR207:gFITm(AA)	This study
FITmSS271AA-2	TGTCCGGAGAAGGAGCGGCTAGGTTAGAGTTCTG	Cloning of pDONR207:gFITm(AA)	This study

SpeI-noATG-FIT	TTTTACTAGTGAAGGAAGAGTCAACGCTCT	Cloning pET-24a(+):FIT/ FITm(AA)/FITm(E)	This study
FITstop-SacI	AAAAGAGCTCTCAAGTAAATGACTTGATGA	Cloning pET-24a(+):FIT/ FITm(AA)/FITm(E) and pET-24a(+):FIT-C/ FITm-C(AA)/FITm-C(E)	This study
SpeI-FIT-C	TTTTACTAGTACTCAACCTTTTCGCGGTAT	Cloning pET-24a(+):FIT-C/ FITm-C(AA)/FITm-C(E)	This study
GST_XbaI.for	AAATCTAGAATGTCCCCTATACTAGGTTATTG	Cloning pET-24a(+):GST	This study
GST_SpeI_BamHI_ SalI.rev	TTTTGTCGACGGATCCACTAGTATCCGATTTTGGAGG	Cloning pET-24a(+):GST	This study
FIT-C B1	GGGGACAAGTTTGTACAAAAAAGCAGGCTTAACTCAACCTTTTCGCGGTATC	Cloning pGBKT7-GW: and pACT2-GW:FIT-C/ FITm-C(AA)/FITm-C(E)	This study
FITst B2	GGGGACCACTTTGTACAAGAAAGCTGGGTTCAAGTAAATGACTTGATGA	Cloning pGBKT7-GW: and pACT2-GW:FIT-C/ FITm-C(AA)/FITm-C(E)	This study

Authors Contribution to Manuscript 1

Regina Gratz

Designed, performed and analyzed following experiments: Yeast assays (Figures 2A, 5C, 6A, 6C), nucleo-cytoplasmic partitioning (Figure 5A), protein mobility (Figure 5B, Supplemental Figure 5), phospho-mutant line analysis (Figure 7, Supplemental Figure 4), Phos-tag assay (Supplemental Figure 3). Contributed to kinase assay (Figure 4B).
Contributed to the writing of the manuscript, prepared figures and reviewed / edited the manuscript.

Tzvetina Brumbarova, Rumen Ivanov, Inga Mohr, Ksenia Trofimov, Prabha Manishankar

Designed, performed and analyzed remaining experiments.

Michael Holtkamp, Uwe Karst

Performed total reflection X-Ray fluorescence experiments.

Johannes Meiser, Philipp Köster, Leonie Steinhorst, Maria Drerup, Sibylle Arendt

Provided plant lines and plasmids.

Petra Bauer, Tzvetina Brumbarova, Jörg Kudla

Designed the outline of the manuscript, supervised the study, provided funding, wrote the manuscript and prepared final figures (T. B.) and reviewed / edited the manuscript.

7 Manuscript 2

Evidence for two-step regulation of FIT, using phospho-mutant activity screening.

Evidence for two-step regulation of FIT, using phospho-mutant activity screening.

Regina Gratz[1], Tzvetina Brumbarova[1], Rumen Ivanov[1], Ksenia Trofimov[1], Rocio Ochoa-Fernandez[2], Tim Blomeier[2], Johannes Meiser[3], Matias Zurbriggen[2,4] and Petra Bauer[1,4,5]

[1]Institute of Botany, Heinrich-Heine University, 40225 Düsseldorf, Germany
[2]Institute of Synthetic Biology, Heinrich-Heine University, 40225 Düsseldorf, Germany
[3]Former address: Department of Biosciences-Plant Biology, Saarland University, 66123 Saarbrücken, Germany and current address: Cancer Research UK Beatson Institute, Glasgow, UK
[4]Cluster of Excellence on Plant Sciences, Heinrich-Heine University, 40225 Düsseldorf, Germany
[5]Corresponding author

Corresponding author: Petra Bauer, Institute of Botany, Heinrich-Heine University, 40225 Düsseldorf, Germany, petra.bauer@hhu.de

List of author contributions:
R. G., T. B., R. I., J. M., M. Z. and P. B. designed the study, R.G., T. B., R. I., K. T., R. O. F., T. B. and J. M. performed research, R. G., T. B., R. I., K. T., R. O. F., T. B., M. Z. and P. B. analyzed data, R. G. wrote the original draft, R. G., T. B. and P. B. reviewed and edited the article, T. B. and P. B. supervised the study, P. B. acquired funding.

Funding: Deutsche Forschungsgemeinschaft grants (Ba 1610/5-1 and Ba 1610/7-1)

Short title: FIT phospho-mutant activity screening

One sentence summary:
A phospho-mutant activity screening of predicted phosphorylation sites uncovers a role of serines for activation and tyrosines for degradation of the iron-regulated transcription factor FIT.

Abstract

Nutritional stress such as iron (Fe) deficiency affects plants in growth and fitness which ultimately leads to crop failure. Post-translational modifications fine-tune the activities of many signaling proteins and transcription factors, enabling dynamic molecular responses to changing environmental conditions. We demonstrated that the key transcription factor in Fe uptake signaling FER-LIKE IRON DEFICIENCY-INDUCED TRANSCRIPTION FACOTR (FIT) is divided into two different pools, in an active and an inactive pool. It however remained unclear which molecular mechanism controls the activity status of FIT. Recently, we could show that the C-terminus of FIT undergoes protein phosphorylation at position Ser272 which subsequently activated the protein. Hence, we asked whether FIT contains additional phosphorylation sites, which may antagonistically regulate FIT activity. Thus, Ser272 and additional predicted phosphorylation sites in its vicinity at the C-terminus of FIT were mutated to phospho-mimicking and non-phosphorylatable sites, and subjected to a phospho-mutant activity screening. We found that phospho-mutations have an influence on FIT localization, nuclear mobility as well as dimerization capacity. Based on a quantitative transactivation assay, we found that the different mutations impact FIT transcriptional activity and the existence of overriding effects among the different target sites. We found an increased FIT activity in phospho-mimicked serine mutants, whereas phospho-mimicked tyrosine mutants were unable to activate the downstream target promoter of *IRT1*. Additionally, we found a compromised stability in one phospho-mimicked tyrosine mutant, mediated by 26S proteasome. Taken together, we propose that FIT-C acts as an integration point as differential phosphorylation depicts a two-step regulatory mechanism for FIT activity.

Introduction

Acquisition of trace elements, such as iron (Fe), is indispensable for metabolic pathways, crop yield and high-quality nutritious food. Biofortification offers the chance to reduce Fe-deficiency anemia in humans (Haas et al., 2016) but relies on elaborate knowledge of plant nutrient sensing, uptake and signaling. Under Fe-deficient conditions (-Fe), *Arabidopsis thaliana*, like other non-graminaceous angiosperms, induces Fe uptake and homeostasis genes and follows a reduction-based Fe acquisition strategy (Strategy I) (Marschner et al., 1986). Due to high amounts of insoluble Fe in the soil (Guerinot and Yi, 1994), plants first acidify the rhizosphere via proton extrusion, chelate ferric Fe (Fe^{3+}) and subsequently reduce it to ferrous Fe (Fe^{2+}), which is mediated by FERRIC REDUCTION OXIDASE 2 (FRO2) (Brumbarova et al., 2015). IRON REGULATED TRANSPORTER 1 (IRT1) then takes up Fe^{2+} into root epidermal cells (Eide et al., 1996; Vert et al., 2002). The expression of components involved in Strategy I Fe uptake is controlled by a complex regulatory network comprising the central regulator FER-LIKE IRON DEFICIENCY-INDUCED TRANSCRIPTION FACTOR (FIT), a subgroup IIIa basic helix-loop-helix (bHLH) protein (Heim et al., 2003; Colangelo and Guerinot, 2004; Jakoby et al., 2004). FIT controls the transcription of 34 Fe responsive genes (Mai et al., 2016), among which *IRT1* displays a robust Fe-deficiency marker gene (Ivanov et al., 2012). The *fit-3* loss-of-function mutant allele develops a strong Fe-deficiency leaf chlorosis and has a lethal phenotype (Jakoby et al., 2004). This displays the pivotal role of FIT in the Fe-deficiency response.

An interplay between external and internal signaling pathways affects the activity of FIT on a molecular level. FIT protein activity is controlled by Fe availability (Jakoby et al., 2004) and is modulated by different signaling molecules as well as hormones (Meiser et al., 2011; Brumbarova et al., 2015; Le et al., 2016). bHLH proteins form homo- and hetero-dimers (Heim et al., 2003). The hetero-dimerization of FIT and members of subgroup Ib bHLH proteins, bHLH038/039/100/101, is needed for downstream activation of FIT target gene expression (Heim et al., 2003; Wang et al., 2007; Yuan et al., 2008; Wang et al., 2013; Naranjo-Arcos et al., 2017). FIT activity is further controlled by direct interactions with proteins coupled to stress and hormone pathways (Brumbarova et al., 2015; Le et al., 2016; Wild et al., 2016; Gratz et al., 2018 (submitted)). Hence, the dynamic addition of FIT interactors enables the cell to quickly react to changes in Fe availability by fine-tuning FIT protein activity.

In a *FIT* overexpression situation, the *FIT* transcript and the FIT protein are present under both Fe sufficient (+Fe) and deficient conditions. However, induction of FIT target genes, *FRO2* and *IRT1,* only occurs upon Fe-deficiency. Moreover, the amount of FIT protein in the -Fe

overexpression situation can by far exceed that of FIT protein in wild-type (WT) at -Fe, although FIT target gene induction remains comparable (Lingam et al., 2011; Meiser et al., 2011). This finding is very interesting because it suggests that FIT protein is divided into rather small active and large inactive pools (Lingam et al., 2011; Meiser et al., 2011; Sivitz et al., 2011). Further, it was shown that FIT undergoes proteasomal degradation (Lingam et al., 2011; Meiser et al., 2011; Sivitz et al., 2011). Although both FIT pools are targets of the proteasome, FIT abundance is often lower at -Fe than at +Fe when overexpressed (Meiser et al., 2011; Sivitz et al., 2011). Presumably in order to maintain Fe-deficiency responses, inactive FIT is constantly activated and active FIT is being degraded to "refresh" target sites, which could be beneficial for the cell to remain responsive to quick changes in nutrient abundance (Lingam et al., 2011; Meiser et al., 2011; Sivitz et al., 2011). One explanation for molecular differentiation between active and inactive FIT forms is the involvement of differential post-translational modifications, for which we could recently provide evidence. We found that a small pool of FIT protein is phosphorylated in plants and identified CBL-INTERACTING PROTEIN KINASE CIPK11 as FIT interaction partner. We demonstrated that the C-terminal part of FIT (FIT-C) is phosphorylated at position Ser272 by CIPK11 and that this site has a positive impact on FIT localization, mobility and dimerization capacity. We concluded that Ser272 phosphorylation renders the FIT protein active (Gratz et al., 2018 (submitted)).

The activity of many transcription factors, such as the bHLH protein INDUCER OF CBF EXPRESSION1 (ICE1), involved in cold-stress responses (Chinnusamy et al., 2003), is regulated by phosphorylation. Cold-induced phosphorylation of Ser278, mediated by SnRK2.6 / OPEN STOMATA 1 (OST1), increased ICE1 stability and promoted downstream target gene expression (Ding et al., 2015). Likewise, MITOGEN-ACTIVATED PROTEIN KINASEs (MAPKs) MAPK3 / MAPK6 facilitate additional ICE1 phosphorylation. However, this had diametrical effects on its stability and lead to proteasomal degradation of ICE1 (Li et al., 2017; Zhao et al., 2017). Hence, phosphorylation events can contribute to the activity of a protein, but an antagonistic mechanism is likewise needed to ensure responsiveness to quickly changing conditions by a balanced protein activity.

Plant tyrosine phosphorylation is mainly associated with proteins having kinase or transferase activity and is overrepresented on nuclear proteins (Sugiyama et al., 2008). Only a few transcription factors were identified to be tyrosine-phosphorylated until now such as *Coptis japonica* WRKY-type transcription factor CjWRKY1, involved in alkaloid biosynthesis (Kato et al., 2007; Yamada and Sato, 2016). A CjWRKY1 tyrosine phospho-mimicking mutant

displayed enhanced cytosolic localization and reduced transactivation activity. Additionally, protein turn-over was shown to be connected to the tyrosine phosphorylation status (Yamada and Sato, 2016).

The predominant regulation of FIT at protein level prompted us to question whether FIT activity is similarly and perhaps even antagonistically regulated by alternate phosphorylation. FIT C-terminus undergoes multiple protein interactions (Lingam et al., 2011; Le et al., 2016; Gratz et al., 2018 (submitted)) and, hence, it was of interest to investigate whether FIT-C possesses additional phosphorylation target sites besides Ser272. We further asked whether one site could reflect a negative regulatory unit and whether tyrosine phosphorylation sites could be predicted and validated. It seemed also conceivable that different phosphorylation sites could exhibit varying significances and hence display a certain hierarchy of phosphorylation events.

Unfortunately, due to the low amounts of FIT protein *in planta* and the small fractions of phosphorylated forms thereof, we were not able to experimentally prove directly individual phosphorylation sites, and to identify any phospho-peptides via LC-MS from enriched FIT protein, derived of plant cells.

For these reasons, we show results from an alternative approach that yielded evidence for novel FIT-C phosphorylation sites. Using a phospho-mutant activity screening we found that phospho-mimicking and non-phosphorylatable mutations affect FIT localization, nuclear mobility and dimerization, besides the known Ser272 site. A quantitative transactivation reporter gene assay indicated, that FIT activity is differentially regulated in these phospho-mutants. Also, one potential phospho-tyrosine was identified, which confers altered FIT protein stability properties. Besides, we expand on the knowledge of position Ser272 phosphorylation, by presenting data that indicate an overriding effect of this position over another site. We propose a model in which serine phosphorylation promotes and tyrosine phosphorylation inhibits FIT activity. This cellular mechanism may serve as tool to fine-tune Fe acquisition from the soil.

Results

Three-step analysis of FIT protein sequence identifies potential novel phosphorylation target sites.

Several bHLH transcription factors are phosphorylated at multiple sites, such as SPEECHLESS (SPCH) (Lampard et al., 2008; Gudesblat et al., 2012; Yang et al., 2015). We asked whether FIT also possesses additional phosphorylation sites, besides the recently identified Ser272 (Gratz et al., 2018 (submitted)). As explained above, we failed to identify FIT peptides by LC-MS and, hence, applied a phospho-mutant activity screening instead. We initially performed a three-step analysis of the FIT protein sequence to predict novel phosphorylation sites.

In the first step, we performed a NetPhos 2.0 (Blom et al., 1999) *in silico* prediction of potential FIT phosphorylation sites. A total of 21 amino acids were predicted, of which six residues were located in FIT-C (Figure 1A). These six C-terminal residues were of high interest, as FIT protein-protein interaction is mainly facilitated via its carboxyl-end (Lingam et al., 2011; Le et al., 2016; Gratz et al., 2018 (submitted)), displaying a regulatory subunit of the protein.

To narrow down the number of potential phosphorylation sites, we analyzed whether these sites are conserved among angiosperms, as we figured this would be the case for a regulatory site. Hence, as a second step, we performed a multiple sequence alignment between full-length Arabidopsis FIT and respective FIT orthologues (Figure 1B). Ser256 is conserved exclusively in the order of the Brassicales, representing the least conserved position among the candidates. Ser221 is conserved within the family of Brassicaceae, as well as in species belonging to the commelinids and fabids. Both serines Ser271 and Ser272 are conserved among the Brassicaceae. Interestingly, however, only one of the two serines is conserved among members of the monocots, superasterids, as well as the remaining superrosids.

Of high interest are two detected tyrosines, as they are highly conserved throughout the angiosperms. FIT orthologues, ranging from the most distant order of Amborellales to the order of Apiales, possess a tyrosine that aligns to Tyr238. Tyr278 was found to be conserved among the order of Brassicales as well as among the commelinids and the lamiids.

We included a full-length sequence alignment between FIT and two *A. thaliana* bHLH proteins, ABORTED MICROSPORES (AT2G16910) and DYSFUNCTIONAL TAPETUM (AT4G21330), which together with FIT belong to the subgroup IIIa bHLH proteins (Heim et al., 2003) (Figure 1C). With respect to C-terminal domains, both proteins do not show substantial sequence similarity with FIT. Also, neither of these two bHLH proteins contain conserved residues that align with predicted FIT phosphorylation target sites. This suggests a

specific function for the predicted sites only in the FIT protein. Given that the identified Tyr residues are predicted to be phosphorylated and are also moderately to highly conserved among angiosperms, makes them interesting candidate sites for a regulatory function.

In a final approach within this three-step analysis framework, we screened the FIT protein sequence for known phosphorylation motifs, surrounding the predicted amino acids. We identified respective motifs for four out of the six predicted phosphorylation target sites (Figure 1D). The motif [pS/pT]X[R/K] (Pearson and Kemp, 1991) encompasses Ser221, which strengthens the assumption of serine phosphorylation at this position. The additional phosphorylation motifs XXpSPX (Kemp and Pearson, 1990; Beausoleil et al., 2004; Luo et al., 2005; Schwartz and Gygi, 2005) and SXXXpS (Fiol et al., 1990) were found to enclose Ser271 and Ser272. This suggests that only one serine undergoes phosphorylation, to which we refer here as Ser272. The highly conserved Tyr238 is part of the motif pYXX[L/I/V] (Argetsinger et al., 2004). Another phosphorylation motif could be assigned to Tyr278, SX[D/E]XpY (Amanchy et al., 2011), which reinforces the hypothesis of tyrosine phosphorylation for both residues.

In summary, the three-step *in silico* prediction, multiple-sequence alignment and phosphorylation motif identification permitted us to identify the four promising phosphorylation target sites: Ser221, Ser272, Tyr238 and Tyr278.

A phospho-mutant activity screening approach was applied to identify whether these suggested target sites might have a regulatory function on FIT activity. To apply such an approach for FIT, we generated phospho-site substitutions by site-directed mutagenesis (FITm) (Figure 1D). Non-phosphorylatable mutations (Ser to Ala- and Tyr to Phe substitutions) as well as phospho-mimicking mutations (Ser or Tyr to Glu substitutions) were created. We recently showed that Ser272 is phosphorylated and relevant for FIT activity (Gratz et al., 2018 (submitted)). During the course of this phospho-mutant activity screening, we found the phospho-mimicking mutant FITm(S221E) to be more active on transcriptional level, than wild-type FIT, whereas FITm(S221A) seemed unaffected. Hence, we additionally created the triple phospho-mutant FITm(S221E / SS271/2AA) to analyze whether FITm(S221E) is dependent Ser272 phosphorylation, comparing it to the controls of single FITm(S221A) and FITm(SS271/2AA). These phospho-mutants were then tested with respect to several FIT regulatory properties and cellular activities, namely protein localization, mobility, interaction, transactivation activity and stability.

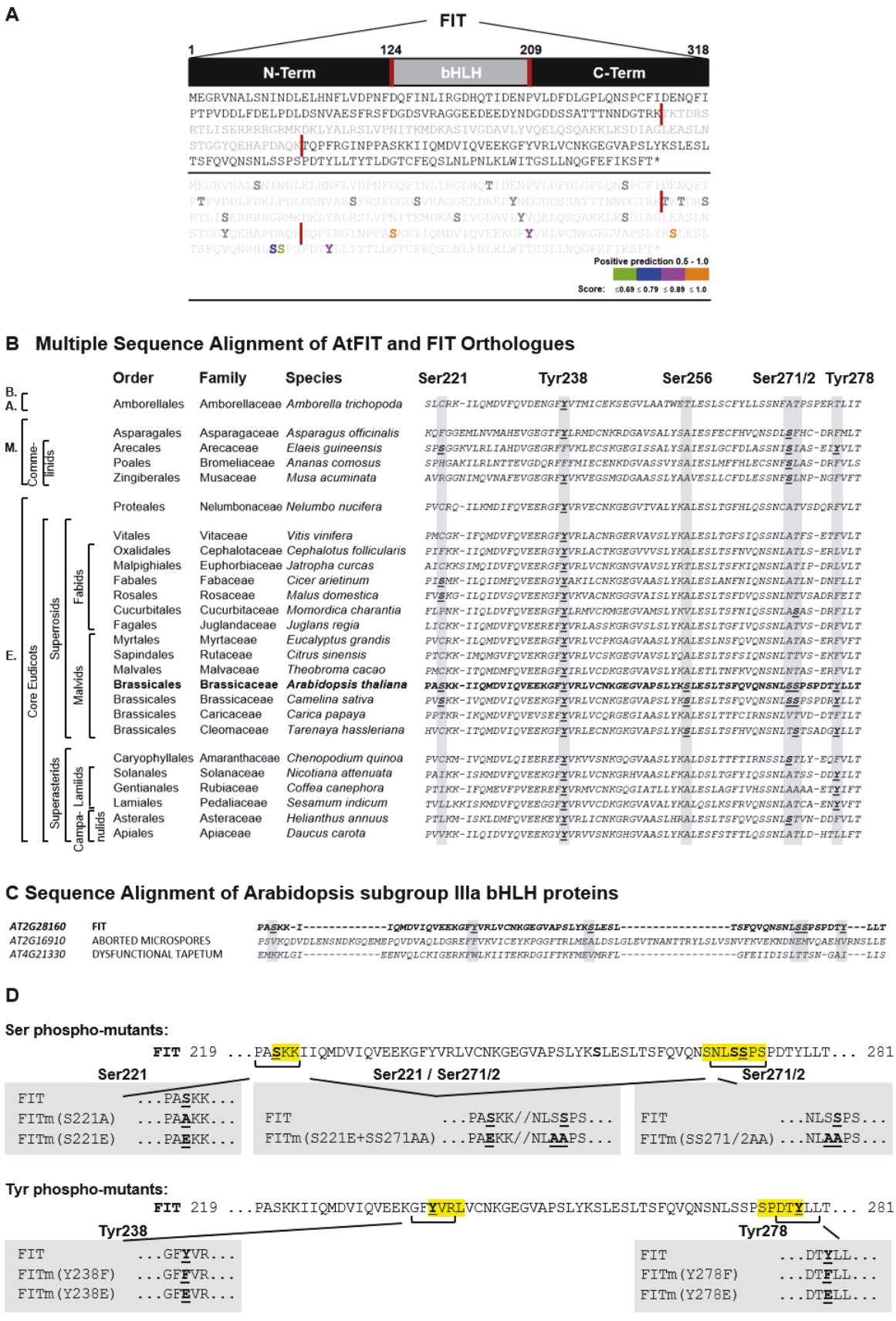

Figure 1. Analysis of FIT protein sequence reveals potential novel phosphorylation target sites in FIT-C. **(A)** Full length amino acid sequence of FIT (top), composed of an amino-terminal- (N-term), basic helix-loop-helix- (bHLH) (grey) and carboxyl-terminal- (C-term) region, divided by red bars. *In silico* prediction by NetPhos2.0 identified potential phosphorylation sites (bottom, bold), of which six are located in FIT-C (bold, colored). Colors reflect the confidence score of the prediction. **(B)** FIT orthologues were identified throughout the

angiosperm kingdom to analyze conserved amino acids. The orthologue of each order with the highest maximum score was aligned against full-length AtFIT (bold). Part of FIT-C term is shown, containing all predicted amino acids (grey, underlined) as in (A). Conserved target sites are marked (bold, underlined). B.A. Basal Angiosperms, M. Monocots, E. Eudicots. **(C)** AtFIT full-length protein sequence was aligned with bHLH proteins AT2G16910 and AT4G21330 (subgroup IIIa). FIT target sites are not conserved between the bHLH proteins. **(D)** Phosphorylated amino acids (underlined) of known phosphorylation motifs (yellow) surrounding predicted FIT target sites as in (A) (bold). FIT target site phospho-mutants (grey boxes) were generated (underlined) by site-directed mutagenesis, creating non-phosphorylatable (Ser to Ala, Tyr to Phe) and phospho-mimicking (Ser, Tyr to Glu) FIT forms.

FIT cellular localization and nuclear mobility depend on the phospho-mutant status.

Post-translational modifications, *e.g.* protein phosphorylation, can affect protein properties and characteristics, such as their subcellular localization (Ju et al., 2012; Ren et al., 2017; Takeo and Ito, 2017). The intracellular trafficking of proteins is central for their function. Although FIT is present in the nucleus (Yuan et al., 2008; Wang et al., 2013), we have found that FIT is also present in the cytoplasm (Gratz et al., 2018 (submitted)), whereby the cytoplasm-to-nucleus ratio was in the range of 3 - 5 (Figure 2). Since the cellular distribution might be part of a regulatory mechanism for FIT, we investigated at first the localization of GFP-tagged FIT phospho-mutants by analyzing their nucleo-cytoplasmic partitioning by confocal imaging. Out of the eight mutants tested, six FIT phospho-mutants showed a significant increase of the cytoplasm-to-nucleus ratio. FITm(SS271/2AA) resulted in a small but significant increase of 50 %, while FITm(S221E) and FITm(S221E / SS271/2AA) displayed a highly increased cytoplasm-to-nucleus ratio of 186 % to 314 % (Figure 2A, Figure 2C). FITm(Y238F), FITm(Y278F) and FITm(Y278E) showed a significantly increased ratio of approximately 152 % to 334 % compared to WT (Figure 2B, Figure 2C). There was no significant increase observed for FITm(S221A) and FITm(Y238E). Overall protein levels in this system were found to be comparable between WT and phospho-mutants (Supplemental Figure 5). Thus, depending on the phospho-mutant status, FIT protein is retained in the cytoplasm.

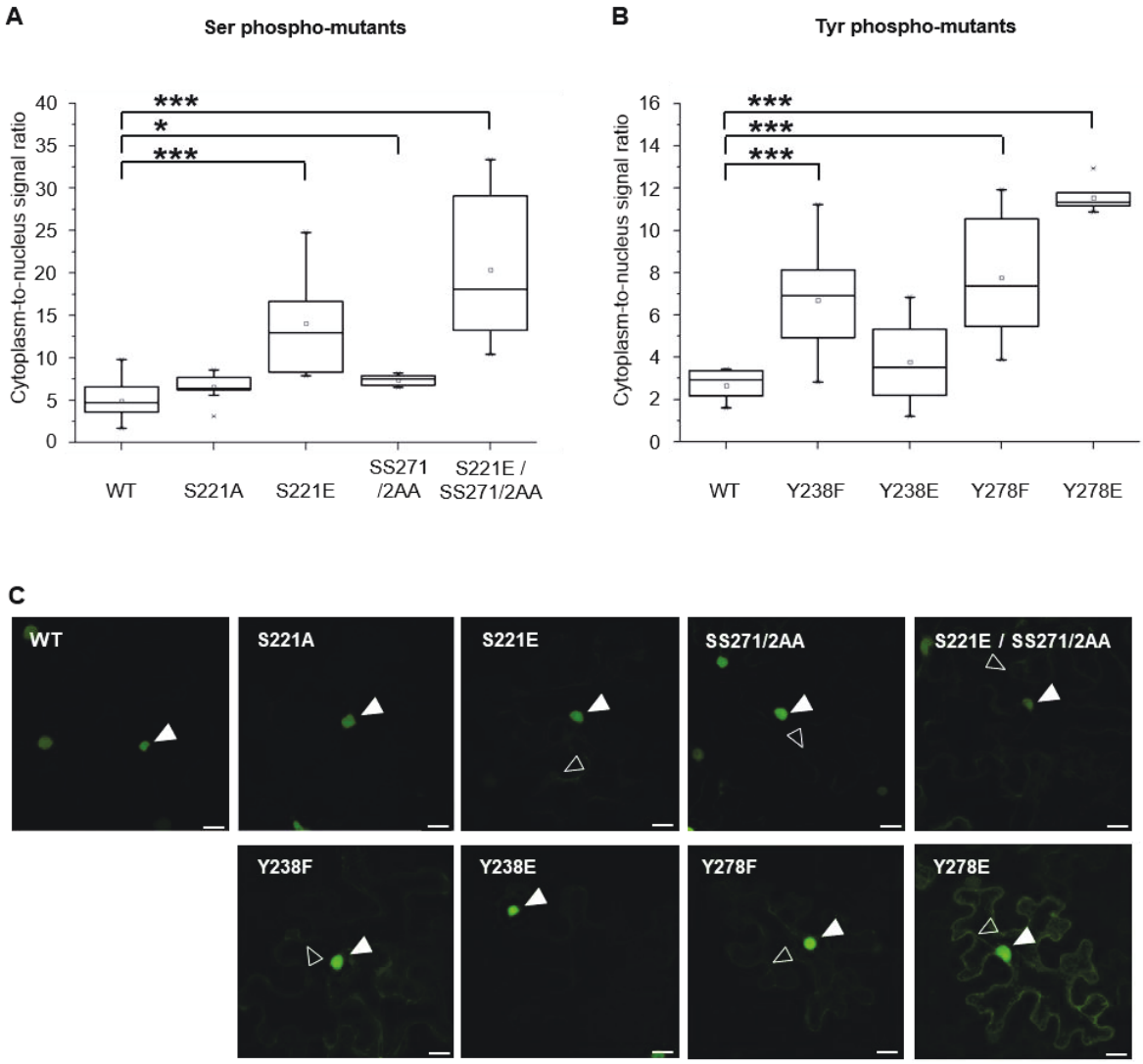

Figure 2. FIT subcellular compartmentalization is altered in phospho-mutants.
(A-B) The subcellular localization of FIT-GFP (WT) and respective phospho-mutants (FITm) was analyzed 48 hours after transient expression in tobacco leaf epidermis cells by laser-scanning confocal microscopy. GFP fluorescence signal intensity was determined in the cytosol and separately in the nucleus. A cytoplasm-to-nucleus signal ratio was calculated. **(A)** Cytoplasm-to-nucleus partitioning is presented for WT and serine- **(B)** and tyrosine phospho-mutants. Asterisks indicate statistical significance between WT and individual mutants, determined by Student's *t*-test (* $P < 0.05$, ** $P < 0.01$, *** $P < 0.001$). Three independent experiments were performed. One representative experiment with 6 - 11 imaged nuclei is shown. **(C)** Representative confocal images of transiently transformed tobacco leaf epidermis cells, expressing FIT-GFP and FITm-GFP. Empty arrowheads indicate significantly enhanced cytoplasmic GFP signal accumulation. Filled arrowheads highlight nuclear signal. Scale bar = 20 μm.

Additionally, nuclear architecture is complex and the motion of molecules in the nucleus could be coupled to their activity status (Reits and Neefjes, 2001). The mobility of nuclear GFP-tagged FIT phospho-mutants was investigated in tobacco leaf epidermal cells by performing Fluorescence Recovery after Photobleaching (FRAP) (Figure 3). We found that the mobile fraction of nuclear, non-mutagenized FIT represents roughly 67 % to 73 %. This mobile fraction was slightly but significantly increased by about 11 % in FITm(SS271/2AA) (Gratz et

al., 2018 (submitted)) and 17 % in FITm(S221E / SS271/2AA) (Figure 3A), whereas it was significantly decreased by 10 % in FITm(Y238E) compared to the respective control (Figure 3B).

In summary, we show that the subcellular localization as well as the nuclear mobility of FIT are affected in individual FIT phospho-mutants. One of the mechanisms by which protein trafficking and mobility can be altered is with respect to protein interactions, which are analyzed next.

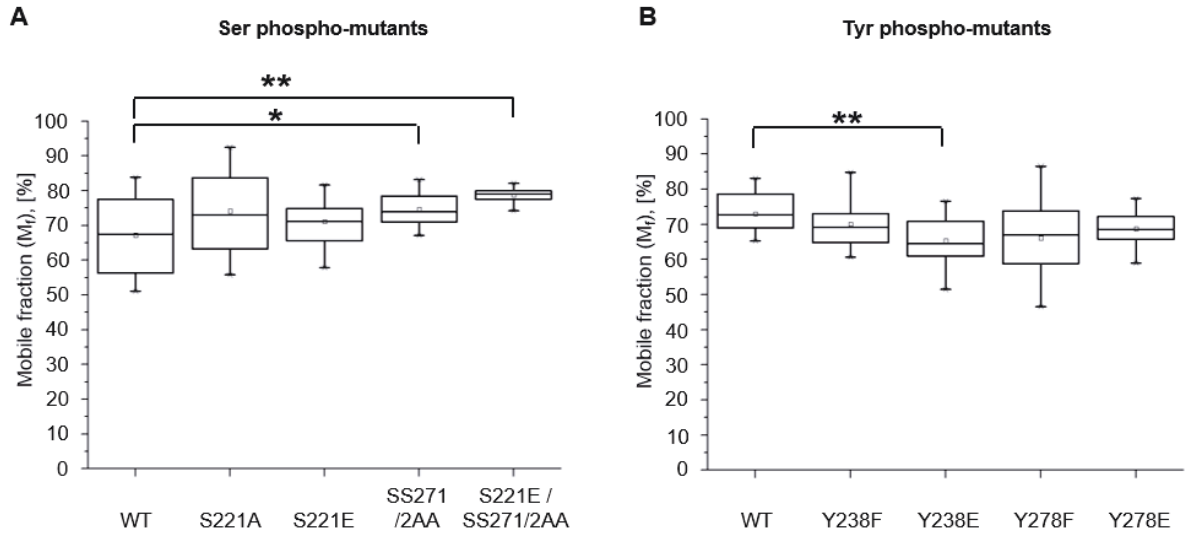

Figure 3. FIT phospho-mutants display altered nuclear mobility.
(A-B) Nuclear mobility of FIT-GFP (WT) and respective FITm was quantified 48 hours post infiltration in tobacco leaf epidermis cells by Fluorescence Recovery after Photobleaching (FRAP). The mobile fraction (M_f) of WT and **(A)** serine- or **(B)** tyrosine phospho-mutants is shown in percent. Statistical significance between WT and individual FITm was calculated with Student's *t*-test and is denoted by asterisks (* $P < 0.05$, ** $P < 0.01$, *** $P < 0.001$). 10 to 17 nuclei were analyzed per construct.

FIT phospho-mutants display altered dimerization capacity.

FIT engages in several protein-protein interactions, which affect Fe uptake from the soil. FIT is capable of forming nuclear homo-dimers as well as hetero-dimers with members of subgroup Ib bHLH transcription factors bHLH038/039/100/101 (Heim et al., 2003; Yuan et al., 2008; Wang et al., 2013). The latter is part of an activating mechanism stimulating FIT downstream responses (Yuan et al., 2008; Wang et al., 2013; Naranjo-Arcos et al., 2017).

We used a semi-quantitative targeted yeast-two hybrid- as well as a quantitative Förster Resonance Energy Transfer - Acceptor Photo Bleaching (FRET-APB) approach *in planta* to address FIT dimerization capacity (Figure 4). BD-FIT full-length showed a high level of auto-activation (Lingam et al., 2011; Le et al., 2016; Gratz et al., 2018 (submitted)). Hence, we investigated the interaction of FIT-C in yeast, but full-length FIT *in planta*. In yeast we found FIT to engage in homo- and hetero-dimerization via FIT-C, not requiring the two helix-loop-helix domains as proposed before (Heim et al., 2003). FIT homo-dimers are formed in yeast

(Figure 4A, Supplemental Figure 2) and *in planta*, with a respective FRET efficiency of 8 % (Figure 4B, 4C). In both systems, in yeast and *in planta*, this interaction capacity was reduced for FITm(S221E), FITm(SS271/2AA) (Gratz et al., 2018 (submitted)) and FITm(S221E / SS271/2AA), compared to WT. FRET efficiency was reduced by 40 % to 61 %. There was no significant difference found for FITm(S221A) relative to the control in both assays. A slight reduction in dimerization capacity was found for FITm(Y238F) in yeast. FRET data supported the reduction, as demonstrated by a significant FRET efficiency decrease of 30 % (Figure 4C). A stronger reduction was found for FITm(Y238E) and FITm(Y278F) in yeast and *in planta* by roughly 60 %. Only FITm(Y278E) showed opposing effects in both systems. Dimerization was inhibited in yeast, whereas *in planta* data displayed an increase in FRET efficiency by 72 % compared to WT. Hence, FIT homo-dimerization is significantly affected in phospho-mutants using two different approaches, consistent in the two assays for seven out of the eight phospho-mutant forms.

Subsequently, FIT hetero-dimerization with bHLH039 was tested. Most phospho-mutants were not found to be affected in either of the two systems, again irrespective of the presence of helix-loop-helix domain. While there was no evidence for hetero-dimerization in the yeast system for FITm(SS271/2AA) and FITm(Y238E) (Figure 4D, Supplemental Figure 3), they displayed a significantly decreased interaction capacity *in planta* by approximately 15 % to 20 % (Figure 4E, 4F). FITm(Y278E) was the only form that concordantly showed reduced dimerization with bHLH039 in yeast and *in planta* by 24 % compared to WT.

Thus, we conclude that the ability of FIT to interact with itself or bHLH039, might be affected by its phosphorylation status.

Phospho-mutants affect FIT transactivation ability.

Next, we investigated promoter induction capacities of FIT phospho-mutants. Full-length FIT, fused to the Gal4 binding domain has a very strong ability to self-activate the reporter gene promoter in the targeted yeast two hybrid assay, even in the presence of 90 mM 3-amino-1,2,4-triazole (3-AT) (Supplemental Figure 4) (Lingam et al., 2011; Le et al., 2016; Gratz et al., 2018 (submitted)). However, we were intrigued by the fact that some phospho-mutant FIT forms, namely FITm(SS271/2AA) (Gratz et al., 2018 (submitted)), FITm(S221E / SS271/2AA) as well as FITm(Y278E) had strongly reduced auto-activation, while there was no detectable difference for all other phospho-mutants compared to the control. We interpret this result as a first indication for a reduced FIT activity, as a direct consequence of the potential phosphorylation status of FIT.

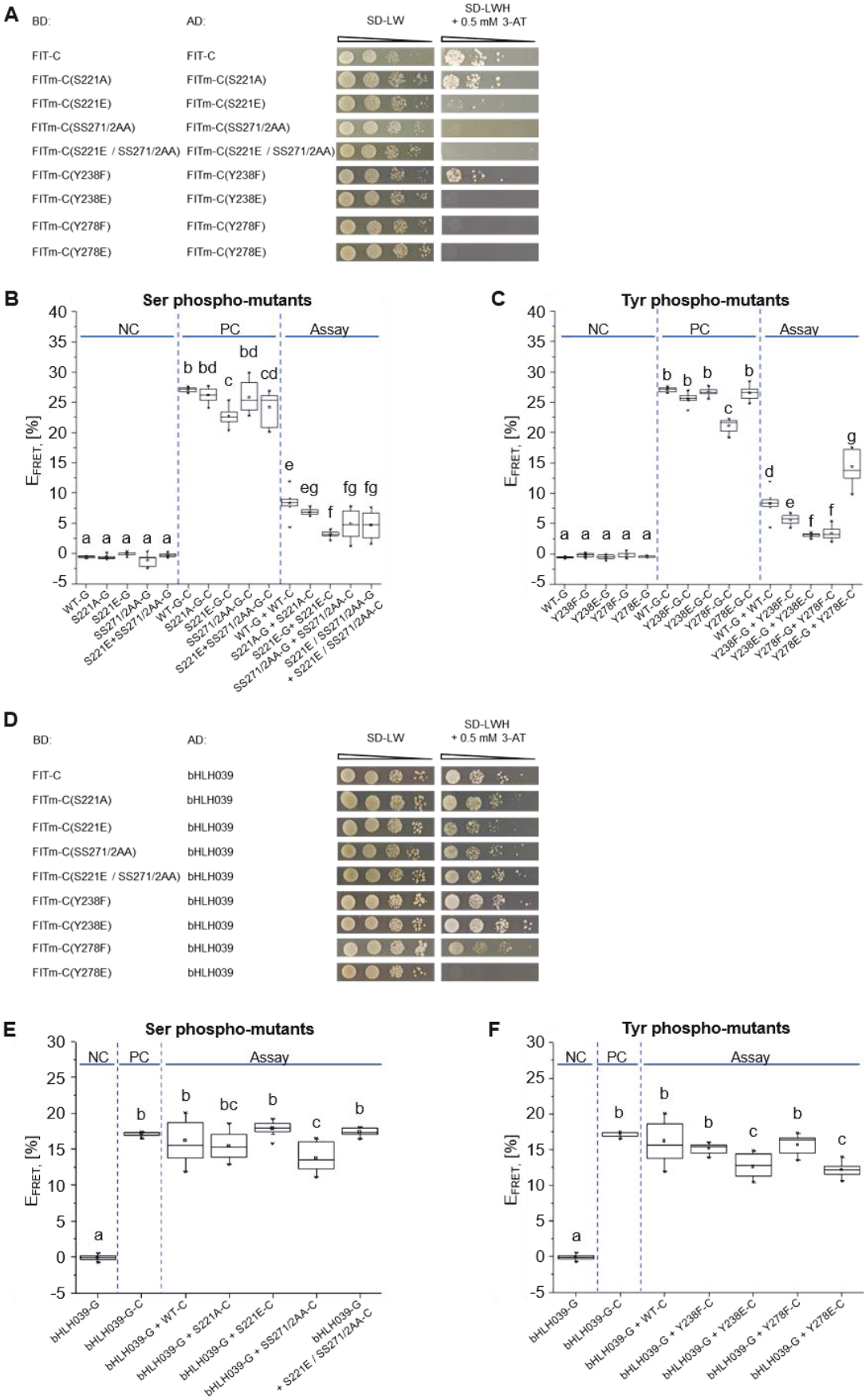

Figure 4. FIT homo- and FIT-bHLH039 hetero-dimerization capacity is affected in phospho-mutants.
(A) FIT and FITm homo-dimerization assay in yeast. Yeast cells were co-transformed with GAL4-binding domain BD-FIT-C and GAL4-activation domain AD-FIT-C plasmids or respective phospho-mutants. A 10-fold dilution

series was spotted onto synthetic defined -Leu, -Trp (SD-LW) plates as growth control (OD_{600} = 1-10^{-3}). To analyze the interaction capacity, yeast was spotted onto SD-LWH plates, containing 0.5 mM 3-amino-1,2,4-triazole (3-AT). **(B-C)** FIT and FITm homo-dimerization assay *in planta*. Förster Resonance Energy Transfer - Acceptor Photo Bleaching (FRET-APB) for GFP- and mCherry-tagged FIT and FITm pairs was measured in plant cell nuclei. GFP-fusion proteins serve as donor-only negative controls (NC). Fusion proteins with GFP-mCherry serve as positive controls (PC). FRET efficiency (E_{FRET}) is the relative increase of GFP intensity following photobleaching of the mCherry acceptor. E_{FRET} is given in percent (Assay). Serine phospho-mutants are presented in **(B)**, tyrosine phospho-mutants in **(C)**. G, GFP; C, mCherry; G-C, GFP-mCherry. Statistical significance is highlighted by different letters and was calculated using one-way ANOVA ($P<0.05$) and Tuckey post-hoc test. At least two independent experiments with 10 imaged nuclei each, were performed. One representative experiment is shown. **(D)** Co-transformed yeast with BD-FIT-C, or respective FITm, and AD-bHLH039 plasmids was spotted like in (A) to analyze FIT hetero-dimerization capacity. **(E-F)** Hetero-dimerization of full-length FIT and bHLH039 *in planta*. FRET efficiency was assessed as in (B). **(E)** E_{FRET} was analyzed for serine- and for **(F)** tyrosine phospho-mutants.

Full-length FIT alone, however, does not initiate FIT target gene induction, neither in yeast nor in plant cells, but it does so in the presence of co-expressed bHLH039 (Yuan et al., 2008; Wang et al., 2013). Since protein interaction with bHLH039 is affected in some FIT phospho-mutants, we addressed whether this translates into changes of transactivation capacities. To provide such evidence we established a quantifiable cellular transactivation assay for the FIT-bHLH039 regulon, based on normalized *SECRETED ALKALINE PHOSPHATASE* (*SEAP*) reporter gene expression, driven by the FIT target promoter *IRT1* (*$IRT1_{pro}$*) in Chinese hamster ovary (CHO) cells. Such synthetic cellular systems are becoming increasingly popular to study gene regulatory modules and the impact of functional variants in the absence of interfering secondary effectors present in plant cells (Braguy and Zurbriggen, 2016). By selective addition of effector plasmids expressing *FIT*, *FITm* or *BHLH039*, we created a tool box to analyze the activity of the transcription factor in dependence of different effectors. An initial proof-of-concept experiment confirmed that FIT and bHLH039 in combination are mandatory to activate *$IRT1_{pro}$*. Neither FIT nor bHLH039 alone initiated *$IRT1_{pro}$* activation (Figure 5A). The combination of FIT and bHLH039 leads to an approximately 7-fold activation of *$IRT1_{pro}$* compared to its background activity, demonstrating suitability of the synthetic cellular assay for comparing WT and FIT phospho-mutants in a reliable and quantitative manner. Therefore, we could replace FIT by respective phospho-mutants and attribute the monitored changes in *$IRT1_{pro}$* activities directly to an altered fitness of the transcription factor. We observed a statistically significant increase in *$IRT1_{pro}$* activity for FITm(S221E) of 25 % compared to WT, whereas a decrease of 27 % - 31 % was detectable for FITm(SS271/2AA) and FITm(S221E / SS271/2AA), respectively. FITm(S221A) activity was comparable to the control (Figure 5B). Out of the four tyrosine phospho-mutants, we found two, FITm(Y238F) and FITm(Y278F), that showed a significant increase in *$IRT1_{pro}$* activity by 20 % and 67 %. However, FITm(Y238E) and FIT(mY278E) displayed a significant decrease in activity by approximately 75 % (Figure 5C).

Currently, we are generating fluorescent protein fusions to confirm the expression of the respective phospho-mutant constructs, which will be analyzed by immuno-blotting. In addition, this will enable us to compare the intracellular localization of the phospho-mutant forms in mammalian cells with the obtained *in planta* data (Figure 2).

In summary, the altered transactivation activity of FIT provides evidence that the predicted phospho-sites are crucial for fine-tuning of transcriptional FIT activity. Indeed, for the three mutant forms FITm(SS271/2AA), FITm(Y238E) and FIT(mY278E), that interacted less with bHLH039 in plant cells, transactivation capacities were lower than for wild-type FIT. However, the phospho-mutant forms interacting similarly as wild-type with bHLH039, showed at least the same level of transactivation as FIT (except FITm(S221E / SS271/2AA).

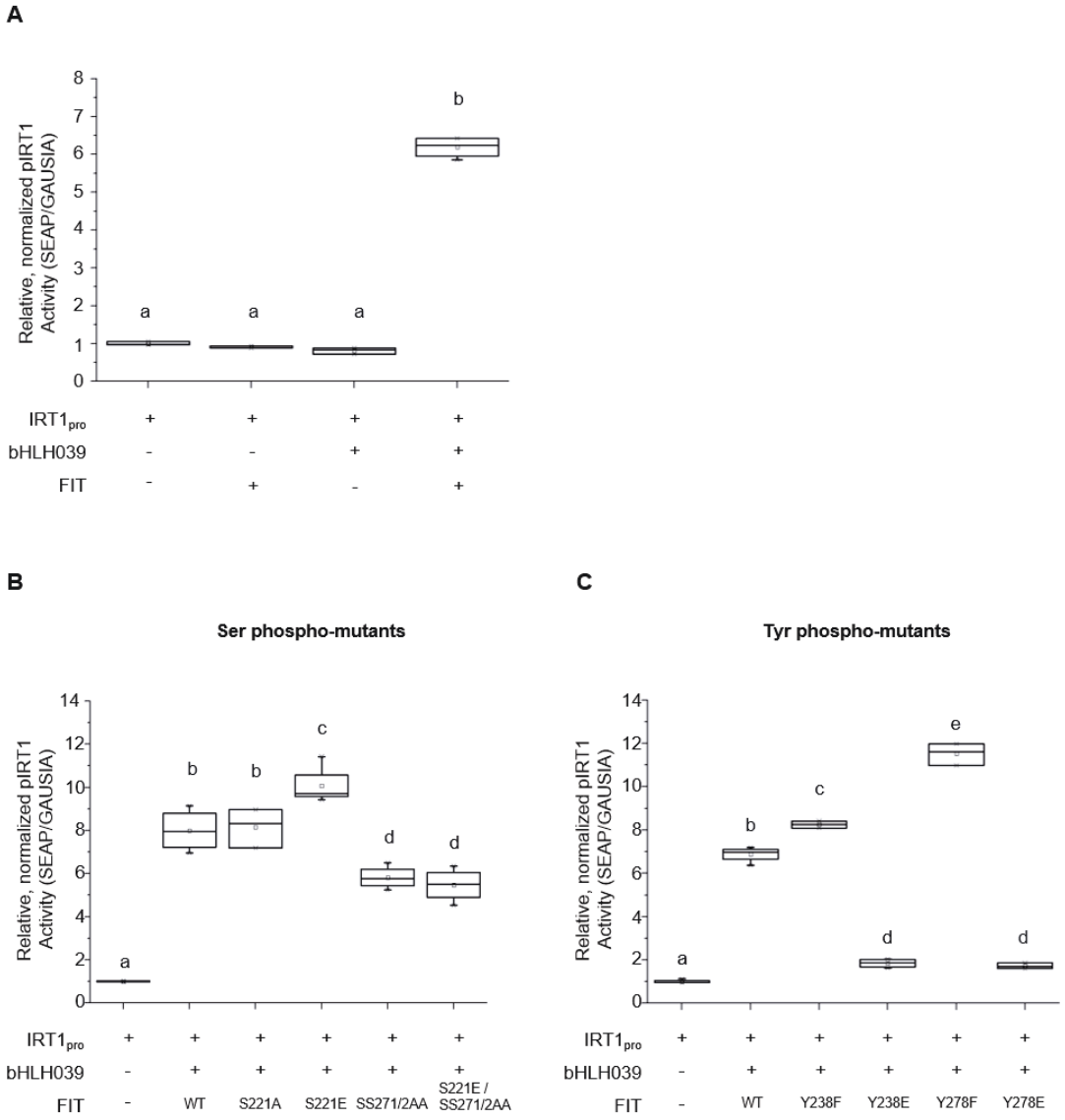

Figure 5. Fine-tuning of FIT transcriptional activity might be modulated by phosphorylation.
(A-C) A quantifiable cellular transactivation assay in Chinese hamster ovary cells (CHO) was used to quantify the ability of FIT or FITm to bind to their target promoter sequence (*IRT1*$_{pro}$) and, hence, induce transcription of the reporter gene (SEAP). Promoter induction was compared to the baseline control, in which only *IRT1*$_{pro}$ was used for transfection. Co-transfected Gaussia luciferase was used for normalization to the transfection efficiency. The

relative, normalized $IRT1_{pro}$ activity is shown. **(A)** Both, FIT and bHLH039 are required to activate $IRT1_{pro}$, defining the minimal framework needed for promoter activation. **(B)** CHO cells were transfected with $IRT1_{pro}$, *bHLH039* and mutagenized or non-mutagenized *FIT* plasmids to analyze FIT and FITm activity. Statistical significance is highlighted by different letters and was calculated using one-way ANOVA ($P<0.05$) and Tuckey post-hoc test. Three independent experiments with each four technical replicates were performed. One representative experiment is shown.

FIT phospho-mutants are altered in protein stability, facilitated by proteasomal degradation.

Protein phosphorylation can be a trigger for protein turnover, as shown for PHYTOCHROME INTERACTING FACTORs (PIFs) (Al-Sady et al., 2006; Shen et al., 2007; Lorrain et al., 2008; Shen et al., 2008; Ni et al., 2013; Ni et al., 2017). Thus, it was an obvious next question whether the previously reported FIT proteasomal degradation (Lingam et al., 2011; Meiser et al., 2011; Sivitz et al., 2011) was changed in phospho-mutants. To this end, we developed a quantified cell-free degradation assay for FIT protein purified from plant cells.

We found that FIT was nearly completely degraded over a time-course of 240 minutes. The addition of the proteasomal inhibitor MG132, however, antagonized the degradation and confirmed proteasomal involvement (Figure 6, Supplemental Figure 5A). We did not observe a significant difference in protein stability for serine phospho-mutants, directly compared to WT (Figure 6A, Supplemental Figure 5B). The same was found for position Tyr238 (Figure 6B, Supplemental Figure 5C). FITm(Y278F) stability was just not significantly different compared to WT. However, a tendency for increased stability was noted ($P = 0.06$ at 240 min, statistically significance is considered $P < 0.05$), whereat FITm(Y278E) displayed a significant decrease in protein stability. Analyzing half-life rates of FITm(Y278E) confirmed the decrease in stability (Supplemental Figure 5D).

These results suggest that a potential tyrosine phosphorylation could be a trigger for faster degradation of the protein.

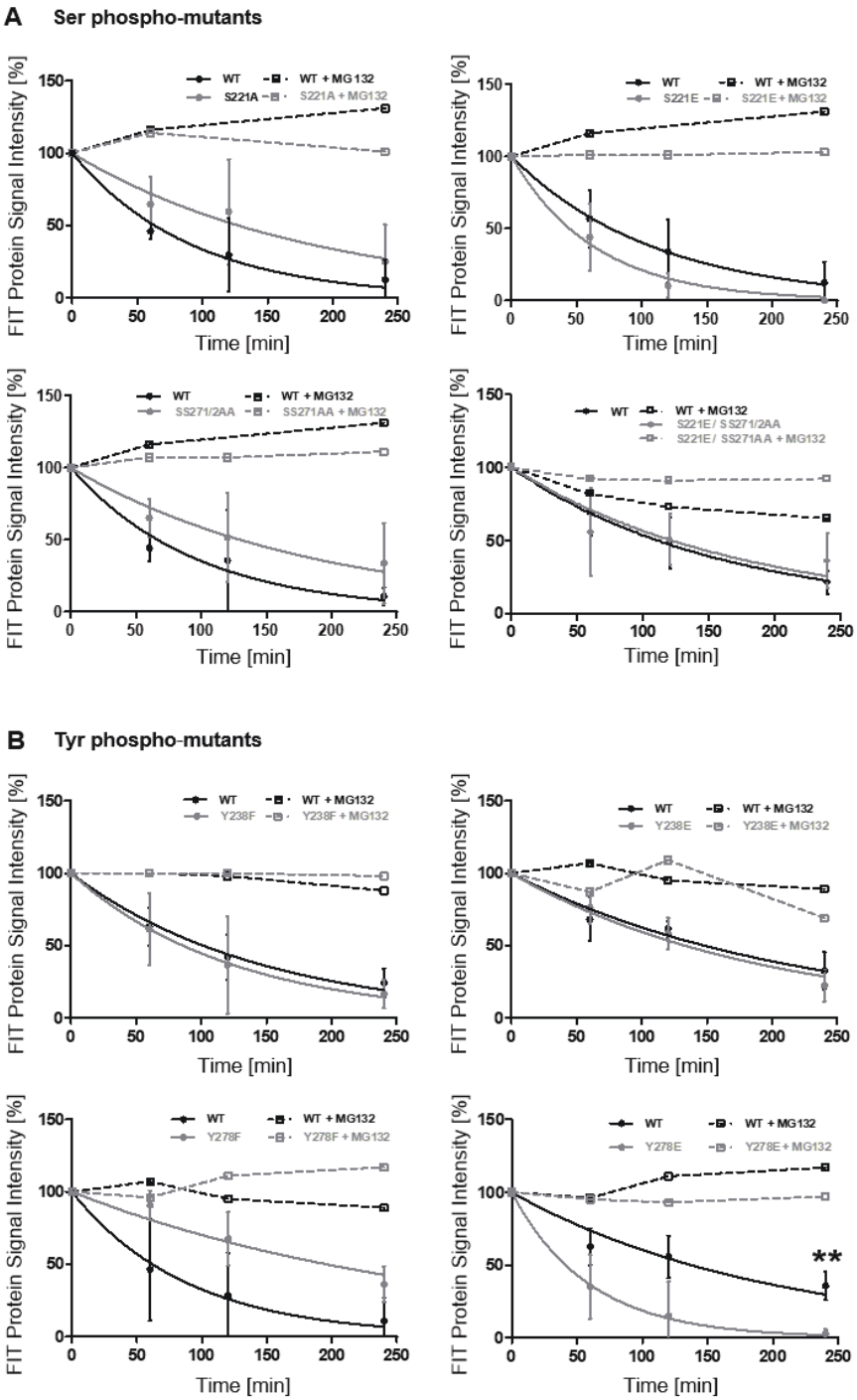

Figure 6. : Tyrosine phospho-mutants are affected by proteasomal degradation.
(A-B) Tobacco leaf epidermal cells were transiently transformed with mutagenized or non-mutagenized FIT-GFP. Equal amounts of total protein extract were transferred to individual reaction tubes, partially treated with the proteasomal-inhibitor MG132 (+MG132) and incubated at 25°C for 0, 60, 120 or 240 minutes. Protein stability was analyzed after immunoblotting of equal protein amounts, using anti-GFP antibody. Quantification of the immunoblot signals allowed plotting the signal intensity over time, displaying protein stability. WT is represented as solid black, FITm-GFP as solid grey curves. **(A)** Protein stability is shown for serine- and **(B)** tyrosine phospho-mutants. Data are means of three ±SD biological replicates. Statistical significance between individual time-points is highlighted by asterisks (Student's t-test, * $P < 0.05$, ** $P < 0.01$, *** $P < 0.001$). MG132 treated samples are illustrated with a dotted curve (n=1).

Discussion

Here, we provide strong indication for a multifaceted phosphorylation control of FIT, involving all four predicted phosphorylation sites in the FIT-C terminus, including tyrosines. Non-phosphorylatable and phospho-mimicking mutants of the four sites caused molecular and cellular FIT phenotypes to various degrees, which we were able to use as the basis for a phospho-mutant activity screening of FIT. Thereby, we could assign different functions to the predicted phospho-sites with respect to regulation of protein localization, mobility, interaction, transactivation and stability. Very interestingly, our data show opposing effects for the predicted serine and tyrosine phosphorylation sites. While serine phosphorylation, with predominance at the previously identified Ser272 site, would activate FIT, tyrosine phosphorylation, particularly at Tyr278, would abolish FIT activity. We suggest a model of FIT protein phosphorylation, involving a two-step regulation mechanism, which modulates the activity status of the protein in the cell. Especially the prospective tyrosine phosphorylation of FIT opens up the way for identifying novel transcription factor regulation mechanisms by a tyrosine kinase, coupled to yet unknown signaling cascades.

Three-step prediction of phosphorylation target sites in FIT-C is validated by phospho-mutant activity screening.

Our analysis of two Ser and two Tyr sites in FIT-C shows that these sites are important for FIT regulatory properties and cellular activities.

We identified these sites using a three-step combination of NetPhos prediction, phylogenetic sequence analysis and known phosphorylation motifs, and narrowed down the 12 Ser, eight Thr and four Tyr existing in FIT-C, to two Ser and two Tyr as probable phosphorylation target sites. Although it was reported previously that FIT seems specific to angiosperms (Carretero-Paulet et al., 2010), this was confirmed in our analysis based on a higher number of analyzed genome sequences. The phylogenetic FIT sequence alignment even suggests that FIT function was acquired in eudicots, because clear sequence similarity of monocot and basal angiosperm FIT-C termini was not evident. Interestingly, however, both Tyr residues are moderately to highly conserved among all angiosperms. Generally, phosphorylated amino acids are often conserved across plant species (Maathuis, 2008; Sugiyama et al., 2008; Nakagami et al., 2010), but especially Tyr phosphorylation is highly evolutionary conserved (Mithoe et al., 2012). Tyr regulation of FIT might therefore be evolutionarily older than the Ser regulation and potentially older than the role of FIT in regulating Strategy I. It could well be that the cretaceous period with the formation of current environment, caused new challenges to plants that required more

efficient Fe acquisition from the soil, and, perhaps, exploration of different new strategies in the evolving branches of angiosperms. In this context FIT might have acquired a different function, albeit still keeping some of its regulatory properties.

Ser272 was demonstrated previously to be a kinase target, promoting FIT action and Fe acquisition upon phosphorylation (Gratz et al., 2018 (submitted)). The genetic analysis, demonstrating the positive effect of Ser272 phosphorylation on FIT activity, was supported by the positive impact of the respective kinase CIPK11. Ser221 could also be targeted by CIPK11, since we know that FIT has additional CIPK target phosphorylation sites (Gratz et al., 2018 (submitted)). However, Ser221 seems to be a minor site as its effect was overruled by Ser272 (Figure 7).

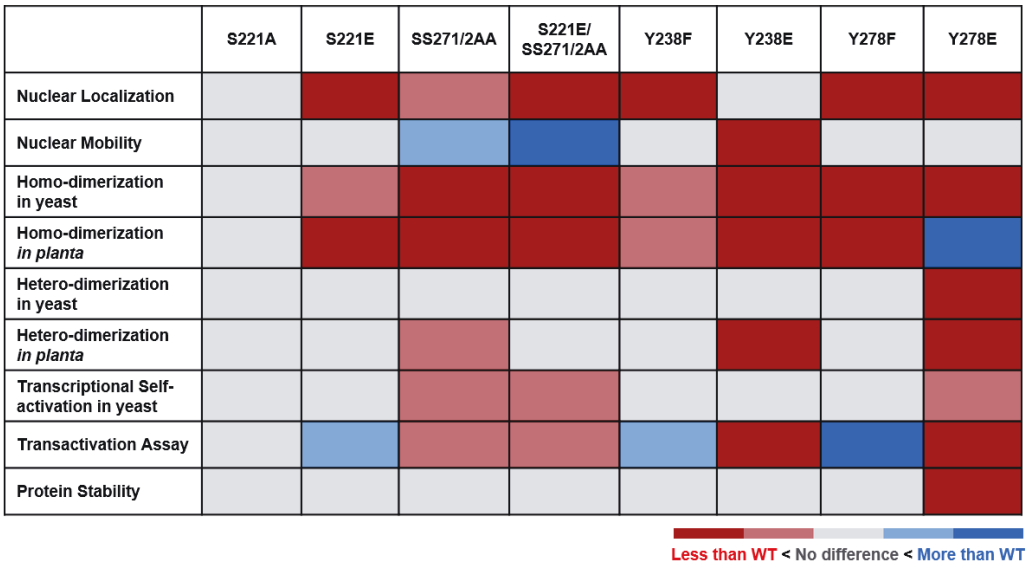

Figure 7. FIT phospho-mutant phenotype screening. A color code was applied, highlighting altered regulatory properties and cellular activities between FIT and FITm. Blue shading indicates a stronger effect in the respective phospho-mutant compared to WT for the conducted experiment. Red shading indicates a reduced effect. Increase of the individual color indicates a stronger effect. No differences between WT and FITm are marked in grey.

The presence of the two Tyr sites was very intriguing. Such phosphorylation has been rarely described to date in plant transcription factors, while based on phospho-proteomics it could be quite important (Sugiyama et al., 2008; van Wijk et al., 2014; Lu et al., 2015). Since substantial knowledge on plant Tyr kinases is lacking and we had failed to identify FIT phospho-peptides, we had undertaken a phospho-mutant activity screening approach, to assess the functional relevance of Ser221, Tyr238 and Tyr278. Such phospho-mutant analyses are widely accepted to identify and characterize functional phosphorylation patterns, and have been reported several times (Yang et al., 2015; Li et al., 2017). The advantage of our approach is that it is relatively fast compared to generation of transgenic lines. Also, various phenotypes can be studied in transient assays and synthetic systems, allowing conclusions on the regulatory module in the

absence of interfering unknown plant effectors. Mutational analysis was based on exchanging Ser and Tyr with either uncharged Ala or Phe, reflecting the non-phosphorylated state, or with Glu, mimicking the negatively charged phosphorylated state. Very interestingly, we found for both Tyr sites, that the opposing mutations gave contrasting phenotypes in several assays (Figure 7). Such contrasting phenotypes are expected for a protein that has different activities in the phosphorylated versus non-phosphorylated state. We see these opposing results as a strong indication for the usefulness of the approach, to identify functional phosphorylation sites. Besides being regulated at Ser272, FIT is thus likely the target of a tyrosine kinase, which opens up a way to connect Fe acquisition regulation to a new signaling pathway in plants.

Ser and Tyr phospho-mutants impact different regulatory properties and cellular activities of FIT.

The phosphorylation-induced local charge differences lead to conformational changes, which ultimately may allow or impede regulatory protein interactions. We measured such effects in a variety of different assays. For example, active shuttling of FIT from the cytoplasm to the nucleus is mediated by the presence of a nuclear localization signal (NLS) (Zhang et al., 2006), which could be masked by either a conformational change or interaction with a regulatory protein, binding to phospho-sites as shown for 14-3-3 proteins (Moorhead et al., 2007). Nuclear translocation of FIT leads to its involvement in complex protein-protein interactions and DNA-binding, associated with transcriptional regulation. Observed changed in FIT phospho-mutant mobility might be due to the binding of FIT to sub-nuclear structures (Bauer et al., 2004). Furthermore, the investigated protein interactions with FIT and bHLH039 could be linked with transactivation abilities, to regulate the responsiveness of the signaling system. When comparing cellular and molecular properties across the different phospho-mutants, we observed a correlation between several read-outs (Figure 7). Hetero-dimerization of FIT and bHLH039 correlated with FIT transactivation ability. This expected correlation was reported previously as bHLH039 interaction is a prerequisite for the FIT-mediated induction of downstream promoter targets (Yuan et al., 2008; Wang et al., 2013; Naranjo-Arcos et al., 2017). Further, we noted that nucleo-cytoplasmic partitioning of FIT largely correlated with FIT homo-dimerization. Perhaps the observed decreased FIT homo-dimerization is the cause of the reduced nuclear localization or vice versa. FIT transactivation ability was uncoupled from nucleo-cytoplasmic partitioning and FIT homo-dimerization, which would go in line with the failure of FIT alone to activate $IRT1_{pro}$. Hence, this phospho-mutant phenotype mapping helps to identify the functional roles of novel regulatory sites.

For the investigation and characterization of FIT properties and its activity, namely its homo- and hetero-dimerization, and transactivation ability, we utilized also non-plant systems. Yeast and mammalian cells are simpler for studying FIT phospho-mutants, as the two cell systems have completely different regulatory mechanisms for Fe uptake. Transferring the FIT-bHLH039 regulon into mammalian cells (this work) and as shown previously for yeast cells (Yuan et al., 2008; Wang et al., 2013), allowed uncoupling the effects of the two transcription factors from any other plant signaling cascade. Interchanging the individual phospho-mutant forms in the mammalian cells, allowed us to calculate normalized mutant effects, which is the hallmark in quantitative and synthetic biology.

Correlation was generally found for FIT homo- and hetero-dimerization assays in between the yeast and plant cell system. There were two discrepancies where the interaction was perturbed in the plant system, but not in yeast (Figure 7). In this case, we gave preference to the plant result, since full-length proteins were analyzed. Only a single case was noted where the plant and yeast system yielded opposing results. That was the case for FITm(Y278E) homo-dimerization, which was increased in plant cells but reduced in yeast. Perhaps, the increased interaction is part of a control mechanism in plants, possibly linked with nuclear structures. However, in contrast to these three cases, there were 13 cases, in which yeast and plant systems gave fully concordant results for the different FIT phospho-mutants. This underlines the general reliability of interaction assays for FIT. Although the studied FIT promoter binding activities were clearly different in the yeast and mammalian assays, yet, there were some consistencies in the responses. Four mutants gave concordant results, while four forms showed minor differences.

Taken together, we have developed a reliable and validated phospho-mutant activity approach that we could successfully apply to identify novel regulation sites of FIT. We found strong indications that these sites are involved in FIT phosphorylation control.

Two-step regulation of FIT activity is mediated via differential phosphorylation.

We have found different regulatory properties and cellular activities of FIT phospho-mutants by applying different assays. Using this approach to gain insight in the existence of additional phosphorylation sites, we can speculate about an antagonistical, two-step regulation of FIT activity, controlled by protein phosphorylation.

In this study, we found FITm(SS271/2AA) transcriptional activity reduced compared to WT. This confirmed our previous results, in which we found reduced FIT target gene expression in stable transgenic lines, expressing FITm(SS271/2AA) in *fit-3* knock-out mutant background.

These lines additionally had a significantly reduced seed Fe content (Gratz et al., 2018 (submitted)). Hence, this verifies our phospho-mutant approach.

With Ser221, we identified a novel possible phosphorylation site in FIT-C. Although the non-phosphorylatable mutant behaved like WT, we found that FITm(S221E) showed increased FIT transactivation capacity. Hence, we believe that FITm(S221E) is a hyper-active FIT form. We propose that potential phosphorylation of the tested serines Ser221 and Ser272 (Gratz et al., 2018 (submitted)) is a prerequisite for bHLH039-dimerization and, thus, initiation of FIT target promoter induction. Thus, serine phosphorylation at these sites might positively affect FIT activity.

For AHA2 proton pump activity it was reported that one phosphorylation site dominates over another. Phosphorylation of Thr881 was sufficient to directly activate the protein, whereas phosphorylation of Thr947 subsequently needed 14-3-3 protein binding to confer increased AHA2 activity (Niittyla et al., 2007). Hence, we studied the effects of a combination of the novel, hyper-active FITm(S221E) and the less active FITm(SS271/2AA) phospho-mutant, as this mutant was described in detail before (Gratz et al., 2018 (submitted)). Regulatory properties between FITm(SS271/2AA / S221E) and FITm(SS271/2AA) were mostly similar, such as increased cytosolic localization and nuclear mobility, as well as reduced homo-dimerization. Ultimately, we could show that the non-phosphorylatable mutant FITm(SS271/2AA) overrides the increase in transcriptional activity of FITm(S221E), rendering FITm(SS271/2AA / S221E) inactive. Hence, we propose that phosphorylation of position Ser272 plays a pivotal role for FIT transcriptional activity, as a loss of this phosphorylation site cannot be rescued by the highly active FITm(S221E) form.

Opposite to this, we identified two potentially phosphorylated tyrosine residues, Tyr238 and Tyr278. Both mutants display an intact bHLH039 binding capacity when present as non-phosphorylatable mutants. As a result of this, we found both FITm(Y238F) and FITm(Y278F) to be significantly more transcriptionally active compared to WT. In general, both mutants displayed the same regulatory properties and cellular activities, as hyper-active FITm(S221E). In contrast to this, the respective phospho-mimicking mutants displayed a significant decrease in dimerization capacity as well as transcriptional activity. In addition, we demonstrated that in particular Tyr278 is of interest with respect to its protein stability. We found the inactive FITm(Y278E) to be less stable and to undergo increased proteasomal degradation. Interestingly, this respective mutant displays very similar characteristics as phospho-mimicked CjWRKY1(Y115E). This phospho-mimicking mutant is impaired in target genes induction and preferentially accumulates in the cytosol, where it is subsequently degraded (Yamada and Sato,

2016). Hence, we propose that, in contrast to the activating mechanism of serine phosphorylation, tyrosine phosphorylation might be a mechanism to render FIT inactive. This phosphorylation might ultimately lead to proteasomal degradation of FIT.

We could show that potential phosphorylation marks on serines might be perceived differently by the cell as tyrosine phosphorylation. Potential phosphorylation of the tested serines promoted FIT activity. It was possible to discriminate between different effects of serine phosphorylation on FIT activity, as Ser272 was dominating over Ser221. We speculate that both serines have to be phosphorylated in order to fully activate FIT. Upon a reduced need for FIT, phosphorylation of Ser272 is prevented, rendering the protein less active (Step 1). If, however, the plant is of no more need for active FIT, tyrosine phosphorylation could be promoted, leading to the complete loss of FIT activity. This could go along with the subsequent degradation of the protein (Figure 8) (Step 2). Tyr278 displays a promising candidate for further analysis in stable transgenic plant lines. This would allow us to test the phospho-mutants for their performance, when environmental challenges, such as Fe-deficiency, are applied.

In summary, a two-step regulation of FIT activity would enable the integration of sudden changes in environmental conditions into a quick response of transcriptional activity.

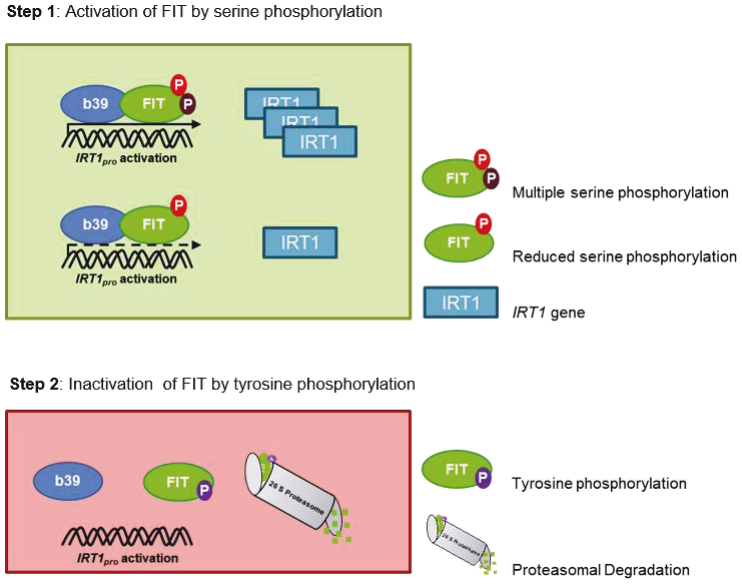

Figure 8: FIT phospho-mutant activity screening suggests a dual regulation of FIT activity conferred by protein phosphorylation. Multi-serine phosphorylation in FIT C-term might be required for full FIT activity. The interaction between phosphorylated FIT and bHLH039 is not obstructed, hence, the dimer can bind to $IRT1_{pro}$. Subsequently, the promotor is activated and FIT target gene expression is initiated. Upon reduction in C-terminal serine phosphorylation, FIT activity might decrease, which is displayed by a diminished in *IRT1* expression (Step 1). In a situation, where no active FIT protein is needed, phosphorylation might target tyrosine residues in FIT-C. This interferes with bHLH039 hetero-dimerization, which thus prevents the expression of FIT target genes. Tyrosine phosphorylated FIT may subsequently undergo 26S-mediated proteasomal degradation (Step 2).

The question remains unanswered to date, which kinases might be involved in phosphorylation of the above identified amino acids. Several kinase families are connected to Fe-deficiency

responses such as MAPKs, targeting Ser and Thr residues. *MAPK3* and *MAPK6* gene expression is upregulated under Fe-deficiency (Ye et al., 2015). The important role of both kinases is displayed in *mapk3* and *mapk6* loss-of function mutants, which show decreased gene expression level of *FRO2* and *IRT1* (Ye et al., 2015). Both kinases are involved in the expression of *ACC SYNTHASE (ACS)* genes (Li et al., 2012; Li et al., 2017) and additionally positively influence Fe acquisition through phosphorylation-based stabilization of ACS proteins, needed for ethylene production (Liu and Zhang, 2004; Joo et al., 2008; Han et al., 2010). Besides, EIN3 was found to be phosphorylated and hence stabilized by MAPK3 and MAPK6 (Yoo et al., 2008). Consequently, ethylene can promote FIT stability and positively influence the Fe-deficiency response (Lingam et al., 2011). Recently, the involvement of serine/threonine kinases CALCIUM-DEPENDENT PROTEIN KINASES (CPKs) CPK5 and CPK6 in *ACS* expression has been shown (Li et al., 2017). Another subfamily of Ca^{2+}-dependent protein kinases, CIPKs, is connected to Fe stress signaling. A recent microarray study revealed two robustly upregulated CIPKs in 6 day old WT seedlings, grown under Fe-deficiency, which are *CIPK11* and *CIPK7* (Mai et al., 2016). Recently, we could elucidate the positive effects of CIPK11 on FIT activity (Gratz et al., submitted), while the involvement of CIPK7 remains still to be revealed.

We find it very interesting that Tyr phosphorylation seems to play such an important role in FIT regulation, as studies of plant Tyr kinases are underrepresented. Similarly, Tyr phosphorylation in humans, for example, was discovered only decades after the first Ser/Thr kinases were analyzed. In parts this might be due to the fact that phosphorylated Tyr are rapidly dephosphorylated, if they are present in an unbound state (Hunter, 2014). The involvement of Tyr phosphorylation in intracellular signal transduction is currently well studied, as this is connected to various severe diseases, such as cancer (Lemmon and Schlessinger, 2010). Out of 90 Tyr kinases, which are encoded in the human genome, 58 are described to be receptor tyrosine kinases (Robinson et al., 2000). In contrast, plant receptor-like kinases (RLK) were initially reported to be Ser/Thr kinases (Shiu and Bleecker, 2001). However, few reports exist, showing tyrosine phosphorylation capacity of RLKs. One example of potential RLKs, connected to Fe signaling, are BRASSINOSTEROID INSENSITIVE 1 (BRI1) and BRASSINOSTEROID INSENSITIVE 1-ASSOCIATED RECEPTOR KINASE 1 (BAK1). Brassinosteroids (BRs) are negative regulators of the Fe uptake, reducing the expression of *CsFRO1* and *CsIRT1* (Wang et al., 2012). Additionally, they were shown to interfere with the Fe homeostasis in Strategy II plants (Wang et al., 2015). Hence, it is possible, that BRI1 and

BAK2 are involved in FIT tyrosine phosphorylation, due to the fact that kinases are dual specificity kinases (Oh et al., 2009; Kim and Wang, 2010; Oh et al., 2010; Jaillais et al., 2011). In addition, other kinases targeting FIT tyrosines might come from the Raf-like subfamilies of MAPKKKs (Jouannic et al., 1999; Ichimura et al., 2002). The phosphorylation motif spanning FIT Tyr238 is a kinase substrate motif of human JANUS KINASE 2 (JAK2) (Argetsinger et al., 2004). The closest plant homologue is the MAPKKK Raf10, which is expressed in roots, responsive to abiotic stresses and is classified as plant tyrosine kinase (Jouannic et al., 1999; Ichimura et al., 2002; Rudrabhatla et al., 2006; Lee et al., 2015).

Taken together, results obtained from our reliable phospho-mutant activity approach enabled us to identify novel regulation sites of FIT. We found strong indications that these sites are involved in FIT phosphorylation, putting a highlight on the promising prospective Tyr sites. We propose that a novel transcription factor regulation mechanisms exists controlling FIT activity, mediated by a tyrosine kinase which is coupled to a yet unknown signaling cascade.

Materials and Methods

Multiple Sequence Alignment of FIT Orthologues

Arabidopsis FIT protein sequence was blasted against every order of the angiosperms (Cole TCH, 2017). The obtained hit with the highest maximum score was re-blasted against the current Arabidopsis TAIR10 protein sequence collection, using TAIR BLAST 2.2.8 for verification. Due to the significance of the *Brassicales*, all families containing FIT orthologues were included. Here, the species of each family with the highest maximum score was chosen. To highlight the FIT specificity of the conserved amino acids, FIT was aligned to both members of *A. thaliana* bHLH subgroup IIIa, AT2G16910 and AT4G21330. The alignment was performed with the MUSCLE algorithm (Edgar, 2004, 2004).

Site-directed Mutagenesis of FIT

Columbia (Col-0) genomic DNA (gDNA) and primer pair FIT B1 and FITnon-stop (ns) B2 were used to amplify full-length *FIT*, which was subsequently cloned into pDONR207, generating the entry clone pDONR207:gFITns (BP reaction, Life Technologies).

In order to generate the different full length phospho-mutant forms of FIT (FITm), pDONR207:gFITns was used as a template for site-directed mutagenesis. To create the non-phosphorylatable form FITm(S221A), primers FITm(S221A) Fw and FITm(S221A)ns Rv were used. For the generation of the opposing, phospho-mimicking mutation FITm(S221E), the primer pair FITm(S221E) Fw and FITm(S221E)ns Rv was utilized. Using the primers FITm(SS271/2AA) Fw and FITm(SS271/2AA)ns Rv, Ser272 was mutated to Ala along with the neighboring Ser 271 to exclude redundancy between both serines, creating the non-phosphorylatable FITm(SS271/2AA) form. pDONR207:gFITns was amplified with the primer pair FITm(Y238F) Fw and FITm(Y238F)ns Rv in order to generate FIT non-phosphorylatable form FITm(Y238F). The opposing phospho-mimicking mutation was obtained by using the primer pair FITm(Y238E) Fw and FITm(Y238E)ns Rv, resulting in the mutant FITm(Y238F). Generation of the phospho-mutant pair FITm(Y278F), non-phosphorylatable, and FITm(Y278E), phospho-mimicking, was obtained by using the primer pair FITm(Y278F) Fw and FITm(Y278F)ns Rv or FITm(Y278E) Fw and FITm(Y278E)ns Rv, respectively.

pDONR207:gFITm(SS271/2AA)ns was amplified with primer pair FITm(S221E) Fw and FITm(S221E)ns Rv to create the triple phospho-mutant pDONR207:gFITm(S221E / SS271/2AA). The subsequent PCR was performed as follows: 95 °C, 30 seconds; 18 cycles of: 95 °C, 30 seconds/ 55 °C, 1 minute/ 72 °C for 2 minutes per 1kb of plasmid length; 72 °C,

7 minutes. The digestion of methylated template DNA was achieved by treating the PCR product with 10 units of *Dpn I* for 1 hour at 37 °C. Subsequently, DH5α *E. coli* cells were transformed. The obtained and sequenced plasmids were used for subsequent experiments.

Construction and Transient Expression of Fluorescent Protein Fusions

For the investigation of FIT and FITm subcellular localization, nuclear mobility and protein stability, C-terminal GFP fusions were generated. FIT and FITm were sub-cloned from the respective pDONR207 entry clones (see Site-directed Mutagenesis of FIT) into the pMDC83 vector (Curtis and Grossniklaus, 2003), generating pMDC83:gFIT(m)ns-GFP (LR reaction; Life Technologies).

For Förster Resonance Energy Transfer - Acceptor Photo Bleaching (FRET-APB) measurements, *FIT* and *FITm* were amplified from cDNA, generated from transiently transformed *Nicotiana benthamiana* (tobacco) leaves expressing pMDC83:gFIT(m)ns-GFP. Primers FIT B1 and FITns B2 were used for amplification. Subsequently, the amplicons were cloned into pDONR207, generating the constructs pDONR207:FIT(m)ns (BP reaction, Life Technologies) and sequenced. Respective clones were used to create C-terminal fusions by sub-cloning into destination vectors pABindGFP, pABindmCherry and pABindFRET (herein named pABindGFPmCherry) (Bleckmann et al., 2010) (LR reaction; Life Technologies), generating pABind:FIT(m)-GFP, pABind:FIT(m)-mCherry and pABind:FIT(m)-GFP-mCherry.

BHLH039 was first amplified from Fe-deficient Col-0 root cDNA with primer pair bHLH039 B1 and bHLH039ns B2 and then cloned into pDONR207 (BP reaction, Life Technologies). The plasmid was sequenced and sub-cloned (LR reaction; Life Technologies) into destination vectors pABindGFP and pABindGFPmCherry (Bleckmann et al., 2010) respectively.

Tobacco epidermal leaf cells were transiently transformed with the Agrobacterium (*Rhizobium radiobacter*) GV3101 (pMP90) strain, containing the respective expression vector (Bleckmann et al., 2010). For inducible FRET vectors, tobacco leaves were sprayed with a 20 µM β-estradiol solution 24 to 48 hours post-infiltration.

Subcellular Localization of FIT-GFP and FITm-GFP

The investigation of the cytoplasm-to-nucleus ratio for FIT-GFP and FITm-GFP (see Construction and Transient Expression of Fluorescent Protein Fusions) was performed 48 hours after tobacco infiltration on a LSM780 laser-scanning confocal microscope (Zeiss). Tobacco cells were imaged using a 40x C-Apochromat water immersion objective at an excitation

wavelength of 488 nm and an emission wavelength of 501 to 530 nm. The pinhole was opened to a maximum diameter of 90 µm. The pixel resolution was 0.208 µm in X and Y and 1 µm in Z. One Z-stack of approximately 20 - 40 slices was acquired for every cell.

A maximum intensity projection of every Z-stack was created, using the ZEN2 Blue Edition software (Zeiss) and the images were subsequently exported to .tiff format. After conversion of the images to the 12-bit grayscale format, the cytoplasm-to-nucleus ratio was calculated (ImageJ software). Total fluorescence signal intensity was first analyzed for the entire cell, excluding the nucleus and then separately for the nucleus. For each construct, 6 - 11 tobacco cells were imaged per experiment. Three independent experiments were performed.

Nuclear Mobility of FIT-GFP and FITm-GFP

Laser-scanning confocal microscopy using a 40x C-Apochromat water immersion objective (LSM 780, Zeiss) was used to analyze the nuclear mobility of FIT-GFP and FITm-GFP fusion protein (see Construction and Transient Expression of Fluorescent Protein Fusions), 48 hours after infiltration of tobacco epidermal leaf cells.

Fluorescence Recovery after Photobleaching (FRAP) was performed within one rectangular region of interest (ROI, 46 x 14 pixels) in the nucleus of a tobacco cell. The initial GFP signal intensity of this ROI before photobleaching was determined during 20 scans at an excitation wavelength of 488 nm and an emission wavelength of 500 to 530 nm. After 20 scans, a bleach with a maximal laser intensity and 50 iterations was applied to the ROI. After the bleach pulse, settings were adjusted to the initial low-intensity imaging and 280 post-bleaching scans were performed over 100 seconds to monitor fluorescence recovery. Fine-tuning of the parameters as well as sufficient control scans ensured that no acquisition bleaching emerged. For correction of background fluorescence of each sample, one additional ROI placed outside of the nucleus, was added. The observed background fluorescence was subtracted from the FRAP values, which were then normalized to the mean of the pre-bleach values. Non-linear curve fitting was performed (GraphPad Prism) in order to assess the final fluorescence intensity (F_{end}). Using the initial fluorescence intensity (F_{pre}) and the fluorescence intensity after photobleaching (F_{post}), the percentage of mobile (M_f) fractions of FIT-GFP and FITm-GFP were calculated according to the equation: $M_f = [(F_{end}-F_{post})/(F_{pre}-F_{post})] * 100$ (Bancaud et al., 2010). For each construct, 10 - 17 nuclei were analyzed.

FIT Homo- and Hetero-dimerization Assay by Targeted Yeast Two-Hybrid

In order to investigate the dimerization capacity of FIT and FITm, the respective C-terminal part was amplified from pDONR207:FIT(m)ns (see Construction and Transient Expression of Fluorescent Protein Fusions) using primers FIT-C B1 and FITst B2.

BHLH039 was amplified from pDONR207:bHLH39ns (see Construction and Transient Expression of Fluorescent Protein Fusions) with the primer pair bHLH039 B1 and bHLH039st B2. The respective amplicons were cloned into pDONR207 (BP reaction, Life Technologies), verified by sequencing and sub-cloning into pGBKT7-GW and pACT2-GW yeast two-hybrid destination vectors (LR reaction, Life Technologies). The obtained constructs pGBKT7-GW:FIT-C(m) or pGBKT7-GW:bHLH039 possess an N-terminal fusion with the GAL4 DNA binding domain (BD). pACT2-GW:FIT-C(m) or pACT2-GW:bHLH039 constructs contain a N-terminal GAL4 DNA activation domain (AD) fusion. Yeast strain AH109 was co-transformed with the respective plasmids. Positive transformants were selected on synthetic defined (SD) media lacking Leu and Trp (SD-LW) and were additionally verified by colony-PCR. To obtain appropriate negative controls, BD-FIT-C(m) and BD-bHLH039 were co-transformed with empty AD plasmids. Additionally, BD empty plasmids were co-transformed with respective AD-FIT-C(m) or AD-bHLH039 plasmids. The combination of pGBT9.BS:CIPK23 and pGAD.GH:cAKT1 served as a positive control (Xu et al., 2006; Le et al., 2016). The screening for positive protein-protein interactions was performed as previously described (Le et al., 2016). Plates were photographed after a one-week (hetero-dimerization) or two-week (homo-dimerization) incubation at 30 °C. pGBKT7-GW and pACT2-GW vectors were kindly provided by Dr. Yves Jacob.

FIT Homo- and Hetero-dimerization Assay by Förster Resonance Energy Transfer - Acceptor Photo Bleaching (FRET-APB) *in planta*

Tobacco leaf epidermal cells were transformed with GFP- and mCherry-tagged protein pairs to measure the homo- (FIT-GFP + FIT-mCherry or FITm-GFP + FITm-mCherry) or the hetero-dimerization (bHLH039-GFP + FIT-mCherry or bHLH039-GFP and FITm-mCherry) efficiency. Donor proteins were additionally transformed single-tagged with GFP and double-tagged with GFP-mCherry to serve as a negative and positive control, respectively (see Construction and Transient Expression of Fluorescent Protein Fusions). 24 hours post-infiltration, gene expression was induced by spraying the leaves with a 20 µM β-estradiol solution. FRET-APB measurements were performed 16 h after induction in nuclei of epidermal cells.

Measurements were operated with ZEN2 Black Edition software (Zeiss) at the confocal laser-scanning-microscope LSM780 (Zeiss). Fluorescence intensity for both fluorophores was detected within 20 frames in a 128 x 128 pixel format and a pixel time of 2.55 µs. After the 5th frame, 100 % laser power (561 nm) was used to bleach mCherry using 80 iterations. FRET efficiency was calculated as percent relative increase of GFP intensity after acceptor photobleaching. At least two independent experiments with 10 measured nuclei each were performed.

FIT Transcriptional Self-activation Assay in Yeast

In order to analyze whether BD-tagged, full length FIT and FITm phospho-mutants alone are able to initiate the *Gal4*-inducible yeast system, full-length FIT and FITm were amplified from the respective template pDONR207:FIT(m)ns (see Construction and Transient Expression of Fluorescent Protein Fusions) by using the primer pair FIT B1 and FITst B2, and cloned into pDONR207 (BP reaction; Life Technologies), generating pDONR207:FIT(m)st. FIT and FIT(m) were sub-cloned (LR reaction; Life Technologies) from the respective pDONR207:FIT(m)st into the pGBKT7-GW vectors, creating N-terminal fusion constructs with the GAL4 DNA binding domain (BD). Yeast strain AH109 was co-transformed with either BD-FIT or BD-FITm, as well as an empty AD plasmid, and selected on SD-LW media. Positive transformants were additionally verified by colony-PCR. The screening for auto-activation was performed by assaying the growth of the yeast colonies on SD-LWH media, containing either 30, 60 or 90 mM 3-amino-1,2,4-triazole (3-AT). A ten-fold dilution series was spotted, ranging from $OD_{600} = 1 - 10^{-3}$. pGBT9.BS:CIPK23 and pGAD.GH:cAKT1 was used as positive control (Xu et al., 2006; Le et al., 2016). A co-transformation control was included by spotting the same dilutions in parallel on selective SD-LW media. Growth of colonies was recorded after a one-week incubation at 30 °C.

Quantitative Transactivation Reporter Gene Assay for FIT in Mammalian Cells

First, plasmids were constructed. Mammalian expression vectors pMZ333 (Beyer et al., 2015) and pKM006 (Muller et al., 2013) were digested with *Not*I/*Xba*I and *EcoR*V/*Nru*I, respectively. In parallel, *FIT* and *FITm* were amplified with aqFIT Fw and aqFIT Rv. As a template, pDONR207:FIT(m)ns was used. *BHLH039* was amplified from pDONR207:bHLH039ns with primers aqBHLH039 Fw and aqBHLH039 Rv. For templates, see Construction and Transient Expression of Fluorescent Protein Fusion.

Col-0 cDNA, extracted from plants grown on Fe-deficient media, was used as a template for *IRT1$_{pro}$*. Primers aqIRT1$_{pro}$ Fw and aqIRT1$_{pro}$ Rv were used for subsequent amplification. The PCR was performed as follows: 95 °C, 30 seconds; 6 cycles of: 95 °C, 10 seconds / 60 °C, 30 seconds (+0.5 °C) / 72 °C, 45 seconds; 29 cycles of: 95 °C, 10 seconds / 55 °C, 30 seconds / 72 °C, 45 seconds; 72 °C, 2 minutes.

The Advanced Quick Assembly (AQUA) cloning approach was used and described previously (Beyer et al., 2015). Briefly, 12 ng linearized vector /1kb vector size was mixed with the PCR amplicon at a molar ratio of 3:1 in a volume of 10 µl ddH_2O. After 1 h of incubation at room temperature, 5 µl of the AQUA DNA mixture was used for subsequent *E.coli* transformation. Single colonies were analyzed by colony-PCR for the presence of the respective insert. Clones were further confirmed by sequencing. Effectors were cloned into pMZ333, creating the constructs pMZ333:FIT(m) and pMZ333:bHLH039. The reporter module comprises pKM195:IRT1$_{pro}$.

The Stuffer plasmid pHB007:BFP was constructed as follows: cDNA for h-mTagBFP2 was synthesized and amplified using the primers oHB018/oHB019. The product was assembled via Gibson cloning into pMZ333 digested with *Not*I/*Xba*I.

For subsequent mammalian cell transfection, Chinese hamster ovary cells (CHO-K1, DSMZ, ACC 110) were cultivated in Ham´s F12 Medium, L-glutamine, 1.176 g L^{-1} $NaHCO_3$ (PAN), supplemented with 10 % fetal bovine serum (FBS, PAN) and 1 % penicillin/streptomycin (PAN). Cells were seeded to a density of 40,000 cells/well in 500 µl of medium in 24-well plates or on glass-coverslips for imaging 24 h prior to transfection. Cells were transfected with respective pMZ333:FIT(m), pMZ333:bHLH039 or pKM195:IRT1$_{pro}$ plasmids (see Plasmid Construction for FIT Transactivation Reporter Gene Assay in Mammalian Cells), using a polyethyleneimine (PEI) method, as described previously (Muller et al., 2014). Briefly, the expression vectors encoding the protein of interest and the reporter module were mixed as indicated to a total amount of 1 µg of DNA (the concentration was adjusted with the stuffer plasmid pHB007:BFP coding for blue fluorescent protein (BFP), when necessary) in a solution of 50 µl Opti-MEM (Life Technologies) for each well. Then, 3.3 µl PEI (Polyscience) from a 1 mg ml^{-1} solution in ddH_2O (adjusted to pH 7.0 and filter sterilized) was diluted in 50 µl Opti-MEM (Life Technologies) per well and then added to the DNA/Opti-MEM mix. The mixture was vortexed immediately and incubated for 15 min at room temperature. Next, 100 µl of the mixture was added to each well of cells and the medium was exchanged 4 h after transfection. For reporter gene determination, the supernatant was collected 48 h after transfection.

For quantitative transactivation reporter gene activity determination, recombinant secreted alkaline phosphatase (SEAP) was quantified in cell culture medium using a colorimetric assay as described previously (Schlatter et al., 2002; Muller et al., 2014). In brief, 200 µl of the cell supernatant was incubated at 65 °C for 30 min in order to inactivate endogenous phosphatases. 80 µl of the heated culture was then mixed with 100 µl of SEAP buffer (20 mM L-homoarginine (Alpha Aeser), 1 mM $MgCl_2$, 21 % (v/v) diethanolamine (Sigma), adjusted to pH 9.8, and 20 µl para-nitrophenyl phosphate (pNPP, AppliChem, 120 mM in ddH_20) in a flat-bottom transparent 96-well plate. The absorbance at 405 nm was measured every minute for 2 h with a Berthold TriStar2 S LB 942 multimode plate reader.

Gaussia luciferase activity was determined as described previously (Remy and Michnick, 2006) by the addition of 20 µl coelenterazine (Roth, 472 mM coelenterazine stock solution in methanol diluted directly before use to 1:1,000 in phosphate-buffered saline PBS) to 80 µl of the cell supernatant in a flat-bottom white 96-well plate. Gaussia luciferase luminescence was measured for 20 min with a Berthold Centro XS LB 960 microplate luminometer.

Quantified Cell-free Degradation Assay

Protein stability was conducted in a quantified cell-free degradation assay. pMDC83:gFIT(m)-GFP (see Construction and Transient Expression of Fluorescent Protein Fusions) was transiently expressed in tobacco leaf epidermal cells. 48 hours post-infiltration, leaves were harvested, shock frozen and subsequently ground in liquid nitrogen. The ground material was solubilized in 2x Protein Loading buffer (124 mM Tris-Cl pH 6.8, 5% SDS, 4% DTT, 20% Glycerol, 0.002% Bromphenol Blue), incubated on a rotating wheel for 10 minutes at room temperature and subsequently pelleted by centrifugation for 10 minutes at 13.000 rpm and 4 °C. The supernatant was transferred into a new reaction tube, containing the total protein extract.

Protein stability was assayed over a time-course of 240 min in total. Subsequently, the total protein extract was equally distributed among four individual reaction tubes. After the respective incubation time of 0, 60, 120 or 240 minutes at 25 °C, samples were denatured for 10 minutes at 95 °C and kept on ice until further processing. FIT-GFP or FITm-GFP protein detection was performed as described previously (Le et al., 2016). Three individual tobacco transformation and degradation assays were performed.

For proteasomal arrest, 100 µM MG132 (AbMole BioScience), dissolved in dimethyl sulfoxide, (DMSO) was added to the protein extract prior to incubation at 25 °C. To monitor the potential

effects of DMSO on FIT protein, DMSO without MG132 was added to the protein extract as a control.

Quantification of the chemiluminescence signal was performed with the "Band Analysis" module present in the AlphaView Software (Cell Biosciences), according to manufacturer's instructions for background corrected signal average. The signal value obtained from the first sample (0 min incubation at 25 °C) was set to 100 % and used to calculate the signal intensities of the remaining samples (60, 120 and 240 min incubation at 25 °C) in direct relation to time-point 0 min. Means (±SD) of obtained values were displayed as fitted curves using non-linear regression (GraphPad Prism). Individual curve fitting of single replicates were performed to calculate the half-life time of the respective FIT form. Means of all 3 half-life times were displayed in box-plots.

Calculation of Outliers and Statistical Analysis

Outlier identification was based on the calculation of the interquartile range and determination of the inner and outer fences within a data-set. A value that was located above the outer fence or below the inner fence was excluded from the analysis (Jacobs and Dinman, 2004). Outlier calculations were applied to the subcellular localization, nuclear mobility, FRET-based protein-protein interaction and to the FIT transactivity reporter gene assay dataset.

Statistical analysis was performed using a two-tailed, unpaired Student's t-test (P-value < 0.05) when comparing an individual phospho-mutant to WT. When comparing WT and phospho-mutants among themselves, P-values ($P<0.05$) were obtained using one-way analysis of variance (ANOVA), followed by a Tukey's post-hoc test performed with OriginLab.

Primer Table

Primer Name	Primer Sequence	Generation of
aqIRT1$_{pro}$ Fw	TTCCCCGAAAAGTGCCACCTG ACGTCGTCGACTAGGAGCAC ATGGATTGACACAT	pKM195:IRT1$_{pro}$
aqIRT1$_{pro}$ Rv	CACTAAACGAGCTCTGCTTAT ATAGGGCTAGCAGATTGTTTA ATGTTTGTGT	pKM195:IRT1$_{pro}$

aqFIT Fw	TTTGTCTTTTATTTCAGGTCCC GGATCGAATTATGGAAGGAA GAGTCAACGC	pMZ333:FIT(m)st
aqFITst Rv	TGTCTGGATCGAAGCTTGGGC TGCAGGTCGACTCAAGTAAAT GACTTGATGA	pMZ333:FIT(m)st
aqBHLH039 Fw	TTTGTCTTTTATTTCAGGTCCC GGATCGAATTATGTGTGCATT AGTACCTCC	pMZ333:bHLH039st
aqBHLH039st Rv	TGTCTGGATCGAAGCTTGGGC TGCAGGTCGACTCATATATAT GAGTTTCCAC	pMZ333:bHLH039st
bHLH039 B1	GGGGACAAGTTTGTACAAAA AAGCAGGCTTCATGTGTGCAT TAGTACCTC	pDONR207:bHLH039 ns/st
bHLH039st B2	GGGGACCACTTTGTACAAGA AAGCTGGGTCTCATATATATG AGTTTCCAC	pDONR207:bHLH039st
bHLH039ns B2	GGGGACCACTTTGTACAAGA AAGCTGGGTCTATATATGAGT TTCCAC	pDONR207:bHLH039ns
FIT B1	GGGGACAAGTTTGTACAAAA AAGCAGGCTTAATGGAAGGA AGAGTCAACGC	pDONR207:gFITns, pDONR207:FIT(m)ns/st
FIT-C B1	GGGGACAAGTTTGTACAAAA AAGCAGGCTTAACTCAACCTT TTCGCGGTATC	pDONR207:FIT(m)-Cst
FITst B2	GGGGACCACTTTGTACAAGA AAGCTGGGTTTCAAGTAAATG ACTTGATGA	pDONR207:FIT(m)st, pDONR207:FIT(m)-Cst
FITns B2	GGGGACCACTTTGTACAAGA AAGCTGGGTTAGTAAATGACT TGATGAATTC	pDONR207:gFITns, pDONR207:FIT(m)-Cns

FITm(S221A) Fw	TATCAATCCTCCTGCAGCCAAAAAAATCATTCA	FIT phospho-mutants
FITm(S221A)ns Rv	TGAATGATTTTTTTGGCTGCAGGAGGATTGATA	FIT phospho-mutants
FITm(S221E) Fw	TATCAATCCTCCTGCAGAGAAAAAAATCATTCA	FIT phospho-mutants
FITm(S221E)ns Rv	TGAATGATTTTTTTCTCTGCAGGAGGATTGATA	FIT phospho-mutants
FITm(SS271/2AA) Fw	CAGAACTCTAACCTAGCCGCTCCTTCTCCGGACA	FIT phospho-mutants
FITm(SS271/2AA)ns Rv	TGTCCGGAGAAGGAGCGGCTAGGTTAGAGTTCTG	FIT phospho-mutants
FITm(Y238F) Fw	GAGGAGAAAGGGTTTTTTGTGAGATTGGTGTGT	FIT phospho-mutants
FITm(Y238F)ns Rv	ACACACCAATCTCACAAAAAACCCTTTCTCCTC	FIT phospho-mutants
FITm(Y238E) Fw	GAGGAGAAAGGGTTTGAAGTGAGATTGGTGTGT	FIT phospho-mutants
FITm(Y238E)ns Rv	ACACACCAATCTCACTTCAAACCCTTTCTCCTC	FIT phospho-mutants
FITm(Y278F) Fw	CCTTCTCCGGACACATTCCTCTTAACATATACC	FIT phospho-mutants
FITm(Y278F)ns Rv	GGTATATGTTAAGAGGAATGTGTCCGGAGAAGG	FIT phospho-mutants
FITm(Y278E) Fw	CCTTCTCCGGACACAGAGCTCTTAACATATACC	FIT phospho-mutants
FITm(Y278E)ns Rv	GGTATATGTTAAGAGCTCTGTGTCCGGAGAAGG	FIT phospho-mutants
oHB018 Fw	CTTTTTGTCTTTTATTTCAGGTCCCGGATCGAATTGCGGCCGCAGGAGGCGCCACCATGAGCGAGGAACTGATCAAAGAAAACATGC	pHB007:BFP

oHB019 Rv	TCATGTCTGGATCGAAGCTTG GGCTGCAGGTCGACTCTAGAT TAGTTCAGCTTGTGGCCCAGC TTAGAAG	pHB007:BFP

Acknowledgments: We are grateful to Elke Wieneke, Gintaute Matthäi, Kai Kirchhoff and Angelika Anna (Heinrich-Heine University, Saarland University) for excellent technical assistance. We are thankful for the contribution of Daniela Lichtblau, Christopher Endres, Laura Tünnermann and Büsra Acaroglu. We appreciate the excellent help from Stefanie Weidtkamp-Peters and the CAi imaging platform at Heinrich-Heine University. Funding from the German Research Foundation is greatly acknowledged (grants Ba1610/5-2 and Ba1610/7-1 to P. B.).

SUPPLEMENTAL INFORMATION

Supplemental Information includes five figures.

SUPPLEMENTAL FIGURES AND LEGENDS

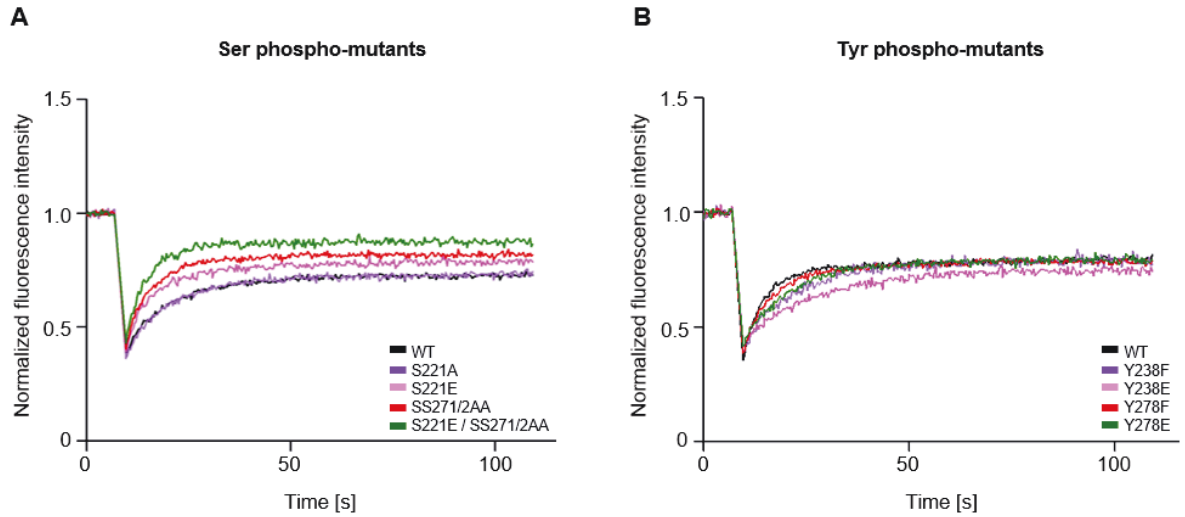

Supplemental Figure 1. Nuclear mobility is altered in FIT phospho-mutants.
(A-B) The nuclear mobility of FIT-GFP (WT) and the respective phospho-mutants was analyzed in tobacco leaf epidermis cells by Fluorescence Recovery after Photobleaching (FRAP). For every mutant, one recording of a representative bleach is shown. The background-corrected and normalized curve comprises the fluorescence intensity as a function of time. The fluorescence intensity is initially stable during the pre-bleach phase, reduced by more than 50% during the bleach and recovers over time. **(A)** WT (black) is shown in comparison to serine- and **(B)** tyrosine phospho-mutants.

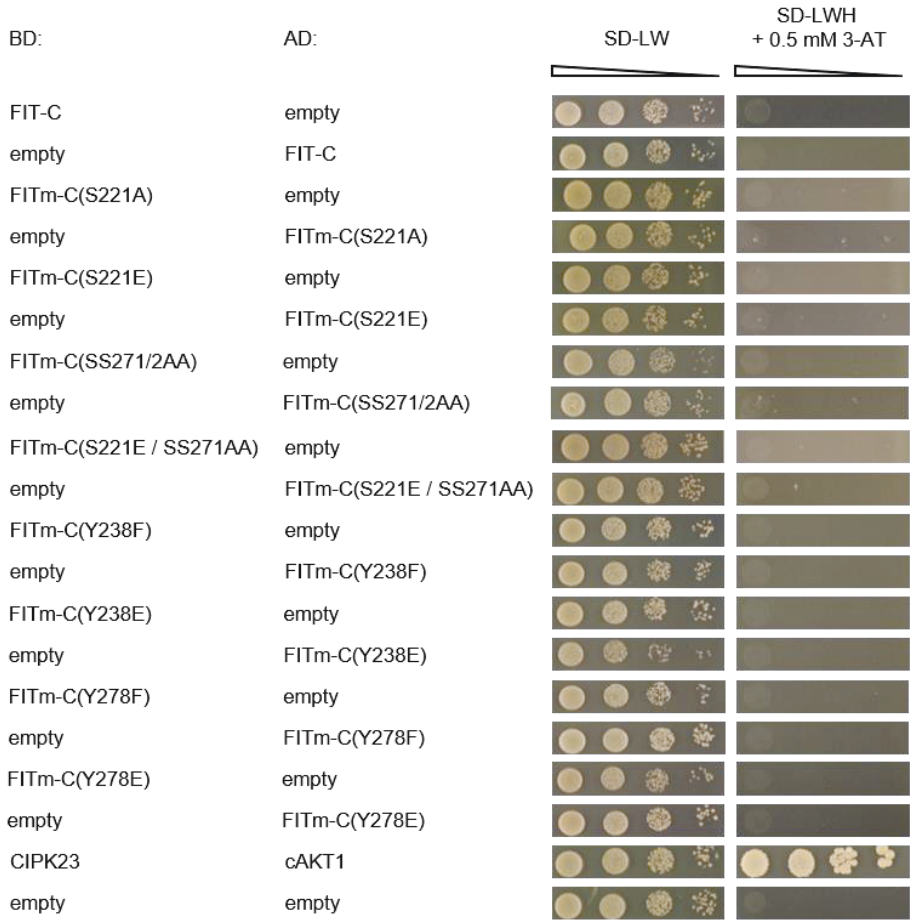

Supplemental Figure 2. FIT homo-dimerization capacity is affected in phospho-mutants.
FIT and FITm homo-dimerization assay in yeast. A 10-fold dilution series of yeast strain AH109, co-transformed with BD-FIT-C, or respective phospho-mutants, and AD-empty plasmids or BD-empty and AD-FIT-C plasmids, or respective phospho-mutants, was spotted onto selection media (OD_{600} = 1-10^{-3}). Growth on synthetic defined media, lacking Leu and Trp (SD-LW), displays a positive co-transformation event. Impeded growth of yeast on media lacking Leu, Trp and His (SD-LWH,) supplemented with 0.5 mM 3-amino-1,2,4-triazole (3-AT), indicates the specificity of the tested protein-protein interaction shown in Fig. 4A. BD-CIPK23 and AD-cAKT1 served as positive control, empty plasmids as negative control.

Supplemental Figure 3. FIT-bHLH039 interaction capacity is affected in phospho-mutants.
(A-B) FIT and FITm hetero-dimerization assay in yeast. **(A)** Yeast cells were co-transformed with BD-FIT-C, or respective phospho-mutant- and AD-empty plasmids, as well as BD-empty- and AD-bHLH039 plasmids. A 10-fold dilution series of yeast strain AH109 was spotted onto selection media (OD_{600} = 1-10^{-3}). Growth on synthetic defined media, lacking Leu and Trp (SD-LW), displays a positive co-transformation event. Impeded growth of yeast on media lacking Leu, Trp and His (SD-LWH,) supplemented with 0.5 mM 3-amino-1,2,4-triazole (3-AT), indicates the specificity of the tested protein-protein interaction shown in Fig. 4D. **(B)** Yeast cells were co-transformed with BD-bHLH039 and AD-FIT-C plasmids, or respective phospho-mutant plasmids. As negative controls, BD-bHLH039 and AD-empty plasmids as well as BD-empty and AD-FIT-C, or respective phospho-mutant plasmids were co-transformed. A 10-fold dilution series was spotted onto synthetic defined -Leu, -Trp (SD-LW) plates as growth control (OD_{600} = 10^{-1}-10^{-3}). To analyze the interaction capacity, yeast was spotted onto SD-LWH plates, containing 0.5 mM 3-amino-1,2,4-triazole (3-AT). BD-CIPK23 and AD-cAKT1 served as positive control, empty plasmids as negative control.

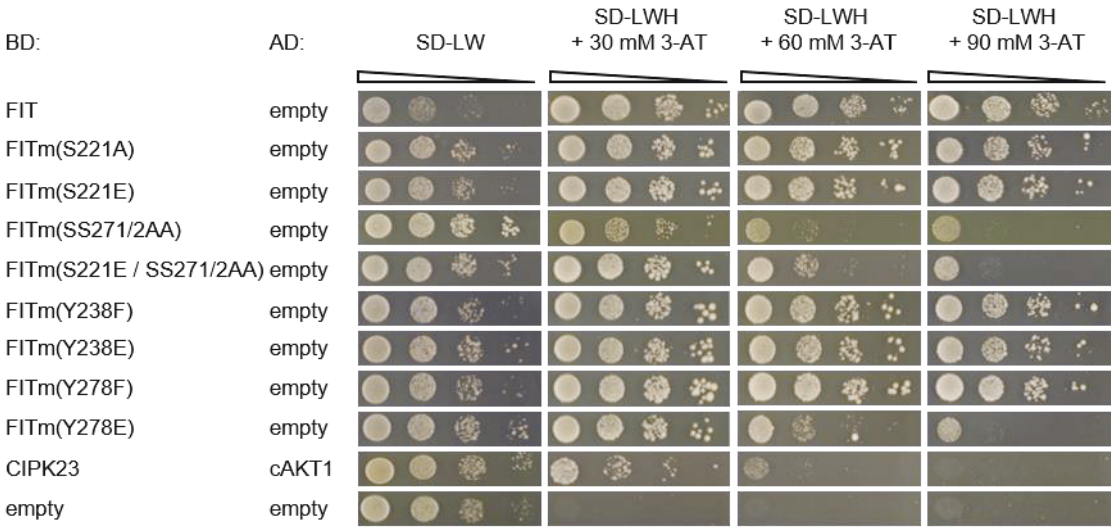

Supplemental Figure 4. Transcriptional self-activation capacity assay of FIT.
Self-activation of the yeast Gal4 transcription machinery mediated by BD-FIT is altered in FIT phospho-mutants. Yeast strain AH109 was co-transformed with respective BD-FIT or BD-FIm and AD-empty plasmids. A 10-fold dilution series was spotted (OD_{600} = 1-10^{-3}) on selection media. Growth on synthetic defined media, lacking Leu and Trp (SD-LW), demonstrates a successful co-transformation. Media lacking Leu, Trp and His (SD-LWH,) supplemented with different concentrations of 3-amino-1,2,4-triazole (3-AT, 30 mM, 60 mM, 90 mM), selects for self-activation of the GAL4-transcription machinery by BD-FIT or BD-FITm. BD-CIPK23 and AD-cAKT1 act as positive control. This interaction is suppressed upon a concentration higher than 60 mM 3-AT. Empty plasmids served as negative control.

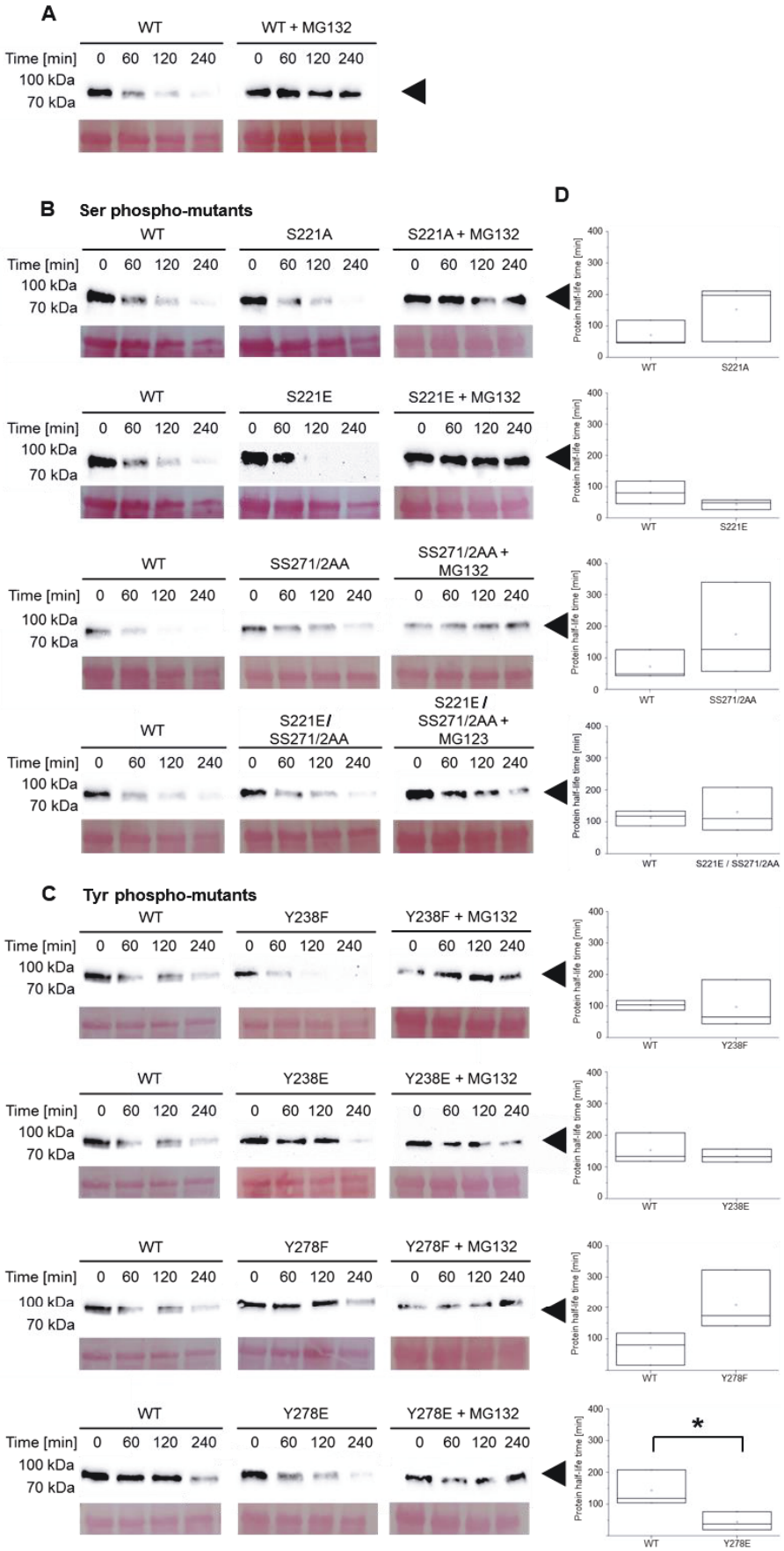

Supplemental Figure 5: Tyrosine phospho-mutants are affected by proteasomal degradation.
Protein stability of **(A)** FIT-GFP, **(B)** serine- and **(C)** tyrosine phospho-mutants was analyzed in a quantified cell-free degradation assay. Equal amounts of transiently transformed tobacco leaf cell extracts were transferred to

individual reaction tubes, partially treated with the proteasomal-inhibitor MG132 (+MG132) and incubated at room temperature for 0, 60, 120 or 240 minutes. Equal amounts of protein were used for immunoblotting. FIT-GFP and FITm-GFP at 70-100 kDa (black arrowhead) was detected using anti-GFP antibody. Ponceau-staining displays equal loading. Three individual transformations and assays were performed to monitor protein stability, one representative image is shown. MG132 treatment was carried out one time (n=1). **(D)** Quantification of the immunoblot signal and calculation of half-life times for FIT-GFP and FITm-GFP. Box-plots represent the half-life times of 3 individual assays. Statistical significance was calculated, using Student's *t*-test and was highlighted by asterisks ($P \leq 0.05$).

References

Al-Sady B, Ni WM, Kircher S, Schafer E, Quail PH (2006) Photoactivated phytochrome induces rapid PIF3 phosphorylation prior to proteasorne-mediated degradation. Molecular Cell 23: 439-446

Amanchy R, Kandasamy K, Mathivanan S, Periaswamy B, Reddy R, Yoon WH, Joore J, Beer MA, Cope L, Pandey A (2011) Identification of Novel Phosphorylation Motifs Through an Integrative Computational and Experimental Analysis of the Human Phosphoproteome. J Proteomics Bioinform 4: 22-35

Argetsinger LS, Kouadio JLK, Steen H, Stensballe A, Jensen ON, Carter-Su C (2004) Autophosphorylation of JAK2 on tyrosines 221 and 570 regulates its activity. Molecular and Cellular Biology 24: 4955-4967

Bancaud A, Huet S, Rabut G, Ellenberg J (2010) Fluorescence perturbation techniques to study mobility and molecular dynamics of proteins in live cells: FRAP, photoactivation, photoconversion, and FLIP. Cold Spring Harb Protoc 2010: pdb.top90

Bauer D, Viczián A, Kircher S, Nobis T, Nitschke R, Kunkel T, Panigrahi KCS, Ádám É, Fejes E, Schäfer E, Nagy F (2004) Constitutive Photomorphogenesis 1 and Multiple Photoreceptors Control Degradation of Phytochrome Interacting Factor 3, a Transcription Factor Required for Light Signaling in Arabidopsis. The Plant Cell 16: 1433-1445

Beausoleil SA, Jedrychowski M, Schwartz D, Elias JE, Villen J, Li J, Cohn MA, Cantley LC, Gygi SP (2004) Large-scale characterization of HeLa cell nuclear phosphoproteins. Proc Natl Acad Sci U S A 101: 12130-12135

Beyer HM, Gonschorek P, Samodelov SL, Meier M, Weber W, Zurbriggen MD (2015) AQUA Cloning: A Versatile and Simple Enzyme-Free Cloning Approach. Plos One 10

Beyer HM, Juillot S, Herbst K, Samodelov SL, Muller K, Schamel WW, Romer W, Schafer E, Nagy F, Strahle U, Weber W, Zurbriggen MD (2015) Red Light-Regulated Reversible Nuclear Localization of Proteins in Mammalian Cells and Zebrafish. ACS Synth Biol 4: 951-958

Bleckmann A, Weidtkamp-Peters S, Seidel CAM, Simon R (2010) Stem Cell Signaling in Arabidopsis Requires CRN to Localize CLV2 to the Plasma Membrane. Plant Physiology 152: 166-176

Blom N, Gammeltoft S, Brunak S (1999) Sequence and structure-based prediction of eukaryotic protein phosphorylation sites. J Mol Biol 294: 1351-1362

Braguy J, Zurbriggen MD (2016) Synthetic strategies for plant signalling studies: molecular toolbox and orthogonal platforms. The Plant Journal 87: 118-138

Brumbarova T, Bauer P, Ivanov R (2015) Molecular mechanisms governing Arabidopsis iron uptake. Trends Plant Sci 20: 124-133

Carretero-Paulet L, Galstyan A, Roig-Villanova I, Martínez-García JF, Bilbao-Castro JR, Robertson DL (2010) Genome-Wide Classification and Evolutionary Analysis of the bHLH Family of Transcription Factors in Arabidopsis, Poplar, Rice, Moss, and Algae. Plant Physiology 153: 1398-1412

Chinnusamy V, Ohta M, Kanrar S, Lee BH, Hong X, Agarwal M, Zhu JK (2003) ICE1: a regulator of cold-induced transcriptome and freezing tolerance in Arabidopsis. Genes Dev 17: 1043-1054

Colangelo EP, Guerinot ML (2004) The essential basic helix-loop-helix protein FIT1 is required for the iron deficiency response. Plant Cell 16: 3400-3412

Cole TCH HH, Stevens PF. (2017) Angiosperm phylogeny poster (APP) – Flowering plant systematics, 2017. PeerJ Preprints

Curtis MD, Grossniklaus U (2003) A gateway cloning vector set for high-throughput functional analysis of genes in planta. Plant Physiol 133: 462-469

Ding Y, Li H, Zhang X, Xie Q, Gong Z, Yang S (2015) OST1 Kinase Modulates Freezing Tolerance by Enhancing ICE1 Stability in Arabidopsis. Developmental Cell 32: 278-289

Edgar RC (2004) MUSCLE: a multiple sequence alignment method with reduced time and space complexity. BMC Bioinformatics 5: 113

Edgar RC (2004) MUSCLE: multiple sequence alignment with high accuracy and high throughput. Nucleic Acids Research 32: 1792-1797

Eide D, Broderius M, Fett J, Guerinot ML (1996) A novel iron-regulated metal transporter from plants identified by functional expression in yeast. Proc Natl Acad Sci U S A 93: 5624-5628

Fiol CJ, Wang AQ, Roeske RW, Roach PJ (1990) Ordered Multisite Protein-Phosphorylation - Analysis of Glycogen-Synthase Kinase-3 Action Using Model Peptide-Substrates. Journal of Biological Chemistry 265: 6061-6065

Gratz R, Manishankar P, Ivanov R, Köster P, Mohr I, Trofimov K, Steinhorst L, Meiser J, Drerup M, Arendt S, Holtkamp M, Karst U, Kudla J, Bauer P, Brumbarova T (2018 (submitted)) CIPK11-dependent phosphorylation modulates dynamic cellular activity of the key transcription factor FIT, promoting iron acquisition.

Gudesblat GE, Schneider-Pizon J, Betti C, Mayerhofer J, Vanhoutte I, van Dongen W, Boeren S, Zhiponova M, de Vries S, Jonak C, Russinova E (2012) SPEECHLESS integrates brassinosteroid and stomata signalling pathways. Nature Cell Biology 14: 548-U214

Guerinot ML, Yi Y (1994) Iron: Nutritious, Noxious, and Not Readily Available. Plant Physiol 104: 815-820

Haas JD, Luna SV, Lung'aho MG, Wenger MJ, Murray-Kolb LE, Beebe S, Gahutu JB, Egli IM (2016) Consuming Iron Biofortified Beans Increases Iron Status in Rwandan Women after 128 Days in a Randomized Controlled Feeding Trial. Journal of Nutrition 146: 1586-1592

Han L, Li GJ, Yang KY, Mao GH, Wang RQ, Liu YD, Zhang SQ (2010) Mitogen-activated protein kinase 3 and 6 regulate Botrytis cinerea-induced ethylene production in Arabidopsis. Plant Journal 64: 114-127

Heim MA, Jakoby M, Werber M, Martin C, Weisshaar B, Bailey PC (2003) The basic helix-loop-helix transcription factor family in plants: A genome-wide study of protein structure and functional diversity. Molecular Biology and Evolution 20: 735-747

Hunter T (2014) The Genesis of Tyrosine Phosphorylation. Cold Spring Harbor Perspectives in Biology 6

Ichimura K, Shinozaki K, Tena G, Sheen J, Henry Y, Champion A, Kreis M, Zhang S, Hirt H, Wilson C (2002) Mitogen-activated protein kinase cascades in plants: a new nomenclature. Trends in plant science 7: 301-308

Ivanov R, Brumbarova T, Bauer P (2012) Fitting into the harsh reality: regulation of iron-deficiency responses in dicotyledonous plants. Mol Plant 5: 27-42

Jacobs JL, Dinman JD (2004) Systematic analysis of bicistronic reporter assay data. Nucleic Acids Research 32

Jaillais Y, Hothorn M, Belkhadir Y, Dabi T, Nimchuk ZL, Meyerowitz EM, Chory J (2011) Tyrosine phosphorylation controls brassinosteroid receptor activation by triggering membrane release of its kinase inhibitor. Genes & Development 25: 232-237

Jakoby M, Wang H-Y, Reidt W, Weisshaar B, Bauer P (2004) FRU (BHLH029) is required for induction of iron mobilization genes in Arabidopsis thaliana. FEBS letters 577: 528-534

Jakoby M, Wang HY, Reidt W, Weisshaar B, Bauer P (2004) FRU (BHLH029) is required for induction of iron mobilization genes in Arabidopsis thaliana. FEBS Lett 577: 528-534

Joo S, Liu Y, Lueth A, Zhang S (2008) MAPK phosphorylation-induced stabilization of ACS6 protein is mediated by the non-catalytic C-terminal domain, which also contains the cis-determinant for rapid degradation by the 26S proteasome pathway. Plant J 54: 129-140

Jouannic S, Hamal A, Leprince A-S, Tregear J, Kreis M, Henry Y (1999) Plant MAP kinase kinase kinases structure, classification and evolution. Gene 233: 1-11

Ju CL, Yoon GM, Shemansky JM, Lin DY, Ying ZI, Chang JH, Garrett WM, Kessenbrock M, Groth G, Tucker ML, Cooper B, Kieber JJ, Chang C (2012) CTR1 phosphorylates the central regulator EIN2 to control ethylene hormone signaling from the ER membrane to the nucleus in Arabidopsis. Proceedings of the National Academy of Sciences of the United States of America 109: 19486-19491

Kato N, Dubouzet E, Kokabu Y, Yoshida S, Taniguchi Y, Dubouzet JG, Yazaki K, Sato F (2007) Identification of a WRKY protein as a transcriptional regulator of benzylisoquinoline alkaloid biosynthesis in Coptis japonica. Plant and cell physiology 48: 8-18

Kemp BE, Pearson RB (1990) Protein-Kinase Recognition Sequence Motifs. Trends in Biochemical Sciences 15: 342-346

Kim T-W, Wang Z-Y (2010) Brassinosteroid Signal Transduction from Receptor Kinases to Transcription Factors. Annual Review of Plant Biology 61: 681-704

Lampard GR, Macalister CA, Bergmann DC (2008) Arabidopsis stomatal initiation is controlled by MAPK-mediated regulation of the bHLH SPEECHLESS. Science 322: 1113-1116

Le CTT, Brumbarova T, Ivanov R, Stoof C, Weber E, Mohrbacher J, Fink-Straube C, Bauer P (2016) ZINC FINGER OF ARABIDOPSIS THALIANA12 (ZAT12) Interacts with FER-LIKE IRON DEFICIENCY- INDUCED TRANSCRIPTION FACTOR (FIT) Linking Iron Deficiency and Oxidative Stress Responses. Plant Physiology 170: 540-557

Lee S-j, Lee MH, Kim J-I, Kim SY (2015) Arabidopsis Putative MAP Kinase Kinase Kinases Raf10 and Raf11 are Positive Regulators of Seed Dormancy and ABA Response. Plant and Cell Physiology 56: 84-97

Lemmon MA, Schlessinger J (2010) Cell signaling by receptor-tyrosine kinases. Cell 141: 1117-1134

Li GJ, Meng XZ, Wang RG, Mao GH, Han L, Liu YD, Zhang SQ (2012) Dual-Level Regulation of ACC Synthase Activity by MPK3/MPK6 Cascade and Its Downstream WRKY Transcription Factor during Ethylene Induction in Arabidopsis. Plos Genetics 8

Li H, Ding Y, Shi Y, Zhang X, Zhang S, Gong Z, Yang S (2017) MPK3- and MPK6-Mediated ICE1 Phosphorylation Negatively Regulates ICE1 Stability and Freezing Tolerance in Arabidopsis. Developmental Cell

Li S, Han X, Yang L, Deng X, Wu H, Zhang M, Liu Y, Zhang S, Xu J (2017) Mitogen-activated protein kinases and calcium-dependent protein kinases are involved in wounding-induced ethylene biosynthesis in Arabidopsis thaliana. Plant Cell Environ

Lingam S, Mohrbacher J, Brumbarova T, Potuschak T, Fink-Straube C, Blondet E, Genschik P, Bauer P (2011) Interaction between the bHLH transcription factor FIT and ETHYLENE INSENSITIVE3/ETHYLENE INSENSITIVE3-LIKE1 reveals molecular linkage between the regulation of iron acquisition and ethylene signaling in Arabidopsis. Plant Cell 23: 1815-1829

Liu YD, Zhang SQ (2004) Phosphorylation of 1-aminocyclopropane-1-carboxylic acid synthase by MPK6, a stress-responsive mitogen-activated protein kinase, induces ethylene biosynthesis in Arabidopsis. Plant Cell 16: 3386-3399

Lorrain S, Allen T, Duek PD, Whitelam GC, Fankhauser C (2008) Phytochrome-mediated inhibition of shade avoidance involves degradation of growth-promoting bHLH transcription factors. Plant Journal 53: 312-323

Lu Q, Helm S, Rödiger A, Baginsky S (2015) On the Extent of Tyrosine Phosphorylation in Chloroplasts. Plant Physiology 169: 996-1000

Luo ML, Reyna S, Wang LS, Yi ZP, Carroll C, Dong LQ, Langlais P, Weintraub ST, Mandarino LJ (2005) Identification of insulin receptor substrate 1 serine/threonine phosphorylation sites using mass spectrometry analysis: Regulatory role of Serine 1223. Endocrinology 146: 4410-4416

Maathuis FJ (2008) Conservation of protein phosphorylation sites within gene families and across species. Plant Signal Behav 3: 1011-1013

Mai H-J, Pateyron S, Bauer P (2016) Iron homeostasis in Arabidopsis thaliana: transcriptomic analyses reveal novel FIT-regulated genes, iron deficiency marker genes and functional gene networks. BMC plant biology 16: 211

Marschner H, Romheld V, Kissel M (1986) Different Strategies in Higher-Plants in Mobilization and Uptake of Iron. Journal of Plant Nutrition 9: 695-713

Meiser J, Lingam S, Bauer P (2011) Posttranslational regulation of the iron deficiency basic helix-loop-helix transcription factor FIT is affected by iron and nitric oxide. Plant Physiol 157: 2154-2166

Mithoe SC, Boersema PJ, Berke L, Snel B, Heck AJR, Menke FLH (2012) Targeted Quantitative Phosphoproteomics Approach for the Detection of Phospho-tyrosine Signaling in Plants. Journal of Proteome Research 11: 438-448

Moorhead G, W. Templeton G, T. Tran H (2007) Role of Protein Kinases, Phosphatases and 14- 3- 3 Proteins in the Control of Primary Plant Metabolism,

Muller K, Engesser R, Metzger S, Schulz S, Kampf MM, Busacker M, Steinberg T, Tomakidi P, Ehrbar M, Nagy F, Timmer J, Zubriggen MD, Weber W (2013) A red/far-red light-responsive bi-stable toggle switch to control gene expression in mammalian cells. Nucleic Acids Res 41: e77

Muller K, Zurbriggen MD, Weber W (2014) Control of gene expression using a red- and far-red light-responsive bi-stable toggle switch. Nature Protocols 9: 622-632

Nakagami H, Sugiyama N, Mochida K, Daudi A, Yoshida Y, Toyoda T, Tomita M, Ishihama Y, Shirasu K (2010) Large-Scale Comparative Phosphoproteomics Identifies Conserved Phosphorylation Sites in Plants. Plant Physiology 153: 1161-1174

Naranjo-Arcos MA, Maurer F, Meiser J, Pateyron S, Fink-Straube C, Bauer P (2017) Dissection of iron signaling and iron accumulation by overexpression of subgroup Ib bHLH039 protein. Scientific Reports 7

Ni W, Xu SL, Gonzalez-Grandio E, Chalkley RJ, Huhmer AFR, Burlingame AL, Wang ZY, Quail PH (2017) PPKs mediate direct signal transfer from phytochrome photoreceptors to transcription factor PIF3. Nat Commun 8: 15236

Ni WM, Xu SL, Chalkley RJ, Pham TND, Guan SH, Maltby DA, Burlingame AL, Wang ZY, Quail PH (2013) Multisite Light-Induced Phosphorylation of the Transcription Factor PIF3 Is Necessary for Both Its Rapid Degradation and Concomitant Negative Feedback Modulation of Photoreceptor phyB Levels in Arabidopsis. Plant Cell 25: 2679-2698

Niittyla T, Fuglsang AT, Palmgren MG, Frommer WB, Schulze WX (2007) Temporal analysis of sucrose-induced phosphorylation changes in plasma membrane proteins of Arabidopsis. Mol Cell Proteomics 6: 1711-1726

Oh M-H, Wang X, Kota U, Goshe MB, Clouse SD, Huber SC (2009) Tyrosine phosphorylation of the BRI1 receptor kinase emerges as a component of brassinosteroid signaling in Arabidopsis. Proceedings of the National Academy of Sciences 106: 658-663

Oh M-H, Wang X, Wu X, Zhao Y, Clouse SD, Huber SC (2010) Autophosphorylation of Tyr-610 in the receptor kinase BAK1 plays a role in brassinosteroid signaling and basal defense gene expression. Proceedings of the National Academy of Sciences of the United States of America 107: 17827-17832

Pearson RB, Kemp BE (1991) Protein-Kinase Phosphorylation Site Sequences and Consensus Specificity Motifs - Tabulations. Methods in Enzymology 200: 62-81

Reits EA, Neefjes JJ (2001) From fixed to FRAP: measuring protein mobility and activity in living cells. Nature cell biology 3: E145

Remy I, Michnick SW (2006) A highly sensitive protein-protein interaction assay based on Gaussia luciferase. Nature Methods 3: 977-979

Ren YJ, Li YY, Jiang YQ, Wu BH, Miao Y (2017) Phosphorylation of WHIRLY1 by CIPK14 Shifts Its Localization and Dual Functions in Arabidopsis. Molecular Plant 10: 749-763

Robinson DR, Wu Y-M, Lin S-F (2000) The protein tyrosine kinase family of the human genome. Oncogene 19: 5548

Rudrabhatla P, Reddy MM, Rajasekharan R (2006) Genome-Wide Analysis and Experimentation of Plant Serine/Threonine/Tyrosine-Specific Protein Kinases. Plant Molecular Biology 60: 293-319

Schlatter S, Rimann M, Kelm J, Fussenegger M (2002) SAMY, a novel mammalian reporter gene derived from Bacillus stearothermophilus alpha-amylase. Gene 282: 19-31

Schwartz D, Gygi SP (2005) An iterative statistical approach to the identification of protein phosphorylation motifs from large-scale data sets. Nature Biotechnology 23: 1391-1398

Shen H, Zhu L, Castillon A, Majee M, Downie B, Huq E (2008) Light-induced phosphorylation and degradation of the negative regulator PHYTOCHROME-INTERACTING FACTOR1 from Arabidopsis depend upon its direct physical interactions with photoactivated phytochromes. Plant Cell 20: 1586-1602

Shen Y, Khanna R, Carle CM, Quail PH (2007) Phytochrome induces rapid PIF5 phosphorylation and degradation in response to red-light activation. Plant Physiology 145: 1043-1051

Shiu S-H, Bleecker AB (2001) Receptor-like kinases from *Arabidopsis* form a monophyletic gene family related to animal receptor kinases. Proceedings of the National Academy of Sciences 98: 10763-10768

Sivitz A, Grinvalds C, Barberon M, Curie C, Vert G (2011) Proteasome-mediated turnover of the transcriptional activator FIT is required for plant iron-deficiency responses. Plant J 66: 1044-1052

Sugiyama N, Nakagami H, Mochida K, Daudi A, Tomita M, Shirasu K, Ishihama Y (2008) Large-scale phosphorylation mapping reveals the extent of tyrosine phosphorylation in Arabidopsis. Molecular Systems Biology 4: 193-193

Takeo K, Ito T (2017) Subcellular localization of VIP1 is regulated by phosphorylation and 14-3-3 proteins. Febs Letters 591: 1972-1981

van Wijk KJ, Friso G, Walther D, Schulze WX (2014) Meta-analysis of Arabidopsis thaliana phospho-proteomics data reveals compartmentalization of phosphorylation motifs. The Plant Cell 26: 2367-2389

Vert G, Grotz N, Dedaldechamp F, Gaymard F, Guerinot ML, Briat JF, Curie C (2002) IRT1, an Arabidopsis transporter essential for iron uptake from the soil and for plant growth. Plant Cell 14: 1223-1233

Wang B, Li G, Zhang W-H (2015) Brassinosteroids are involved in Fe homeostasis in rice (Oryza sativa L.). Journal of Experimental Botany 66: 2749-2761

Wang B, Li Y, Zhang WH (2012) Brassinosteroids are involved in response of cucumber (Cucumis sativus) to iron deficiency. Ann Bot 110: 681-688

Wang HY, Klatte M, Jakoby M, Baumlein H, Weisshaar B, Bauer P (2007) Iron deficiency-mediated stress regulation of four subgroup Ib BHLH genes in Arabidopsis thaliana. Planta 226: 897-908

Wang N, Cui Y, Liu Y, Fan H, Du J, Huang Z, Yuan Y, Wu H, Ling HQ (2013) Requirement and functional redundancy of Ib subgroup bHLH proteins for iron deficiency responses and uptake in Arabidopsis thaliana. Mol Plant 6: 503-513

Wang N, Cui Y, Liu Y, Fan HJ, Du J, Huang ZA, Yuan YX, Wu HL, Ling HQ (2013) Requirement and Functional Redundancy of Ib Subgroup bHLH Proteins for Iron Deficiency Responses and Uptake in Arabidopsis thaliana. Molecular Plant 6: 503-513

Wild M, Davière J-M, Regnault T, Sakvarelidze-Achard L, Carrera E, Lopez Diaz I, Cayrel A, Dubeaux G, Vert G, Achard P (2016) Tissue-Specific Regulation of Gibberellin Signaling Fine-Tunes Arabidopsis Iron-Deficiency Responses. Developmental Cell 37: 190-200

Xu J, Li HD, Chen LQ, Wang Y, Liu LL, He L, Wu WH (2006) A protein kinase, interacting with two calcineurin B-like proteins, regulates K+ transporter AKT1 in Arabidopsis. Cell 125: 1347-1360

Yamada Y, Sato F (2016) Tyrosine phosphorylation and protein degradation control the transcriptional activity of WRKY involved in benzylisoquinoline alkaloid biosynthesis. Scientific Reports 6: 31988

Yang KZ, Jiang M, Wang M, Xue S, Zhu LL, Wang HZ, Zou JJ, Lee EK, Sack F, Le J (2015) Phosphorylation of Serine 186 of bHLH Transcription Factor SPEECHLESS Promotes Stomatal Development in Arabidopsis. Molecular Plant 8: 783-795

Ye LX, Li L, Wang L, Wang SD, Li S, Du J, Zhang SQ, Shou HX (2015) MPK3/MPK6 are involved in iron deficiency-induced ethylene production in Arabidopsis. Frontiers in Plant Science 6

Yoo SD, Cho YH, Tena G, Xiong Y, Sheen J (2008) Dual control of nuclear EIN3 by bifurcate MAPK cascades in C2H4 signalling. Nature 451: 789-U781

Yuan Y, Wu H, Wang N, Li J, Zhao W, Du J, Wang D, Ling HQ (2008) FIT interacts with AtbHLH38 and AtbHLH39 in regulating iron uptake gene expression for iron homeostasis in Arabidopsis. Cell Res 18: 385-397

Zhang J, Zhu HF, Liang H, Liu KF, Zhang AM, Ling HQ, Wang DW (2006) Further analysis of the function of AtBHLH29 in regulating the iron uptake process in Arabidopsis thaliana. Journal of Integrative Plant Biology 48: 75-84

Zhao C, Wang P, Si T, Hsu C-C, Wang L, Zayed O, Yu Z, Zhu Y, Dong J, Tao WA, Zhu J-K (2017) MAP Kinase Cascades Regulate the Cold Response by Modulating ICE1 Protein Stability. Developmental Cell

Authors Contribution to Manuscript 2

Regina Gratz

Designed, performed and analyzed all experiments, except FRET, wrote the manuscript, designed final figures and reviewed / edited the manuscript.

Ksenia Trofimov, Rocio Ochoa-Fernandez and Tim Blomeier

Performed and analyzed FRET experiments (K. T.). Helped designing, performing and analyzing the quantitative transactivation reporter gene assay (R. O. F., T. B.).

Tzvetina Brumbarova, Rumen Ivanov,

Helped in designing, performing and analyzing experiments, reviewed / edited the manuscript and supervised the study.

Johannes Meiser

Helped designing the phospho-mutants approach.

Matias Zurbriggen

Supervised and provided support for the quantitative transactivation reporter gene assay.

Petra Bauer

Designed the outline of the manuscript, supervised the study, provided funding and reviewed / edited the manuscript.

8 Concluding Remarks

The results of our study suggest a dual regulation of FIT protein activity, in which phosphorylation of selected Ser promote the activity, whereas phosphorylation of selected Tyr have a repressive effect.

We concordantly showed Fe-deficiency-induced Ca^{2+} transients in the same subcellular compartments in which FIT is highly expressed [1]. We propose that the Ca^{2+} sensors CBL1/CBL9 are involved in the Fe-deficiency signal transmission, as *cbl1/9* loss-of-function mutants show a decreased Fe reductase activity. CBL1/CBL9 are known interaction partners of the protein kinase CIPK11 [2], which we found to interact with FIT. The CBL1/CBL9 - CIPK11 module induces CIPK11 kinase activity which leads to FIT phosphorylation. We found that phospho-mimicked FIT at position Ser272 is a prerequisite for proper subcellular localization, mobility and dimerization in transient assays. Transgenic lines carrying the respective non-phosphorylatable Ser272 had reduced FIT activity as well as reduced seed Fe content. In summary, we could show that an Fe-deficiency-based Ca^{2+} transient activates CIPK11, which in turn phosphorylates and, hence, activates FIT (Figure 5A).

The integration of abiotic stress signals to transcriptional responses have been shown in the past. The antagonistical regulation of SPCH activity is a suitable comparison for a possible multi-layer FIT regulation, as it was shown that (i) one abiotic factor can have opposing effects on phosphorylation-triggered downstream processes [3-5] and (ii) that the regulation of protein activity can be mediated by different kinases, having antagonistic effects [6, 7]. Taking the SPCH regulation as model for FIT regulation, we asked if FIT also undergoes multifaceted phosphorylation control and whether one site could potentially reflect a negative regulatory unit. In addition we asked if Tyr phosphorylation sites could be predicted and validated.

In an exhaustive and reliable phospho-mutant activity screening, we indeed found two highly promising Tyr sites with an expected regulatory function. In a series of different assays, in which we were screening for altered regulatory FIT properties and cellular activities, mostly contrasting phenotypes for both Tyr sites were found, when phospho-mimicking and non-phosphorylatable FIT forms were compared. Interestingly, respective phospho-mimicking forms showed a decreased bHLH039-interaction capacity and thus, a reduced activity of these FIT forms was anticipated. Indeed, we verified a reduced transcriptional activity of the phospho-mimicked mutants in a controlled synthetic assay. Tyr278 appeared to be of high interest, as it displayed a reduced protein stability in addition to being inactive. Based on these intriguing results, we propose the following model, in which hypothetically, tyrosine phosphorylation displays an antagonistical way to modify FIT activity by deactivating and

destabilizing FIT (Figure 5B). Hence, we identified two molecular mechanisms to fine-tune FIT activity, either by Ser phosphorylation-based activation or via Tyr phosphorylation-based inactivation.

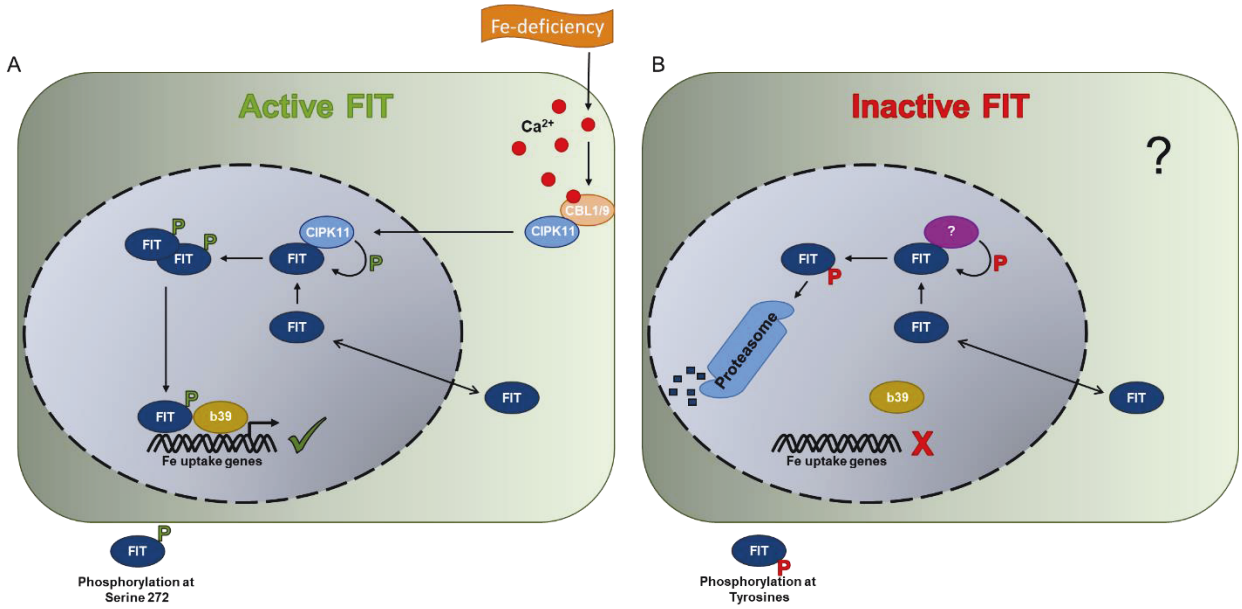

Figure 5: FIT activity is controlled by post-translational modifications. **(A)** Under Fe-deficiency, FIT is phosphorylated at Ser272, mediated by the CBL1/9 – CIPK11 module. Phosphorylated FIT displays an active FIT form and can interact with itself and bHLH039 (b39). This interaction promotes downstream target gene expression. **(B)** Potential phosphorylation of Tyr residues might display a mechanism to inactivate FIT via the decrease of hetero-dimerization. Inactive FIT forms might undergo proteasomal degradation. It is not known, which signals and kinases inhibit FIT activity.

The discovery of possible Tyr phosphorylation sites in FIT is very interesting, as Tyr phosphorylation in plants is a newly emerging topic. In the animal kingdom, Tyr phosphorylation is studied more in detail and connected with signal transduction, mediated by receptor tyrosine kinases. For a long time it was assumed that Tyr phosphorylation was playing a minor role in plant protein regulation [8]. Recent phospho-proteomic data *in planta* revealed, however that phospho-tyrosines account for 4.3 % of all phosphorylation events, which is more as reported for animals [9, 10]. Identified peptides were considerably more often multiply phosphorylated, which is very interesting in the context of our two identified regulatory Tyr sites. Also, mainly nuclear proteins were found to be Tyr phosphorylated [9]. This displays, that Tyr phosphorylation *in planta* is a promising tool for protein -possibly transcription factor- regulation, as it might be the case for FIT.

We suggest a model of FIT protein phosphorylation involving a two-step regulation mechanism in which Ser phosphorylation is beneficial for FIT activity and Tyr phosphorylation renders the protein inactive.

References

1. Jakoby, M., et al., *FRU (BHLH029) is required for induction of iron mobilization genes in Arabidopsis thaliana.* FEBS letters, 2004. 577(3): p. 528-534.
2. Albrecht, V., et al., *The NAF domain defines a novel protein–protein interaction module conserved in Ca(2+)-regulated kinases.* The EMBO Journal, 2001. 20(5): p. 1051-1063.
3. Kim, T.-W., et al., *Brassinosteroid regulates stomatal development by GSK3-mediated inhibition of a MAPK pathway.* Nature, 2012. 482(7385): p. 419-422.
4. Khan, M., et al., *Brassinosteroid-regulated GSK3/Shaggy-like Kinases Phosphorylate Mitogen-activated Protein (MAP) Kinase Kinases, Which Control Stomata Development in Arabidopsis thaliana.* Journal of Biological Chemistry, 2013. 288(11): p. 7519-7527.
5. Gudesblat, G.E., et al., *SPEECHLESS integrates brassinosteroid and stomata signalling pathways.* Nature Cell Biology, 2012. 14(5): p. 548-U214.
6. Yang, K.Z., et al., *Phosphorylation of Serine 186 of bHLH Transcription Factor SPEECHLESS Promotes Stomatal Development in Arabidopsis.* Molecular Plant, 2015. 8(5): p. 783-795.
7. Lampard, G.R., C.A. Macalister, and D.C. Bergmann, *Arabidopsis stomatal initiation is controlled by MAPK-mediated regulation of the bHLH SPEECHLESS.* Science, 2008. 322(5904): p. 1113-6.
8. van Bentem, S.d.l.F. and H. Hirt, *Protein tyrosine phosphorylation in plants: more abundant than expected?* Trends in plant science, 2009. 14(2): p. 71-76.
9. Sugiyama, N., et al., *Large-scale phosphorylation mapping reveals the extent of tyrosine phosphorylation in Arabidopsis.* Molecular Systems Biology, 2008. 4: p. 193-193.
10. Mithoe, S.C., et al., *Targeted Quantitative Phosphoproteomics Approach for the Detection of Phospho-tyrosine Signaling in Plants.* Journal of Proteome Research, 2012. 11(1): p. 438-448.